UNIVERSITY OF KWAZULU-NATAL

THE SYNTHESIS, CHARACTERISATION AND ANTIBACTERIAL ACTIVITY OF BENZIMIDAZOLE-OXADIAZOLE HYBRIDS

2022

AISHWARYA NISHAN BANTHO

THE SYNTHESIS, CHARACTERISATION AND ANTIBACTERIAL ACTIVITY OF BENZIMIDAZOLE-OXADIAZOLE HYBRIDS

AISHWARYA NISHAN BANTHO

2022

A thesis submitted to the School of Chemistry and Physics, College of Agriculture, Engineering and Science, University of KwaZulu-Natal, Westville, for the degree of Master of Science in Chemistry.

This thesis has been prepared according to **Format 1** as outlined in the Information for the guidance of examiners of Higher degrees, which states:

Format 1: As a single coherent book, with a single Introduction, Materials and Methods, Results, Discussion, Conclusion and References.

As the candidate's supervisor, I have approved this thesis for submission.

Supervisor: Date.27 March 2022……………

Professor Neil A. Koorbanally

ABSTRACT

In the mission to combat antimicrobial resistance (AMR), molecular hybridisation was one of the methodologies used in designing new antibiotics agents. Since benzimidazole and oxadiazole moieties are well known and used for their diverse and overlapping medicinal applications, a series of 2-trifluoromethylbenzimidazole-oxadiazole hybrid molecules were synthesised to investigate their potential as antibacterial compounds. The synthesis was performed through a six-step synthetic pathway to produce twelve novel hybrids with yields of 70-97%. These compounds were elucidated by NMR, and HR-MS, CHN analysis and XRD were used to confirm their structures. The application of the molecular hybrids against AMR was determined by testing the synthesised compounds on Gram-positive (*Staphylococcus aureus* and Methicillin-resistant *Staphylococcus aureus*) and Gram-negative (*Klebsiella pneumoniae*, *Escherichia coli*, *Salmonella typhimurium* and *Pseudomonas aeruginosa*) bacterial strains. A hit compound **7k** was identified as it displayed a minimum bactericidal concentration (MBC) of 4 µM against *K. pneumoniae*, three-fold better than the standard drug ciprofloxacin.

Keywords: Benzimidazole, oxadiazole, molecular hybridisation, structural elucidation and antibacterial assay

GRAPHICAL ABSTRACT

7k
MBC = 4 μM
against *K. pneumoniae*
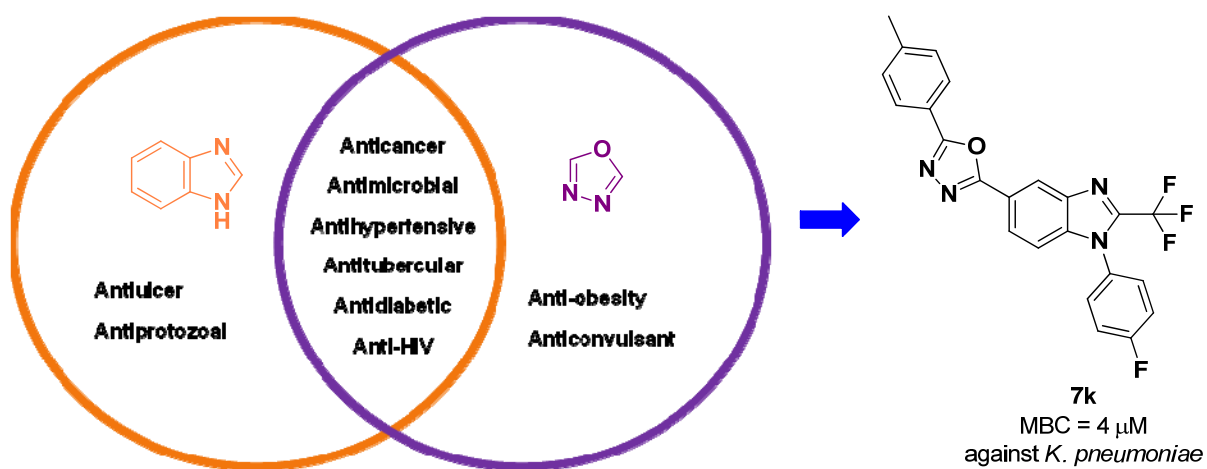
STRUCTURES OF COMPOUNDS
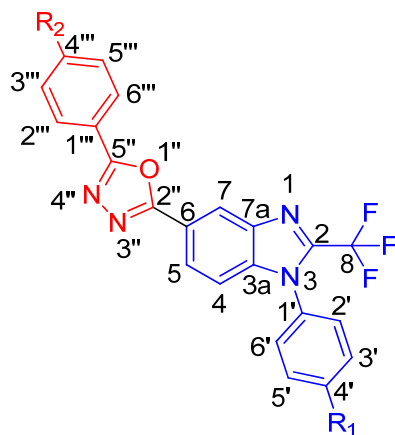
7a-l

Compound	R₁	R₂	Compound	R₁	R₂
7a	H	H	**7g**	F	H
7b	H	Br	**7h**	F	Br
7c	H	Cl	**7i**	F	Cl
7d	H	F	**7j**	F	F
7e	H	Me	**7k**	F	Me
7f	H	MeO	**7l**	F	MeO

ABBREVIATIONS

^{13}C NMR	Carbon-13 Nuclear Magnetic Resonance Spectroscopy
^{1}H NMR	Proton Nuclear Magnetic Resonance Spectroscopy
3D-QSAR	3Dimensional-Quantitative structure-activity relationships
4CR	Four component reaction
ADME	Absorption, distribution, metabolism and excretion
Akt	Ak strain transforming (Protein kinase B)
AMR	Antimicrobial resistance
Anti-TB	Antitubercular
APT	Attached proton test
AT$_1$	Angiotensin II receptor antagonists
ATP	Adenosine triphosphate
AZT	Azidothymidine
BAS	Bronsted active sites
BK$_{Ca}$	Large conductance calcium-activated potassium channels
Caco-2	Human colorectal adenocarcinoma cells
CC$_{50}$	50% Cytotoxic concentration
cGMP	Cyclic guanosine monophosphate
CLL	Chronic lymphocytic leukaemia
cLogP	Compound's logarithmic partition coefficient between octanol and water
COSY	Correlated Nuclear Magnetic Resonance Spectroscopy
COX-2	Cyclooxygenase enzyme
Cu(II)@DAC-Betti	Copper immobilised dialdehyde cellulose-Betti biocatalyst
d	Doublet
DABAL-Me$_3$	Bis(trimethylaluminum)-1,4-diazabicyclo[2.2.2]octane adduct
dd	Double doublet
ddd	Doublet of doublets of doublets
DDQ	2,3-Dichloro-5,6-dicyano-1,4-benzoquinone
DEAD	Diethyl azodicarboxylate
DIPEA	*N*, *N*-diisopropylethylamine
DMF	Dimethyl formamide
DMSO	Dimethyl sulfoxide
DNA	Deoxyribonucleic acid

DPPH	2,2-Diphenyl-1-picryhydrazyl
Ec	*Escherichia coli*
EC_{50}	Half maximal effective concentration
EGFR	Epidermal growth factor receptor
EMMN	Ethoxymethylenemalononitrile
FAK	Focal adhesion kinase
FDA	Food and drug administration
FT-IR	Fourier Transform – Infrared Spectroscopy
FtsZ	Filamenting temperature-sensitive mutant Z
GLR-G2	Amidoamine G2 polymer
GSK-3β	Glycogen synthase kinase 3 beta enzyme
GST	Glutathione S-transferase
H^+/K^+ ATPase	Hydrogen/potassium adenosine triphosphatase
HATU	1-[Bis(dimethylamino)methylene]-1*H*-1,2,3-triazolo[4,5-*b*]pyridium 3-oxide hexafluorophosphate
HCCLM3	Hepatocellular carcinoma cell line
HCT	Human colorectal carcinoma cell line
HCV	Hepatitis C virus
HepG2	Liver hepatocellular carcinoma
Hf-BTC	Hafnium-1,3,5-tricarboxylate
Hf-MOF	Hafnium-metal organic framework
HIV-1	Human immunodeficiency virus type 1
HMBC	Heteronuclear Multiple Bond Coherence
HPAILs	Heteropolyanion-based ionic liquids
HPHT	High pressure high temperature
HRMS	High-Resolution Mass Spectrometry
HSQC	Heteronuclear Multiple Quantum Coherence
HT-29	Colon adenocarcinoma
IBD	Iodobenzene diacetate
IC_{50}	Half-maximal inhibitory concentration
IC_{90}	90% of the maximal inhibition
INH	Isoniazid
InhA	Inhibin subunit alpha (protein coding gene)
Kp	*Klebsiella pneumoniae*

MBC	Minimum bactericidal concentration
MCF-7	Human breast cancer cell line
MCR	Multicomponent reaction
MDA-MB-231	Breast adenocarcinoma
MDR	Multidrug-resistant
MeCN	Acetonitrile
MFC	Minimum fungicidal concentration
MH	Molecular hybridisation
MIC	Minimum inhibitory concentration
miR-21	MicroRNA 21
MRSA	Methicillin-resistant *Staphylococcus aureus*
MS	Mass spectroscopy
MT-4 cells	Human T-cell line
MTB	*Mycobacterium tuberculosis*
MTB-H$_{37}$Rv	*Mycobacterium tuberculosis* H$_{37}$Rv strain
MW	Microwave
NF-κB	Nuclear factor kappa B
NHL	non-Hodgkin lymphoma
NMP	*N*-Methyl-2-pyrrolidone
NMR	Nuclear magnetic resonance
NNRTIs	Non-nucleoside reverse transcriptase inhibitors
NRK-52E	Normal rat kidney tubular epithelial cells
NSAIDs	Nonsteroidal anti-inflammatory drugs
OLEDs	Organic light-emitting diodes
ORTEP	Oak Ridge Thermal Ellipsoid Plot
Pa	*Pseudomonas aeruginosa*
PhI(OAc)$_2$	Phenyl iododiacetate
pMIC	Planktonic minimum inhibitory concentration
PPA	Polyphosphoric acid
Rf	Retention Factor
RNA	Ribonucleic acid
RT	Reverse transcriptase inhibitors
s	Singlet
Sa	*Staphylococcus aureus*

SAR	Structure-activity relationship
SARS-CoV-2	Severe acute respiratory syndrome coronavirus 2
SC-XRD	Single crystal X-Ray Diffraction
SEM	Scanning electron microscopy
SI	Selectivity index
S_N2	Nucleophilic substitution reaction
S_NAr	Nucleophilic aromatic substitution reaction
SPPS	Solid-phase peptide synthesis
St	*Salmonella typhimurium*
STAT	Signal transducer and activator of transcription
t	Triplet
T3P®	Propylphosphonic anhydride solution
TBZ	1-(2,6-Difluorophenyl)-1*H*,3*H*-thiazolo[3,4a]benzimidazole
TEM	Transmission electron microscopy
Tf$_2$O/Py	Trifluoromethanesulfonic anhydride/pyridine system
TFA	Trifluoroacetic acid
TFBen	Benzene-1,3,5-triyl triformate
THF	Tetrahydrofuran
TLC	Thin Layer Chromatography
TMDS	Tetramethyldisiloxane
TsCl	Tosyl chloride
UV	Ultraviolet
Vero	Monkey kidney epithelial cells
WHO	World Health Organisation
XDR	Extremely drug-resistant
XRD	X-ray diffraction

DECLARATIONS

DECLARATION 1 – PLAGIARISM

I, **Aishwarya Nishan Bantho** declare that

1. The research reported in this thesis is my original research, except where otherwise indicated.

2. This thesis has not been submitted for any degree or examination at any other university.

3. This thesis does not contain other persons' data, pictures, graphs or other information, unless specifically acknowledged as being sourced from other persons.

4. This thesis does not contain other persons' writing, unless specifically acknowledged as being sourced from other researchers. Where other written sources have been quoted, then:

   a. their words have been re-written but the general information attributed to them have been referenced, and

   b. where their exact words have been used, then their writing has been placed in italics and inside quotation marks, and referenced.

5. This thesis does not contain text, graphics or tables copied and pasted from the Internet, unless specifically acknowledged, and the source being detailed in the thesis and in the References section/s.

Signed ………………………………………………………… Date 27th March 2022

Aishwarya Nishan Bantho, BSc (HONS) (UKZN)

ACKNOWLEDGEMENTS

Jai Shri Ram

Table of Contents

List of Figures

List of Tables

Chapter 1   Introduction

Paul Ehrlich (1854-1915) is considered the father of medicinal chemistry. He coined the term "chemotherapy", involving the synthesis of chemical entities to treat bacterial infections (Parascandola, 1981). He theorised that molecules containing particular functional groups could target and destroy pathogenic cells without affecting the host cell (Valent et al., 2016). As a result, chemical drugs were developed to treat specific diseases with low toxicity. Ehrlich referred to these chemicals as 'magic bullets' (Zauberkugeln), which are capable of locating their target without being cytotoxic to the surrounding cells (Witkop, 1999). He was known for the synthesis of the first antibiotic, arsphenamine, used to treat syphilis and commercialised as salvarsan® in 1909 (Valent et al., 2016).

Salvarsan® was administered in low dosages due to side effects caused at higher quantities, resulting in the spirochetes (syphilis microorganism) acquiring resistance to the drug (Kasten, 1996). However, for 20 years, salvarsan® and its chemical derivative neosalvarsan were the only two drug treatments available for bacterial infections. Then the medicinal landscape changed dramatically in 1928 with the discovery of penicillin by Sir Alexander Flemming. Penicillin was recognised as a more effective alternative for treating syphilis and other severe bacterial infections (Bosch and Rosich, 2008). Since then, medicine has grown in leaps and bounds, culminating in modern medicine today, with pharmacies stocking a wide variety of drugs to treat a range of illnesses and diseases. The general steps in drug discovery include hit identification and confirmation, hit to lead, lead optimisation, pre-clinical studies and clinical trials (Li and Kang, 2020b; Shi and Zhang, 2021).

Nuclear magnetic resonance (NMR), mass spectrometry (MS) and X-ray diffraction (XRD) are some of the advances in instrumentation used widely to identify and elucidate structures of

complex molecules during the early stages of drug discovery. These instrumental tools, particularly NMR and XRD, have been useful in the drug discovery process, especially regarding structure-activity relationships and drug target identification for structure-based drug design (Grant, 2009; Li and Kang, 2020b; Shi and Zhang, 2021).

Drug targets are generally DNA, RNA and proteins, including enzymes, receptors, transport and ion channels in disease-causing organisms (Baig et al., 2014). Compounds that act as inhibitors or modulators are synthesised for these purposes once identified. Natural products identified and isolated from plant, animal, marine and fungal sources, as well as the vast library of synthetic compounds available in the literature, serve as sources for drug design. When designing a drug, specific physicochemical properties are monitored to improve the drug-likeness of the molecule (Baig et al., 2014). This is done taking Lipinski's Rule of Five into consideration: a molecule should not contain greater than five hydrogen bond donors (total number of hydroxyl and amine groups); ten hydrogen bond acceptors (oxygen and hydrogen atoms); have a molecular weight more than 500 Daltons; and a partition coefficient cLogP (a measure of lipophilicity) greater than five (Benet et al., 2016). A violation of this rule might result in poor absorption and permeation of the drug molecule.

Small molecules are quite popular in the pharmaceutical industry due to simple chemical modification, quicker distribution and tissue penetration within the human body, and the administration via multiple routes, especially orally (Yang et al., 2020). In addition to their small size and physiochemical properties, the molecules are effective inhibitors of enzymes and various protein-protein systems. This allows for high binding affinities by duplicating fundamental binding interactions to be achieved, and the rigid structure can bring about conformational changes in the protein target site, enhancing binding energies (Fry, 2006).

Some small molecules are allosteric modifiers, changing the protein conformation, which in turn changes the active site of the enzyme (Fry, 2006; Li and Kang, 2020a). As a result, the enzyme cannot bind to its substrate rendering it inactive to perform its biological activities within the cell. Small molecule drugs are also designed to target cell surface receptors (G protein-coupled receptors), responsible for mediating intracellular and extracellular responses, affecting the microorganism's homeostasis (Homan and Tesmer, 2014; Zhao et al., 2016; Ayoub, 2018).

Heterocyclic motifs are considered one of the most significant backbones in small molecule drug discovery, and normally include heteroatoms such as oxygen, nitrogen, and sulfur. Some heterocyclic moieties can be found in naturally occurring bioactive substances such as amino acids, vitamins, nucleic acids, hormones and antibiotics (Gomtsyan, 2012; Heravi and Zadsirjan, 2020). Almost 75% of small molecule drugs possess a nitrogen heterocycle (Kerru et al., 2020). The prevalence and efficacy of *N*-heterocycles are accredited to the improved potency, specificity and stability due to nitrogen's ability to readily bond with DNA and target proteins through hydrogen bonding interactions (Heravi and Zadsirjan, 2020).

Lazar and her team introduced a novel drug design strategy known as "drug evolution", based on reproductive recombination of parent genomes found in biological evolution, to generate chemical libraries to find new drugs or drug candidates (Lazar et al., 2004). This concept is more commonly known as molecular hybridisation (MH), where two or more compounds containing biologically active pharmacophores are combined to create a hybrid molecule (Viegas Junior et al., 2007). Several hybrid compounds have been synthesised, and some have been identified as antimicrobial, antitubercular, and anti-inflammatory compounds, and candidates for neurodegenerative diseases amongst many other bioactivities (Rane and

Telvekar, 2010; Bosquesi et al., 2011; Gündüz et al., 2019; Ramprasad et al., 2019; Gontijo et al., 2020). The hybrids have demonstrated that additional functional groups and moieties can be effective on mulpitle target enzymes.

The synthesis of lead drugs with comparable activity to existing ones but with fewer side effects will lead to a plethora of drugs, positively impacting human health and well-being.

1.1 Antibiotics – antimicrobial resistance and modes of action

There is currently a global shortage of antibiotics due to the emergence of drug-resistant pathogens and the non-existence of new, innovative antimicrobials in the clinical pipeline. Drug resistance is acquired through new mechanisms, such as limited drug uptake, enhanced efflux pumps, modification of antibiotic inactivating enzymes, and drug inactivation (through drug degradation or chemical modification) (Reygaert, 2018). Gram-negative bacteria are considered a significant threat as a consequence of built resistance to last-resort antibiotics (carbapenems, fluoroquinolones and colistin). According to the World Health Organisation (WHO, 2021), the rate of resistance of urinary tract infections caused by *Klebsiella pneumoniae* and *Escherichia coli* to the antibiotic ciprofloxacin has escalated to 79.4% and 92.9%, respectively. The last line of defence against these resistant Enterobacteriaceae is colistin; however, drug resistance has been isolated in immunocompromised cancer patients (Zafer et al., 2019).

Almost half the pre-clinical antibiotic projects involve small molecules. A large proportion of these projects aim to create targets for Gram-negative bacteria (Theuretzbacher et al., 2020). Generally, a good antibiotic is known to eradicate bacterial infections rapidly with relatively

low cytotoxicity and primarily target enzymes responsible for a specific function in the biochemical pathway of the bacterial cell. These antibacterial agents can be categorised according to their modes of action, such as inhibition in the synthesis of cell walls, proteins, nucleic acids, depolarization of cell membranes and inhibition of metabolic pathways.

Most classes of small molecule antibiotics include *β*-lactams, fluoroquinolones, azoles, rifampicins and sulfonamides (Figure 1.1). These drugs have different mechanisms of antibacterial activity; *β*-lactams affect the synthesis of peptidoglycan (responsible for cell wall formation), whereas fluoroquinolones inhibit supercoiling and replication of bacterial DNA (interaction with DNA gyrase and topoisomerase IV) (Hughes and Karlén, 2014). Nitroimidazole is believed to be reduced within the bacterium to the amine. It interacts with intracellular targets of the microorganism, disrupting the homeostasis of the cell, ultimately leading to cell death (Weir and Le, 2021). Rifampicins suppress DNA transcription into RNA by interacting with DNA-dependent RNA polymerase, and sulfonamides inhibit the metabolic pathway of dihydropteroate synthetase, dihydropteroate being an important intermediate in folate synthesis, vital for bacterial cell division and homeostasis (Hughes and Karlén, 2014; Hutchings et al., 2019).
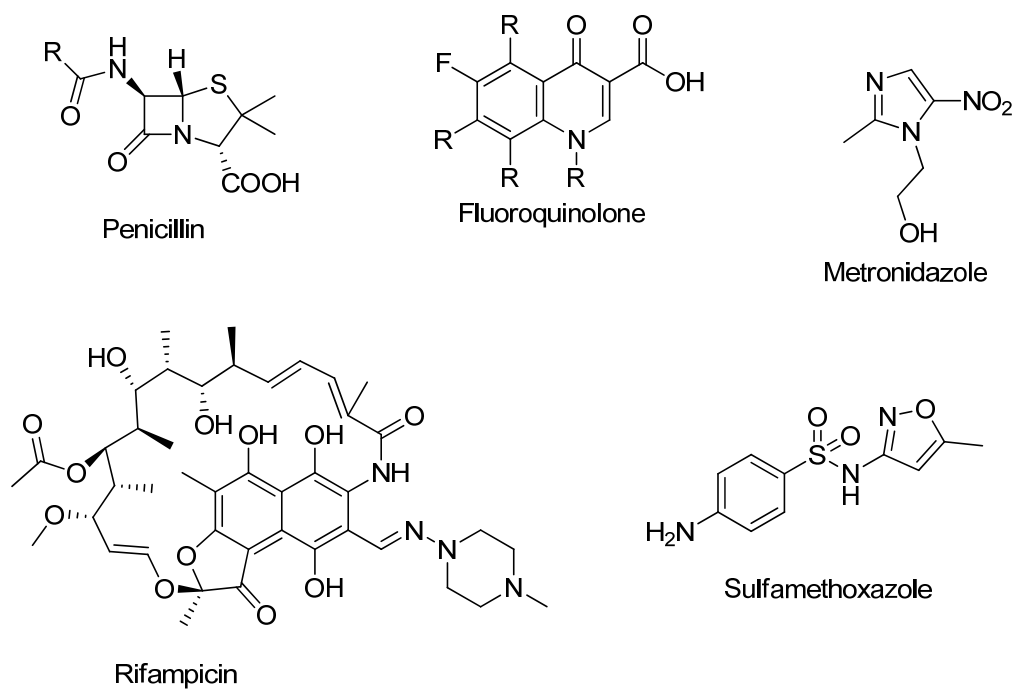
Figure 1.1 Classes of small molecule antibiotics

Although there has been much success in treating bacterial infections over the years with the current classes of antibiotics, there has been a gradual regression in antibiotic discovery and development, leading to an alarming increase in antimicrobial resistance (AMR) worldwide. Overuse and misuse of antibiotics, self-medicating and unnecessary use of antibiotics has resulted in bacterial genetic makeup mutation, resulting in resistance to current drug regimens and promoting bacteria to "superbug" status (Adegoke et al., 2016). Although a natural evolutionary process, it is accelerated by improper use of antibiotic medication, leading to severe infection rates. AMR is one of the key reasons it is difficult to treat infectious diseases such as acute respiratory and meningeal, diarrhoeal and sexually transmitted infections as there are limited options for treatment (Crowther-Gibson et al., 2011).

Most antibiotics discovered during the golden era are still being used today. However, AMR has reduced their efficacy. Various drug strategies used to treat bacteria resistant to commonly

used antibiotics have been employed. One of these is combination therapy, which involves using two or more therapeutic agents to treat bacterial infections. However, drug-drug interactions need to be considered, as adverse drug reactions, hospitalisation and death may occur (Ansari, 2010).

Combination therapy also improves drug efficacy and reduces the duration of treatment compared to monotherapy. There are three distinct modes of combination therapy: the inhibition of targets via various pathways, inhibiting different targets using the same pathway and inhibiting the same target with the same pathway (Fischbach, 2011). Antibiotics are recognised to have contraindications when taken with other drugs. An example is decreasing the effectiveness of oral contraception. A wide range of antibiotics such as ciprofloxacin, clarithromycin, erythromycin, metronidazole or trimethoprim-sulfamethoxazole is known to increase the effect of the anticoagulant Warfarin, which requires the use of another antibiotic (Ansari, 2010).

Molecular hybridisation is a more advantageous design as it supersedes combinational therapy by reducing the risk of drug-drug interactions and improving pharmacodynamic and pharmacokinetic interactions (Sunil et al., 2019). Hence, it was the primary concept used to develop bioactive molecules.

1.2   Benzimidazoles

1.2.1   History and structural features of benzimidazoles

Benzimidazoles are classified as planar aromatic, nitrogen-containing heterocycles. The benzimidazole skeleton is composed of a six-membered benzene ring fused to a five-membered imidazole ring. When combined, these moieties offer their original properties and enhance

physicochemical properties. Figure 1.2 shows that the imidazole pharmacophore introduces a pyrrole (imino group) and pyridine-like (tertiary) nitrogen atoms at positions 1 and 3, making the compound amphoteric. The benzene ring offers additional support to the molecule through its conjugated system, which improves the compound's stability and additional points for functionalisation.
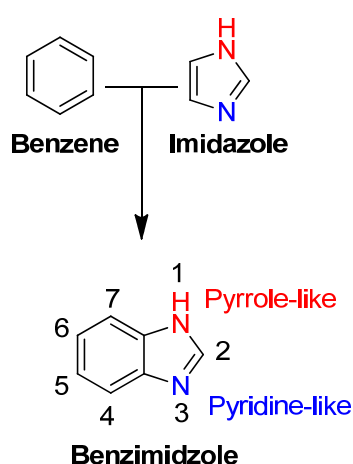
Figure 1.2 Structure of benzimidazole exhibiting pyrrole and pyridine-like properties

Hobrecker synthesised the first benzimidazole, 2,5 or 2,6-dimethylbenzimidazole, by reducing 2-nitro-4-methylacetanilide, using granulated tin and hydrochloric acid. The cyclised product was formed through an intramolecular condensation reaction (Scheme 1.1) (Hobrecker, 1872; Wright, 1951). Later, Fischer and Romer reacted the same dimethylbenzimidazole with methyl iodide to form tautomers of trimethylbenzimidazoles of similar yields (Fischer, 1905). When the N1 hydrogen is free (unsubstituted) and unhindered, it undergoes prototropic tautomerisation between the annular nitrogen atoms. The proton is found on either one of the nitrogen atoms at a given time; hence, the tautomeric forms are in equilibrium (Figure 1.3). This phenomenon is seen more prominently for unsymmetrical benzimidazoles containing substituents on the benzene ring (R_1).
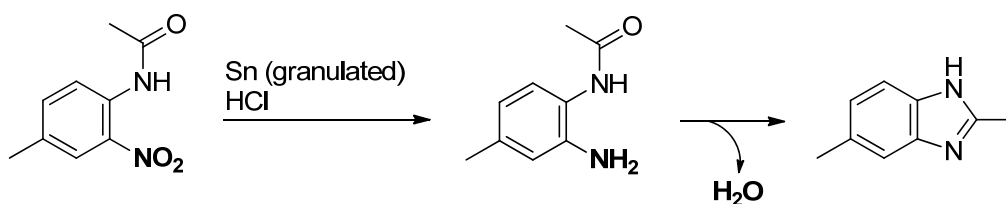
Scheme 1.1 Synthesis of 2,5 or 2,6-dimethylbenzimidazole via intramolecular cyclisation
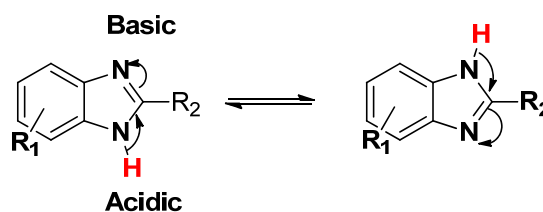
Figure 1.3 Tautomeric forms of benzimidazole in equilibrium

The tautomeric rate can be influenced by steric and electronic effects of substituents (R_2) at position 2. Unsubstituted (H) and electron-withdrawing groups tend to increase the rate of tautomerisation, whereas sterically hindered and electron-donating groups slow it down (Nieto et al., 2014). The rate of tautomerisation and type of deuterated solvent greatly impacts the NMR spectra of benzimidazoles. The faster the movement of the proton, the more the chemical shifts become equivalent and overlap. Hence, the assignment of some resonances become problematic. This also results in ^{13}C NMR resonances, even the protonated resonances, being either very weak or absent from the spectra, a problem overcome by adding a substituent onto one of the nitrogen atoms of the benzimidazole (Cheddie et al., 2020).

Karl Folkers and his group at Merck managed to isolate naturally occurring vitamin B_{12} (cobalamin) from liver extracts to complete the series of B vitamin compounds comprising of: B1 (thiamine), B2 (riboflavin), B3 (niacin), B5 (pantothenic acid), B6 (pyridoxine) and B11

(folic acid) (Gu and Li, 2016). Vitamin B_{12} was of particular interest as it was used to treat pernicious anaemia and shown to support cellular function for DNA synthesis and stability, and protein and lipid production (Rickes et al., 1948; Todorova et al., 2017).

In determining the structure of vitamin $B_{12,}$ a degradation product of 5,6-dimethylbenzimidazole was produced by acid hydrolysis and validated by condensing 4,5-diamino-1,2-methylbenzene with formic acid (Brink and Folkers, 1950). After the structure of vitamin B_{12} was elucidated, it was found that the benzimidazole scaffold was an inherent part of the α-axial ligand *N*-ribosyl-dimethylbenzimidazole, coordinated to cobalt and responsible for therapeutic properties (Brink and Folkers, 1950; Bonnett, 1963; Scott and Molloy, 2012). As a result, much attention was given to using benzimidazoles as medicinal agents.

Due to benzimidazole being a structural inhibitor and present in vitamin B_{12} (Figure 1.4), it behaves competitively with the vitamin (Woolley, 1944). Hence, benzimidazoles can be active against microorganisms that synthesise the vitamin. Despite this, bacteria synthesising vitamin B_{12} are generally non-pathogenic (*Propionibacterium* genus) and are used to manufacture the vitamin for commercial use (Piwowarek et al., 2018).

Benzimidazoles are also known as structural isosteres of naturally occurring compounds that are common building blocks for biopolymers and are therefore regards asactive substances due to their interaction with biomolecules (Narasimhan et al., 2012). This group includes purines found in naturally occurring nucleotides such as guanine and adenine (two of the four chemical bases in DNA), as well as uric acid and caffeine (Kamanna, 2019). Purine plays an essential role in the biosynthesis of DNA, RNA, and the proteins in the cell walls of bacteria. Hence, it was postulated that the antibacterial activity of benzimidazoles is due to being bio-isosteres to

purine (Song and Ma, 2016; Bistrović et al., 2018). Therefore, the benzimidazole moiety can become a competitive inhibitor and substitute purine, preventing growth, or eradicating the bacteria.
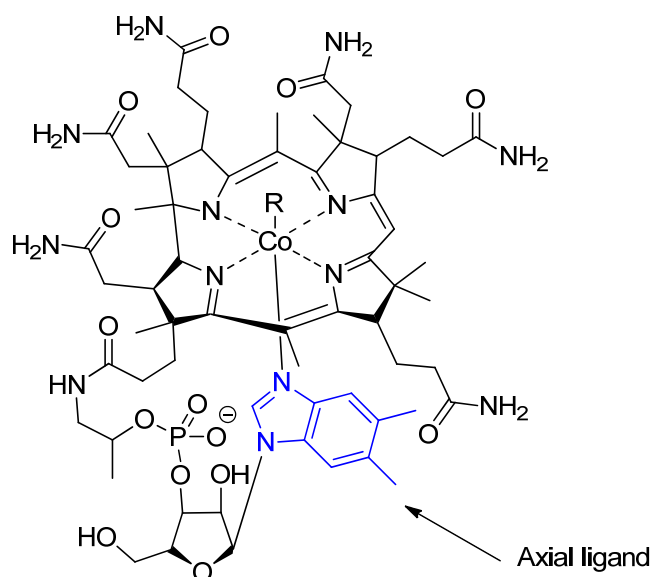
Figure 1.4 Structure of vitamin B_{12}

The bicyclic scaffold has been explored extensively in drug development due to its electron-rich and unique structural features that allow the compound to bind to therapeutic sites, enabling diverse pharmacological activities (Gaba and Mohan, 2016). Thus, the benzimidazole pharmacophore has been incorporated into several drugs such as albendazole, mebendazole and flubendazole (anthelmintics), telmisartan and candesartan (anti-hypertensives), omeprazole, rabeprazole and lansoprazole (antiulcer activity), tecastemizole (anti-parasitic) (Xie et al., 2017), thiabendazole and benomyl (antifungals), bendamustine hydrochloride (anticancer) and astemizole (antihistaminic and antiparasitic) (Bansal and Silakari, 2012; Xie et al., 2017) (Figure 1.5).
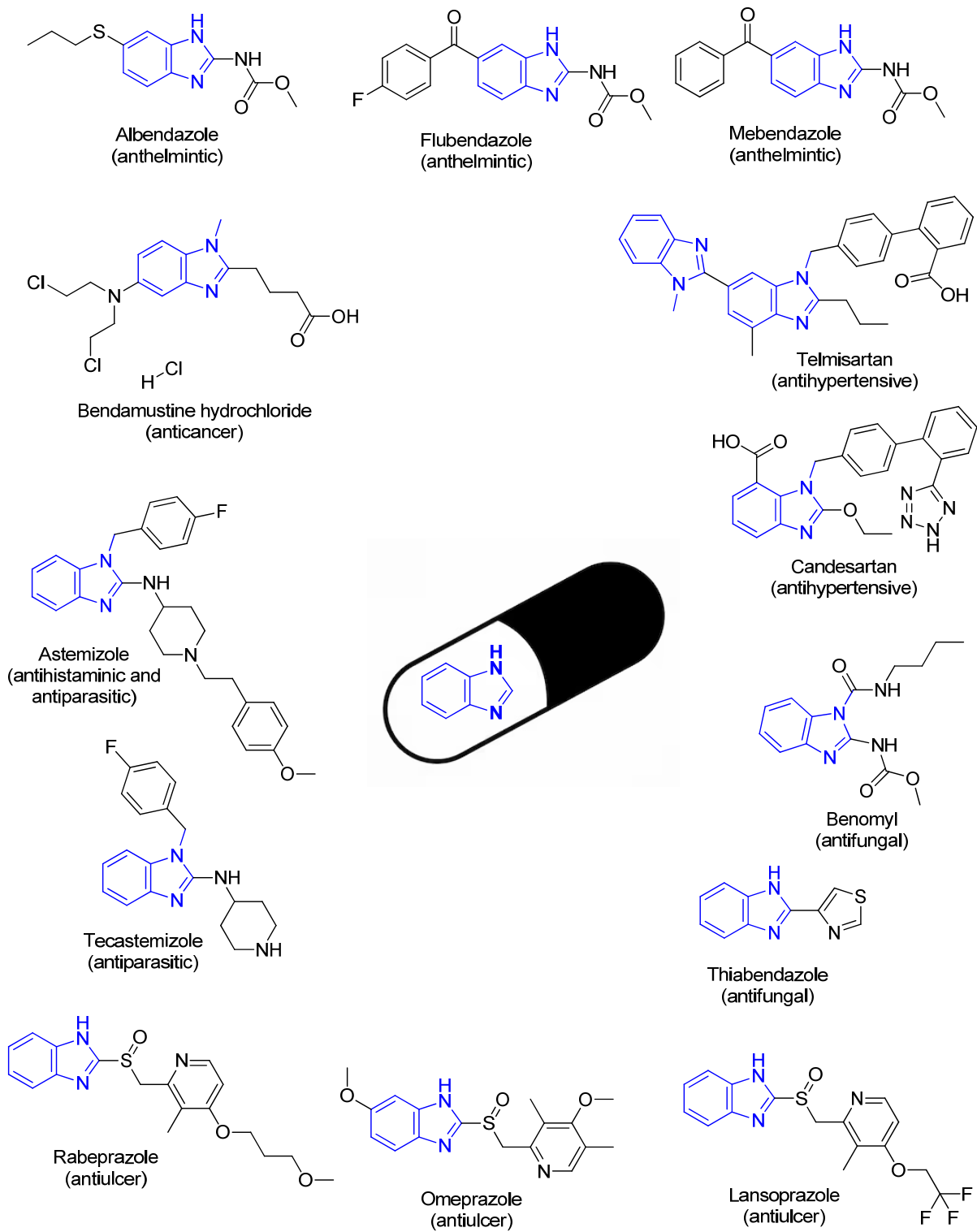
Figure 1.5 Drugs containing the benzimidazole pharmacophore

1.2.2   Synthesis of benzimidazoles

Generally, benzimidazoles are synthesised by condensing benzene derivatives with nitrogen atoms *ortho* to each other (*o*-phenylenediamine) and compounds containing electron-deficient carbons (acids, aldehydes, ketones, esters, acid anhydrides, amides, acid chlorides and nitriles) under various conditions. Mechanistically, charge density on the carbonyl carbon or cyanocarbon for nitriles significantly impact the reaction pathway due to different transition-state intermediates created before forming the cyclised product. The precursors involved can either be unsubstituted or include specific functional groups for key steps in the reaction scheme or construct the benzimidazole skeleton to be mono-, di- or tri-substituted, providing a particular pharmacological activity.

Although Hobrecker was the first to synthesise benzimidazoles through intramolecular cyclisation, Ladenburg and Phillips worked extensively to prepare the moiety via the more popular condensation reaction. Hence, the synthesis of benzimidazoles is commonly known as the Ladenburg or Phillips method, Phillips modification or Ladenburg-Phillips reaction (Ladenburg, 1875; Phillips, 1928; Wang, 2010).

1.2.2.1   Syntheses involving the *ortho*-phenylenediamine precursor

Reaction with acids

The synthesis of benzimidazoles using carboxylic acids is the most popular method which generally reacts with most phenylenediamines in good yields. Ladenburg was the first to condense carbonyl compounds with diamines by reacting 4-methyl-*o*-phenylenediamine with acetic acid through simple reflux (Ladenburg, 1875). The reaction goes through the pathway to form an acetamide intermediate as created in Hobrecker's reaction to form the dimethylated benzimidazole (Scheme 1.2). Phillip modified this method via acid catalysis by adding dilute

mineral acid (4N hydrochloric acid), which improved yield and allowed for milder temperature conditions (Phillips, 1928).
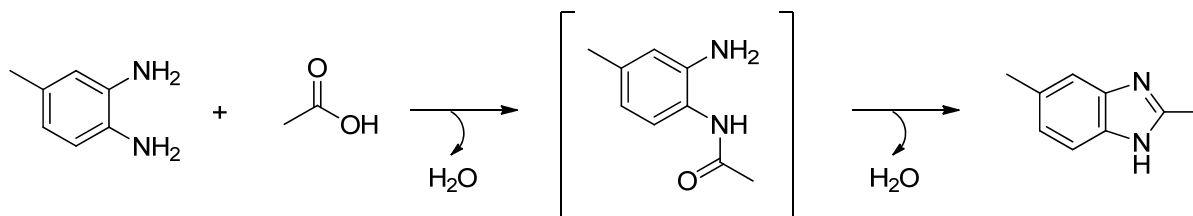
Scheme 1.2 Synthesis of dimethylbenzimidazole via cyclisation of acetamide intermediate

The hydrochloric acid acts as a catalyst to form a carbonium ion which can be easily attacked by the lone pair of electrons on one of the amine groups (Scheme 1.3). This method is so efficient that it is still used to produce 2-substituted benzimidazoles (Gozelle et al., 2019). Other methods include using strong or weak acids such as sulfuric, *p*-toluenesulfonic polyphosphoric acid (PPA), acetic acid, or boric acid to catalyse the reaction.

Furthermore, *N*-substituted *o*-phenylenediamines are also condensed with a variety of carboxylic acids and their derivatives to form 1,2-substituted benzimidazoles. Recently, *N*-methyl-*o*-phenylenediamine and various aromatic acids were reacted with PPA. Kashid et al. (2019) used PPA as both catalyst and solvent, which was thought to be more economical and reactive. When protic and aprotic solvents were used with 1% PPA, yields of 20-72% was obtained. However, an excellent yield of 95% was acquired when only PPA was used. This was attributed to better solubility and dehydration compared to organic solvents.
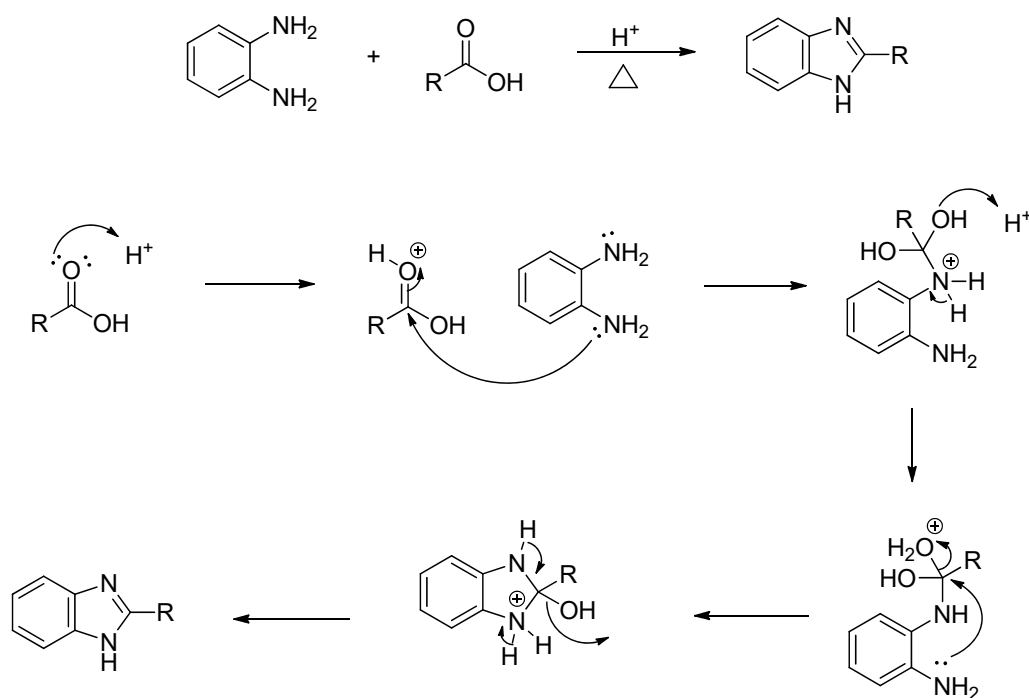
Scheme 1.3 General mechanism for the synthesis of benzimidazoles through acid catalysis

Reaction with aldehydes and ketones

Early attempts at condensation with an aldehyde (salicylaldehyde) and diamine at 110-120 °C produced "aldehydines" (1,2-disubstituted benzimidazoles) in addition to 2-substituted benzimidazoles (Ladenburg and Rügheimer, 1878). Due to the oxidative nature of the reaction, copper salts (copper acetate) in water or alcohol were introduced to the diamine and aldehyde, resulting in good yields of 2-substituted benzimidazole, commonly known as the Weidenhagen reaction (Weidenhagen, 1936). This method is also used with ketones. However, it is done to a lesser extent with unsymmetrical ketones due to mixtures forming by eliminating the alkyl group or affecting the yield. Therefore, it would be suitable to use *N*-substituted benzimidazoles to control substitution of the diamine and elimination of the alkyl groups.

Aldehydes and ketones are more receptive to attack by the amino group that contain more electrophilic centres compared to the other carbonyl groups. However, these carbonyls do not

possess good leaving groups, and therefore harsher conditions are required for cyclisation to the benzimidazole. Aldehydes are now being condensed in the presence of a mineral acid or metal catalyst using oxidizing agents such as oxygen (O_2) (Reddy et al., 2016), sodium metabisulfite ($Na_2S_2O_5$) (Garcia-Aranda et al., 2020), hydrogen peroxide (H_2O_2) (Rahimi and Soleimani, 2020), iodobenzene diacetate (IBD) (Du and Luo, 2010), potassium persulfate ($K_2S_2O_8$) (Kumar et al., 2010) and 2,3-dichloro-5,6-dicyano-1,4-benzoquinone (DDQ) (Naeimi and Babaei, 2017). Generally, the synthesis with ketones involves C-C bond cleavage between the carbonyl and alkyl/aryl groups for the C-N bond formation with *ortho*-phenylenediamine with the use of iodine as a catalyst or selenium dioxide as an oxidising reagent (Ravi et al., 2017; Khan et al., 2019).

Intriguingly, Smitha and Sreekumar (2016) synthesised 2-substituted benzimidazoles and 2,2-substituted benzimidazoles by coordinating aldehydes and ketones, respectively, to GLR-G2 copper complex to generate a more electrophilic carbonyl carbon intermediate. The formation of 2-substituted benzimidazole goes through route 1 via oxidative cyclodehydrogenation of the *in-situ* Schiff base followed by the aromatization of the dihydrobenzimidazole via aerial oxidation. The diamine follows route 2 when cyclised with a ketone to directly form the dihydrobenzimidazole intermediate, which creates the 2,2-disubstituted benzimidazole through oxidation (Scheme 1.4).
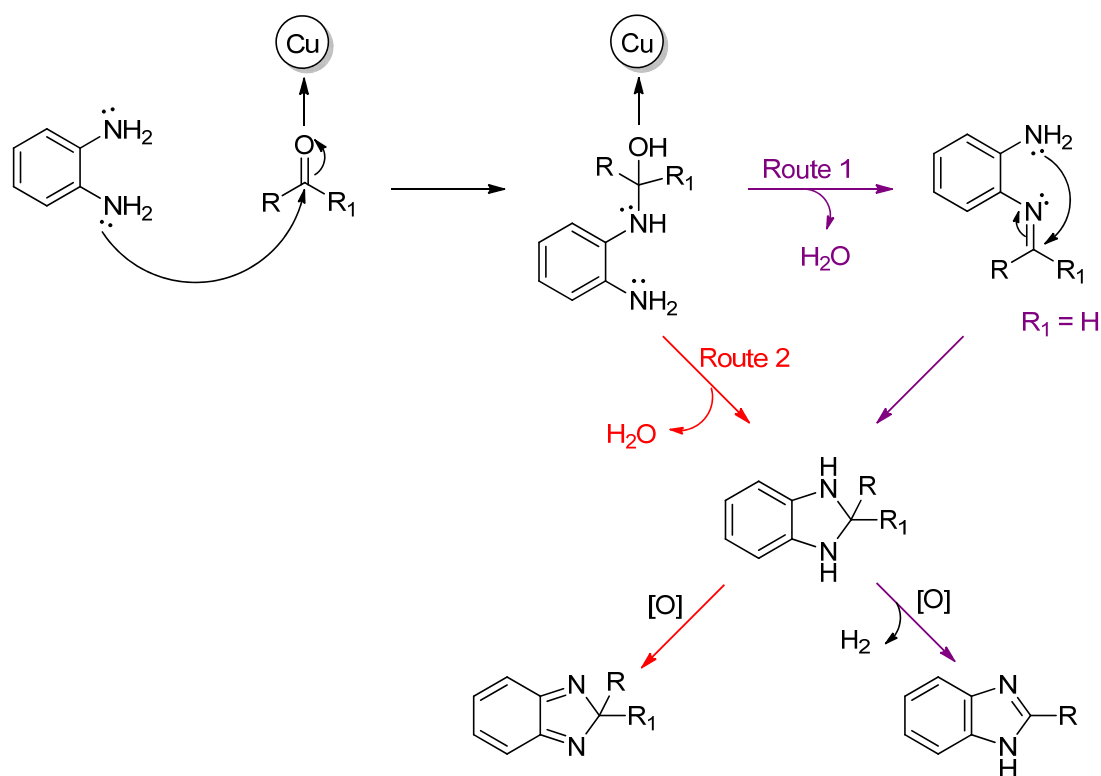
Scheme 1.4 Proposed mechanism for the synthesis of 2- and 2,2-substituted benzimidazoles using to GLR-G2 copper complex

Reaction with acid anhydrides

Benzimidazoles synthesised from acid anhydrides are not as extensive as acids, even though the reaction goes through the same acetamide intermediate after substitution. The condensation of *o*-phenylenediamine with acetic anhydride via acid catalysis with hydrochloric acid and *p*-toluenesulfonic acid resulted in average yields of 69% and 41% (Hashtroudi et al., 2000; Elshihawy and Hammad, 2013). However, the addition of metal catalysts (alumina and potassium fluoride) and organic catalysts (1,3,2-benzodithiazole and 1,1,3,3-tetraoxide) significantly enhanced the yield to 89 and 84%, respectively (Barbero et al., 2012; Khalili and Sardarian, 2012).

Interestingly the synthesis of 2-benzimidazoles from butyric anhydride revealed that the reaction goes through the formation of bisacetamide intermediates, with ring closure finally occurring through the Phillips condensation reaction shown in Scheme 1.5 (Schoepf et al., 2020a; Schoepf et al., 2020b). A greener, one-step method was investigated by condensing *N*-phenyl-*o*-phenylenediamine with benzoic anhydride in water without the addition of a catalyst (Nagao et al., 2016). The reaction was performed through a HPHT (high pressure high temperature) water microflow chemical procedure to produce good yields, but the addition of *N*-methyl-2-pyrrolidone (NMP) to water (1:9) resulted in excellent yields.
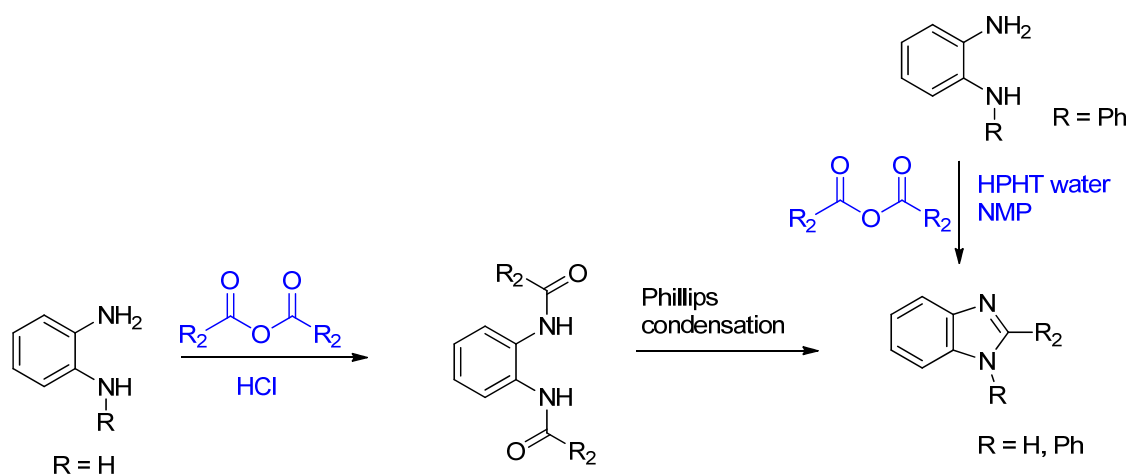
Scheme 1.5 Condensation reactions with acid anhydrides forming benzimidazoles with *o*-phenylenediamines

Reaction with amides and nitriles

Synthesis with amides resulted in exceptional yields at optimum conditions. Kattimani et al. (2015) created 2-benzimidazoles with unsubstituted and various substituted *o*-phenylenediamine with DMF and a series of amides. The reaction conditions involved conventional heating or microwave irradiation in the presence of hydrochloric acid. Complete conversion was not obtained between *o*-phenylenediamine and DMF at room temperature,

however, the reaction occurred within 1 hour at 100 °C. The same was true for substituted *o*-phenylenediamine. The reaction for substituted *o*-phenylenediamine was carried out under MW irradiation (150 W) in 2 minutes with exceptional yields of 94-96%. Moderate to good yields were obtained when *o*-phenylenediamine was condensed with amides via conventional heating (40-78%), whereas excellent yields (80-95%) were obtained with MW irradiation at 150 °C within 40-60 minutes. Hence, MW irradiation is a suitable method to condense *o*-phenylenediamines and amides regardless of substitution.

The reaction is thought to go through the formation of the benzimidazoline intermediate, produced by hydrochloric acid protonating DMF and driving the diamine to attack the electrophilically enhanced carbonyl group. This is followed by the dimethylamine group leaving. The second amino group then attacks the carbonium ion, and finally, the simple benzimidazole is formed through dehydration (Scheme 1.6). However, it has been reported that the condensation of *o*-phenylenediamine goes through the formation of the amidine intermediate (Scheme 1.7) (Lellmann and Hailer, 1893; v. Niementowski, 1897; Marinescu, 2019).
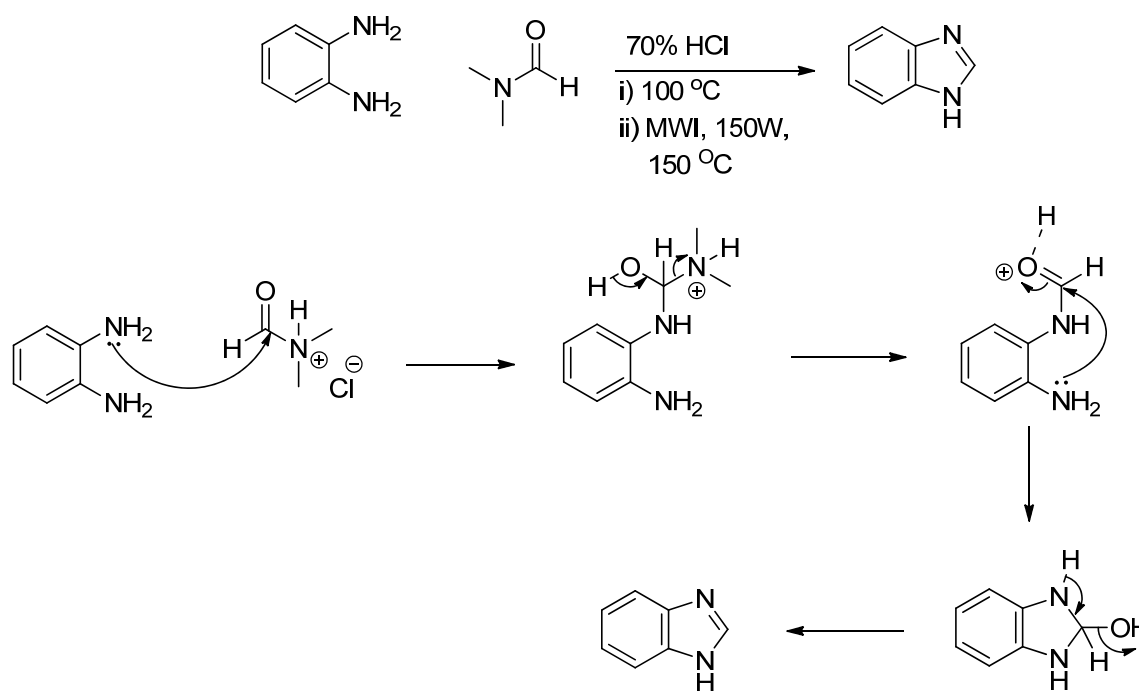
Scheme 1.6 Synthesis of benzimidazoles from DMF hydrochloride
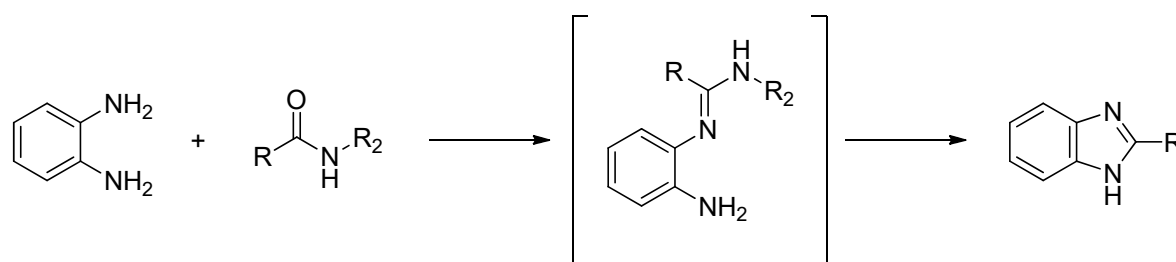
Scheme 1.7 Condensation of *o*-phenylenediamine with amides forming benzimidazoles through an amidine intermediate

Nitriles are known as ring-closing agents when condensed with *o*-phenylenediamine to form benzimidazoles. In preliminary experiments, Hölljes and Wagner (1944) reacted *o*-phenylenediamine with benzonitrile at 200 °C in a sealed tube for 6 or 24 hours and reported no product formation. However, 2-phenylbenzimidazole was produced with *o*-phenylenediamine dihydrochloride, indicating the need for acid to be used to catalyse the reaction. Hence, the nitrile reacted with hydrochloric acid to form the imidoyl chloride,

susceptible to nucleophilic attack by the diamine to form the highly reactive amidine intermediate. The reaction then undergoes intramolecular cyclisation to form the benzimidazole (Scheme 1.8).
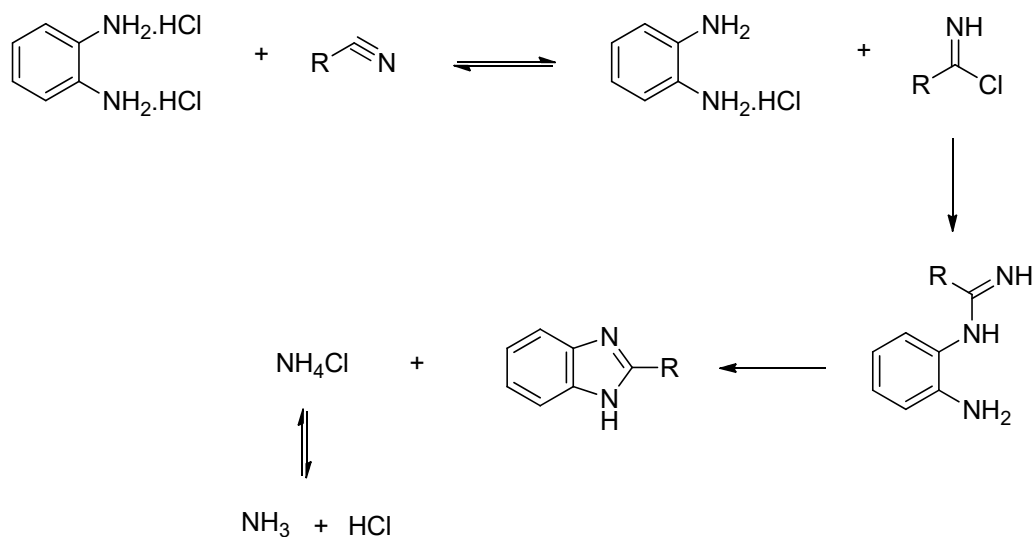
Scheme 1.8 Synthetic route to the formation of 2-substituted benzimidazoles using nitriles

There are two other plausible synthetic routes for the synthesis of 2-substituted benzimidazoles using nitriles. One is the conversion of nitrile to an amide intermediate through acid hydrolysis that forms the product through the amidine intermediate. The second could be the conversion of the nitrile to the carboxylic acid, which would then undergo the Phillips condensation reaction to form the 2-substituted benzimidazole (Scheme 1.9).
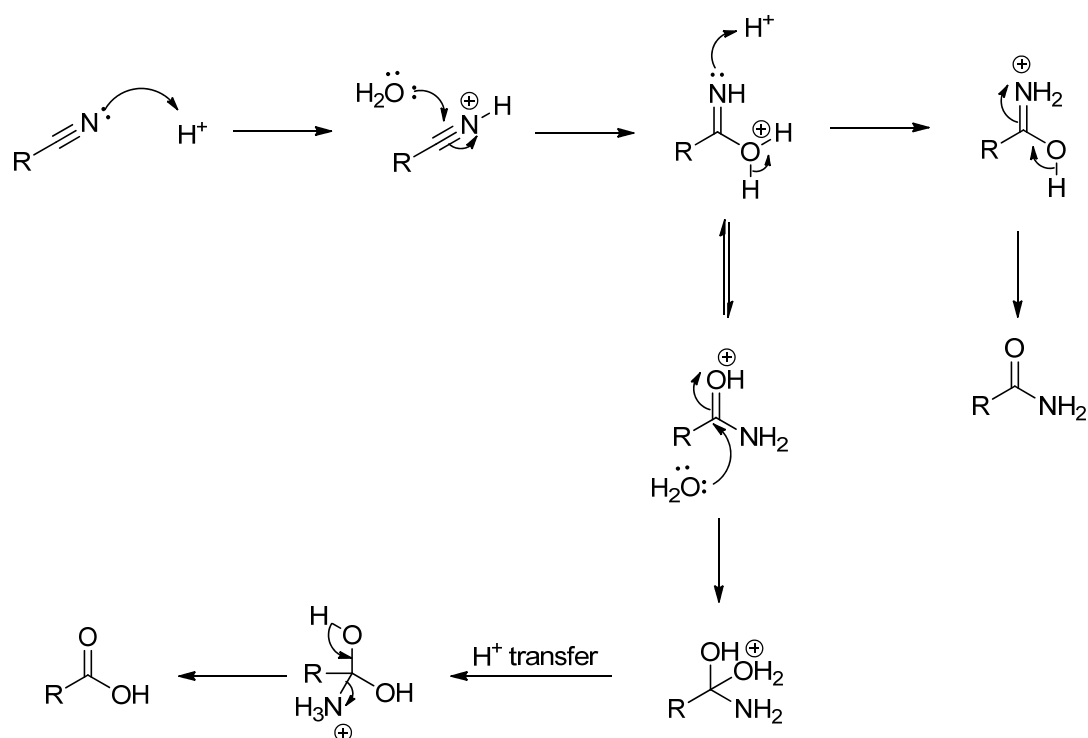
Scheme 1.9 Acid hydrolysis of nitriles to amides and carboxylic acids

Howe (1969) presented a novel reaction that formed 1-aminomethylenemalonitrile benzimidazoles using ethoxymethylenemalononitrile (EMMN) under mild conditions. The synthesis of the final product followed two synthetic routes. Firstly 1*H*-benzimidazole was treated with EMMN and malononitrile in ethanol to form the final product via the 1-*H* substitution. The second synthetic route involved reacting *o*-phenylenediamine with 2 moles of EMMN in ethanol which formed the dimalononitrile intermediate that underwent intramolecular ring cyclisation in *N, N*-dimethylacetamide to produce the benzimidazole (Scheme 1.10).
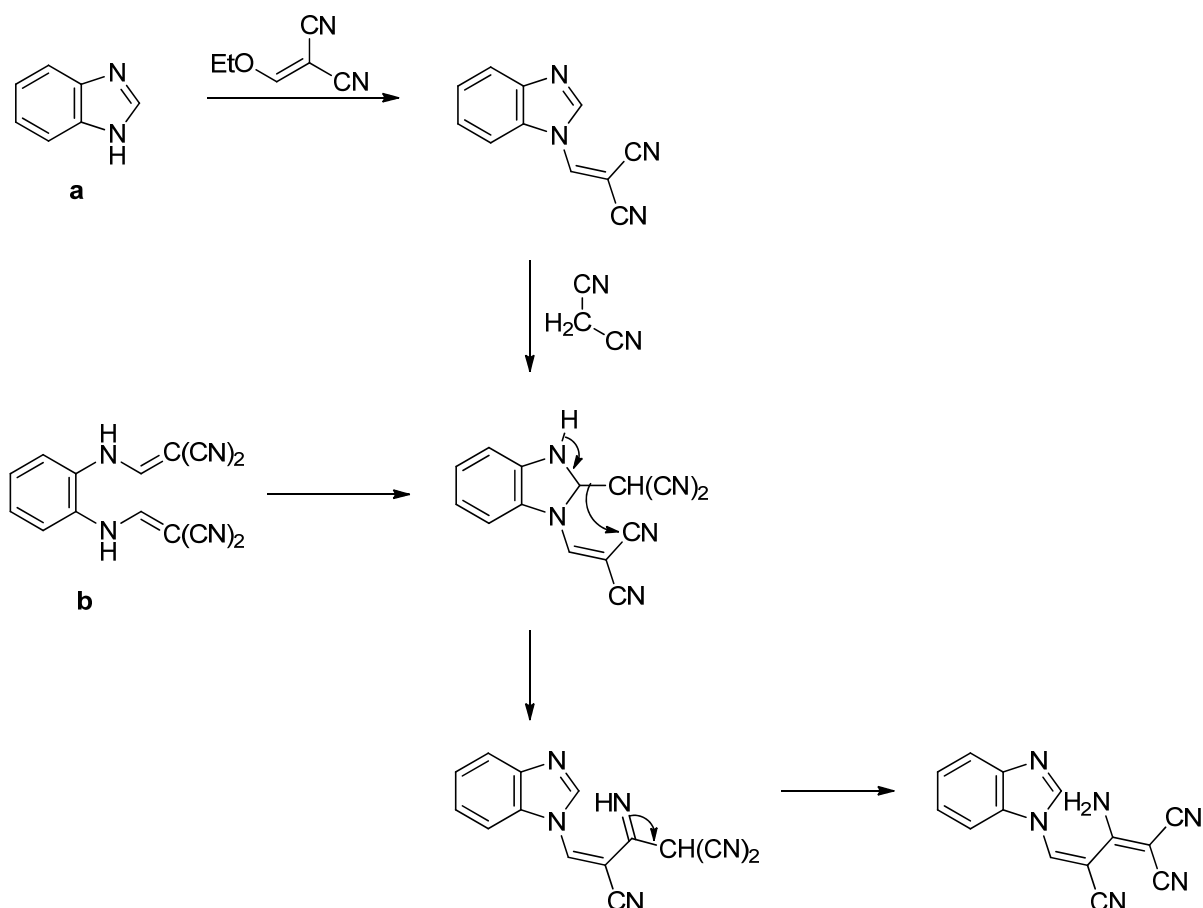
Scheme 1.10 Synthesis of 1-aminomethylenemalonitrile benzimidazoles using 1*H*-benzimidazole (**a**) and *o*-phenylenediamine-1,2-dimalononitrile (**b**)

Most synthetic reactions require a primary amine to attach additional scaffolds, functional groups, or to form salts. The synthesis of 2-aminobenzimidazole was performed by reacting *o*-phenylenediamine with cyanogen bromide in excellent yields (Sethi et al., 2018). Previously, sulphonate salts of 2-amino-5-chlorobenzimidazole were prepared by reacting *p*-chloro-*o*-phenylenediamine with cyanogen bromide followed by the treatment with substituted arylsulfonic acids to form the salts (Leonard et al., 1947) (Scheme 1.11).
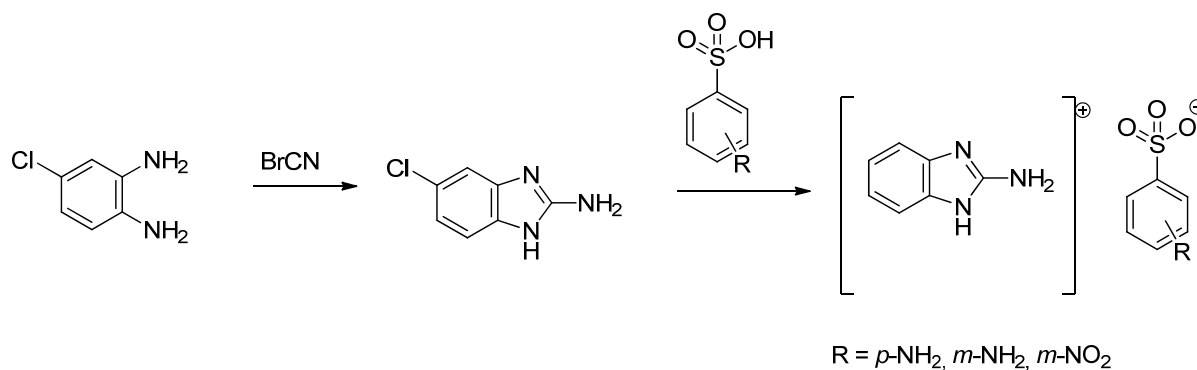
Scheme 1.11 Synthesis of 2-amino-5-chlorobenzimidazole sulfonate salts

Reaction with esters

The condensation of *o*-phenylenediamine with carboxylic activated esters are very common due to their commercial availability. In addition, esters require simple reaction conditions, even with complex precursors, owing to the possession of excellent leaving groups. Lactones (cyclic esters of carboxylic acids) were successfully condensed with *o*-phenylenediamine in water to form 2-substituted benzimidazoles. For example, D-gluco-D-gulo-heptonic lactone underwent a ring-opening reaction when condensed with the diamine to form 2-[D-gluco-D-gulo-hepto-hexahydroxyhexyl]-benzimidazole (Scheme 1.12) (Haskins and Hudson, 1939).
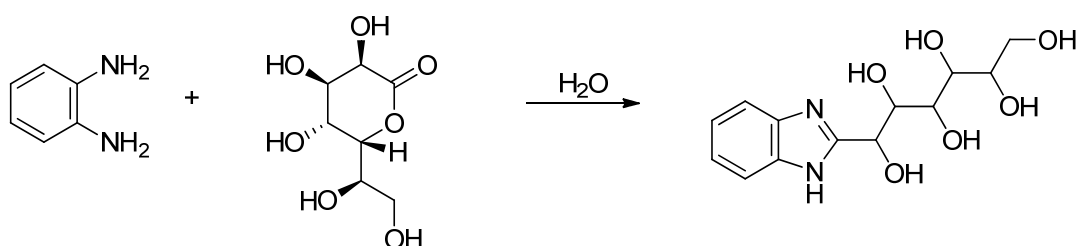
Scheme 1.12 Synthesis of 2-[D-gluco-D-gulo-hepto-hexahydroxyhexyl]-benzimidazole
through the ring-opening reaction of D-gluco-D-gulo-heptonic lactone

Unexpectedly the formation of 2-phenylbenzimidazole (40%), with a low yield of the anticipated amide product, was reported during the condensation of *o*-phenylenediamine with

methyl benzoate in the presence of 0.8 mol% DABAL-Me$_3$ in toluene (Dubois et al., 2013). The Lewis acid DABAL-Me$_3$, a safer counterpart to the pyrolytic trimethylaluminum, is known for synthesising amides. However, due to the DABAL-Me$_3$ dehydrating nature, the 2-aminophenylamide intermediate cyclised to form the benzimidazole. Pinder et al. (2014) drastically improved the yield to 94% by increasing the mole ratio of DABAL-Me$_3$ to 2%. This optimised condition was also successfully applied to functionalised *o*-phenylenediamine derivatives with alkyl, aryl and heteroaryl esters. Hence this reaction is suitable for forming a wide range of benzimidazoles, given that non-participating functional groups are not esters.

Ionic liquids have gained popularity due to their versatile applications, such as being used as catalysts and media in reaction systems. Heteropolyanion-based ionic liquids (HPAILs) possess high melting points, thermal and chemical stability that provides simplicity, low toxicity, easy separation, and can be recycled, similar to solid acid catalysts, leading to the development of greener and efficient media (Yadavalli and Vaidya, 2020). Hence, a solvent-free procedure was developed using microwave-assisted HPAILs catalysis for direct amidation of esters (Fu et al., 2015). The *N*-formylation of *o*-phenylenediamine was performed with formic ester and optimised condition of 2 mol % 1-(3-sulfopropyl)pyridium phosphotungstate ([PyPS]$_3$PW$_{12}$O$_{40}$) to form 1*H*-benzo[*d*]imidazole in an excellent yield (90%).

Reaction with acid chlorides
Acid chlorides are the most reactive species from the acid derivatives. Hence, reaction conditions need to be controlled when reacting acyl chlorides with *o*-phenylenediamine, since the diamine can be mono- or diacylated to form *N*-acyl-1,2-phenylenediamine and *N*, *N''*-diacyl-1,2-phenylenediamine respectively. Subsequently, these intermediates formed 2-substituted benzimidazoles or 2,4-disubstituted benzodiazepines upon cyclisation. Tandon and

Kumar (2004) synthesised *N*-acyl-1,2-phenylenediamine by reacting the diamine with one equivalent of acid chloride at 0 °C in dry dioxane and *N, N''*-diacyl-1,2-phenylenediamine using two equivalents of acid chloride. The intermediates were cyclised *in situ* using a Lewis acid $BF_3.EtO_2$ (boron trifluoride etherate) in excellent yields (Scheme 1.13).
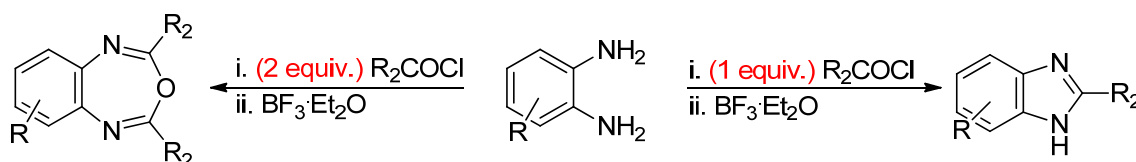
Scheme 1.13 Synthesis of 2-substituted benzimidazoles and 2,4-disubstituted benzodiazepines from substituted diamines using $BF_3.EtO_2$

Zeolites and heteropolyacids are important industrial catalysts and have been reported to catalyse the reaction between *o*-phenylenediamine and acyl chlorides with heteropolyacids, especially $H_{14}[NaP_5W_{30}O_{110}]$, resulting in better yields than zeolites (Heravi et al., 2006; Heravi et al., 2007). Heteropolyacids are not very selective with unhindered acyl chlorides. As a result, benzodiazepines are formed as a slight by-product. Nevertheless, the yields remain > 96% compared to zeolites (Heravi et al., 2007). The reaction is thought to go through the Bronsted acid mechanism based on the hydrogen atoms present on the Bronsted active sites (BAS) on the zeolite framework (Lukyanov et al., 2014). Furthermore, due to the numerous tungsten atoms and protons, the catalyst provides many active sites and lowers the activation barrier to cyclise the intermediate.

A Hafnium-metal organic framework (Hf-MOF), Hf-BTC, can also be employed to cyclise acyl chlorides to *o*-phenylenediamine using microwave irradiation under solvent free-conditions (Nguyen et al., 2021). Fascinatingly the catalysts behave as a dual Bronsted and Lewis acidic catalyst to protonate the acyl chloride carbonyl group and subsequently undergoes

nucleophilic substitution by the chloride, which is promoted by the nucleophilic attack of the diamine. The intermediate then undergoes cyclodehydrogenation and gets deprotonated by the Hf-BTC to form the benzimidazole compound (Scheme 1.14). Due to the high probability that the diamine can be diacylated, usually, *N*-substituted-*o*-phenylenediamines are used to create benzimidazoles.
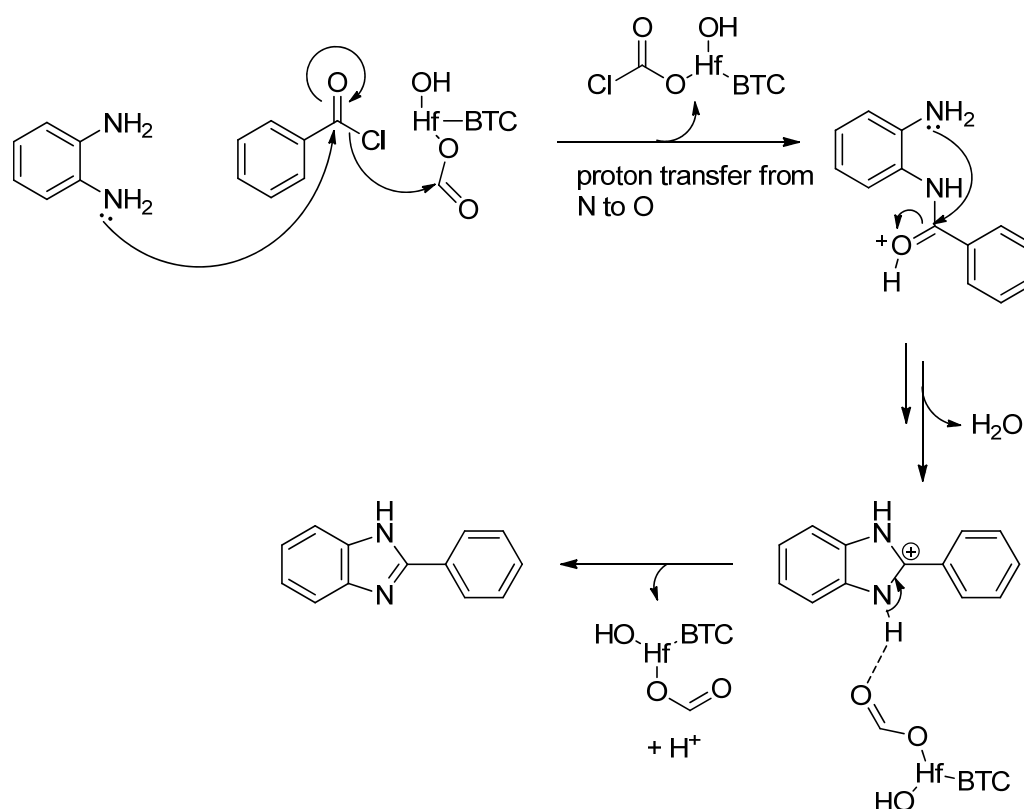
Scheme 1.14 Proposed mechanism for the synthesis of 2-phenylbenzimidazole using a Hf-BTC catalyst

Summary of reactions with o-phenylenediamine

Scheme 1.15 elegantly summarises the synthetic routes for the development of benzimidazoles using various precusors. The synthesis of the benzimidazole via routes 1-3 uses the substrate *ortho*-phenylenediamine that goes through the formation of three different intermediates, namely, an amide when reacted with acids and its derivatives, amidine for amine-containing

precusors and benzimidazoline for aldehydes and ketones. Furthermore, route 4 makes use of
o-nitroanilines that undergoes reductive cyclisation and route 5 the intramolecular cyclisation
of quinoxalines.
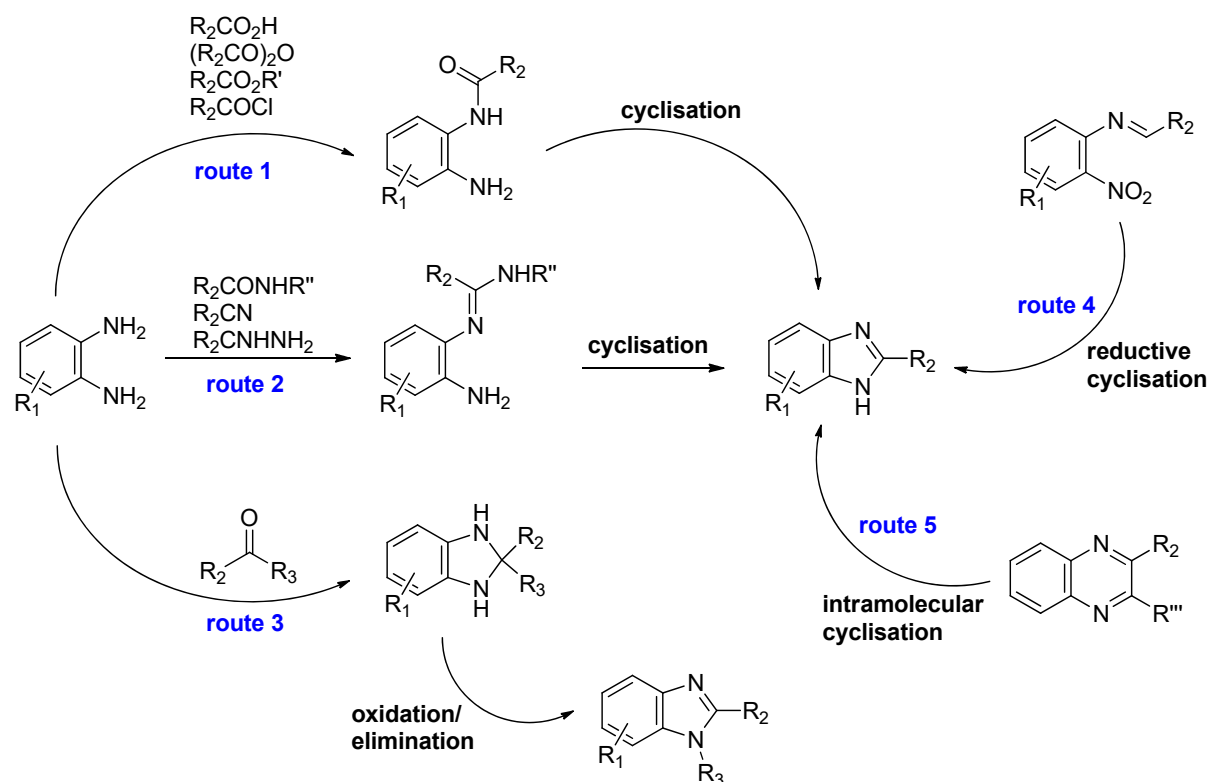
Scheme 1.15 Synthetic routes for the formation of the benzimidazole scaffold

Other precursors

The synthesis of benzimidazoles is not only restricted to *o*-phenylenediamine, and generally,
other precursors are required to synthesise highly complex and functionalised benzimidazoles
that provide a specific application.

Ortho-nitroanilines and N-substituted amidines

In some instances, *o*-phenylenediamine derivatives are created from *ortho*-nitroanilines
through a nucleophilic aromatic substitution (S_NAr) reaction with anilines followed by the

reduction of the nitro group to form a *N*-substituted diamine derivative. As previously mentioned, these intermediates can be reacted with a wide range of precursors to form benzimidazoles.

Yoon et al. (2015) synthesised novel benzimidazoles by esterifying 4-fluoro-3-nitrobenzoic acid through sulfuric catalysis in ethanol. The fluoro group on the ethylbenzoate intermediate was then substituted by different amines using *N, N*-diisopropylethylamine (DIPEA) and dry DCM. The derivatised *o*-nitroaniline was then reduced with ammonium formate and 10% Pd/C to yield the *N*-substituted-1,2-phenylenediamine (60%). The benzimidazoles were formed by cyclising the phenylenediamine with substituted adducts of aromatic aldehydes (Scheme 1.16).
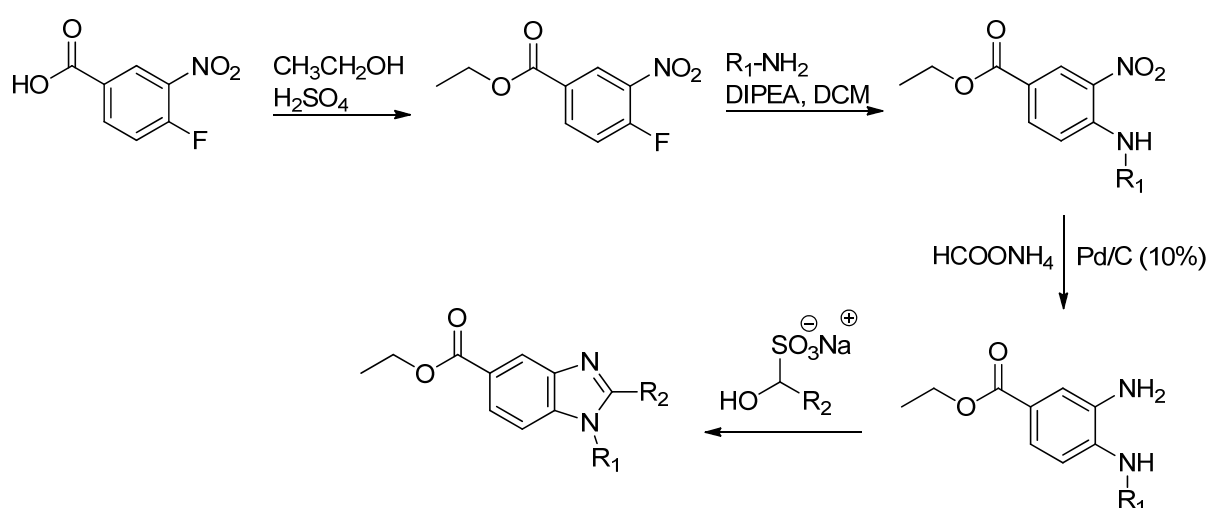
Scheme 1.16 Synthesis of 1,2-disubstituted benzimidazoles from 4-fluoro-3-nitrobenzoic acid

Other reducing systems used to convert the nitro group into an amine on the *o*-nitroaniline include stannous chloride and concentrated HCl in methanol (Perin et al., 2021), thiourea dioxide in the presence of NaOH (Zhong et al., 2020), and most commonly, a Pd/C catalyst under hydrogen atmosphere (Bandarage et al., 2009; Sasmal et al., 2011).

A two-step synthetic route to synthesise benzimidazoles was reported by the *N*-arylation of 2-fluoronitrobenzene with amidine to result in a carboximidamide intermediate through nucleophilic substitution (Gupta et al., 2010). This intermediate was reduced using 10% Pd/C in ethanol to form the amidine intermediate, which underwent intramolecular cyclisation to form 2-substituted benzimidazoles. A more efficient one-pot approach was recently presented whereby the nitro group on 1-fluoro-2-nitrobenzene behaved as a leaving group (Sayahi et al., 2018). The coordination of a copper (I) ion catalysed the reaction for the intermediate to undergo intramolecular cyclisation with the elimination of nitrite (NO_2^-) and the regeneration of the copper bromide catalyst, forming 2-arylbenzimidazoles (Sunke et al., 2016; Sayahi et al., 2018) (Scheme 1.17).
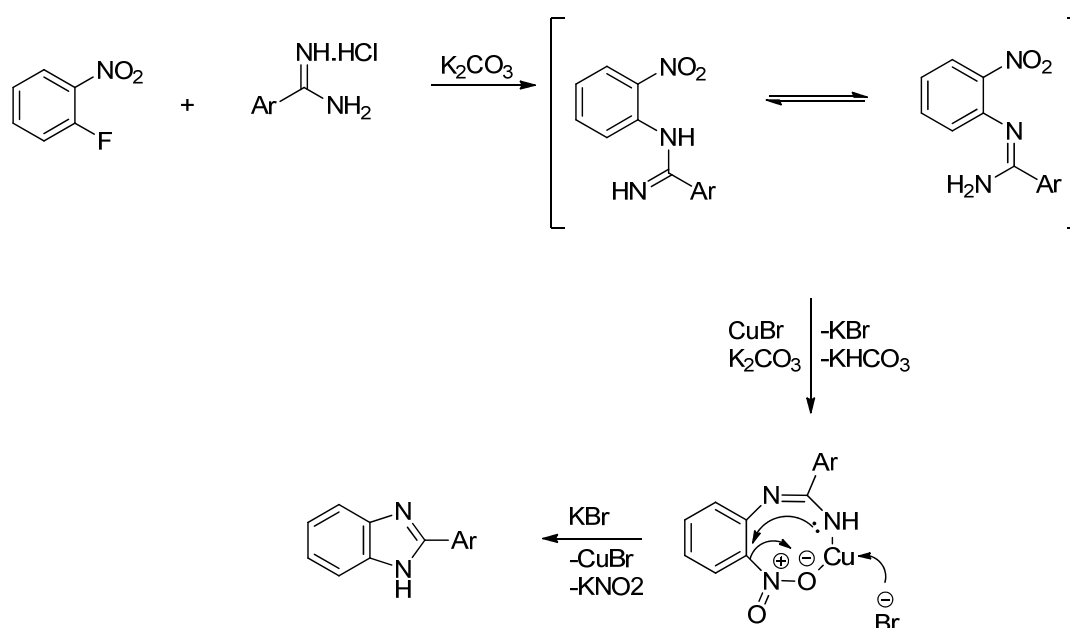
Scheme 1.17 Synthesis of 2-arylbenzimidazoles through a carboximidamide intermediate using copper bromide

Quinoxaline

Taylor and McKillop (1965) showed that an unusual ring contraction occurred when pure 2,3-diphenylquinoxaline was reacted with potassium amide in ammonia to yield the product in

32%. Based on spectroscopic evidence and an independent study of condensing *o*-phenylenediamine and benzaldehyde in the presence of cupric acetate (Weidenhagen reaction), the product was discovered to be 2-phenylbenzimidazole. It was proposed that the amide ion attacked C-2 and resulted in a rearrangement to form the benzimidazole (Scheme 1.18). Due to the low yields obtained from this rearrangement, quinoxalines are generally condensed with *o*-phenylenediamines to form quinoxaline-benzimidazoles, bisbenzimidazoles or benzodiazepinoquinoxaline (Kalinin et al., 2000; Mamedov et al., 2006; Yaragorla and Vijaya Babu, 2017).
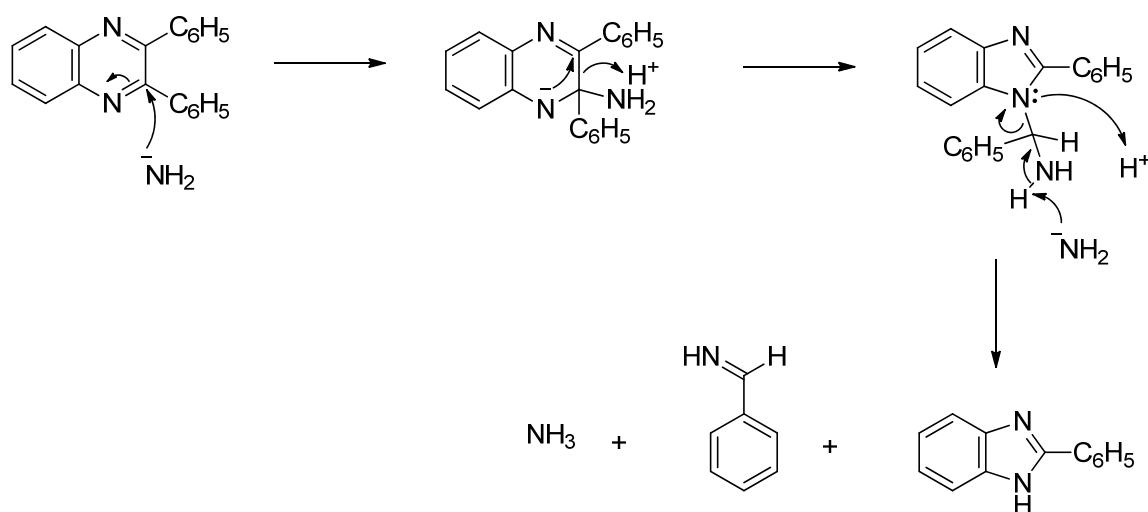
Scheme 1.18 Rearrangement of 2,3-diphenylquinoxaline to 2-phenylbenzimidzole using potassium amide

1.2.3 Bioactivity of benzimidazoles

Many studies incorporate benzimidazoles with other pharmacophores based on it being an isostere of purine, present in vitamin B_{12}, and having lower cytotoxicity due to interactions with biopolymers. During the mid-1900s, the benzimidazole scaffold showed promise to be used as potential therapeutic agents (Woolley, 1944; Hirschberg et al., 1957; Stone and Mullins, 1963; Bishop et al., 1964; Méhes et al., 1966). Initially, benzimidazoles were used as

plant fungicides and veterinary anthelmintics, which led to the discovery and development of the first benzimidazole drug suitable for human consumption, thiabendazole, used to treat infections caused by helminths (Stone and Mullins, 1963; Kamanna, 2019).

Today, benzimidazoles are known to show a broad spectrum of bioactivities, such as antibacterial (Breijyeh et al., 2020), anticancer (Cheong et al., 2018), antiulcer (Radhamanalan et al., 2018), anti-inflammatory (Veerasamy et al., 2021), anti-analgesic (Eswayah et al., 2017), anti-oxidant (Tumosienė et al., 2018), antihypertensive (Insa et al., 2019), anti-tubercular (Chaturvedi et al., 2018), and anti-HIV (Kanwal et al., 2019).

Antibacterial activity

The growth inhibition of 1*H*-benzo[d]imidazole against *Escherichia coli* and *Streptococcus lactis* displayed a half-maximal inhibitory concentration (IC_{50}) of 300 µg mL^{-1} and 725 µg mL^{-1} (Woolley, 1944). In contrast, electron-donating and withdrawing benzimidazole derivatives at position 2 was reported to decrease the bacteriostatic effect of the pharmacophore.

Some fluorine-containing benzimidazoles with one or more electron-withdrawing groups on the benzene ring (Figure 1.6) showed moderate to excellent minimum inhibitory concentrations (MICs) against *Staphylococcus aureus*, *Streptococcus pyogenes*, *Klebsiella aerogenes* and *E. coli*. An unsubstituted benzimidazole was reported to be inactive to these bacterial strains. Introducing a trifluoromethyl group at position 2 in compound **1.1** improved the benzimidazole's activity, as it was selective against *S. pyogenes* at 125 µg mL^{-1}, however, 2-pentafluoroethylbenzimidazole (**1.2**) proved to be more active against all strains with better activity of 15 µg mL^{-1} against *S. pyogenes* (Bishop et al., 1964). The most effective compound from the series was 2,4,5-tristrifluorobenzimidazole (**1.3**) that had excellent MIC values toward

S. pyogenes (0.24 µg mL^{-1}) and *S. aureus* (0.97 µg mL^{-1}). Hence the presence of electron-withdrawing groups on the benzimidazole moiety improves the bacteriostatic activity.

1.1
2-Trifluorobenzimidazole
S. pyogenes MIC = 125 µg/mL

1.2
2-Pentafluoroethylbenzimidazole
S. pyogenes MIC = 15 µg/mL

1.3
2,4,5-Trisfluorobenzimidazole
S. pyogenes MIC = 0.24 µg/mL
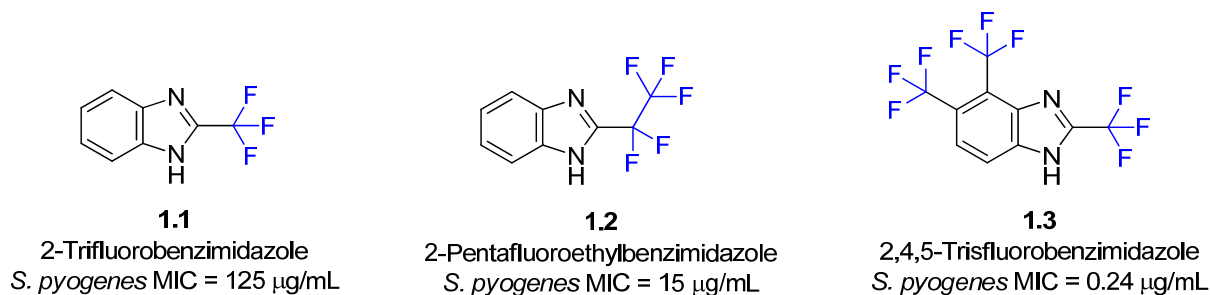
Figure 1.6 Structures of fluorinated benzimidazoles with MICs against *S. pyogenes*

The 1,2-disubstituted benzimidazoles (Figure 1.7) bearing a phenyl ring at position 2 and benzyl or 4-methylbenzyl group at position 1 (compounds **1.4** and **1.5**) were identified as potential antibacterial agents on account of the good activity displayed against TolC–mutant *E. coli* (strain lacking efflux gene responsible for resistance to antibiotics), with MIC values of 16 and 8 µg mL^{-1} (Bandyopadhyay et al., 2011; Dokla et al., 2020). However, potent antibacterial activity of 2 µg mL^{-1} was observed when R$_1$ had a 4-methyl group and R$_2$ a 3-methanesulfonamide group (**1.6**), better or comparable than the standard drug linezolid (Dokla et al., 2020). The methanesulfonamide compound displayed no significant cytotoxicity against human colorectal (Caco-2) and monkey kidney epithelial (Vero) cells, as the compound concentration to reduce 50% cell viability (CC$_{50}$) was greater than 128 µg mL^{-1}.

Interestingly this set of benzimidazole compounds had insufficient activity toward other Gram-negative bacteria, specifically *E. coli* BW25113, which contains the gene for the active efflux system. This indicated that these compounds were ineffective against the high efflux. An improved synergetic effect was observed against *E. coli* BW25113 and other Gram-negative bacteria (8 or 16 µg mL^{-1}) upon the addition of the cell permeabilising agent, colistin to the

methanesulfonamide compound (**1.6**). Hence, combining these antibacterial agents can be considered potential combinational therapy against drug-resistant Gram-negative bacteria.
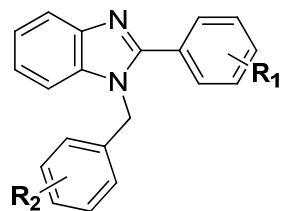
Compound	R_1	R_2	MIC $\mu g\ mL^{-1}$
1.4	H	H	16
1.5	H	$4\text{-}CH_3$	8
1.6	$3\text{-}NHSO_2CH_3$	$4\text{-}CH_3$	2
Linezolid			8

Figure 1.7 Structure of 1,2-benzimidazoles (**1.4-1.6**) showing antibacterial activity against TolC–mutant *E. coli* in comparison with Linezolid

Some benzimidazole-thiophene-carboxamide derivatives **1.8-1.9** (Figure 1.8) compared to the carboxylic acid parent molecule (**1.7**) displayed broad-spectrum antibacterial activity. In addition, these molecules exhibited activity against *B. subtilis*, *S. aureus*, *E. coli* and *T. thermophilus* with MIC values approximately six-fold better than ofloxacin. Structure-activity relationship (SAR) studies revealed that aromatic carboxamides containing electron-withdrawing groups at specific sites on the ring were regarded as the most active from the series (Hooda et al., 2021). Especially dinitro (**1.8**) or dichloro (**1.9**) groups at 2,4 or 2,5 positions, respectively, which was also determined via *in silico* molecular docking studies.

1.8: R = 2,4-dinitro
1.9: R = 2,5-dicloro

1.7
Parent molecule
pMIC = 1.57-1.88 μM/mL

1.8-1.9
Carboxamide derivatives
pMIC = 2.29-2.61 μM/mL

Ofloxacin
pMIC = 0.44 μM/mL
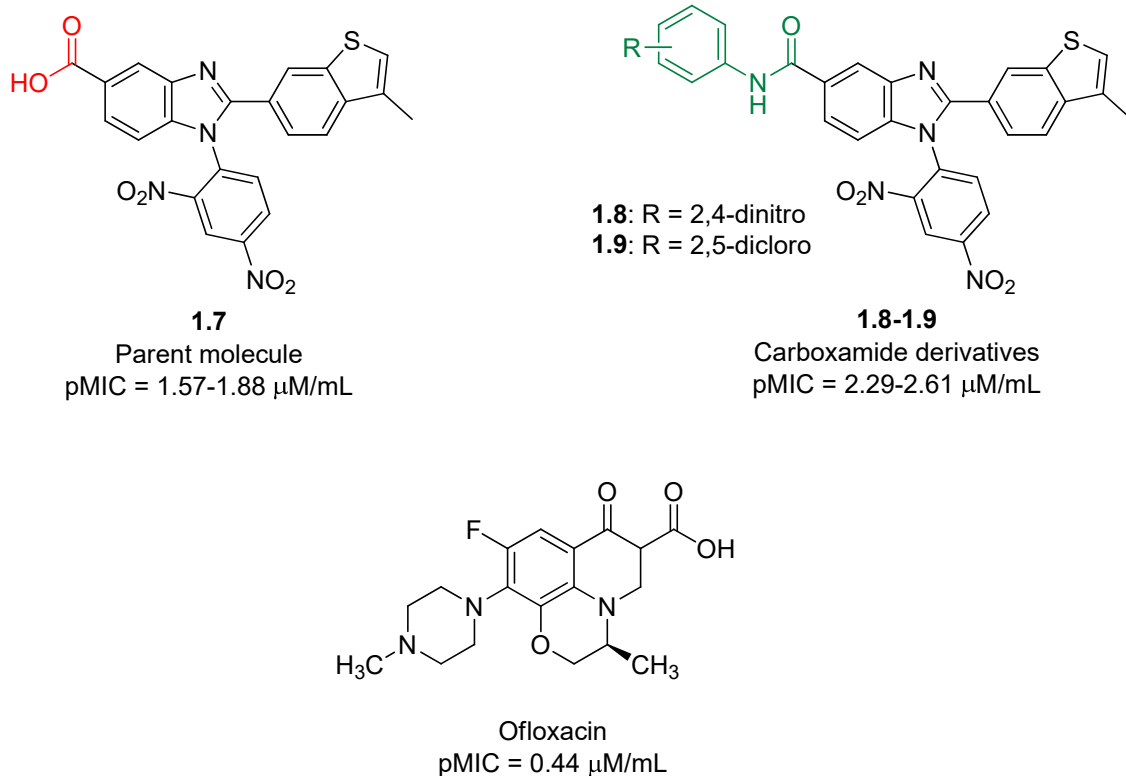
Figure 1.8 Structures and pMIC (μM/mL) of benzimidazole-thiophene-carboxamide derivatives

Benzimidazoles containing amino acids were shown to be promising alternatives to the antibacterial drug ciprofloxacin. Two chiral benzimidazoles derived from *S*-alanine, containing bromo (**1.10**) and chloro (**1.11**) derivatives at position 5 (Figure 1.9), showed comparable MIC values of 32 μg mL^{-1} towards MRSA HG-1 and MRSA BIG 0050 bacterial strains (Alasmary et al., 2015). The chirality of antibacterial agents significantly impacts bioactivity as the consequence of the ability to bind to cellular targets in bacteria through a recognition phenomenon (Paris, 2012).   Benzimidazole-acetamido derivatives (Figure 1.9) exhibited similar antibacterial activity to ciprofloxacin against *E. coli* with a MIC of 0.98 μg mL^{-1} (Abdel-Wahab et al., 2016).
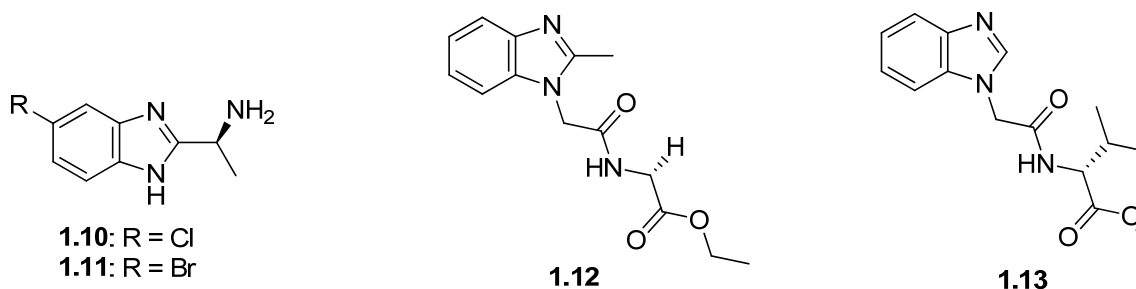
Figure 1.9 Promising benzimidazoles as antibacterial agents

Gejalakshmi et al. (2018) integrated a five-membered thiazolidinone ring onto the benzimidazole scaffold at position 1 (**1.14** in Figure 1.10), which improved its antimicrobial activity. The 4-methyl derivative had the best activity against *S. aureus* and *E. coli* with zones of inhibition of 17 and 19 mm. Heightened zones of inhibition against *E. coli* of 20-25 mm were observed for benzimidazoles containing a thiazolidinone ring at position 2 (**1.17**), the methyl derivative having a MIC of 9 µg mL^{-1}. These compounds also exhibited higher activity than their Schiff base counterparts **1.15** and four-membered azetidinones **1.16** evaluated in the series (Figure 1.10) (Panneer Selvam et al., 2011).
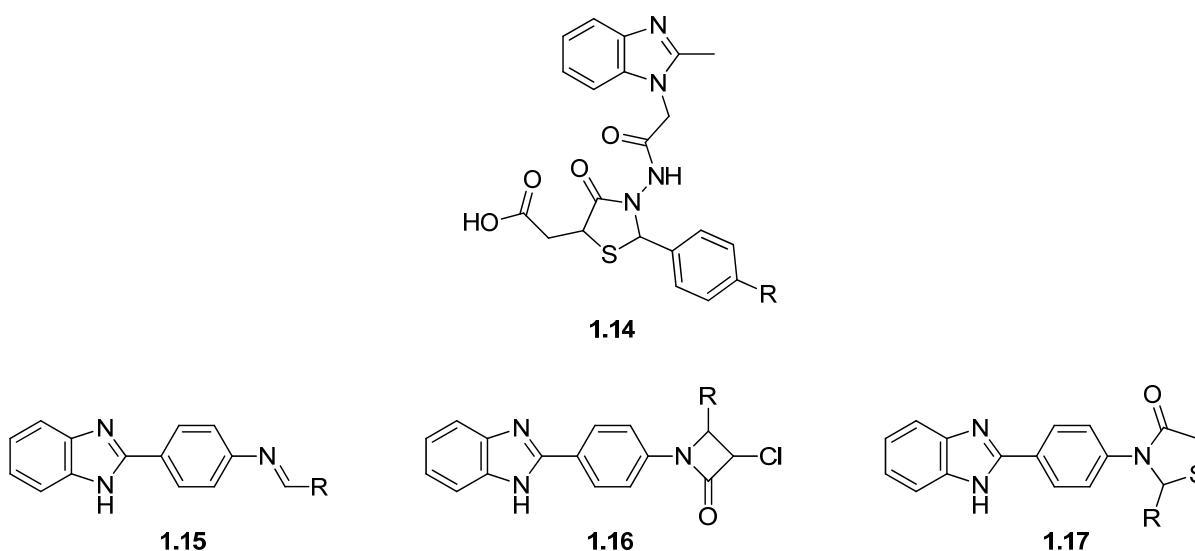
Figure 1.10 Structures of benzimidazoles containing Schiff bases, four-membered azetidinones and five-membered thiazolidinone rings

Substituted benzimidazole chalcones **1.18** (Figure 1.11) with a methoxy derivative at the *para*-position showed an inhibition zone of 20 mm against *E. coli,* equivalent to the standard ciprofloxacin (Chigurupati et al., 2013). However, benzimidazole-pyrazole hybrids **1.19** (Figure 1.11) synthesised from a simple ring closure reaction of various benzimidazole aminochalcones displayed superior activity. SAR studies revealed that electron-withdrawing groups on the phenyl ring attached to the pyrazole exhibited better activity than electron-donating groups, whereas the unsubstituted compound showed average activity. The benzimidazole-pyrazole containing a 4-trifluoromethyl group was discovered to be a hit molecule as it had MIC values of 3.9 µg mL^{-1} and 7.81 µg mL^{-1} against *M. luteus* and *E. coli* compared to ciprofloxacin of 7.81 µg mL^{-1} and 15.62 µg mL$^{-1,}$ respectively (Krishnanjaneyulu et al., 2014).
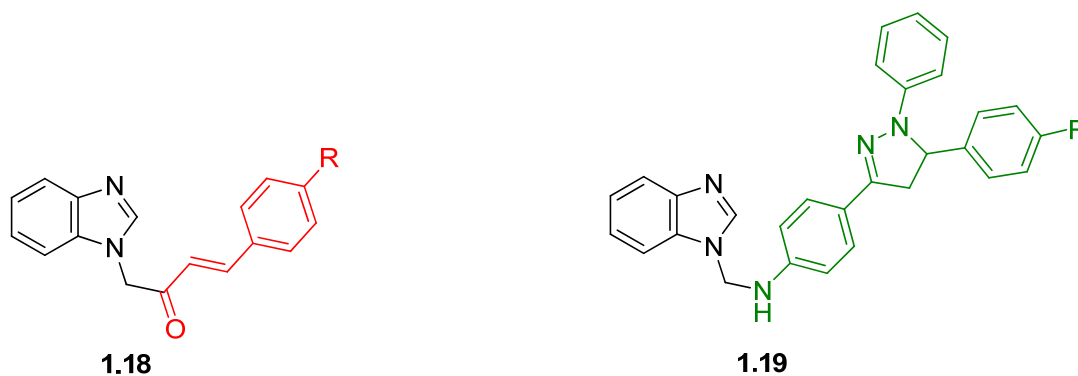
Figure 1.11 Structures of hybrid benzimidazole chalcones and pyrazole derivatives

Anticancer

Hirschberg et al. (1957) introduced a benzimidazole nucleus with a nitrogen mustard group at the imidazole carbon (**1.20,** Figure 1.12) to improve the efficacy of alkylating agents while lowering the toxicity to normal host cells. The benzimidazole mustard showed enhanced antitumor activity toward glandular adenocarcinomas (Ehrlich ascites carcinoma, mammary

carcinomas 755 and EO-771) and soft tissue and bone (sarcoma 180) with no evidence of toxicity at carcinostatic concentrations.
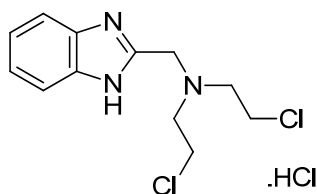
1.20

Figure 1.12 Structure of 2-nitrogen mustard benzimidazole

Further development of benzimidazole mustards led to the synthesis of bendamustine hydrochloride, a bifunctional chemotherapy drug with alkylating and antimetabolite properties for the treatment of chronic lymphocytic leukaemia (CLL) and non-Hodgkin lymphoma (NHL) (Bhatia et al., 2020). Although bendamustine is considered less toxic than previous regimens, side effects and adverse cutaneous reactions have been reported, as with all chemotherapy treatments (Carilli et al., 2014).

A set of mono-substituted benzimidazoles conjugated with various heterocycles at the 2-position were evaluated as glutathione S-transferase (GST) inhibitors in an attempt to overcome multidrug resistance anticancer chemotherapy. Compounds **1.21-1.24** (Figure 1.13), which had potent inhibition toward GST enzyme (IC$_{50}$ values of 0.00067-0.0065 µg mL^{-1}) was tested for their anticancer activity against breast (MCF-7) and colon (HCT) carcinoma cell lines. Benzimidazole-isoxazole **1.21** displayed three-fold more potency than the standard ethacrynic acid, whereas benzimidazole-2-methyl-3-acetyl-pyridine **1.24** was ten-fold more potent. However, these compounds were less cytotoxic against MCF-7 (7.5, 15.5 µg mL^{-1}) and

HCT (7.5, 33.8 μg mL^{-1}) than benzimidazole-sulfonamide with a 3-oxopropyl linker **1.22** and

benzimidazole-2-methylpyridine-3-carboxylate **1.23** of 2.7-4.9 μg mL^{-1}.
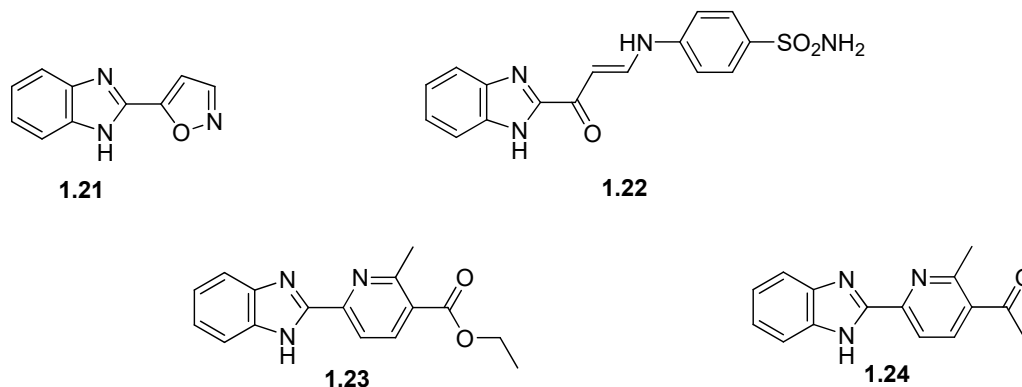
Compound	GST IC$_{50}$ (μg mL^{-1})	MCF-7 IC$_{50}$ (μg mL^{-1})	HCT IC$_{50}$ (μg mL^{-1})
1.21	0.0017	7.5	7.5
1.22	0.0065	2.7	3.7
1.23	0.0024	3.2	4.9
1.24	0.00067	15.5	33.8
Ethacrynic acid	0.0055	-	-
Doxorubicin	-	1.2	1.4

Figure 1.13 Structures of 2-substituted benzimidazoles and their IC$_{50}$ values against GST

enzyme, MCF-7 and HCT cell lines

Disubstituted benzimidazoles (Figure 1.14) containing benzyl derivatives at position 1 and a

p-tolyl ring at position 2 produced antiproliferation against MCF-7 and HepG2 cancer cell lines

(Akkoç, 2020). The presence of electron-withdrawing groups, specifically methyl in the *para*-

position of the benzyl ring, showed increased cytotoxic activities toward HepG2 with an IC$_{50}$

value of 48.17 μM compared to the standard 5-fluorouracil (55.48 μM).
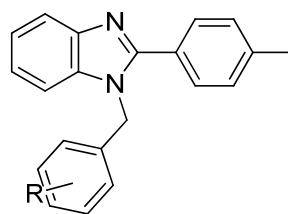
1.25

Figure 1.14 Structure of 1,2-disubstituted benzimidazoles screened against MCF-7 and HepG2

Anti-inflammatory, analgesic, antiulcer and anti-oxidant

Gastrointestinal tract disorders have been associated with the frequent use of nonsteroidal anti-inflammatory drugs (NSAIDs) to relieve pain and reduce inflammation. Novel *N*-sulfonyl benzimidazoles containing alkyl and aryl derivatives at position 5 (**1.26 a-i** in Figure 1.15) exhibited poor anti-inflammatory effects of 6.7-10.8% reduction in edema (swelling) (Gaba et al., 2010). However, the reduction of the nitro aryl to amino derivatives resulted in a comparable anti-inflammatory response of 33-39% edema reduction and analgesic activity of 51-57% writhing inhibition than standard drugs indomethacin (43%) and aspirin (58%) with lower gastric ulcerogenicity (**1.26 j-l** in Figure 1.15).

The chemical modification of *N*-sulfonyl benzimidazoles with the placement of an amine group at position 2 of the benzimidazole **1.27 a-i** also displayed similar activity to the standard drugs. These compounds were classified as gastrointestinal-safe anti-inflammatory analgesic agents due to their anti-oxidant properties, which contributed to the influence of electron-donating substituents (Gaba et al., 2015). Hence 3,4-dimethylated benzimidazole (**1.27 i**) demonstrated the most significant therapeutic effect.

R$_1$ = **a**, CH$_3$
    b, C$_2$H$_5$
    c, C$_3$H$_7$
    d, C$_4$H$_9$
    e, 2-ClC$_7$H$_6$
    f, 4-ClC$_7$H$_6$
    g, 2-NO$_2$C$_6$H$_4$
    h, 4-NO$_2$C$_6$H$_4$
    i, 4-NO$_2$C$_7$H$_6$

1.26 a-l

g-i $\Longrightarrow$ R$_1$ = **j**, 2-NH$_2$C$_6$H$_4$
    k, 4-NH$_2$C$_6$H$_4$
    l, 4-NH$_2$C$_7$H$_6$

1.27 a-i

R$_2$ = **a**, H   R$_2$ = **g**, 2,6-di-Cl
    b, 3-NO$_2$ **h**, 3,5-di-Cl
    c, 4-NO$_2$ **i**, 3,4-di-CH$_3$
    d, 2-CH$_3$
    e, 3-CH$_3$
    f, 4-CH$_3$
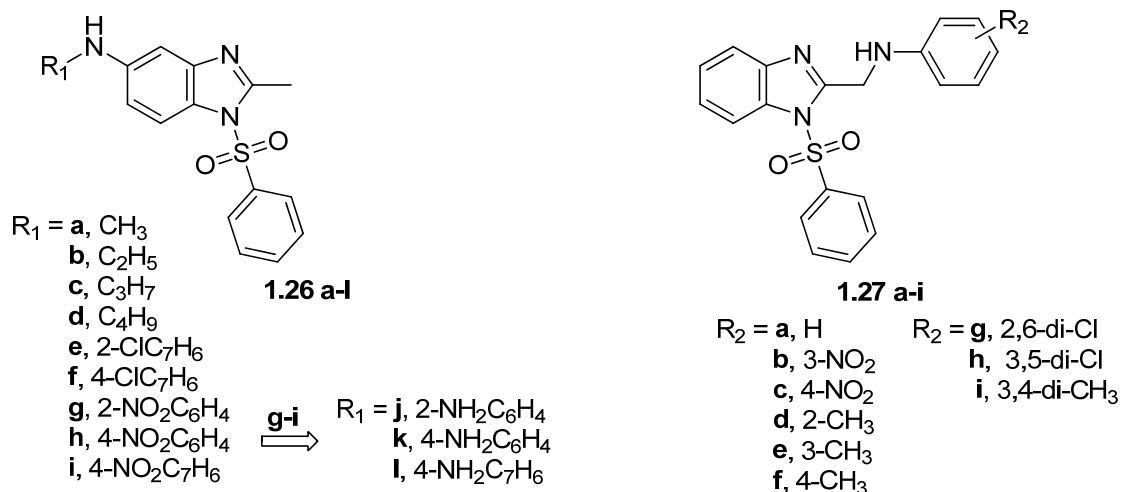
Figure 1.15 *N*-sulfonyl-benzimidazoles with gastrointestinal properties

The majority of proton pump inhibitors available on the market include benzimidazole sulfoxide derivatives as the core nucleus (omeprazole, esomeprazole, lansoprazole and rabeprazole) that inhibits the release of protons by binding to the enzyme, hydrogen/potassium adenosine triphosphatase (H$^+$/K$^+$ ATPase), reducing the content of gastric acid (Alfahad et al., 2021). Substituted 2-mercaptobenzimidazoles (**1.28 a-c** in Figure 1.16) showed promise as gastroprotective agents similar to omeprazole at a dosage level of 10 mg kg^{-1} (Reddy et al., 2011). Furthermore, Khan et al. (2020) found through molecular docking that amino acid conjugated 2-mercaptobenzimidazole compounds (**1.29 a-b**) had good binding affinities and inhibitory effects with H$^+$/K$^+$ ATPase of -8.7 and -8.2 kcal/mol, and the inflammatory cyclooxygenase (COX-2) enzyme (-8.7 and -9.8 kcal/mol).

A new class of H$^+$/K$^+$ ATPase inhibitors, 2-mercaptobenzimidazole-pyrazoles **1.30,** were discovered as lead molecules based on their anti-ulcer activity, binding properties, drug-likeness and acute toxicity. Compounds possessed 72-83% of superior anti-ulcer properties at 500 µg kg^{-1}, whereas omeprazole had an inhibition level of 83% at 30 mg kg^{-1} (Noor et al., 2017).

1.28 a-c

a: n = 1, R = H
b: n = 3, R = H
c: n = 3, R = OCH₃

1.29 a

1.29 b

1.30

R₁	R₂
C₆H₅	H
C₆H₅	2-OH
2-OHC₆H₄	2-OH
2-OHC₆H₄	3-OH, 4-OCH₃
4-OHC₆H₄NH	2-OH
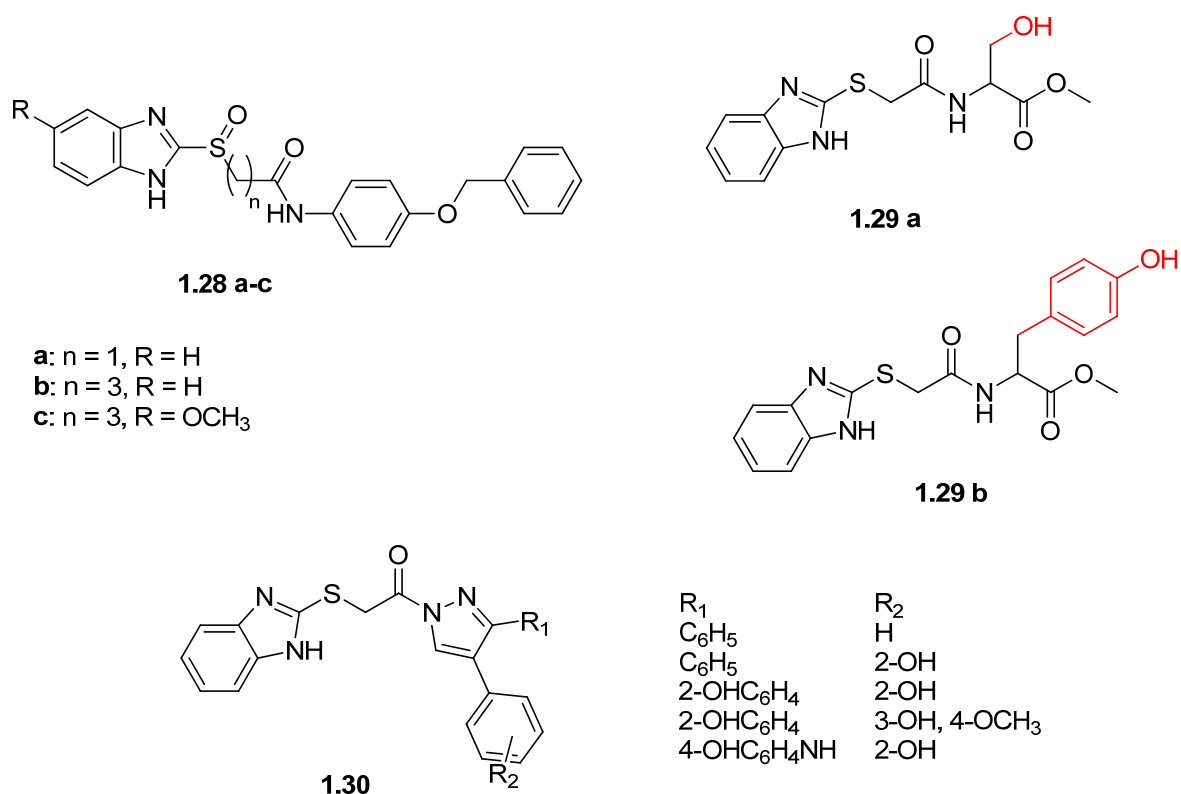
Figure 1.16 Gastroprotective 2-mercaptobenzimidazoles

Antihypertensive

Candesartan and Telmisartan (Figure 1.5) are a class of benzimidazole anti-hypertensive drugs that work as angiotensin II receptor antagonists (AT₁) to treat hypertension. Wu et al. (2019) altered the structure of Telmisartan by replacing the biphenyl moiety with an *N*-phenyl indole group for enhanced efficacy with low toxicity. The molecule was modified further to include an alkyl carbamoyl group with a phenyl ring at position 6, instead of the methyl benzimidazole, for additional hydrogen bonding. The benzimidazoles containing phenylethyl (n=2) was more accessible to the AT₁ cavity pocket and bound strongly to the receptor sites. Additionally, the propyl group at position 2 aided in significant binding affinities compared to other alkyl chains. The attachment of the indole moiety at position 4 was shown to be better than position 5.

A radioligand binding assay (^{125}I Ang II) showed that compounds **1.31 a-b** lowered blood pressure to 57.6 mmHg at 10 mg kg^{-1}. This was more effective than the control drug, Losartan. The highest affinity to the AT$_1$ receptor was displayed by compound **1.31 a** with an IC$_{50}$ value of 2.3 nM and inhibitor constant Ki of 1.9 nM. In comparison, Losartan had an IC$_{50}$ of 14.6 nM and Ki of 10.5 nM. A more straightforward and effective adjustment of Telmisartan was the addition of trifluoromethyl groups on the alkyl chain at position 2 of the benzimidazole nucleus (**1.32 a-b** in Figure 1.17), resulting in desirable electronic effects with the AT$_1$ receptor (Wu et al., 2020). The inhibitory effects indicated that the trifluoropropyl group in **1.32 a** was the optimal hydrophobic substituent as the mean blood pressure after 10 mg kg^{-1} oral administration was 74.5 mmHg. In addition, the IC$_{50}$ and Ki was 0.8 nM and 0.6 nM respectively, more potent than telmisartan (IC$_{50}$ = 3.8 nM, Ki = 2.8 nM).

A series of small molecular weight benzimidazoles (**1.33** in Figure 1.17) was designed with a phenyl ring at position 2 instead of the *N*-biphenyl group present in Telmisartan and Candesartan (Figure 1.5) (Iqbal et al., 2021). The 2-fluorophenyl benzimidazole displayed the most effective concentration-dependent vasorelaxation response of 97.8%. The vasorelaxant mechanisms occurred through increased cyclic guanosine monophosphate (cGMP) levels in tissue, inhibition of L-type calcium channels and opening of BK$_{Ca}$ channel blockers as targets of vasorelaxation without toxicity.
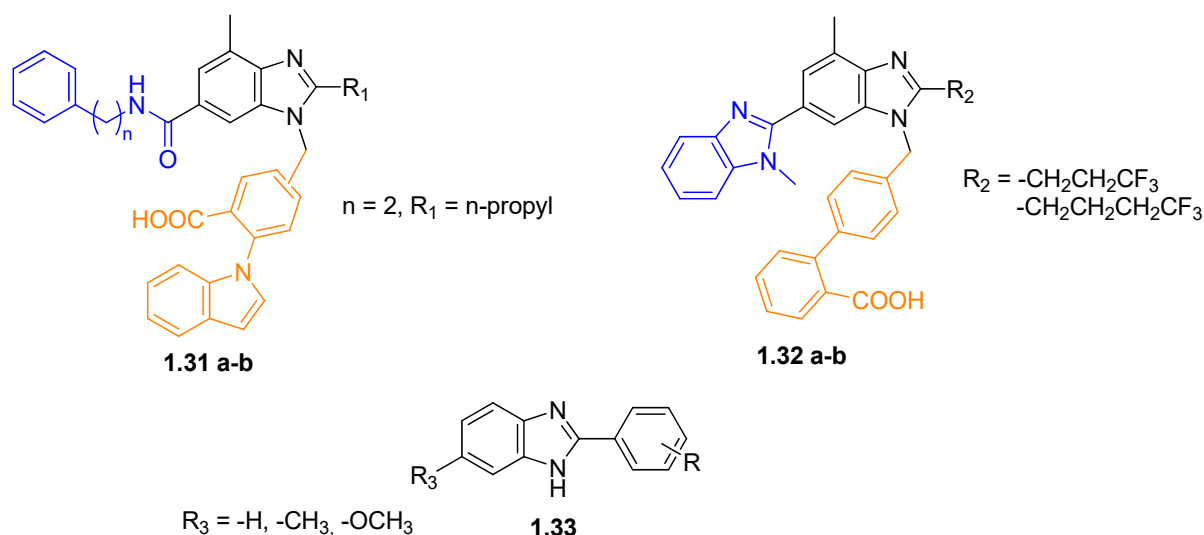
Figure 1.17 Potential antihypertensive agents containing the benzimidazole nucleus

Antitubercular

Benzimidazoles have been considered possible antitubercular agents, attributed to similar structures as indoles which are present in mycobacterial InhA inhibitors (Genz-10850) (Kuo et al., 2003; Yeong et al., 2017).

Benzimidazole esters with various aromatic derivatives at position 2 were screened against *Mycobacterium tuberculosis* $H_{37}R_V$ strain (MTB-$H_{37}R_V$). The most active product was 2-(4-(trifluoromethyl)phenyl)-1*H*-benzo[d]imidazole-5-carboxylate (**1.34**, Figure 1.18) with IC_{50} of 11.27, IC_{90} of 12.65 and MIC of 50.00 µM, using the Alamar Blue method. This was more active than the reference drugs cycloserine and pyrimethamine, but less active than the first-line drug isoniazid. However, the compound showed potential activity against isoniazid, rifampin and ofloxacin multidrug-resistant MTB strains with MIC of 15.24, 30.50 and 60.00 µM (Yeong et al., 2017).

Generally, disubstituted benzimidazoles at positions 2,5 and 2,6 generate possible anti-TB agents (Keri et al., 2016). Jiménez-Juárez et al. (2020) demonstrated that 2,5-disubstituted benzimidazoles **1.35 a** and **1.36 a** had effective *in vitro* inhibition against MTB-H$_{37}$Rv with MIC values of 19.4-89.6 nM compared to the *N*-alkylated 1,2,5-trisubstituted benzimidazoles **1.35 b** and **1.36 b** (>182 nM). Molecular docking studies suggested that the disubstituted benzimidazole interacts with the FtsZ protein responsible for septum formation and cell division, whereas the trisubstituted benzimidazoles were restricted from the binding site.
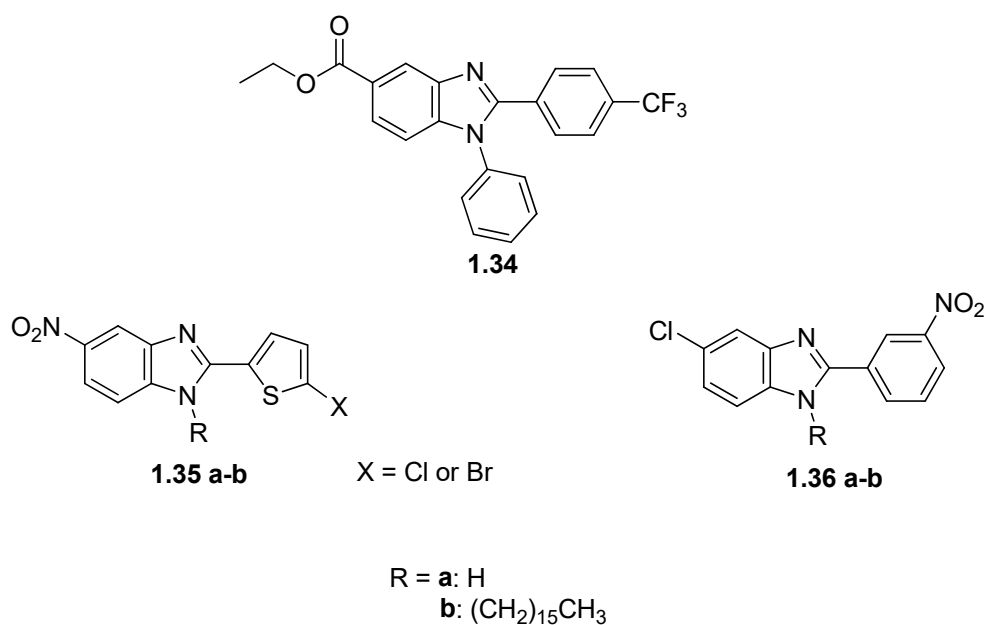
Figure 1.18 Di- and tri-substituted benzimidazoles with antitubercular activity

Anti-HIV

Serval *N*-aryl-benzimidazoles have been designed as non-nucleoside reverse transcriptase inhibitors (NNRTIs) for the treatment of human immunodeficiency virus type 1 (HIV-1) due to the lower chances of mutation expected in the region and possible application in multiple antiretroviral therapies (Roth et al., 1997; Chimirri et al., 1999; Rao et al., 2002; Monforte et al., 2018; Wang et al., 2019b; Srivastava et al., 2020).

Chimirri et al. (1991) developed a novel class of thiazolobenzimidazole reverse transcriptase (RT) inhibitors (**1.37** in Figure 1.19) and discovered the highly potent lead molecule, 1-(2,6-difluorophenyl)-1*H*,3*H*-thiazolo[3,4a]benzimidazole (TBZ). The compound owes its biological activity to its energy minimised "butterfly-like" conformation due to planar π-electron rings and a hydrogen bond acceptor, important features for binding to RT allosteric sites and suppressing the replication of the virus (Chimirri et al., 1997). However, the molecule's stability suffers as the thiazolo ring of TBZ undergoes metabolic oxidation to the weaker sulfoxide and sulfone metabolites, reducing the therapeutic effect (El Dareer et al., 1993).

Roth et al. (1997) revealed through retrosynthesis that the synthetic equivalent of TBZ is *N*-benzyl-2-alkylbenzimidazoles through the ring-opening of the thiazolo ring (Figure 1.19). Additionally, the structure retains its "butterfly-like" confirmation, crucial for the molecule to fit in the NNRTI binding pocket and interact with the key residues. The best inhibitor from the series 1-(2,6-difluorobenzyl)-2-(2,6-difluorophenyl)-4-methylbenzimidazole (**1.39**) had a low IC$_{50}$ value of 200 nM, approximately 3-fold better than TBZ (500 nM) against wild-type RT. Additionally, the compound showed excellent activity against RT resistant strains (containing amino acid residues) and no cytotoxic effects at < 10 mM.

A hit compound (**1.40**) was identified from a series of *N*-aryl-2-arylthioacetamidobenzimidazoles which proved to be an effective NNRTI at EC$_{50}$ of 24 nM in MT-4 cells with better inhibitory activity than nevirapine at 180 nM (Monforte et al., 2018). Furthermore, the compound's high selectivity index (SI) suggests its suitability as an antiretroviral drug candidate. Wang et al. (2019b), through 3D-QSAR studies, showed that

anti-HIV activity is produced by having hydrogen acceptor groups (sulphonamide) on the arylacetamide moiety at the *para*-position. Moreover, the presence of the 3,5-dimethylphenyl group enables interaction with amino acid residues.

1.37
Lead molecule
(TBZ)

1.38
N-benzyl-2-alkylbenzimidazole

1.39

1.40
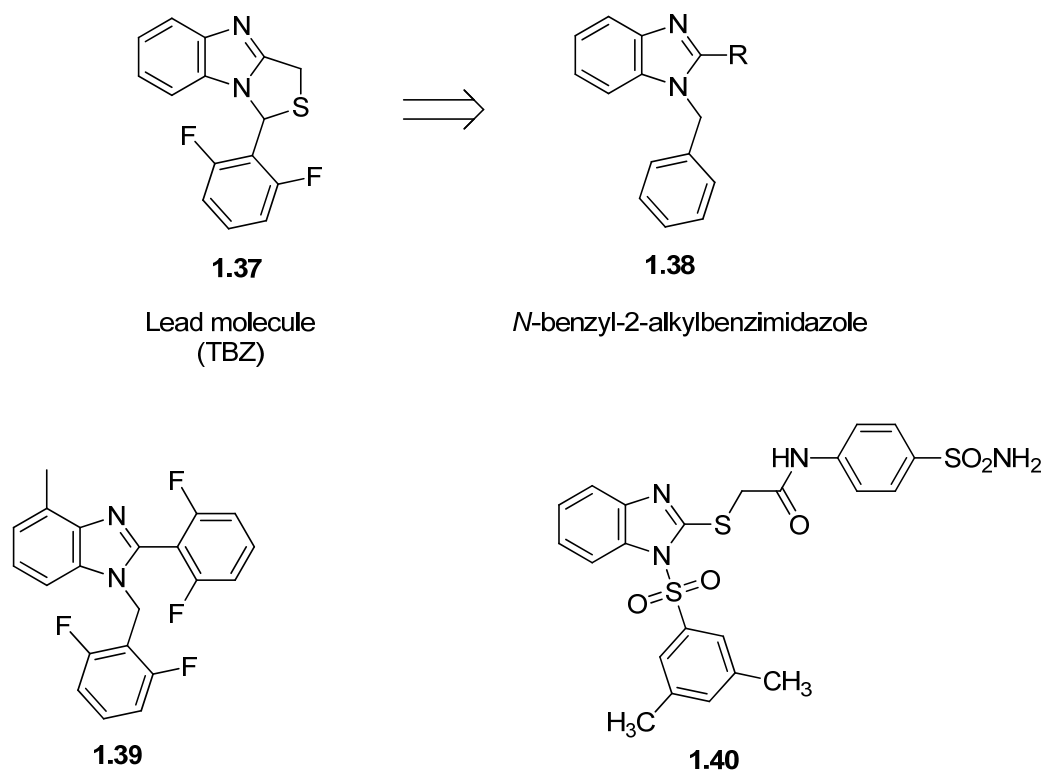
Figure 1.19 Benzimidazoles with potential anti-HIV activity

1.3   Oxadiazoles

1.3.1   History and structural features of oxadiazoles

Oxadiazoles are monocyclic five-membered heterocycles, containing one oxygen and two nitrogen atoms in four isomeric forms (Glomb et al., 2018). The first synthesis was recorded at the end of the 19th century with the formation of 3,4-diphenyl-1,2,5-oxadiazole (**I**) from the dehydration of diphenylglyoxime, and closely followed by the synthesis of 3,5-disubstituted 1,2,4-oxadiazoles (**II**) through the thermal cyclisation of benzamidoxime with benzoyl

chloride, benzotrichloride or benzoic acid (Figure 1.20) (Goldschmidt, 1883; Tiemann and Krüger, 1884).

Later, 2,5-disubstituted 1,3,4-oxadiazoles (**III**) were synthesised by dehydrating symmetrical acid hydrazides using phosphorous pentoxide or zinc chloride (Figure 1.20) (Stollé, 1899). However, the 1,2,3-isomer (**IV**) is hypothetical, as it experiences ring strain due to the weak N-O σ-bond resulting in a relatively more stable ring open acyldiazomethane molecule. It is presumed to be formed via the 1,3-dipolar cycloaddition of nitrous oxide with alkynes (Figure 1.20) (Huisgen, 1980).

The unsubstituted form of the isomers was prepared in the 1960s. Moussebois et al. (1962) formylated formamidoxime with acetic formic anhydride to form a formyl intermediate which was cyclised to create the 1,2,4-oxadiazole (Figure 1.21). The thermally stable parent molecule, 1,2,5-oxadiazole (furazan), was synthesised by the dehydration of glyoxime using succinic anhydride (Figure 1.21) (Olofson and Michelman, 1965). Ainsworth (1965) showed that the cyclisation of ethyl formate formylhydrazone through thermolysis produced 1,3,4-oxadiazole (Figure 1.21).
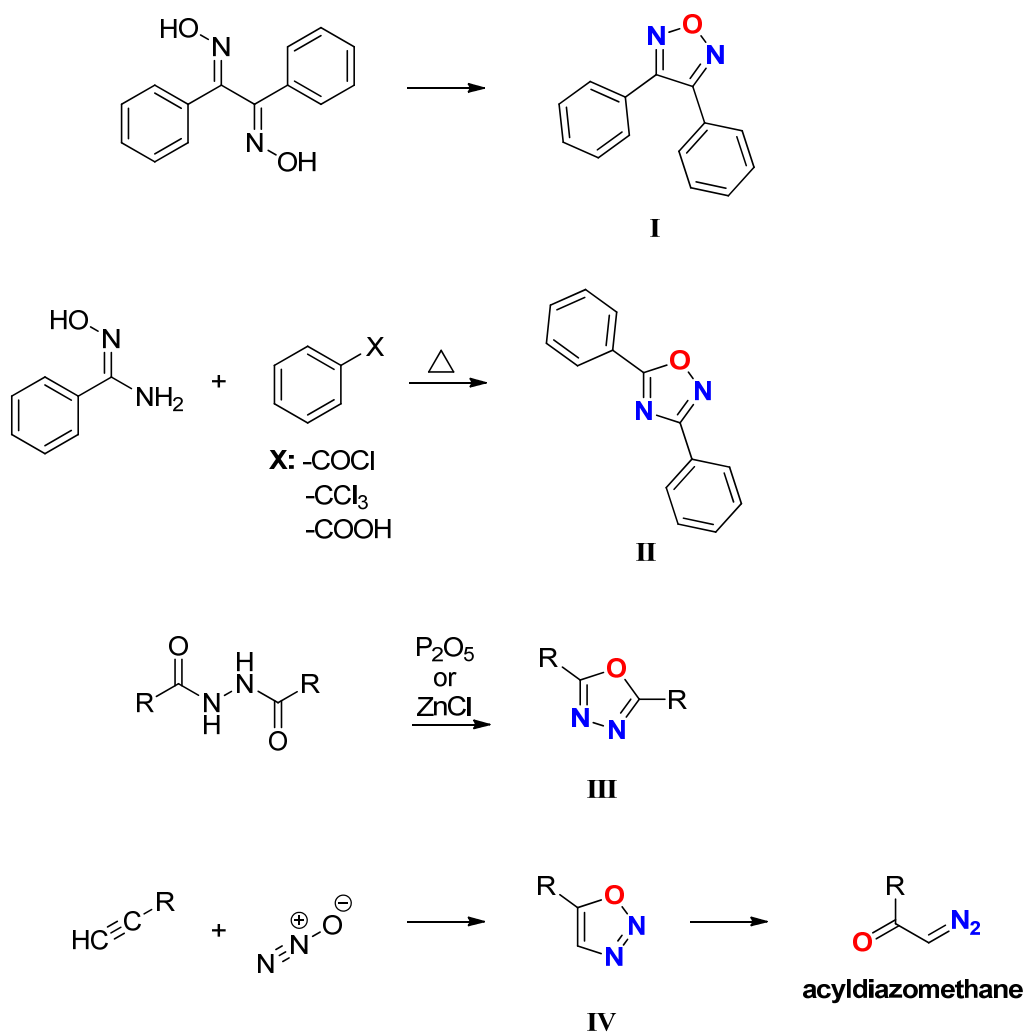
Figure 1.20 Synthesis of some of the first substituted oxadiazole isomers
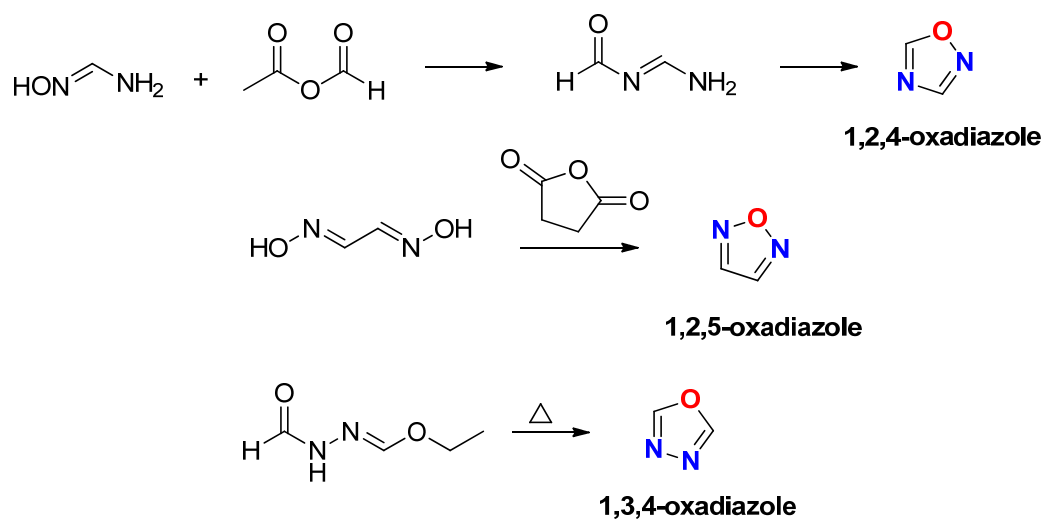
Figure 1.21 Synthesis of unsubstituted five-membered oxadiazole isomers

The 1,2,4-oxadiazole ring is the only naturally occurring isomer isolated from a marine organism, *Phidiana militaris*, as two 3-substituted indole alkaloids, phidianidines A and B (Figure 1.22) (Carbone et al., 2011). These compounds are known to exhibit potent *in vitro* cytotoxicity toward tumour and benign mammalian cell lines. Over the years, various synthetic oxadiazole derivatives were widely used in medicinal chemistry, dyestuff, corrosion inhibitors and electron-transport material for OLEDs (Srinivas et al., 2011; Wu et al., 2018; Siwach and Verma, 2020; Nadi et al., 2021).
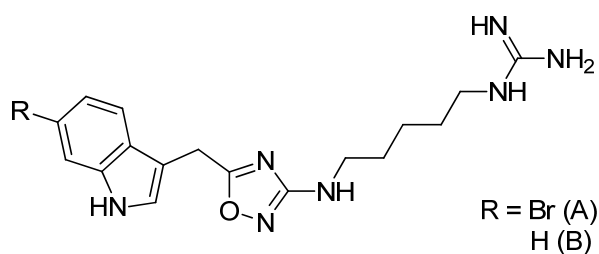
Phidianidine A or B

Figure 1.22 Natural products phidianidine A and B containing the 1,2,4-oxadiazole moiety

The 1,2,4- and 1,3,4-oxadiazole moiety was shown to have pharmacological activities (Figure 1.23). Some drugs with the 1,2,4-oxadiazole scaffold include ozanimod, an immunomodulating agent for the treatment of multiple sclerosis and ulcerative colitis; oxolamine, a cough suppressant; and ataluren, used for the treatment of Duchenne muscular dystrophy. Pleconaril, an investigational antiviral drug for the treatment of asthma and cold symptoms, has shown potential inhibitory activity to the SARS-CoV-2 spike protein (Calligari et al., 2020).

The only commercially available and FDA approved drug containing the 1,3,4-oxadiazole moiety is the antiretroviral raltegravir, used for the treatment of HIV, but now being repurposed for the treatment of SARS-CoV-2 (Indu et al., 2020). A few other lead compounds are undergoing investigational trials as potential therapeutic agents such as zibotentan (to treat

prostate cancer), freselestat (chronic obstructive pulmonary disease treatment), GSK-356278

(for Huntington's disease, anxiety, and depressive disorders) and GW-493838 (for neuropathic

pain) (Figure 1.23) (Wishart et al., 2018).
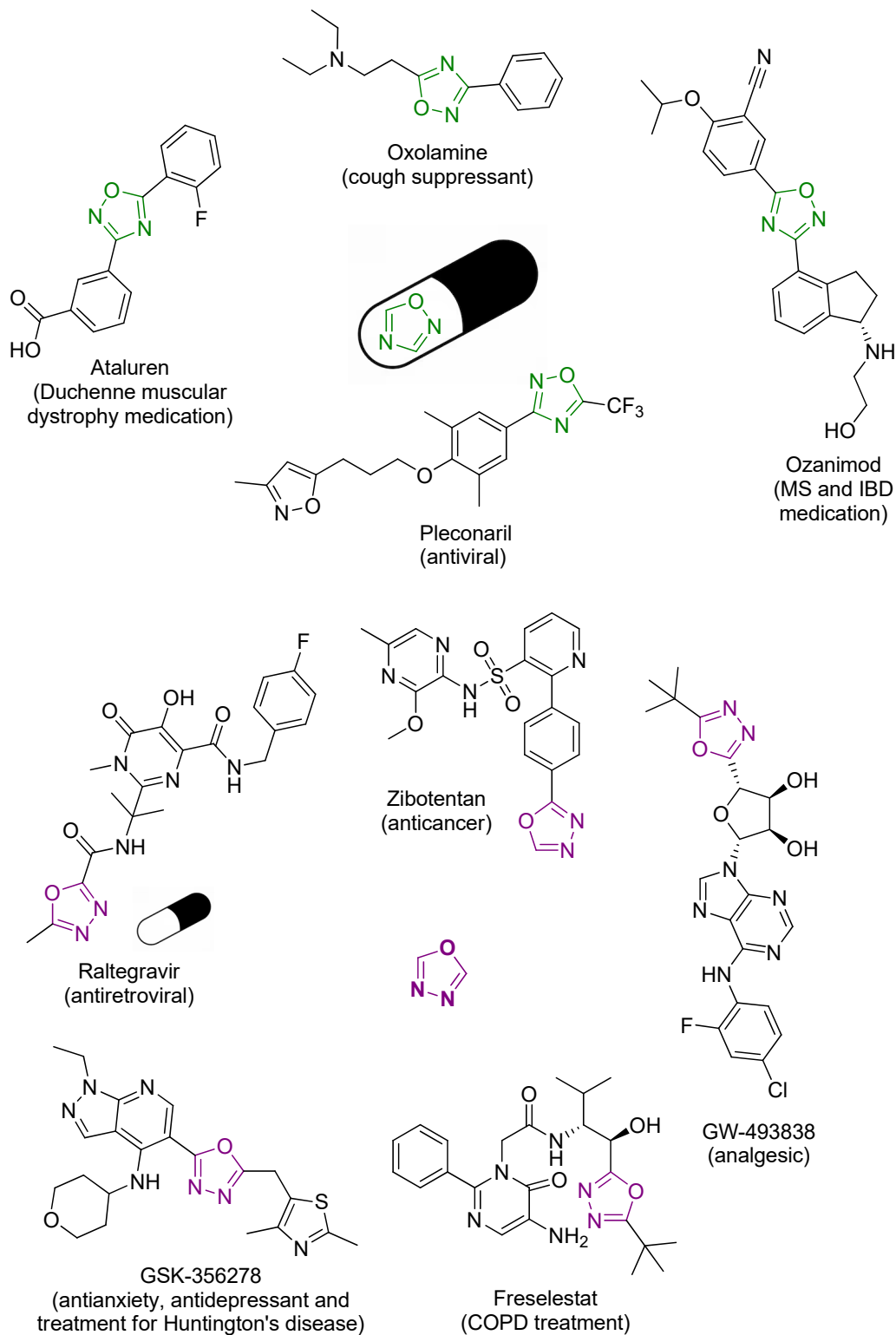
Figure 1.23 1,2,5- and 1,3,4-Oxadiazoles with pharmacological activity

1.3.2 Synthesis of oxadiazoles

The synthesis of 1,3,4-oxadiazoles has been popular, due to its broad spectrum of applications. For this reason, it was selected to be integrated onto the benzimidazole scaffold. Generally, 1,3,4-oxadiazoles were synthesised from acyl hydrazides (Scheme 1.19) via cyclisation with *ortho*-esters, oxidative one-pot reaction with benzoic acids, condensation with carbon disulphide, dehydrocyclisation of diacylhydrazides or the oxidation of acylhydrazones, *N*-acylsemicarbazides and acylthiosemicarbazides. Additionally, 1,3,4-oxadiazoles have been formed using other substrates such as semicarbazides to form semicarbazones, multicomponent reactions and the thermal decomposition of 5-substituted 1*H*-tetrazoles.
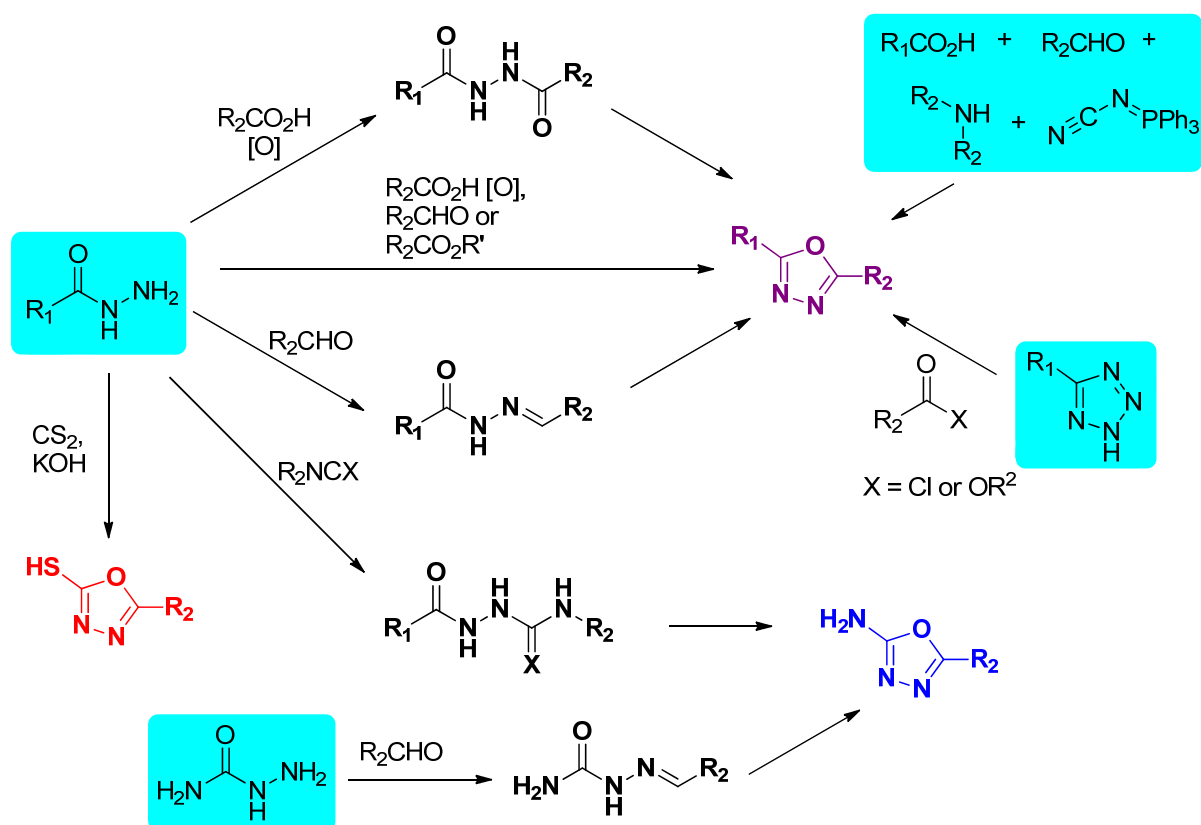
Scheme 1.19 Various synthetic pathways for the synthesis of 1,3,4-oxadiazoles

1.3.2.1 Acyl hydrazides and its derivatives

One-pot synthesis

Monosubstituted 1,3,4-oxadiazoles containing aryl or alkyl groups at position 2 (Scheme 1.20) was first reported in good yields by condensing aromatic acid hydrazide in excess ethyl orthoformate or the thermal ring closure of alkyl hydrazines (Ainsworth, 1955; Ainsworth and Hackler, 1966). Recently, Yin et al. (2018) presented that benzene-1,3,5-triyl triformate (TFBen) can be used as a carbon source in the presence of TFA as a catalyst. Interestingly, these monosubstituted derivatives have also been developed through the oxidative cleavage of C(sp)-H, C(sp^2)-H or C(sp^3)-H bonds via iodine-mediated direct annulation of hydrazides (Gao et al., 2015; Fan et al., 2016).
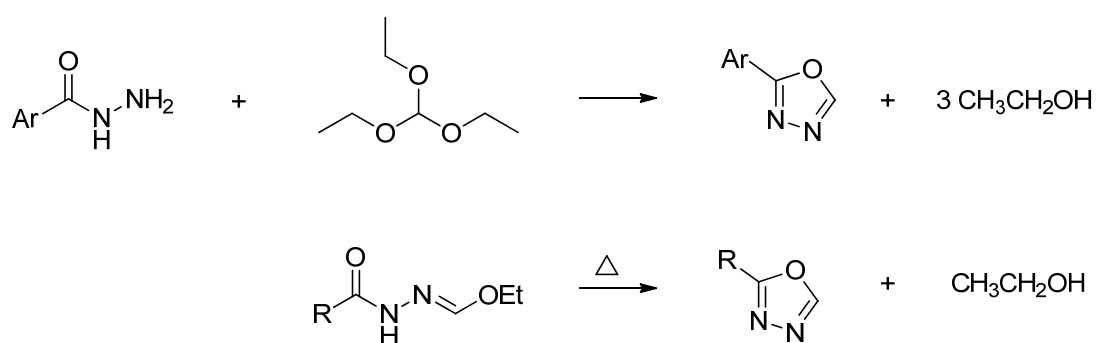
Scheme 1.20 Synthesis of mono-aryl or alkyl 1,3,4-oxadiazoles

Scheme 1.21 shows the proposed mechanism, whereby the substrates undergo iodination and oxidation to form the acyl iodide intermediate, which is then converted to glyoxal through the Kornblum oxidation with DMSO. The acid hydrazide and glyoxal react to generate the acyl hydrazone that undergoes iodisation via a potassium carbonate (K$_2$CO$_3$)-promoted reaction. The iodide intermediate then gets cyclised through an S$_N$2'-type reaction and aromatisation reactions to form the five-membered ring. Lastly, the acyl 1,3,4-oxadiazole undergoes deacylation in the presence of K$_2$CO$_3$.
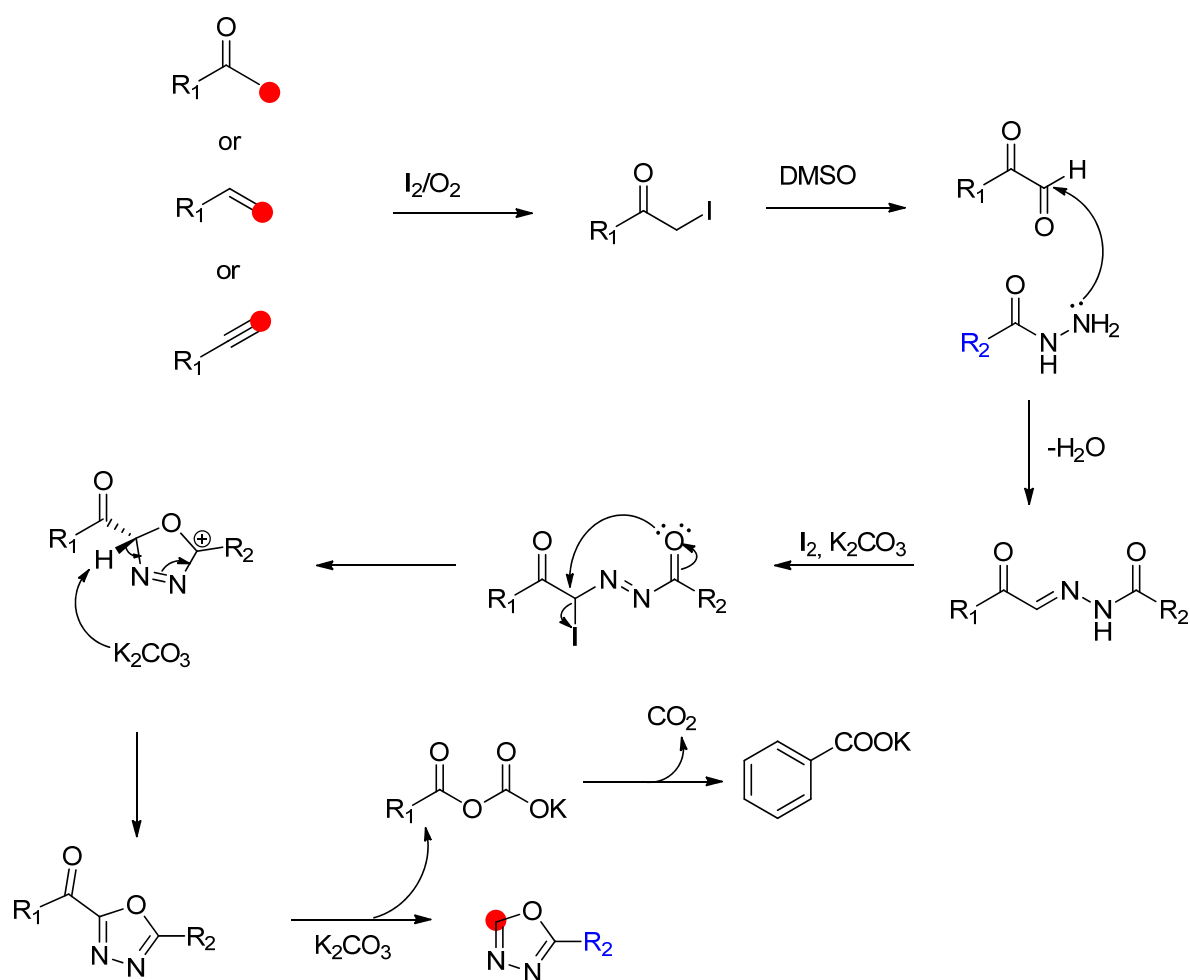
Scheme 1.21 Formation of 1,3,4-oxadiazoles via oxidative bond cleavage of C(sp)-H, C(sp^2)-H or C(sp^3)-H bonds

Disubstituted 1,3,4-oxadiazoles bearing various substituents at the 2 and 5 positions generally involve a one-pot synthetic approach from acyl hydrazide derivatives and carboxylic acids using a dehydrating agent such as phosphorus oxychloride (POCl$_3$). Chandrakantha et al. (2010) synthesised a series of 2-(2-fluoro-4-methoxyphenyl)-5-substituted-1,3,4-oxadiazoles by refluxing an acyl hydrazide with various aromatic carboxylic acids with POCl$_3$. This common reagent was also employed for the microwave-assisted phenyl-5-(2,3,5,6-tetrafluoro-phenyl)-[1,3,4]-oxadiazoles (Dhotre et al., 2020), 3-[5-(substituted phenyl)-[1,3,4] oxadiazol-

2-yl)-1*H*-indazole hybrid molecule (Raut et al., 2021) and newly discovered three-winged unique fan-like oxadiazoles (Rabie, 2021) (Scheme 1.22).

Other one-step ring-closing agents include coupling/cyclodehydration reagent Deoxo-Fluor (Kangani et al., 2006), the mild propylphosphonic anhydride (T3P®) (Augustine et al., 2009), a combination of HATU (coupling agent) and Burgess reagent (dehydrating reagent) (Li and Dickson, 2009), and the catalyst cerium (IV) ammonium nitrate (Behalo, 2016).

Chandrakantha et al. (2010)

Dhotre et al. (2020)

Raut et al. (2021)

Rabie (2021)
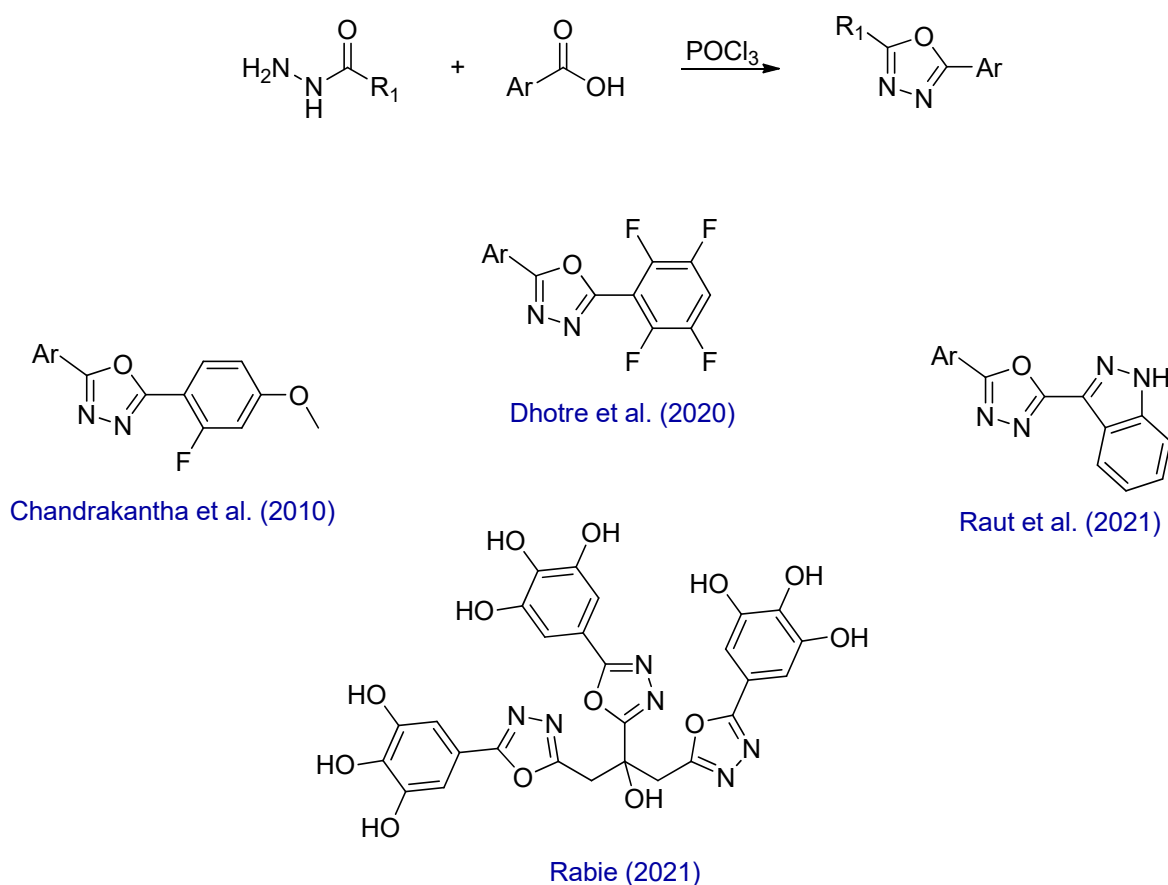
Scheme 1.22 Synthesis and structures of various 1,3,4-oxadiazoles using a dehydrating agent, POCl₃

Carbon disulphide (CS$_2$) is a sulfur source for 5-substituted-1,3,4-oxadiazole-2-thiols when reacted with acid hydrazides in a basic medium (Scheme 1.23). Jha et al. (2010) synthesised these sulfur-containing oxadiazoles by reacting aroylhyrazides in ethanol at 0°C with carbon disulphide and potassium hydroxide. Using the same reagents, a potential antitubercular agent 4-(5-mercapto-1,3,4-oxadiazol-2-yl)phenol was synthesised from 4-hydroxybenzohydrazide (Makane et al., 2019). As depicted in Scheme 1.23, the generation of thiol compounds can be subsequently converted into various thioethers (Kahl et al., 2019; Azizian et al., 2020; Song et al., 2021).
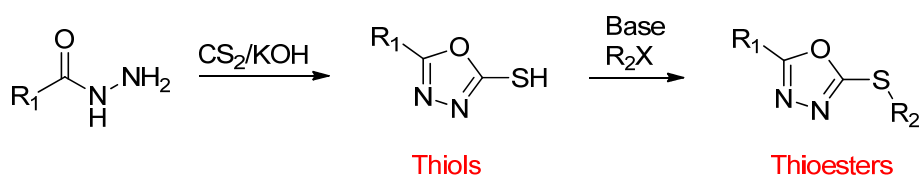
Scheme 1.23 Synthesis of 5-substituted-1,3,4-oxadiazole-2-thiols from carbon disulphide in basic media and subsequent reaction to thioesters

Diacylhydrazides

Diacylhydrazides are cyclised to 2,5-disubstituted 1,3,4-oxadiazoles using different reagents and catalysts (Scheme 1.24). Lashkari et al. (2020) described a method of using unsupported and supported phosphinium dibromide systems to prepare the oxadiazole derivatives. Nano-silica-anchored PPh$_2$/Br was more effective than Ph$_3$P/Br$_2$ due to the purification of an easier by-product (Ph$_2$PO) compared to the arduous triphenyl phosphine oxide (Ph$_3$PO). More conventional cyclising reagents used over the years include phosphorous oxychloride (POCl$_3$) (Wu et al., 2018), tosyl chloride (TsCl) and *N, N*-diisopropylethylamine (DIPEA) (Saglam et al., 2021), thionyl chloride (SOCl$_2$) (Mikhailov et al., 2020), trifluoromethanesulfonic

anhydride/pyridine (Tf$_2$O/Py) (Zabiulla et al., 2020), phosphorous pentoxide (P$_2$O$_5$) and polyphosphoric acid (PPA) (Du et al., 2019).

Scheme 1.24 The cyclisation of diacylhydrazides to form 2,5-disubstituted 1,3,4-oxadiazoles

N-acylhydrazones

N-acylhydrazones are cyclised to 1,3,4-oxadiazoles using various oxidising agents (Scheme 1.25). Garg and Raghav (2016) synthesised 2,5-disubstituted 1,3,4-oxadiazoles through oxidative cyclisation of *N*-acylhydrazones in dichloromethane with iodobenzenediacetate and acetic acid as a catalyst. However, a catalyst was not required when hypervalent phenyl iododiacetate (PhI(OAc)$_2$) was used (Taha et al., 2019). Hypervalent *in situ* iodine species were generated via the auto-oxidation of isobutyraldehyde to acyloxy radicals under an oxygen atmosphere that reacted with *p*-anisolyl iodide, to cyclise *N*-acylhydrazones into substituted oxadiazoles (Chauhan et al., 2019). Some acylhydrazones underwent dehydrogenative cyclisation using a palladium catalyst in the presence of caesium carbonate (Jiang et al., 2018). Milder reaction conditions were reported with the use of Dess-Martian periodinane or a biocatalyst, Cu(II)@DAC-Betti and K$_2$CO$_3$ in the presence of air (Dobrotă et al., 2009; Bahri et al., 2021).
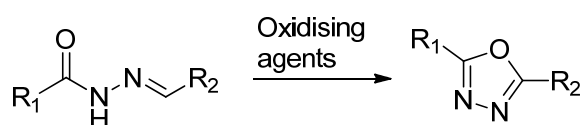
Scheme 1.25 Cyclisation of *N*-acylhydrazones to 2,5-disubstituted 1,3,4-oxadiazoles using oxidising agents

Semicarbazides

N-acylsemicarbazides and acylthiosemicarbazides are formed by a reaction with acyl hydrazides and isocyanate or isothiocyanate, respectively (Prabhu and Sureshbabu, 2012). These precursors are then cyclised using an appropriate reagent to form 2-amino-1,3,4-oxadiazoles (Scheme 1.26). 1-Cinnamonyl-4-phenyl and 1-oleyl-4-phenyl semicarbazides were subjected to a simple acid catalysed intramolecular cyclisation using sulfuric acid to afford substituted 1,3,4-oxadiazole (Scheme 1.26) in high yields of 78 and 89 % (Asghar et al., 2010). Vosátka et al. (2018) synthesised *N*-substituted 5-(pyridine-4-yl)-1,3,4-oxadiazol-2-amines in moderate yields of 52-68% with triphenylphosphine, 1,2-dibromo-1,1,2,2-tetrachloroethane and triethylamine (Et$_3$N) in the presence of an anhydrous solvent system (CH$_3$CN/THF).

Acylthiosemicarbazides have been reported to have higher reactivity than their semicarbazide analogues due to their significantly higher conversion under the same conditions - a tosyl chloride/pyridine-promoted cyclisation (Dolman et al., 2006). Li et al. (2019) presented a new procedure for synthesising 2-acylamino-1,3,4-oxadiazole derivatives from acylthiosemicarbazides in moderate to good yields using the desulfurising agent potassium oxide in water at 60°C. Recently, Aly et al. (2020) synthesised 5-(1,4(1,4)-dibenzenacyclohexaphane-1^2-yl)-*N*-substituted-1,3,4-oxadiazol-2-amines (60-68%) through the cyclisation of paracyclophanyl-acylthiosemicarbazides, using Et$_3$N in THF.
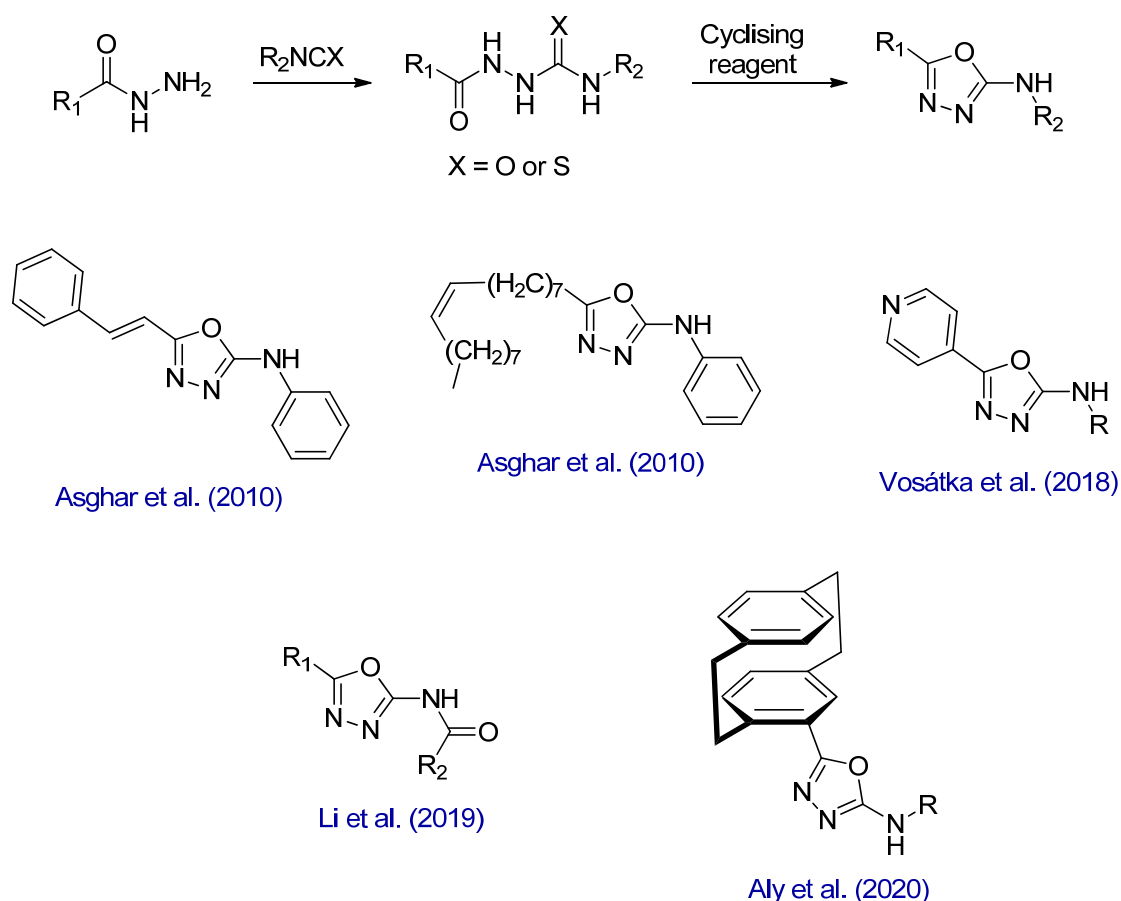
Scheme 1.26 Synthesis of semicarbazides followed by cyclisation to form 2-amino-1,3,4-oxadiazoles

1.3.2.2 Other substrates

Semicarbazones

Semicarbazones can be cyclised under various techniques to form 2-amino-1,3,4-oxadiazoles (Scheme 1.27). Lotfi et al. (2011) performed anodic oxidation on semicarbazone derivatives by using the supporting electrolyte lithium perchlorate (LiClO$_4$) through electrolysis. An ultrasound-assisted synthesis using *N*-bromosuccinimide (NBS) in sodium acetate afforded the products at elevated purities and satisfactory yields (57-92%); however, reacting the substrates in bromine, sodium acetate and acetic acid at 60°C for 2 hours resulted in a 70-95% yield (Borsoi et al., 2017; Kaur et al., 2019).

Scheme 1.27 Synthesis of 2-amino-1,3,4-oxadiazoles through various cyclisation techniques of semicarbazones

Multicomponent reactions

Multicomponent reactions (MCR) are considered advantageous over stepwise reactions, in view of the potential to generate various new chemical entities (NCEs) in a one-pot arrangement and are regarded as a more environmentally friendly process (few synthetic steps, energy usage, and waste creation) (Zhu et al., 2015; John et al., 2021). Ramazani and Rezaei (2010) presented a novel procedure for the synthesised α-amino 1,3,4-oxidazoles through an Ugi-4CR/aza-Wittig reaction. The four-component reaction involved odourless (*N*-isocyanoimino)triphenylphosphorane and selected secondary amines, carboxylic acids, and aromatic aldehydes in dichloromethane at ambient temperature without the use of a catalyst.

The probable mechanism (Scheme 1.28) published was the formation of the iminium ion through the condensation of the carboxylic acid with the benzaldehyde and secondary amine. The iminium ion is then thought to have undergone nucleophilic attack by the (*N*-isocyanoimino)triphenylphosphorane to form the nitrilium intermediate that the acid's conjugate base could have attacked to create a 1:1:1 adduct. The adduct then undergoes the aza-Wittig intramolecular reaction with the iminophosphorane moiety and the carbonyl group of the ester to form the five-membered ring. The phosphorane group reacts strongly with the oxide ion to form the triphenylphosphine oxide and the final 2,5-disubstitued 1,3,4-oxadiazole (Ramazani and Rezaei, 2010).
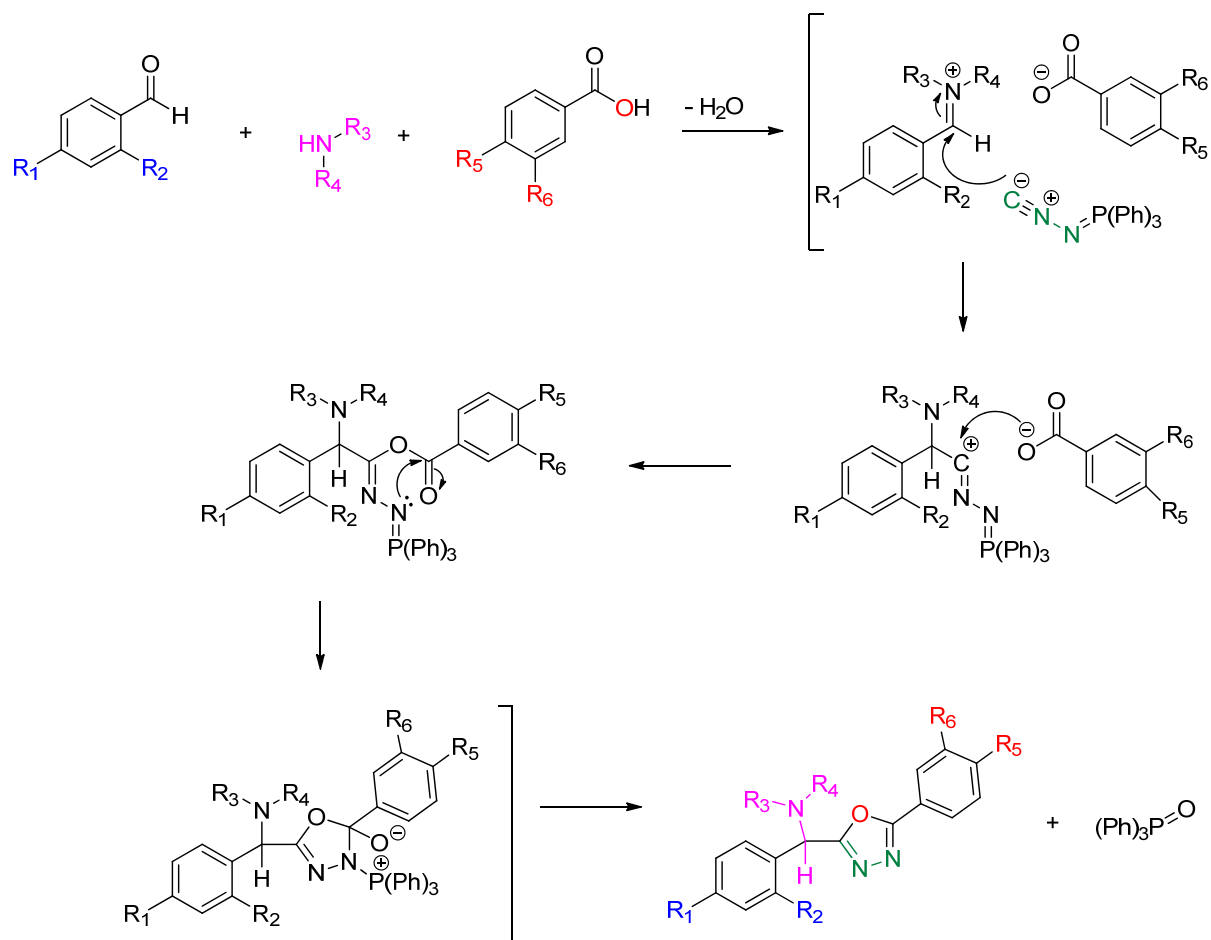
Scheme 1.28 Proposed mechanism for the synthesis of 2,5-disubstituted 1,3,4-oxadiazoles through an Ugi-4CR/aza-Wittig reaction

The synthesis of α-amino oxadiazoles using tertiary amides or lactams were performed in a three-component iridium-catalysed reductive coupling reaction (Scheme 1.29). The chemoselective Vaska's complex (IrCl(CO)(PPh$_3$)$_2$) and tetramethyldisiloxane (TMDS) were vital components for the formation of the iminium ion from the sterically hindered reagents (Matheau-Raven and Dixon, 2021). The construction of other 2,5-disubstituted 1,3,4-oxadiazole pharmacophores via MCR-based procedures have been reported. Sun et al. (2021) synthesised 5-(1,2,3,4-tetrahyroisoquinolin-1-yl)-1,3,4-oxadiazoles using a diethyl azodicarboxylate (DEAD)-promoted oxidative Ugi/aza-Wittig reaction. DEAD acts as both an oxidant to generate the key iminium ion and a base to form the carboxylate ion (Scheme 1.30).
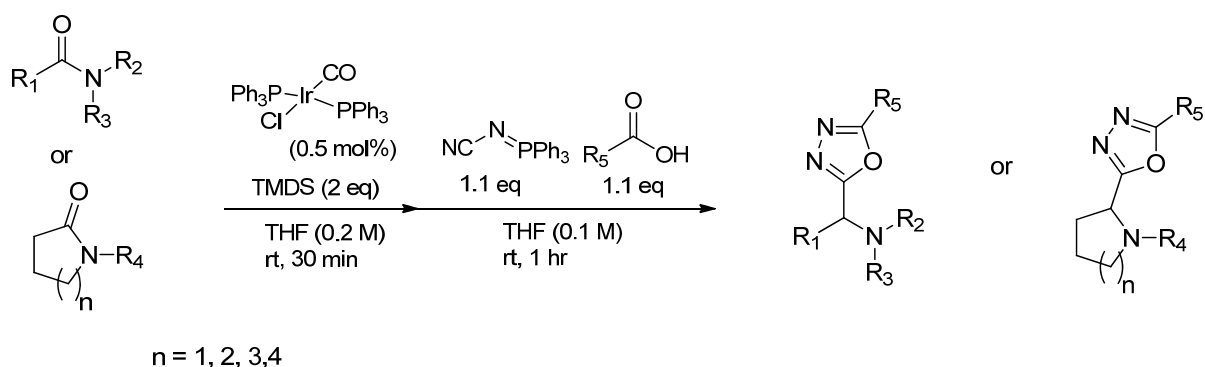
Scheme 1.29 Synthesis of α-amino 1,3,4-oxadiazoles via the functionalisation of lactams and tertiary amides
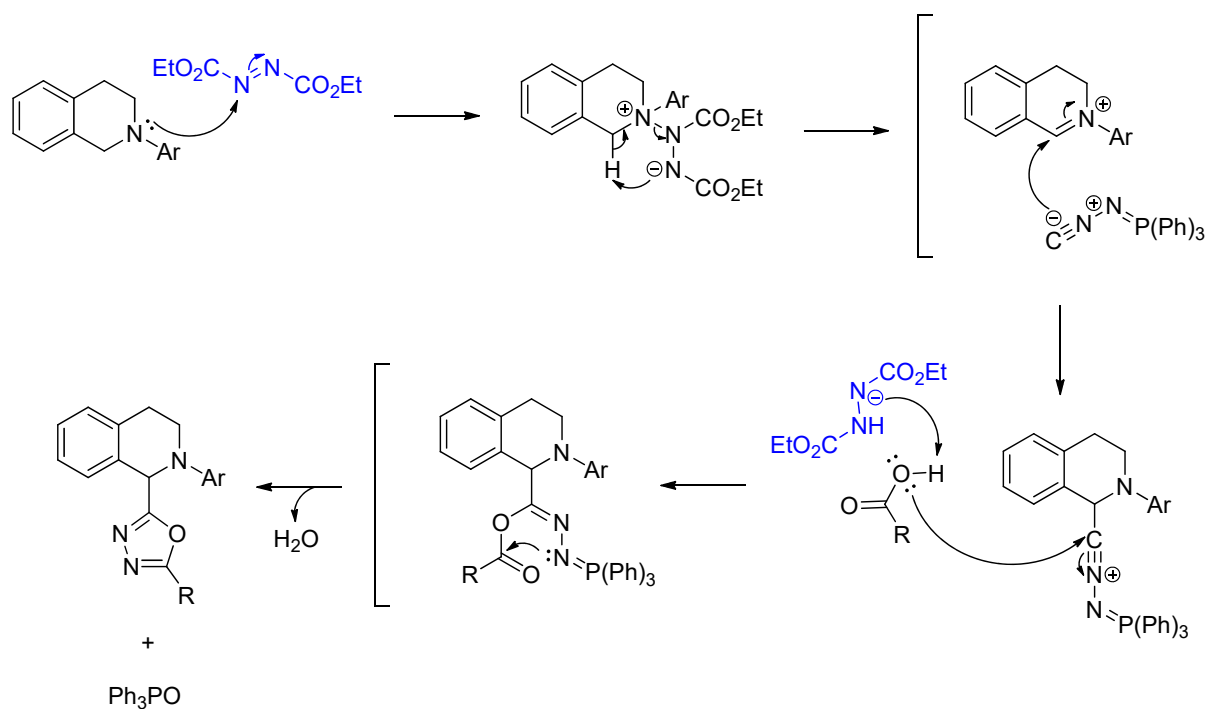
Scheme 1.30 Synthesis of 5-(1,2,3,4-tetrahyroisoquinolin-1-yl)-1,3,4-oxadiazoles through a DEAD-promoted oxidative Ugi/aza-Wittig reaction

Disubstituted 1,3,4-oxadiazoles can also be synthesised by the thermal decomposition of a 5-substituted 1*H*-tetrazole nucleus with electrophiles (acyl chlorides and anhydrides), generally known as the Huisgen reaction (Reichart and Kappe, 2012). A 1,5-dipole intermediate, nitrile

imine (Scheme 1.31), is formed by the elimination of nitrogen, which is further cyclised to form the 1,3,4-oxadiazole ring (Huisgen et al., 1958). The energy input to develop the nitrile imine was recently extended to include HTHP continuous flow and a UV-induced approach (Reichart and Kappe, 2012; Green et al., 2020).
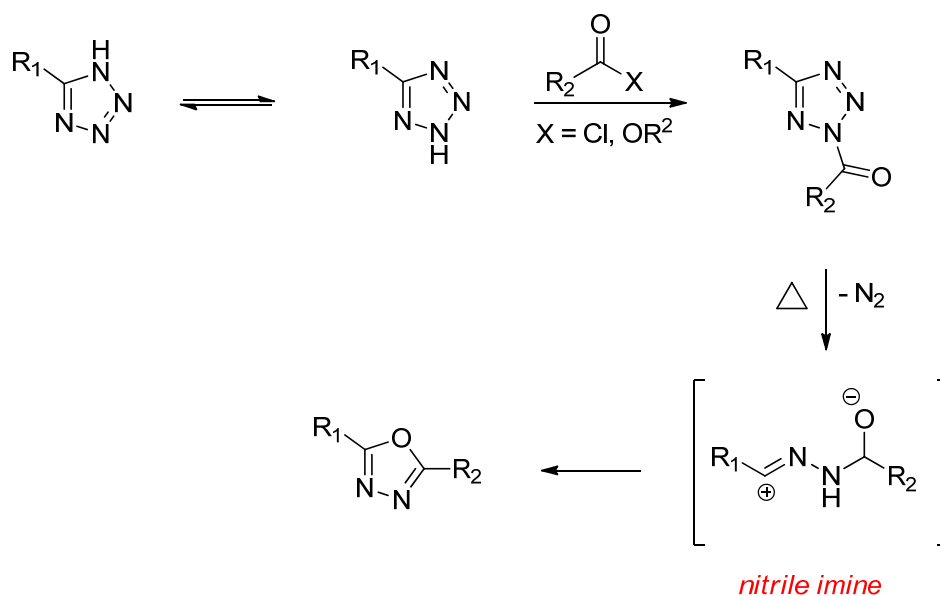
Scheme 1.31 Thermal decomposition of 5-substituted 1*H*-tetrazole to 2,5-disubstituted 1,3,4-oxadiazole

1.3.3   Bioactivity of oxadiazoles

The 1,3,4-oxadiazole ring is a potent pharmacophore; its possible pharmacological activities could be due to the toxophoric -N=C-O- linkage, hydrogen bond acceptor properties due to its π-stacking interactions and capability to bind to ligands (Siwach and Verma, 2020; Glomb and Świątek, 2021). Furthermore, oxadiazoles are considered as bioisostere replacements of amides and esters of drug molecules. The introduction of the ring is known to improve the pharmacokinetics and *in vivo* activity due to the increase in metabolic stability and reduction in lipophilicity that increases the water solubility in a molecule compared to the other isomers (Boström et al., 2011; Wang et al., 2019a).

Antibacterial

Three different 1,3,4-oxadiazole derivatives (**1.41**-**1.43** in Figure 1.24) exhibited antibacterial activity against Methicillin-resistant and susceptible *S. aureus*, with MIC values of 4-32 µg mL^{-1} for planktonic cells and a dose-dependent manner was observed for biofilms of 8-32 µg mL^{-1} (Zheng et al., 2018). However, the standard vancomycin had better MIC values against the strains, with compounds **1.41** and **1.42** being comparable only against MRSA USA300 (4 µg mL^{-1}). A series of 2-acylamino-1,3,4-oxadiazoles showed no significant antibiotic activity against *E. coli,* but compound **1.44 a** with a nitro group at R_1 and methyl group R_2 was active against *S. aureus* with an MIC of 1.56 mg mL^{-1} (Li et al., 2019). The other two compounds, **1.44 b** and **c** had higher activity toward *B. subtilis* (MIC of 0.78 mg mL^{-1}), although the positive control, Levofloxacin, remained a better antibacterial agent with MIC 0.05 and 0.20 mg mL^{-1} against *S. aureus* and *B. subtilis* respectively.

Oxadiazole hybrid molecules clubbed with isoxazole **1.45** showed enhanced activity against Gram-positive and -negative bacteria than the standard Ampicillin (Shingare et al., 2018). Guo et al. (2019) designed a new class of norfloxacin-1,3,4-oxadiazole hybrids **1.46** with most of the target molecules displaying equal or improved activity against clinical drug-resistant MRSA isolates compared to their antibiotic precursor norfloxacin and standard vancomycin. The derivative with a methoxy group at the *meta*-position demonstrated superior time-kill kinetics and damaged bacterial membranes after a short period. Moreover, this compound had low cytotoxicity with an IC$_{50}$ value of >200 µg mL^{-1} to normal rat kidney tubular epithelial cells (NRK-52E).
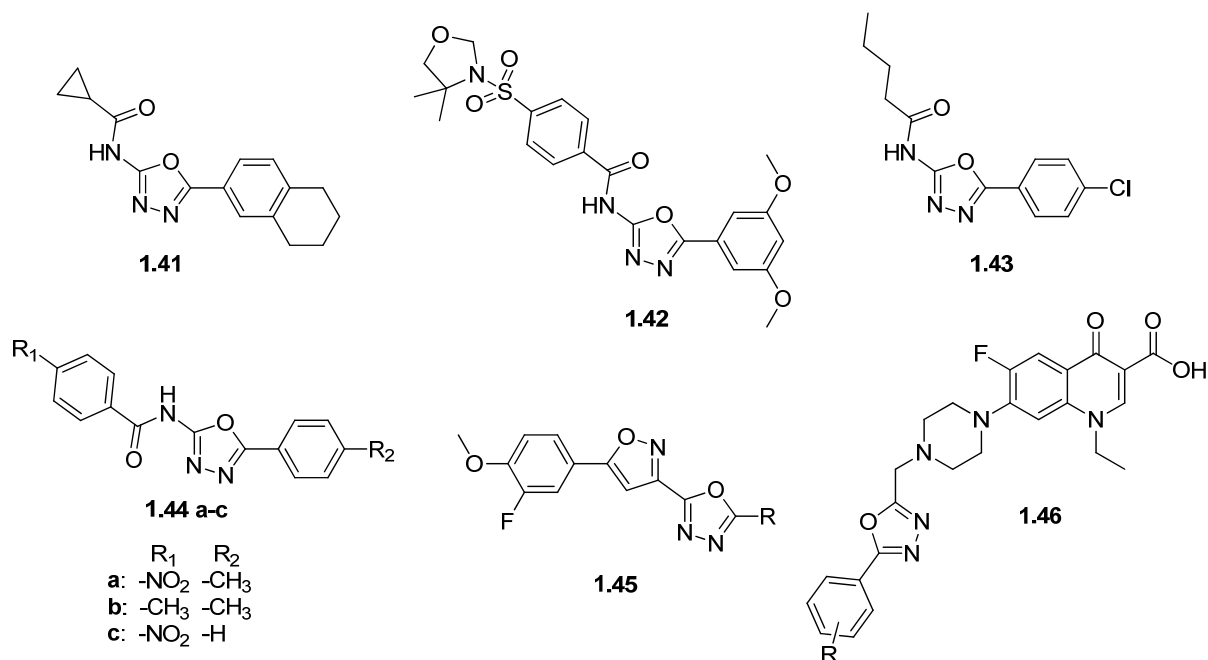
Figure 1.24 2,5-Disubstituted 1,3,4-oxadiazoles with antibacterial activity

Anticancer

Target therapy is a promising strategy in treating cancer by inhibiting proteins and genes responsible for cancer cell survival and growth. Chemotherapeutic agents 2,5-diaryl-1,3,4-oxadiazoles exhibited a strong cytotoxic effect against colon adenocarcinoma (HT-29) and breast adenocarcinoma (MDA-MB-231) than cisplatin and doxorubicin. Compound **1.47** (Figure 1.25) showed the most favourable impact from the series with low toxicological risks. According, to predictive studies, the probable targets for the compounds are through the inhibition of STAT3 and interaction with miR-21 (Stecoza et al., 2021). A lead compound **1.48** presented potential antiproliferative effects against HCCLM3 cells with an IC$_{50}$ of 27.5 μM with *in vitro* and *in silico* results demonstrated that NF-κB signalling was the target (Mohan et al., 2018).

The oxadiazole **1.49** proved to be a potent antiproliferative agent against renal cancer (UO-31) with IC$_{50}$ of 5.7 nM, more cytotoxic than doxorubicin (7.4 nM). This compound even displayed

epidermal growth factor receptor (EGFR) inhibition of two-fold potency greater than erlotinib and could have interacted with essential amino acids (Met769 and Leu768) present in the ATP binding pocket of the kinase enzyme (El-Sayed et al., 2019). Compound **1.50** had superior cytotoxicity effects against human lung adenocarcinoma A549 and C6 rat glioma with excellent interactions and binding affinities in Akt and FAK active sites (Altıntop et al., 2018). *In silico* ADME predicted that compounds **1.49** and **1.50** (Figure 1.25) could be further developed as potential orally available anticancer drugs.

1.47

STAT3 and miR-21
inhibitors

1.48

NF-κB
inhibitor

1.49

EGFR
inhibitor

1.50
Akt and FAK
Inhibitors
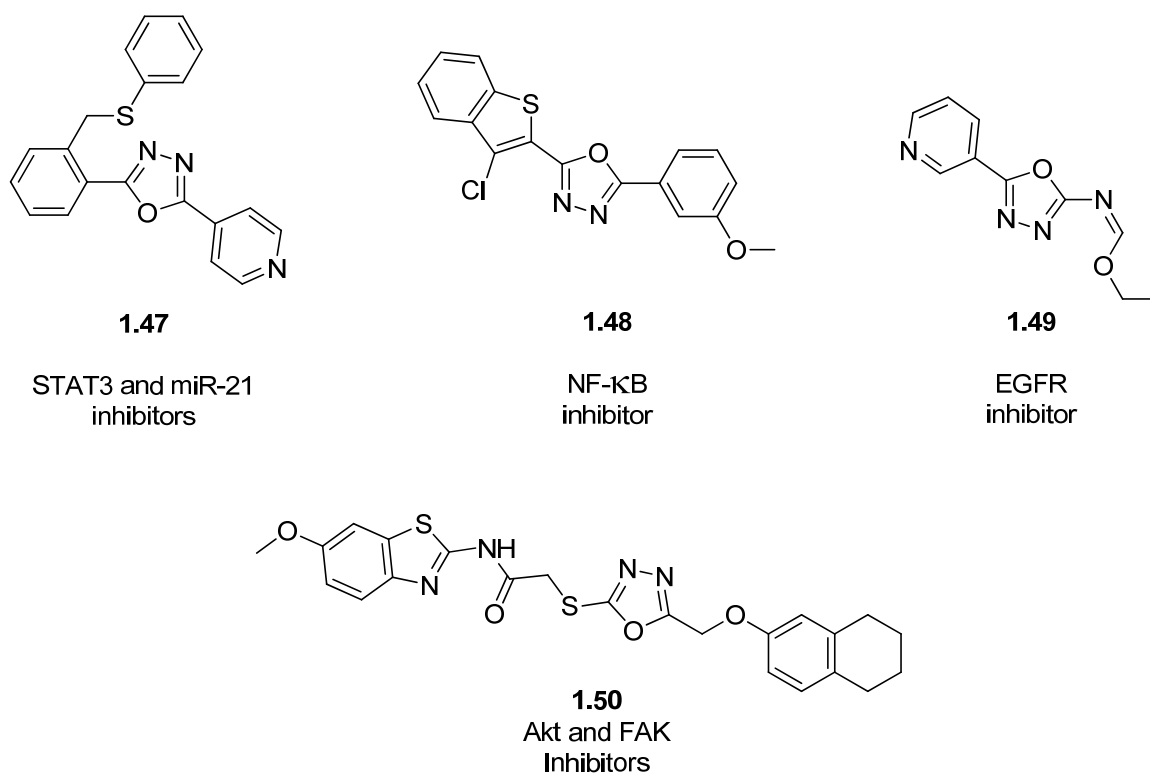
Figure 1.25 Potential chemotherapeutic agents containing the 2,5-disubstituted 1,3,4-oxadiazole moiety

Antiviral

Reverse transcriptase inhibitors **1.51 a-b** (Figure 1.26) possessed C-nucleoside analogues D-galactopentitolyl and D-xylotetritolyl. The free hydroxyl group present on the 1,3,4-

oxadiazolylthio sugar hydrazone **1.51 b** increased antiviral activity to an IC$_{50}$ of 1.44 μM (El-Sayed et al., 2009). HIV integrase inhibitors are another approach as the nitrogen atoms in the 1,3,4-oxadiazole moiety are involved in Mg^{2+} chelation (Alimi Livani et al., 2018; Parizadeh et al., 2018). Diazocoumarins were designed to mimic integrase strand transfer inhibitors (INSTIs), and compound **1.52** displayed anti-HIV activity at 100 μM with a 52% inhibition rate of p24 expression, which was close to the standard AZT of 58% (Alimi Livani et al., 2018). Molecular docking studies revealed that the 4-chlorobenzyl group sits in the same active site and position as the 4-fluorobenzyl group in raltegravir.

Zuo et al. (2016) synthesised several hepatitis C virus (HCV) inhibitors with **1.53** presenting potent activity with an EC$_{50}$ value of 39 nM and without cytotoxic effects (CC$_{50}$ >10 μM). *S*-benzyl- and *S*-alkylphthalimide hybrids (**1.54 a-b** in Figure 1.26) were discovered as potential dengue protease inhibitors, displaying IC$_{50}$ values of 13.9 and 15.1 μM (Hamdani et al., 2020). According to computational studies, the hybrids repress the virus by occupying the allosteric cleft of the protease.
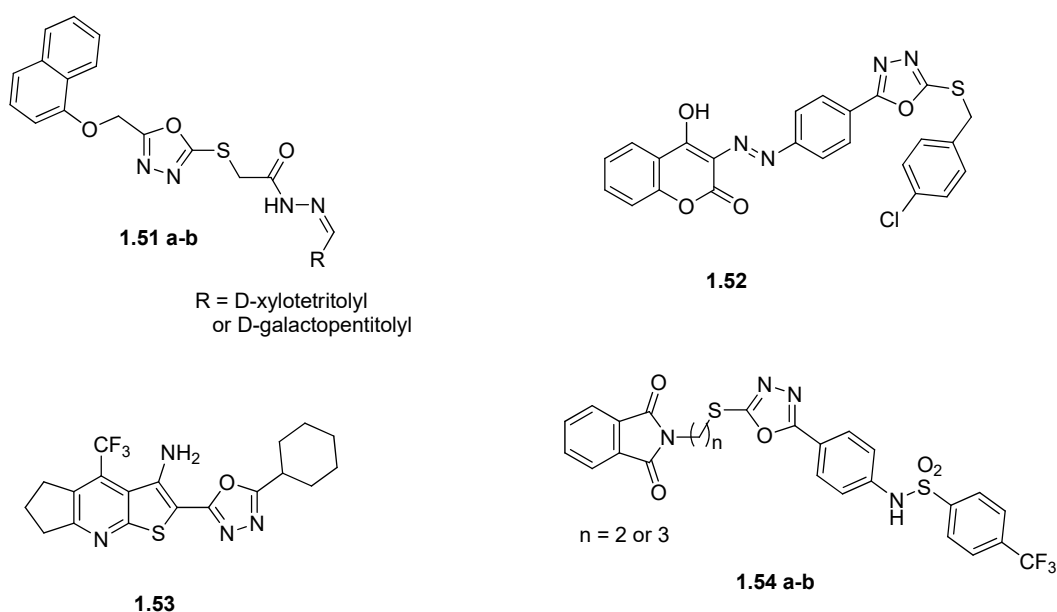
Figure 1.26 Antiviral agents containing the 1,3,4-oxadiazole moiety

Antitubercular

Some 1,3,4-oxadiazole molecules have been designed with the oxidative cyclisation of isoniazid (INH) with other pharmacologically active scaffolds. Khan et al. (2017) synthesised novel 2,5-disubstituted-1,3,4-oxaidazoles **1.55 a-d** by cyclising INH with four different fluoroquinolones (ciprofloxacin, norfloxacin, gatifloxacin and ofloxacin) using POCl3 (Scheme 1.32) with the expectation that the compounds would have lower toxicity than INH. The MICs of the four oxadiazoles tested against MTB-H$_{37}$R$_V$ were 6.25 µg mL^{-1}, comparable to its precursor INH (3.12 µg mL^{-1}).
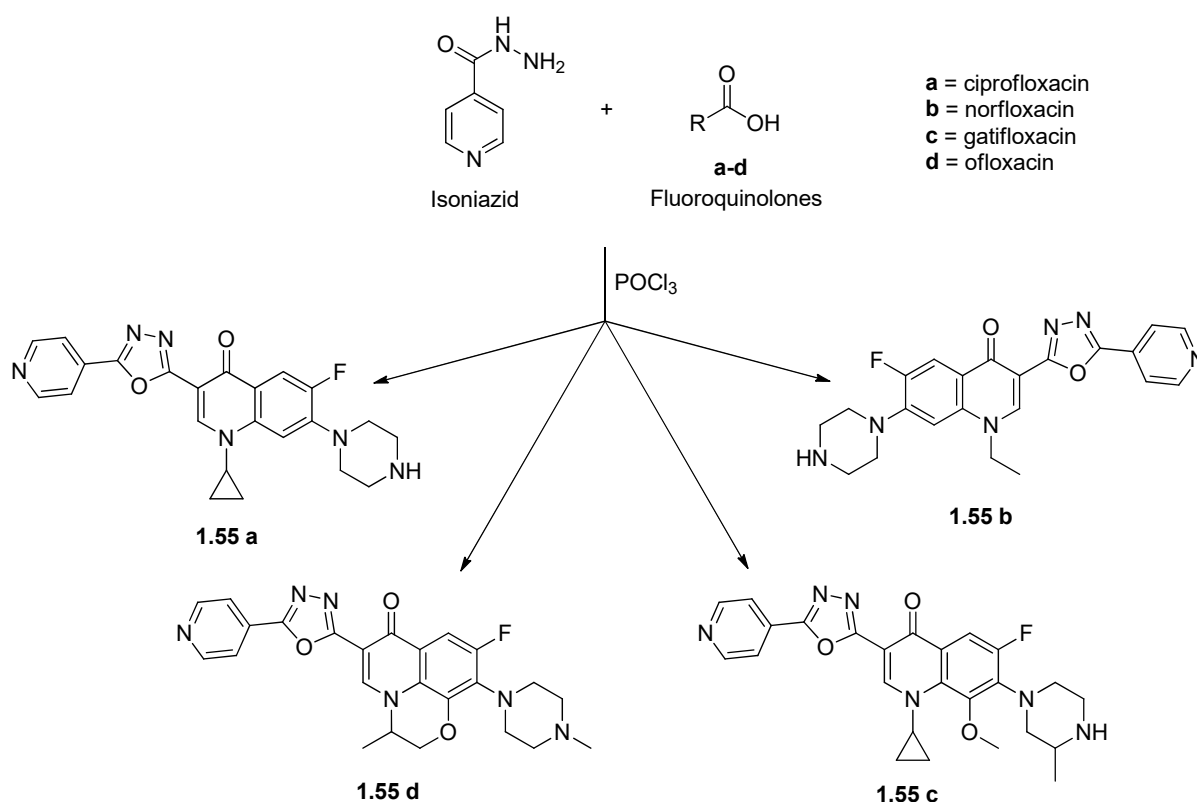
Scheme 1.32 Synthesis of 1,3,4-oxadiazoles from the hybridisation of INH with fluoroquinolones

N-dodecyl-5-(pyridine-4-yl)1,3,4-oxadiazol-2-amine **1.56** (Figure 1.27) was synthesised from INH precursor, previously mentioned in the synthesis of semicarbazides, and inhibited the

growth of susceptible and multidrug-resistant (MDR) and extensively drug-resistant (XDR) *M. tuberculosis* strains with MIC values of 4-8 µM. Additionally, the compound is a potential drug for resistant-TB as its mode of action is INH-independent, and it does not show cross-resistance to other clinical drugs (Vosátka et al., 2018).

The antitubercular activity of 1,3,4-oxadiazoles bearing benzofuranylamide was evaluated against *M. tuberculosis* H$_{37}$Ra (ATCC 25177) (Tambe et al., 2018). The 2-trifluoromethyl phenyl acetylene derivative (**1.57 a** in Figure 1.27) had a moderate activity with an IC$_{50}$ value of 8.8 µg mL^{-1} and an improvement in activity of 2.8 µg mL^{-1} was reported when the trifluoromethyl group was in the *para*-position (**1.57 b**). According to molecular docking, the mechanism of action follows the same pathway as INH through the inhibition of the InhA enzyme responsible for the biosynthesis of mycolic acid (required for the synthesis of the cell wall). Dhumal et al. (2016) assessed 2-pyridinyl substituted thiazolyl-5-aryl-1,3,4-oxadiazoles against the H$_{37}$Ra strain with poor IC$_{50}$ values >30 µg mL^{-1}. A few compounds from the set with electron-donating and withdrawing group at the *ortho*-position (**1.58 a-d**) showed inhibitory activity against the *M. bovis* BCG strain with concentrations <3 µg mL^{-1}.
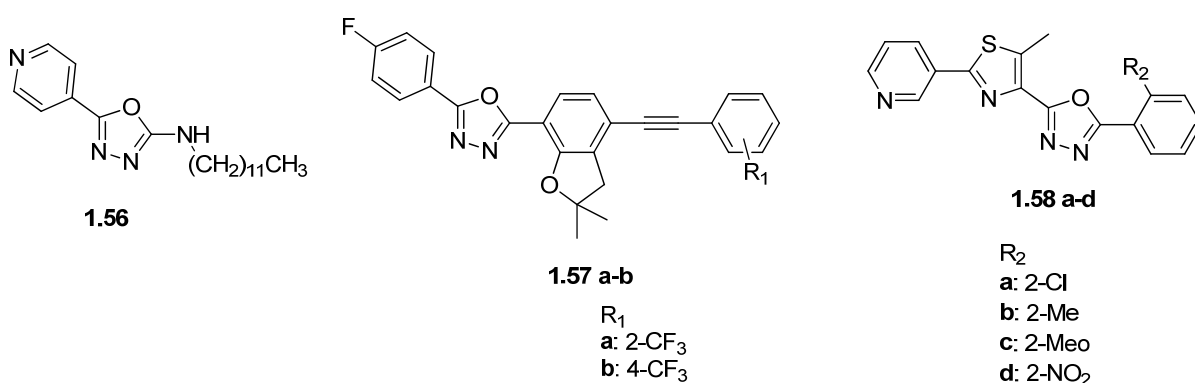
Figure 1.27 Structures of potential antitubercular agents

Antifungal

Two 1,3,4-oxadiazoles (**1.59** and **1.60** in Figure 1.28) were evaluated for their antifungal activity against *Candida albicans,* with both compounds having MICs of 32 μg mL^{-1}. The mechanism of action determined through SEM and TEM images showed that the compounds inhibited thioredoxin reductase and affected the fungal cell internally. Moreover, these compounds exhibited low cytotoxicity with a reduction in spleen and renal fungal burden (Capoci et al., 2019). Ultrasound-assisted, 5-(4-fluorophenyl)-1,3,4-oxadiazole-2-thiol (**1.61 a**) had a minimum fungicidal concentration (MFC) of 4 μg mL^{-1}, eight-fold better than the positive control terbinafine. In contrast, the 3-bromo derivative (**1.61 b**) showed similar activity against *C. albicans* of 64 μg mL^{-1} (Yarmohammadi et al., 2021).

A library of isoxazole-substituted-1,3,4-oxadiazoles (**1.62 a-k**) showed significant toxicity to selected pathogenic fungi *Aspergillus niger*, *Chrysosporium tropicum*, *Rhizopus oryzae*, *Fusarium moniliforme* and *Curvularia lunata* at 100 μg mL^{-1} in comparison to the reference drug clotrimazole (Marri et al., 2018). Compounds **1.62 b, d** and **f** exhibited remarkable growth inhibition, which could be attributed to the 4-chloro, 4-nitro and 3-bromo substituents. Furthermore, **1.62 d** had superior activity against all the fungal strains except for *C. lunata*, on account of **1.62 f**.
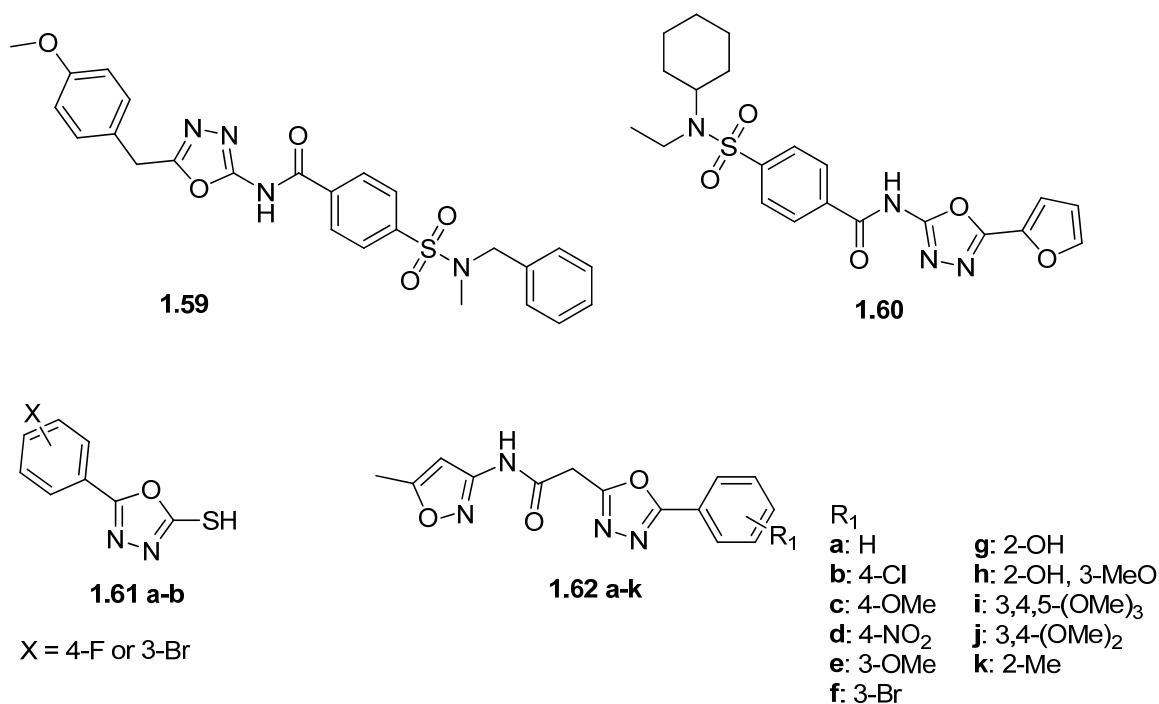
Figure 1.28 Structures of 1,3,4-oxadiazoles with antifungal activity

Plant pathogenic fungi are a major concern in agriculture, and 1,3,4-oxadiazoles can be used in disease control. 2-Ferrocenyl-5-aryl-1,3,4-oxadiazoles (**1.63** in Figure 1.29) displayed potent activity against *Gibberella nicotiancola*, *Gibberella saubinettii* and *Fusarium oxysporum f. sp. Niveum* at 125 µg mL^{-1} than the antifungal hymexazol (Ge et al., 2019). The presence of electron-donating groups, 4-methyl and 4-methoxy, on the phenyl moiety, increases the activity against *G. saubinettii* (EC$_{50}$ = 0.008 µg mL^{-1}) and *F. oxysporum f. sp. Niveum* (EC$_{50}$ = 2 ng mL^{-1}), whereas 4-fluoro was more selective to *G. nicotiancola* (EC$_{50}$ = 3 ng mL^{-1}). Wen et al. (2019) synthesised a resveratrol-inspired, 1,3,4-oxadiazole-thiophene-containing stilbene (**1.64**) with an EC$_{50}$ of 155.4 and 248.2 µg mL^{-1} against *Botrytis cinerea* and *Colletotrichum lagenarium*, more superior to resveratrol (263.1 and 342.6 µg mL^{-1}).
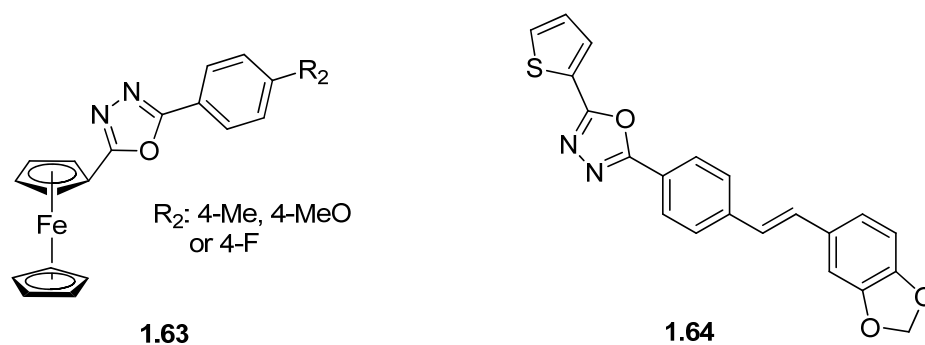
Figure 1.29 Plant pathogenic antifungals containing the 1,3,4-oxadiazole moiety

Antidiabetic

A small library of 7-azaindole based 1,3,4-oxadiazoles were screened for their α-glucosidase potential. The derivative containing a 3-trifluoromethyl group had a noteworthy IC_{50} value of 0.46 μM from the series (**1.65** in Figure 1.30) (Izgi et al., 2022). Potential anti-hyperglycaemic agent (**1.66**) displayed effective glucose reduction to 157.15 mg dL^{-1} than the standard drug pioglitazone (154.39 mg dL^{-1}) and had excellent α-glucosidase inhibition of 0.21 μM (Bhutani et al., 2019). Selvaraj et al. (2019) presented a sulfonamide-1,3,4-oxadiazole bearing an indole moiety (**1.67**) that was capable of targeting and inhibiting the α-amylase enzyme with an IC_{50} of 2.34 μM, comparable to the standard drug acarbose (2.53 μM).
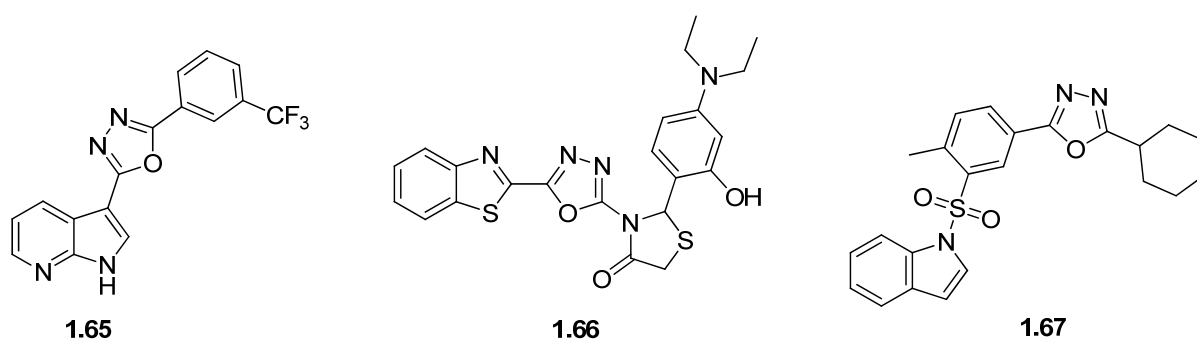
Figure 1.30 Chemical structures of potential antidiabetic agents

1.4 Benzimidazole-oxadiazole hybrids – synthesis and bioactivity

The synthesis of benzimidazole-oxadiazole hybrids generally occurs with cyclising an acyl hydrazide group attached to various positions of the benzimidazole scaffold with different carbon sources and reagents such as substituted benzoic acids and the dehydrating agent $POCl_3$ or carbon disulphide in basic media (Rathore et al., 2017; Karaburun et al., 2019). Intramolecular cyclisation of benzimidazole hydrazones has also been performed using acetic anhydride and phenyliodoacetate (Ibrahim et al., 2018; Taha et al., 2020). The incorporation of five-membered oxadiazole moieties onto the benzimidazole scaffold resulted in compounds with superior bioactivity.

Desai and Kotadiya (2014) synthesised benzimidazoles bearing 1,3,4-oxadiazole derivatives at position 2 of the scaffold with excellent antimicrobial activity. Compounds with fluoro and nitro groups in the *para*-position of the phenyl group (**1.68 a-b** in Figure 1.31) exhibited potent antibacterial activity against two Gram-positive and two Gram-negative bacteria, *S. aureus*, *S. pyogenes*, *E. coli* and *P. aeruginosa*, respectively, with MIC values lower (<25 μg mL^{-1}) than the antibiotic chloramphenicol (50 μg mL^{-1}). Furthermore, these compounds had good antifungal activity, ten-fold more active against *C. albicans* and two-fold higher against *A. niger* and *A. clavatus* compared to griseofulvin.

Benzimidazoles containing a 1,3,4-oxadiazole moiety at position 1 (**1.69 a-b** in Figure 1.31) were screened for their antimicrobial, antitubercular and antioxidant activities (Bhati et al., 2020). Compound (**1.69 a-b**) with a nitro group in the *meta*-position had comparable antibacterial activity to the standard drug streptomycin, moderate antifungal activity against *Aspergillus parasiticus* (MIC of 25 mg mL^{-1}) and potent DPPH scavenging activity with IC$_{50}$ of 24.85 μg mL^{-1} in comparison to ascorbic acid (62.91 μg mL^{-1}). Superior antitubercular

activity of 1.60 µg mL^{-1} was noted for the unsubstituted aryl compound compared to first-line drugs pyrazinamide and streptomycin (3.12 and 6.25 µg mL^{-1}) and second-line drug ciprofloxacin (3.12 µg mL^{-1}).
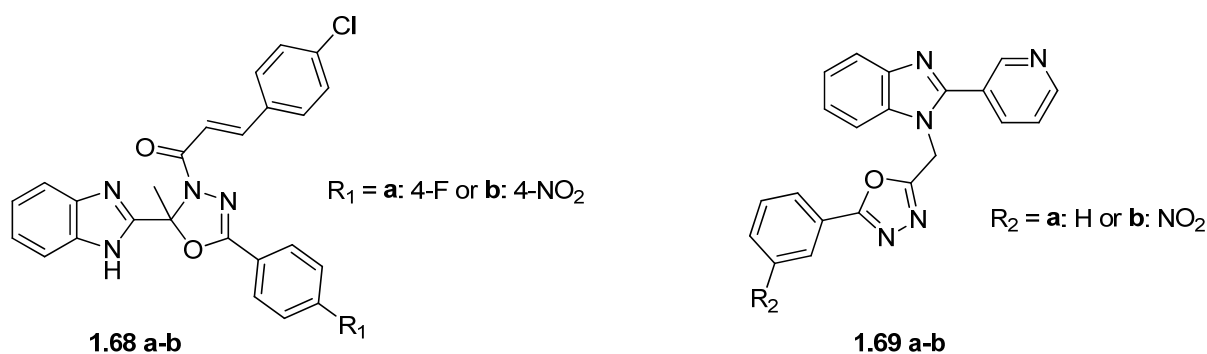
Figure 1.31 Chemical structures of benzimidazole-oxadiazole hybrids possessing various biological activities

Several benzimidazole-oxadiazole have been introduced as potential inhibitory agents because of the interactions and binding modes to specific pockets in the enzymes. Zawawi et al. (2015) synthesised *β*-glucuronidase inhibitors (**1.70** in Figure 1.32) with IC$_{50}$ values of 2.14 - 46.14 µM, more effective than D-saccharic acid 1,4-lactone (48.4 µM). A few benzimidazole-oxadiazoles (**1.71 a-d**) were identified as possible *α*-glycosidase inhibitors with IC$_{50}$ values of 2.6 - 9.50 µM, more effective than the reference acarbose 38.45 µM (Taha et al., 2020). Tantray et al. (2016) synthesised hybrids (**1.72**) that had GSK-3β inhibitory activity with sub-micromolar IC$_{50}$ values and displayed good antidepressant activity.

Benzimidazole-oxadiazoles have been reported to exhibit intense cytotoxic activities to selected cancer cell lines (Acar Çevik et al., 2020; Katikireddy et al., 2021). Compounds (**1.73 a-h** in Figure 1.32) were determined as human topoisomerase type I inhibitors owing to the interaction with the DNA topoisomerase I enzyme and had similar activity as the known

inhibitor camptothecin (Acar Çevik et al., 2020). Benzimidazole-1,3,4-oxadiazol-2-*N*-alkyl/aryl amines containing chloro substituents (**1.74 a-c**) were identified as EGFR inhibitors due to fundamental interactions similar to the standard doxorubicin (Katikireddy et al., 2021).

1.70
β-glucuronidase inhibitors

1.71 a-d
α-glycosidase inhibitors

R_1
a: 2,3-OH
b: 2,5-OH
c: 3,4-OH
d: 4-F

1.72
GSK-3β inhibitors

1.73 a-h
Topoisomerase type I inhibitors

	R_1	R_2
a: -OH or **e**: -OC$_2$H$_5$		-CH$_3$
b: -OH or **f**: -OC$_2$H$_5$		-C$_2$H$_5$
c: -OH or **g**: -OC$_2$H$_5$		
d: -OH or **h**: -OC$_2$H$_5$		

1.74 a-c
EGFR inhibitors

R_3
a: ClCH$_2$CH$_2$-
b: 4-ClC$_6$H$_4$-
c: 2,4-(Cl)$_2$C$_6$H$_3$-
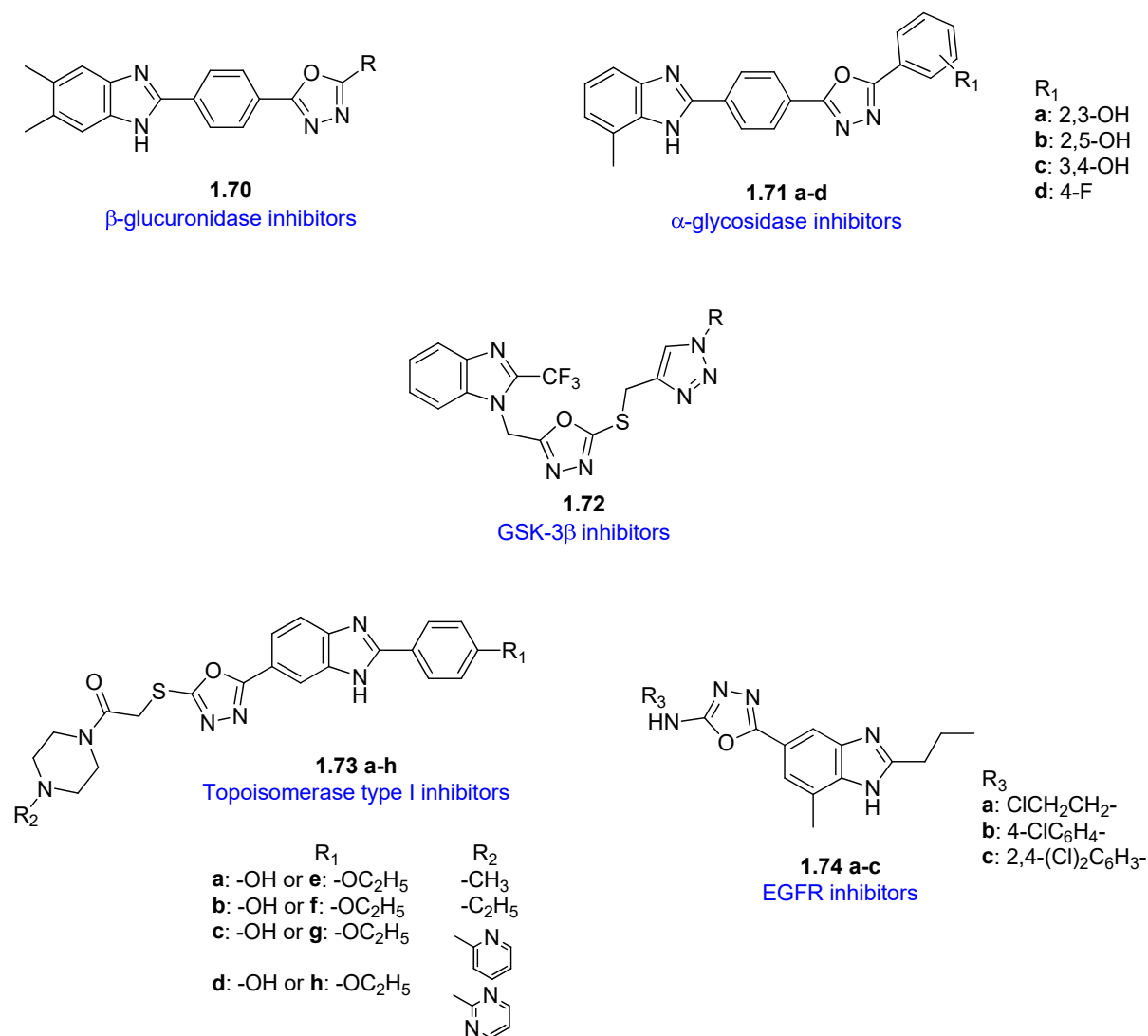
Figure 1.32 Benzimidazole-oxadiazole hybrids with inhibitory activity

75

1.5   Hypothesis, aims and objectives

Hypothesis

Given that benzimidazoles and oxadiazoles are privileged heterocycles with individual modes of action and activity against various biological targets, it is hypothesised that the hybridisation of these two pharmacophores with different electron-withdrawing and electron-donating substituents on the scaffolds may result in the identification of a potential hit molecules with antibaterial activity to tackle the rise in antimicrobial resistance.

Aim

To identify antibacterial hit molecules from a series of benzimidazole-oxadiazole hybrids.

Objectives

1.   To synthesise a small library of benzimidazole-oxadiazole hybrids

2.   To characterise the synthesised compounds using nuclear magnetic resonance spectroscopy and mass spectrometry.

3.   To determine the antibacterial activity of the synthesised compounds.

4.   To identify hit compounds that can be developed further into an antibacterial drug.

Chapter 2 Results and Discussion

This chapter reports on the synthesis of the benzimidazole-oxadiazole hybrids, its design, failed attempts at other schemes, the structural elucidation of the library of synthesised compounds and their antibacterial activity.

2.1 Failed and trial reactions

2.1.1 Benzimidazole dipeptides

The initial idea was to couple *N*-protected dipeptides to the benzimidazole moiety **A** (Scheme 2.1). The dipeptides were formed through a benzotriazole mediated solution phase technique as reported in Ibrahim et al. (2011) (Scheme 2.2). This method was reported to avoid epimerisation and hydrolysis through a faster coupling rate than solid-phase peptide synthesis (SPPS). The role of the benzotriazole was to activate the carboxyl end of the amino acid to serve as a leaving group for the second amino acid (Scheme 2.2).

In order to effectively activate the *N*-protected amino acid with benzotriazole, different conditions were investigated, such as reaction time and temperature, aprotic solvents, varying the starting material ratios, and using different protected amino acids. The optimum conditions were stirring one equivalent of amino acid with 1.2 equivalents of thionyl chloride in dry THF for two hours at room temperature, and then adding on the benzotriazole. As a result, two activated amino acids were synthesised, Fmoc-alanine-benzotriazole and Z-tryptophan-benzotriazole. Subsequently, two dipeptides were successfully synthesised: Z-tryptophan-methionine (aa1) and Fmoc-alanine-phenylalanine (aa2), using mild triethylamine conditions, and a water-acetonitrile solvent system. (7:3) (Scheme 2.2).

Unfortunately, these dipeptides did not couple to the amino group of **A** in Scheme 2.1. Despite using different coupling reagents such as dicyclohexyl carbodiimide, 4-(dimethylamino)pyridine in dichloromethane, 1-ethyl-3-(3-dimethylaminopropyl) carbodiimide or hydroxybenzotriazole in triethylamine, the coupling was still unsuccessful.
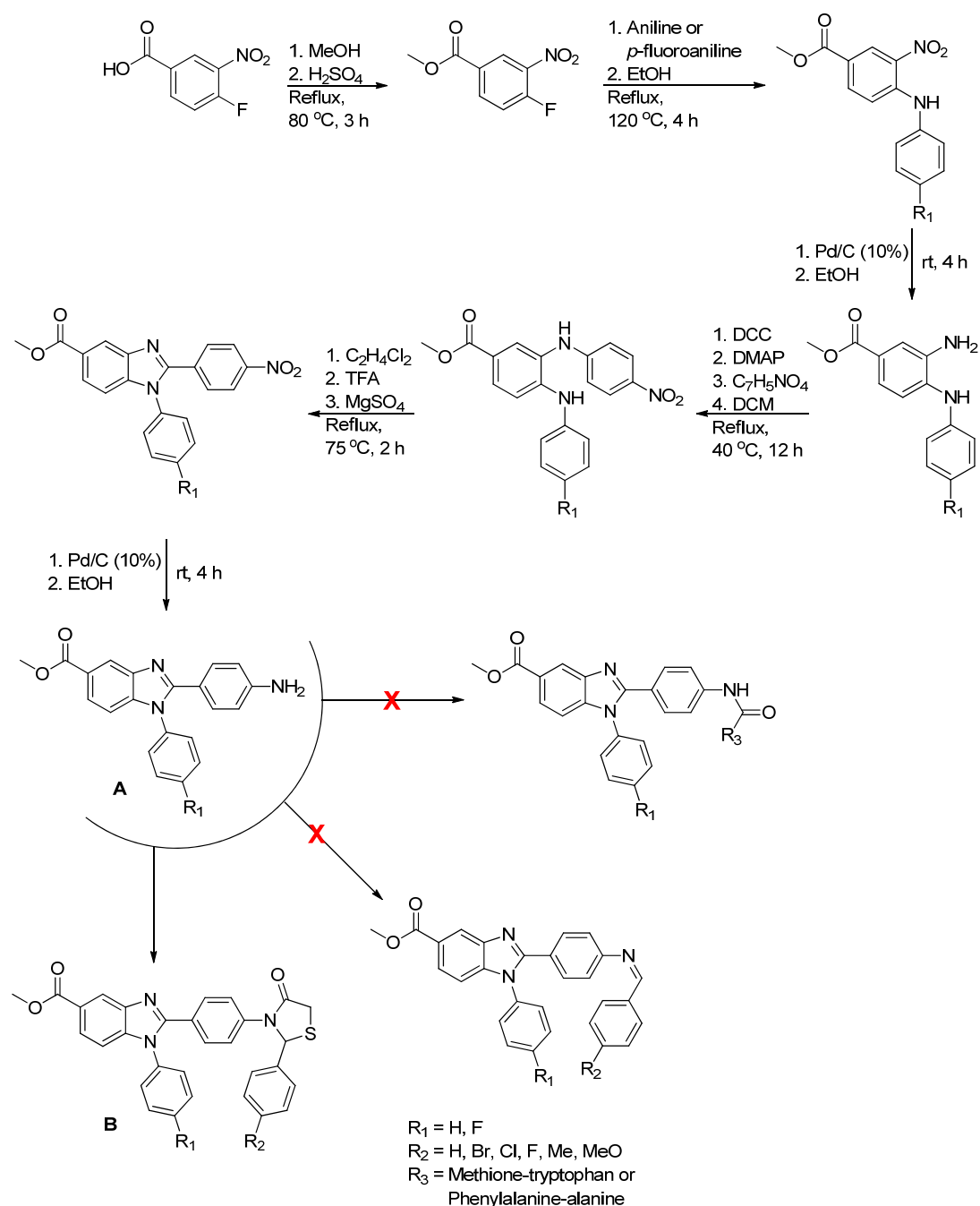
Scheme 2.1 The pathway for synthesising various benzimidazole hybrid molecules

R_1 = -CH_3 (Alanine)
     -Ph-NH-CH=C-CH_2-CH (Tryptophan)
R_2 = -Ph (Phenylalanine)
     -CH_2SCH_3 (Methionine)

aa 1, R_1 = -CH_3, R_2 = -Ph
aa 2, R_1 = -Ph-NH-CH=C-CH_2-CH,
         R_2 = -CH_2SCH_3
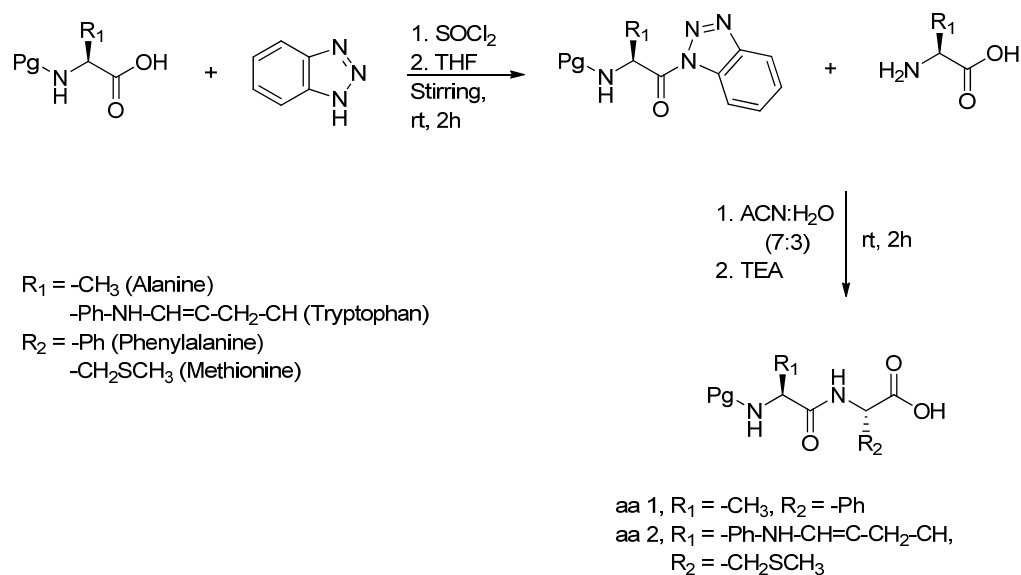
Scheme 2.2 Synthesis of dipeptides through a solution phase technique

The benzimidazole intermediate **A** (Scheme 2.1) was then subjected to a much simpler reaction, a Schiff base reaction with benzaldehydes to form imines. However, this reaction also did not work, despite using various reaction conditions. It was postulated that the lone pair of electrons on the primary amine was delocalised with the benzimidazole, a highly conjugated system, and as such this, lone pair was not available for imine formation with aldehydes.

Benzimidazole thiazolidinone hybrids **B** were already being investigated in our laboratory (Cheddie, 2018). This was tried on intermediate **A** and was found to work well, using toluene as a solvent; however, this design was too similar to work already being carried out.

2.1.2 Benzimidazole chalcones

A second scheme was designed to produce benzimidazole chalcones (Scheme 2.3). The benzimidazole alcohol intermediate was synthesis with lactic acid. The intermediates in this scheme were all synthesised in good yields. Initially, an attempt was made to oxidise the alcohol intermediate **C** to the aldehyde with selenium dioxide and then condense this

intermediate with various acetophenones. However, this reaction did not work well, and when oxidation did occur, complete oxidation all the way to the carboxylic acid occurred.

Thus, it was decided to oxidise the alcohol **C** (Scheme 2.3) to ketones **D** with chromium trioxide, which worked well in yields in excess of 80%. Due to tautomerisation occurring, it was necessary to methylate the nitrogen on the benzimidazole scaffold. This was tried before and after oxidation to the ketone. After oxidation to the ketone, the yields were much better at 88%, with methylation of the alcohol intermediate only resulting in a yield of 50%. It must be noted that separation of the methylated intermediates **E1** and **E2** was a tedious process, as the compounds had very similar retention factors on silica. Disappointingly, attempts to condense the acetophenone with aldehydes forming chalcones were unsuccessful, despite trying several methods, altering basic conditions, and trying condensations under reported acidic conditions.

Surprisingly, a Claisen Schmidt condensation on the unmethylated benzimidazole **D** was successful, and a small library of these compounds were synthesised with halogenated and methoxylated benzaldehydes **F** (Scheme 2.4). The methoxy derivatives however were only partially soluble in DMSO, making it a challenge to obtain NMR data to verify the synthesis of those derivatives.

The chalcones were further reacted with hydrazine hydrate and glacial acetic acid to form a pyrazole, which improved the compound's solubility in DMSO, but not in other organic solvents commonly used. The benzimidazole pyrazole hybrids were then methylated, forming two isomers **G1** and **G2**. These isomers were however difficult to separate using conventional chromatographic techniques due to solubility issues in organic solvents. Even when it was managed to successfully separate one of the *para*-chlorinated derivatives, NMR spectra were

difficult to obtain due to its insolubility in DMSO. This insolubility in DMSO prompted work on this project to be stopped, as DMSO was also the medium used to carry out bioassays, and solubility issues would ultimately lead to problems.
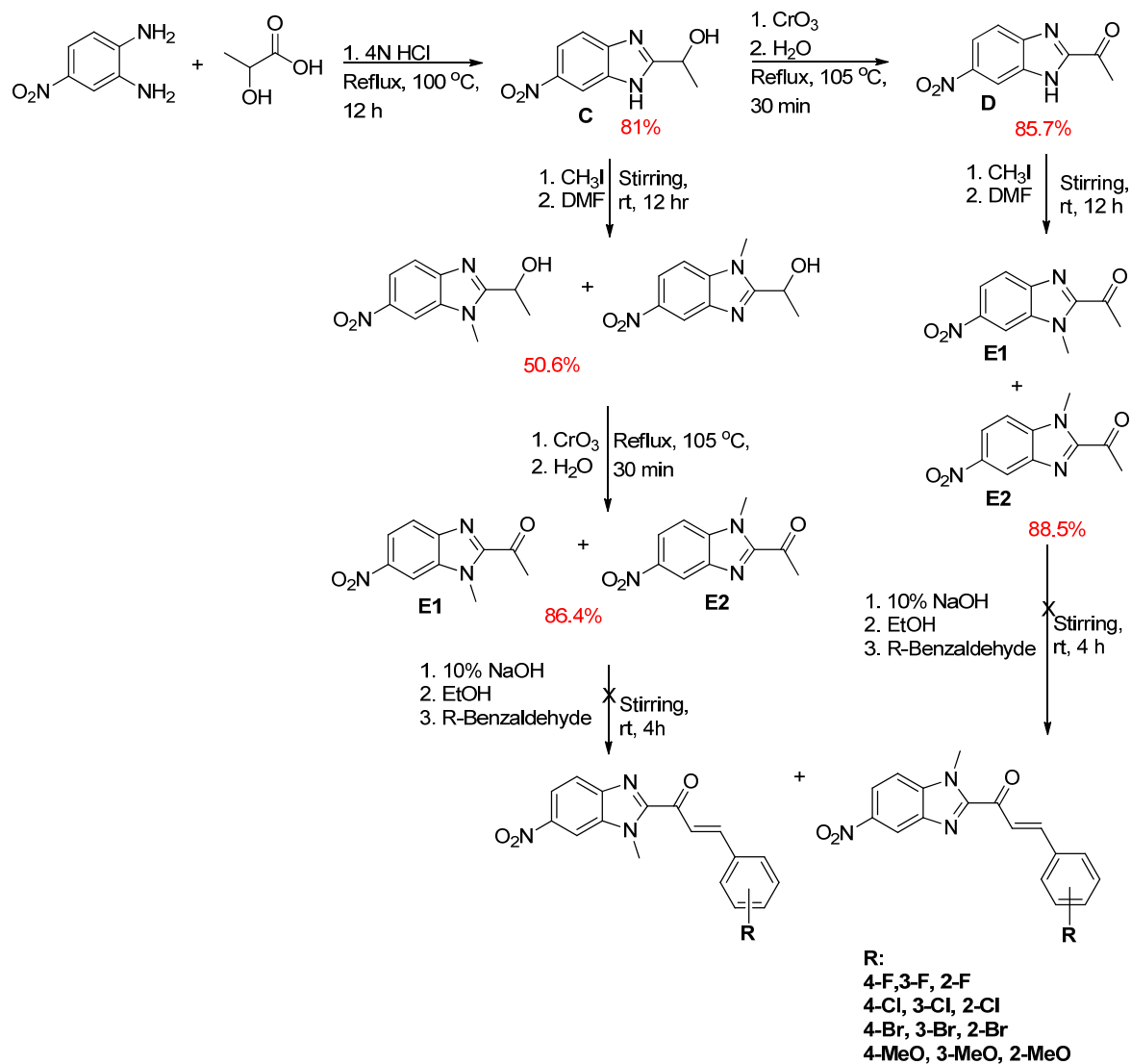
Scheme 2.3 Synthesis scheme to nitrobenzimidazole chalcone derivatives
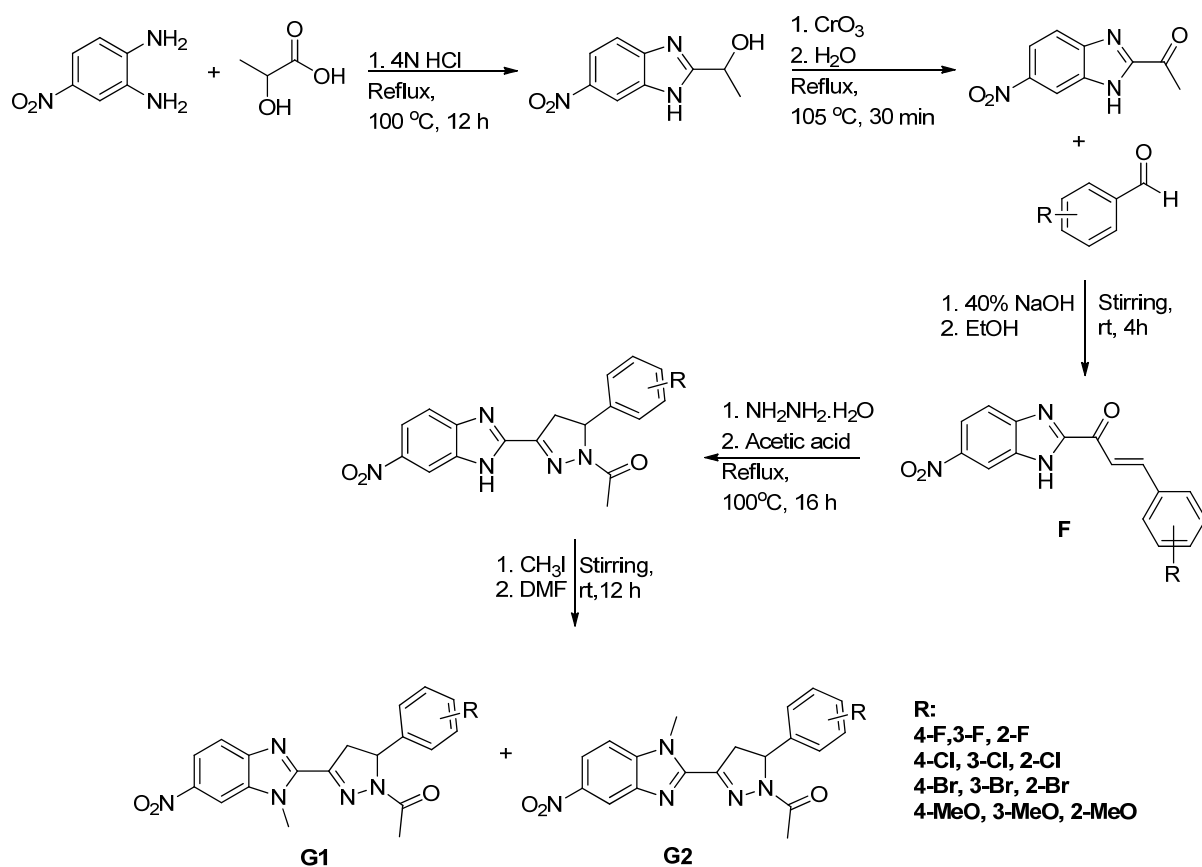
Scheme 2.4 Synthetic scheme to nitrobenzimidazole-pyrazole hybrids

The challenges experienced in the previous two projects influenced the design of the scheme that was eventually successful. The benzimidazole scaffold was constructed by replacing the phenylamine moiety at position 2 with a trifluoromethyl group, since fluorine atoms are known to improve certain pharmacokinetic and physiochemical properties – increased metabolic stability, improved membrane permeation (lipophilicity) and superior binding affinities to target proteins (Shah and Westwell, 2007). Furthermore, it was decided to synthesise the benzimidazoles from *N*-substituted-*o*-phenylenediamines to prevent tautomerisation and use other positions on the benzimidazole to conjugate with other moieties.

2.2 Synthesis of benzimidazole oxadiazoles

The final design involved the synthesis of a small library of sixteen benzimidazole oxadiazole hybrids (Scheme 2.5). The design contained a six-step synthetic pathway. The synthetic scheme began with Fischer esterification of 4-fluoro-3-nitrobenzoic acid, which was initially esterified with methanol producing **2**, and subsequently underwent a nucleophilic substitution with aniline, introducing a 4-aminophenyl moiety (**3a-b**). The nitro group was then reduced with hydrogen over a palladium/carbon catalyst, converting it to the amine. The diamine **4a-b** was transformed to the benzimidazole **5a-b** with trifluoracetic acid and into the hydrazide **6a-b** with hydrazine. The final oxadiazole hybrids were formed from **6a-b**, benzoic acids and phosphoryl chloride producing 12 hybrid compounds with hydrogen, halogens, methyl and methoxy groups present on the *para*-position of the phenyl group on the oxadiazole moiety, and hydrogen or fluorine at the *para*-position of the phenyl group on the benzimidazole moiety.

Similar intermediates to **3-6** were also synthesised using methylamine instead of anilines in the second step with good yields of between 70-96%. However, the final methylated hybrid molecules were unstable in all deuterated solvents. Hence, aniline and 4-fluoroaniline were the only amines used to form the benzimidazoles.

In the substitution reaction, the nitro group deactivated the aromatic ring, making the fluorine a good leaving group. The aniline was used in excess to ensure the reaction proceeded to completion. Ethyl acetate and 4 N hydrochloric acid was used to remove excess aniline. Excellent yields were obtained for intermediates (**3a-b**) at 98% and 90% respectively. In the hydrogenation reaction, the duration of the reaction for the phenylamine derivative **3a** was 20 hours as opposed to 4 hours for the fluorophenylamine derivative **3b**. It is postulated that the fluorine atom also coordinates loosely to the metal, allowing for a faster reduction. Even

though the diamino intermediates (**4a-b**) had to be purified by column chromatography, the compounds were isolated in excellent yields of 92% and 87% respectively.
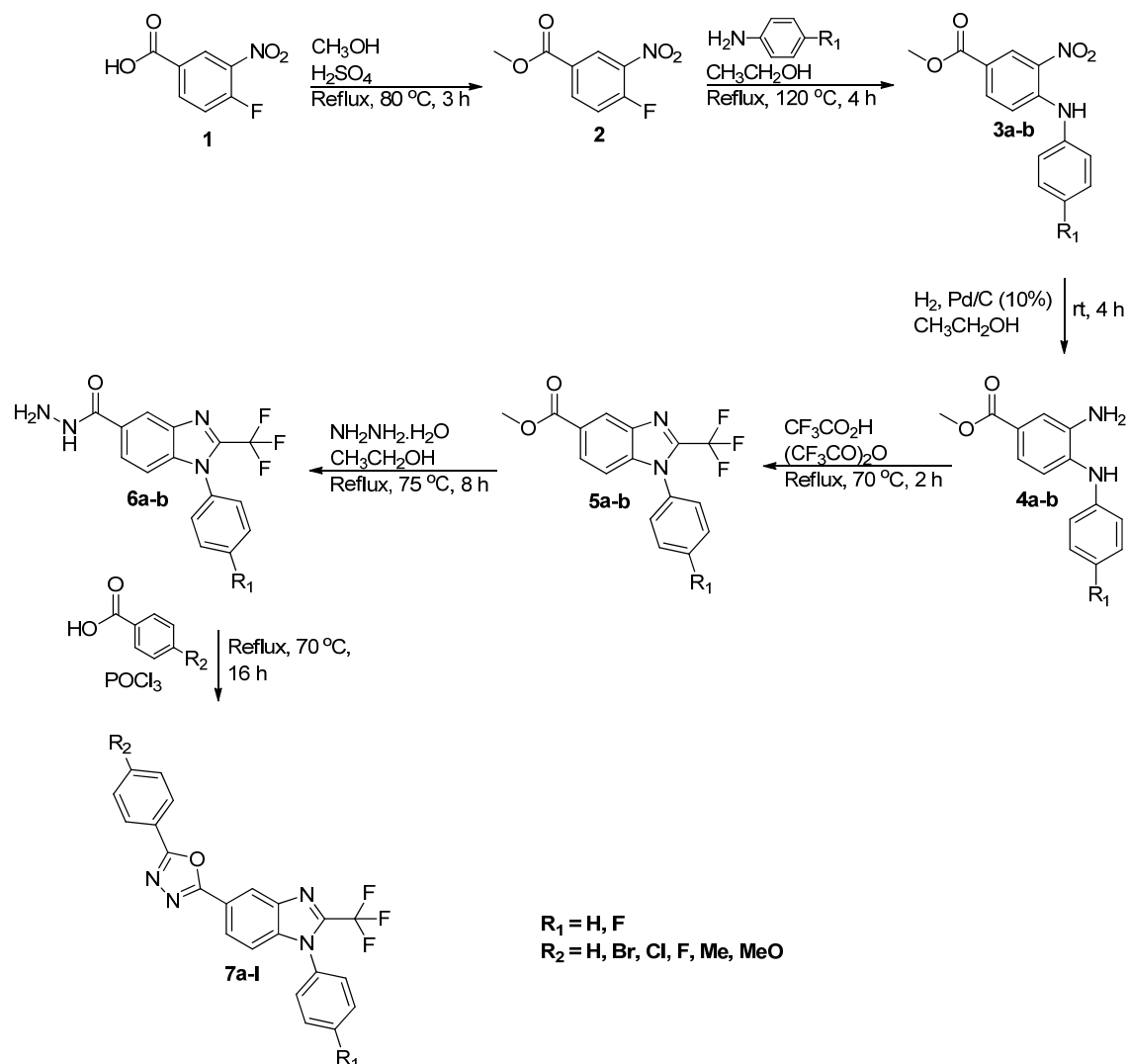
Scheme 2.5 Synthetic route to benzimidazole-oxadiazole hybrids **7a-l**

Efficient cyclisation to the benzimidazoles **5a-b** was not observed with trifluoroacetic acid alone, and a mixture of trifluoroacetic acid and trifluoroacetic acid anhydride was needed for good conversion with yields of 87% and 90% respectively. Conversion to the hydrazides **6a-b** were also very efficient with yields of 96% and 98% being recorded. The melting point, Rf values in ethyl acetate:hexane 1:4 and yields obtained for each intermediate is summarised in

Table 2.1. As can be seen by the yields being approximately 90% and higher for all intermediate steps, this is a highly efficient synthetic scheme.

Table 2.1 Retention factor (Rf in ethyl acetate:hexane 1:4), melting point (ºC), yield (%) and HRMS data of intermediates
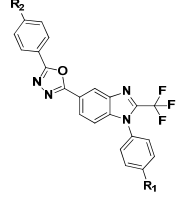
No.	R_1	Rf	Melting point/ °C	Yield/ %	HRMS data
2	-	0.58	65-66	93	-
3a	H	0.67	126-127	98	-
3b	F	0.70	157-158	90	-
4a	H	0.28	88-89	92	-
4b	F	0.20	133-134	87	-
5a	H	0.63	-	87	-
5b	F	0.65	-	90	-
6a	H	0.00	145-146	96	319.0814 [M-H]
6b	F	0.00	148-149	98	417.1009 [M+H+DMSO]

Twelve benzimidazole-oxadiazole hybrids were successfully synthesised with six benzoic acids using phosphoryl chloride and heating under reflux for 16 hours (Scheme 2.5). The reaction was also attempted with *para* hydroxybenzoic acid and *para* nitrobenzoic acid, but these reactions were unsuccessful, as low yields less than 20% were obtained for the crude products, which were also difficult to separate because of solubility issues in organic solvents. Initially, a 1:1 molar ratio of benzimidazole hydrazide (**6a-b**) and benzoic acid was used but resulted in poor yields (42-54%). Microwave irradiation was also tried without major improvement. It was discovered that the benzoic acids were reacting with itself, forming benzophenones. This was deduced after isolating 4,4′-dichlorobenzophenone from one of the reaction mixtures and led to increasing the ratio of benzoic acid added to 2 molar equivalents.

This modification led to the yield of the final step being between 61- 97%. Overall yields of the final product were between 42 - 68%.

Table 2.2 Retention factor (Rf in ethyl acetate:hexane 1:4), melting points (°C), final step and overall yields (%), and HRMS data of the benzimidazole-oxadiazole hybrids **7a-l**

	R_1	R_2	Melting point/ °C	Rf	Final step yield/ %	Overall yield/ %	HRMS data
7a	H	H	179-180	0.42	70	49	407.1132 [M+H]
7b	H	Br	186-187	0.50	70	49	563.0385 [M+H+DMSO]
7c	H	Cl	173-174	0.47	83	58	519.0892 [M+H+DMSO]
7d	H	F	170-171	0.44	76	53	503.1179 [M+H+DMSO]
7e	H	CH_3	173-174	0.44	89	62	443.1083 [M+Na]
7f	H	CH_3O	169-170	0.22	97	68	515.1382 [M+H+DMSO]
7g	F	H	183-184	0.44	85	58	503.1187 [M+H+DMSO]
7h	F	Br	192-193	0.52	78	54	-
7i	F	Cl	215-216	0.52	61	42	537.0786 [M+H+DMSO]
7j	F	F	195-196	0.46	82	57	521.1084 [M+H+DMSO]
7k	F	CH_3	162-163	0.46	88	60	517.1328 [M+H+DMSO]
7l	F	CH_3O	211-212	0.28	97	67	533.1286 [M+H+DMSO]

In general, the yields of the final compounds where an electron donating methyl or methoxy group was present on the benzoic acid were higher than those where the benzoic acid was unsubstituted or when electron withdrawing halogens were present. The reason for this is not quite clear, however these differences in yields were not appreciable.

In general, the melting points for all the fluorinated benzimidazole derivatives **7g-7l** (those compounds with a *para* substituted fluorobenzene ring at the nitrogen of the benzimidazole) were higher than those with an unsubstituted phenyl group at the nitrogen (**7a-f**), with the exception of **7e** (Figure 2.1). This is probably due to stronger intermolecular forces occurring with the fluorinated phenyl group such as hydrogen bonding. For the unsubstituted group (**7a-f**), the melting point decreased as the size of the halogen on the benzoic acid derived phenyl group decreased. With the fluorinated compounds (**7g-7l**), the chloro derivative **7i** had the highest melting point with the bromo and fluoro derivatives (**7h** and **7j**) having similar melting points. The highest melting points were experienced by the chloro (**7i**) and methoxy derivatives (**7l**) where the phenyl group on the nitrogen was fluorinated, and the lowest melting point was when a methyl substituent was present on the phenyl ring derived by the benzoic acid (**7k**).
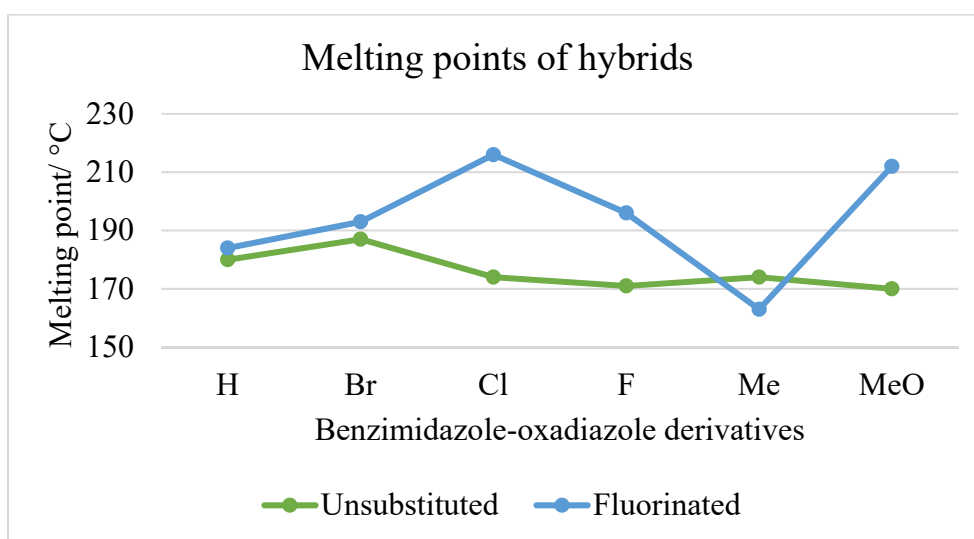
Figure 2.1 Melting points of the benzimidazole-oxadiazole derivatives **7a-7l**

All the final benzimidazole-oxadiazole hybrids were elucidated by mainly Nuclear Magnetic Resonance (NMR) spectroscopy (1D and 2D) and confirmed with High-Resolution Mass Spectrometry (HRMS) and elemental analysis. NMR spectroscopy was also used to determine whether the intermediates had formed and whether or not the level of purity was acceptable for the next stage. Intermediates **6a-b** were novel intermediates and were therefore also fully characterised.

2.3 Structural elucidation

2.3.1 Characterisation of intermediates

Confirmation of the ester **2** was provided by the ester methyl group (H-8) at δ 3.88. H-1, H-4 and H-5 were identified by their splitting patterns and coupling constant; H-1 a double doublet at δ 8.53 split by H-5 (2.1 Hz) and the F (7.5 Hz); H-4 a double doublet at δ 7.70 split by H-5 (8.7 Hz) and the F (11.0 Hz), and H-5 a doublet of doublet of doublets (ddd) at δ 7.92 split by H-4 (8.7 Hz), H-1 (2.1 Hz) and the F (4.2 Hz) (Figure 2.2). The ^{13}C NMR data was also easily elucidated with the methyl carbon appearing at δ 53.4, and the protonated carbons C-1, C-4 and C-5 appearing at δ 127.5 (d, $J = 1.6$ Hz), δ 119.8 (d, $J = 21.8$ Hz) and δ 137.2 (d, $J = 10.5$ Hz). The ester carbonyl carbon could be seen at δ 164.3, the fluorinated carbon as a doublet at δ 157.7 ($J = 268.3$ Hz), and C-6 at δ 127.1 ($J = 3.7$ Hz) (Figure 2.3).
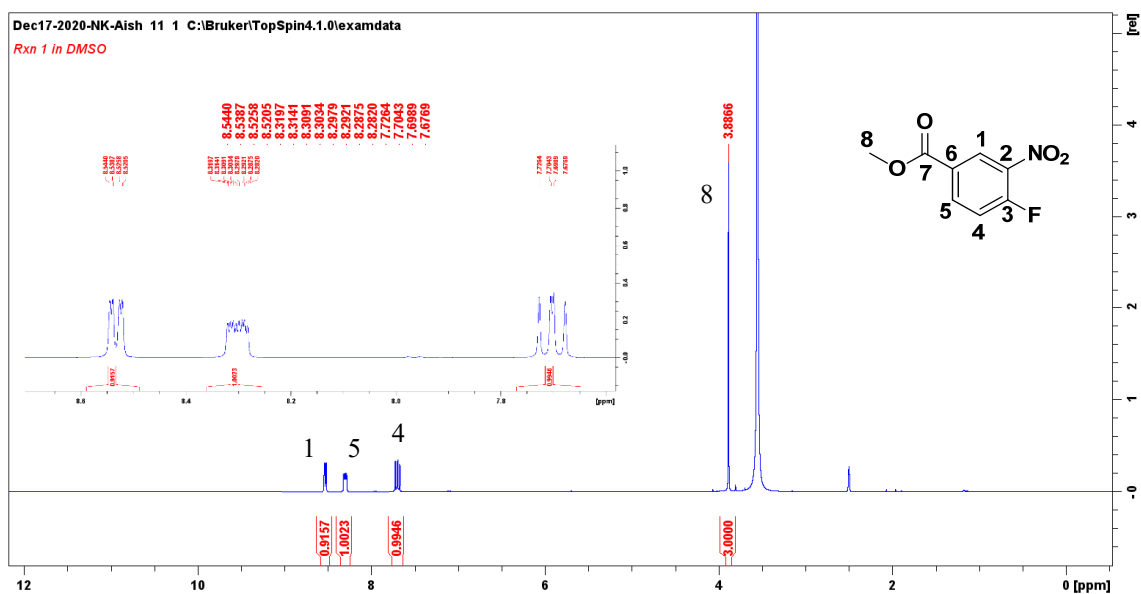
Figure 2.2 ^{1}H NMR spectrum of methyl 4-fluoro-3-nitrobenzoate **2**
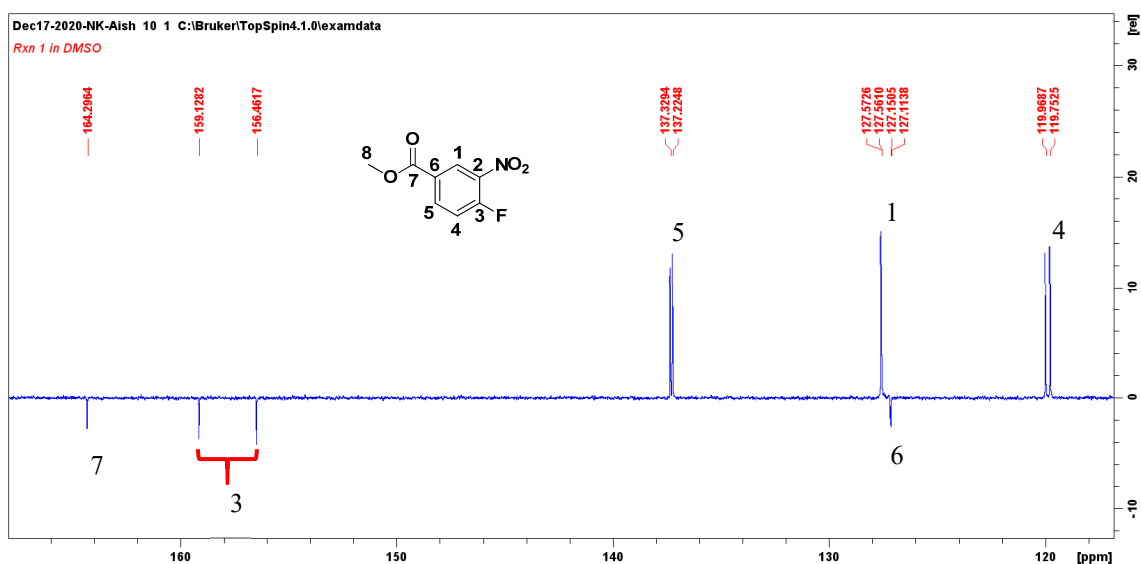
Figure 2.3 ^{13}C NMR spectrum of methyl 4-fluoro-3-nitrobenzoate **2**

When the phenylamine group was substituted onto the ring, the ^{1}H NMR spectrum of this intermediate showed eight aromatic protons, including the methyl group proton resonance at δ 3.83 and an amino proton at δ 9.83 (Figure 2.4). The splitting patterns of the proton on the ester aromatic ring now changed considerably as the fluorine was notably absent. H-1 was a doublet at δ 8.63 with a small coupling constant of 1.7 Hz, typical of *meta* coupling, H-5 a

doublet of doublets at δ 7.92 with J = 8.9 and 1.8 Hz and H-4 a more upfield shift at δ 7.12, a

doublet with a coupling constant of 8.8 Hz. The phenylamine ring protons were present as a

two-proton triplet at δ 7.47 with J = 8.0 Hz, assigned to H-3'/5', a one-proton triplet at δ 7.30

(H-4'), and a two-proton proton doublet at δ 7.36 (H-2'/6'). The coupling constants of these

protons were 8.0 Hz.

The ^{13}C NMR spectrum showed the ester carbonyl carbon at δ 165.1 and the singlet carbon

resonances at δ 145.9, 138.5, 132.5 and 118.4 for C-3, C-1', C-2 and C-6. The phenylamine

carbon resonances were present at δ 130.1 (C-3'/5'), 126.7 (C-4') and 125.6 (C-2'/6'), and C-

1, C-4 and C-5, the protonated carbon resonances on the ester aromatic ring at δ 128.6, 116.8

and 135.9 respectively (Figure 2.5).
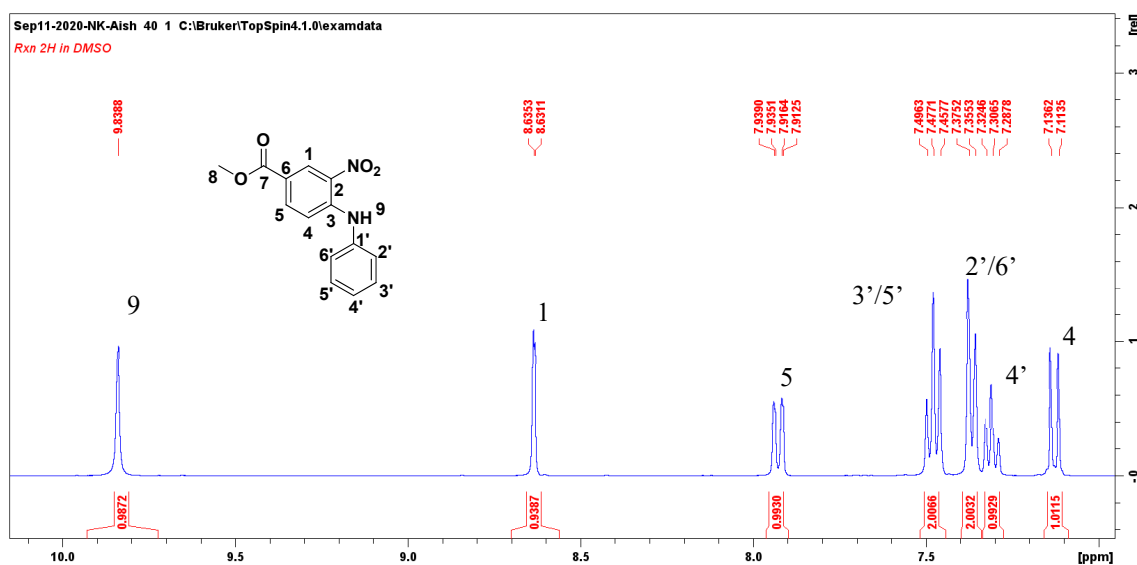
Figure 2.4 ^{1}H NMR spectrum of methyl 3-nitro-4-(phenylamino)benzoate **3a**
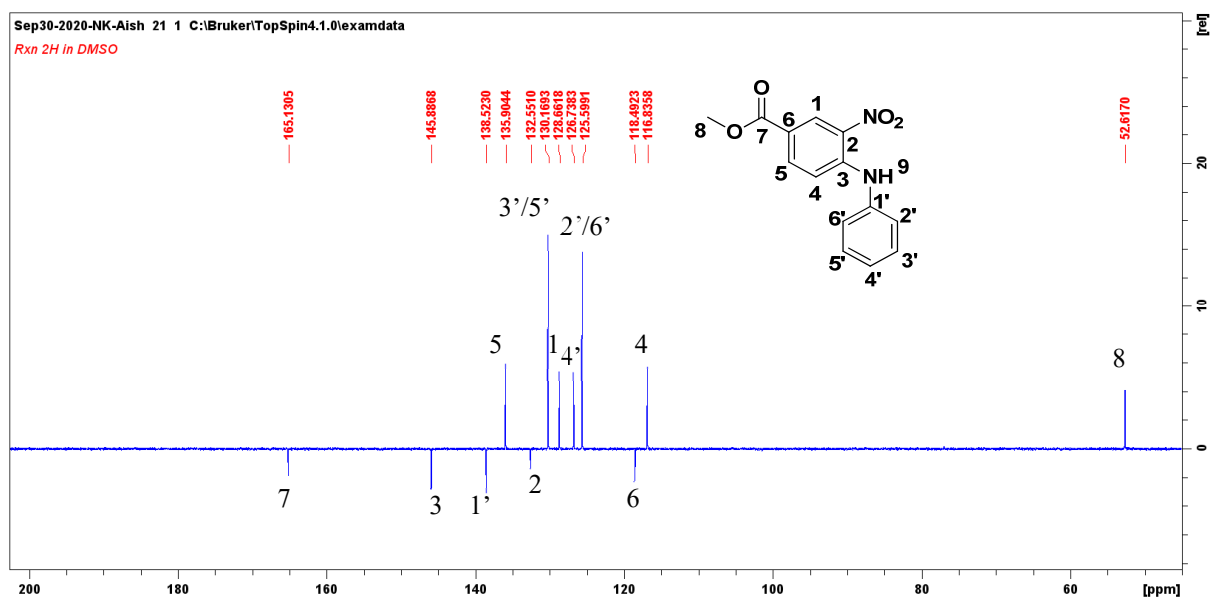
Figure 2.5 ^{13}C NMR spectrum of methyl 3-nitro-4-(phenylamino)benzoate **3a**

Reduction of the nitro group was determined by the appearance of the primary amine (H-10) as a two-proton singlet at δ 5.04. In intermediate 3, the *ortho* and *para* protons to the nitro group were deshielded and separated from the phenylamine group protons, however in the diamine; these proton resonances were all in the same region between δ 6.80 to δ 7.40. However, H-1, H-5 and H-4 could easily be identified as the spectrum was well resolved into a doublet at δ 7.35 (J = 1.6 Hz), a doublet of doublets at δ 7.17 (J = 8.3 and 1.6 Hz) and a doublet at δ 7.07 (J = 8.3 Hz) respectively. The phenylamine group protons were present as a two proton triplet at δ 7.23 (J = 8.1 Hz) for H-3'/5', a two proton doublet at δ 7.00 (J = 7.7 Hz) for H-2'/6' and a one proton triplet at δ 6.85 (J = 7.3 Hz) for H-4'.

The ^{13}C NMR spectrum was similar to the nitro precursor with the exception that C-1, C-5, C-4' and C-2'/6' were all now more upfield at δ 116.1, 119.1, 120.6 and 118.1 respectively due to the reduction of the nitro group to the amine.
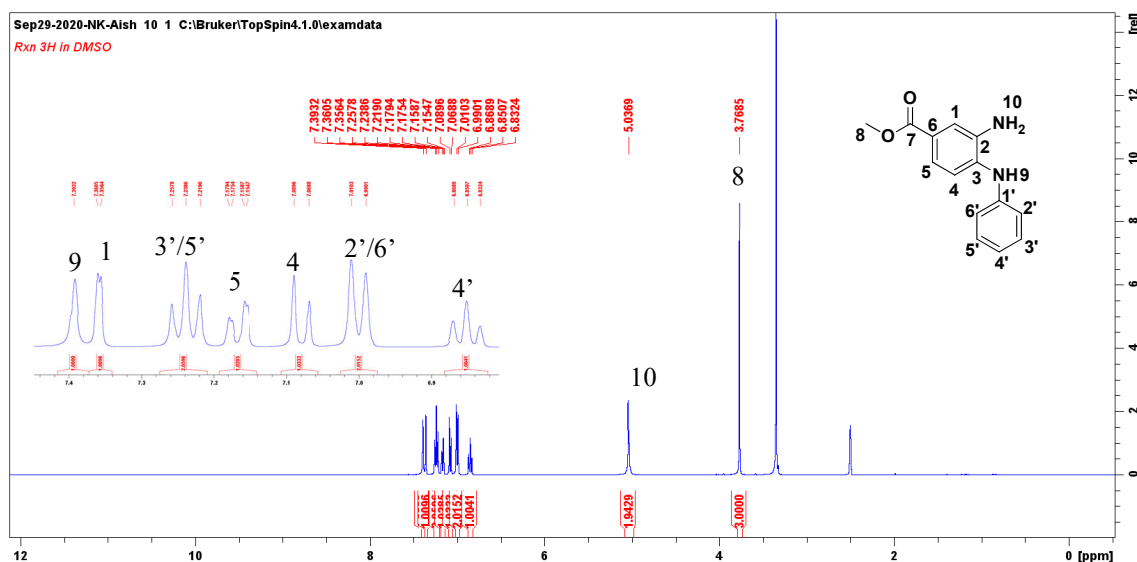
Figure 2.6 ^{1}H NMR spectrum of methyl 3-amino-4-(phenylamino)benzoate **4a**
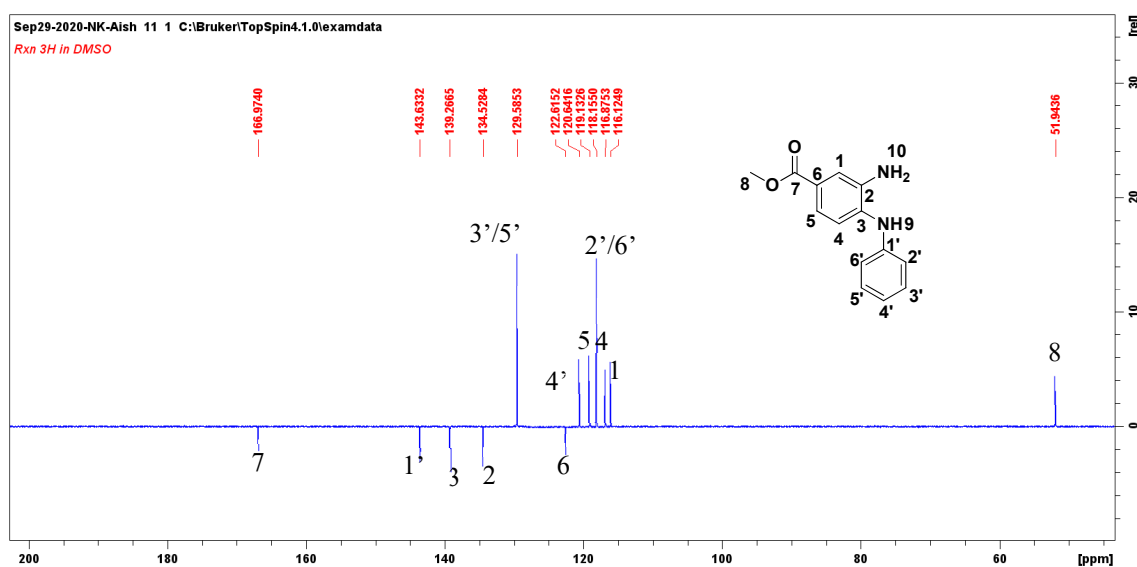
Figure 2.7 ^{13}C NMR spectrum of methyl 3-amino-4-(phenylamino)benzoate **4a**

Cyclisation of the diamine ester with trifluoroacetic acid and trifluoroacetic anhydride resulted in the formation of the 2-trifluoromethylbenzimidazole **5a**, whose ^{1}H NMR spectrum was rather simple and elegant compared to the precursor **4a**. Compared to **4a**, the H-9 and H-10 proton resonances disappeared and the H-2' to H-6' resonances all coalesced as a five-proton broadened singlet at δ 7.67. The other three resonances in the aromatic region, a slightly

broadened singlet, doublet of doublets (seen by an expansion) and a doublet was attributed respectively to H-7 at δ 8.50, H-5 at δ 8.04 and H-4 at δ 7.29 (Figure 2.8). The *meta* coupling was 1.3 Hz and *ortho* coupling 8.7 Hz. The ester methyl resonance appeared as a singlet at δ 3.90.

In the ^{13}C attached proton test (APT) of **5a**, six aromatic protonated carbon resonances could be seen at δ 130.9 (C-4'), 130.5 (C-3'/5'), 128.0 (C-2'/6'), 127.2 (C-5), 123.1 (C-7), and 112.3 (C-4). The three carbon resonances adjacent to the nitrogen were present slightly more deshielded at δ 140.4 (C-3a), 140.1 (C-7a) and 133.9 (C-1'). C-6, to which the ester was attached, appeared at δ 126.1. Due to the trifluoromethyl group, both C-10 and C-2 appeared as quartets at δ 118.9 ($J = 272.2$ Hz) and δ 142.1 ($J = 38.3$ Hz) respectively (Figure 2.9). C-2 was more deshielded being at the centre of two nitrogen atoms. The ester carbonyl C-8 was present at δ 166.5 and the ester methyl group at δ 52.7.
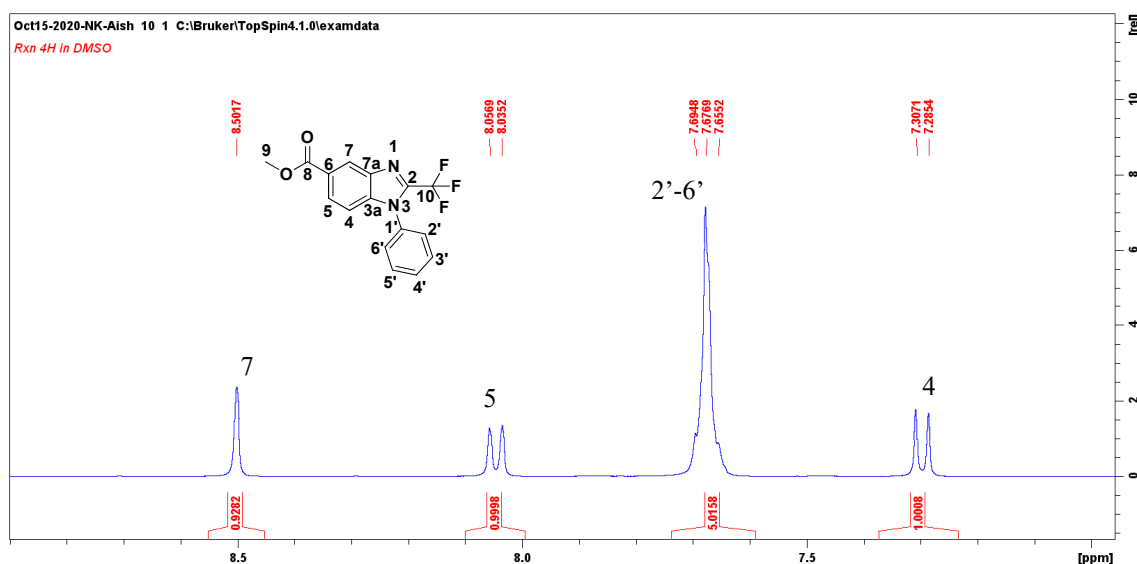
Figure 2.8 ^{1}H NMR spectrum of methyl 1-phenyl-2-(trifluoromethyl)-1*H*-benzo[d]imidazole-5-carboxylate **5a**
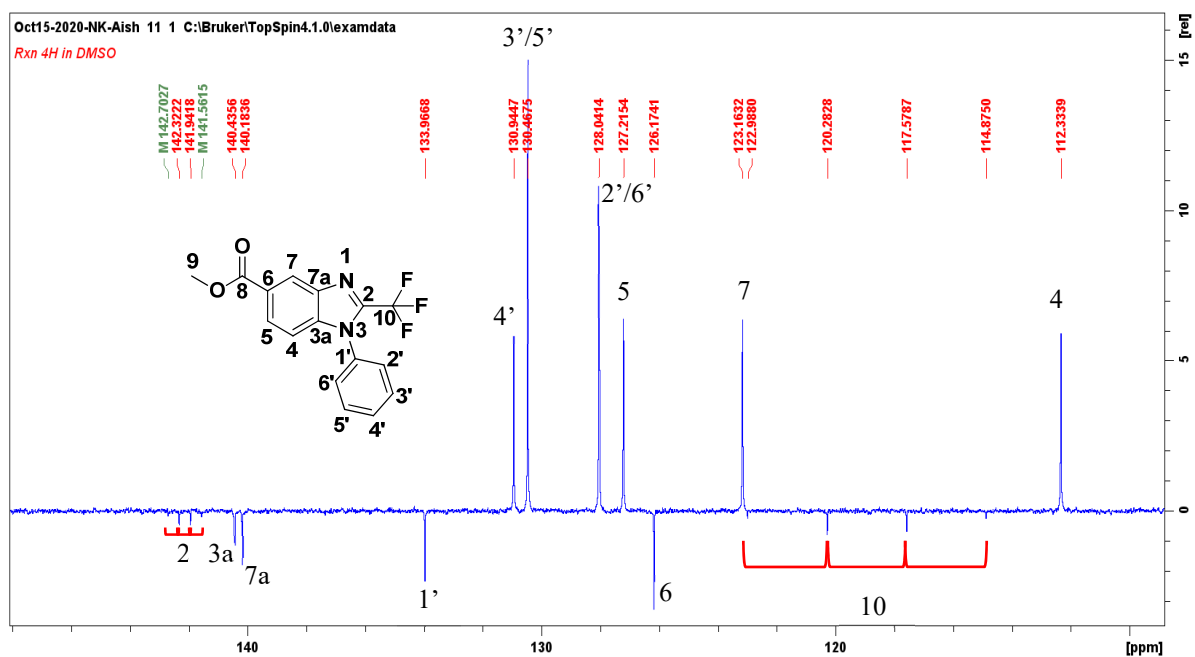
Figure 2.9 ^{13}C NMR spectrum of methyl 1-phenyl-2-(trifluoromethyl)-1*H*-benzo[d]imidazole-5-carboxylate **5a**

When hydrazine converted the benzimidazole ester to the hydrazide **6a**, the ^{1}H NMR spectrum was similar to its precursor **5a** with the exception of the disappearance of the ester methyl group at δ 3.89 and the appearance of the NH protons on the hydrazide group, a one-proton resonance at δ 9.93 (H-9) and two-proton resonance at δ 4.54 (H-10) (Figure 2.10). The ^{13}C NMR spectrum of **6a** was very similar to **5a** with the notable absence of the ester methyl carbon resonance. Interestingly, the carbonyl chemical shift of the acyl hydrazide was similar to the ester at δ 166 (Figure 2.11).
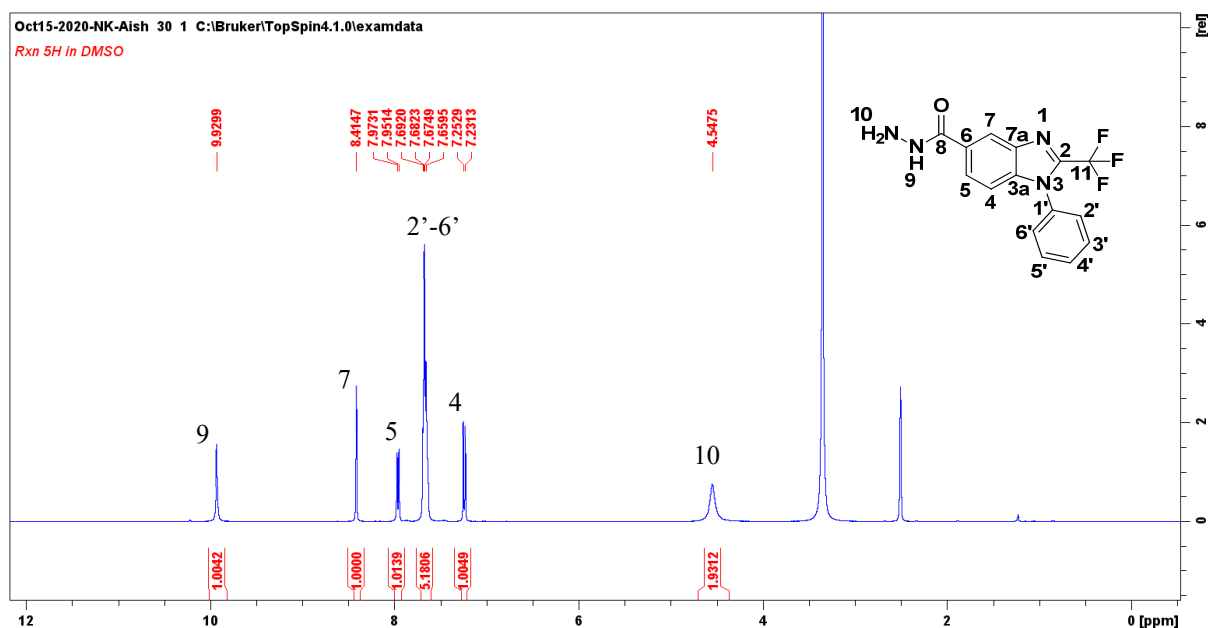
Figure 2.10 ^{1}H NMR spectrum of 1-phenyl-2-(trifluoromethyl)-1*H*-benzo[d]imidazole-5-carbohydrazide **6a**
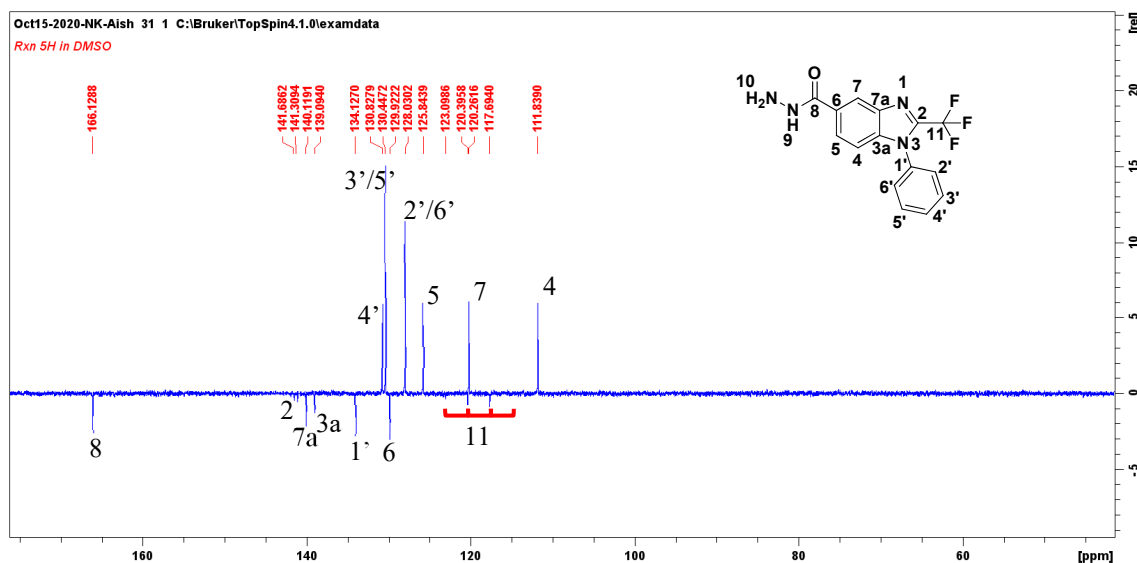
Figure 2.11 ^{13}C NMR spectrum of 1-phenyl-2-(trifluoromethyl)-1*H*-benzo[d]imidazole-5-carbohydrazide **6a**

The 4-fluorophenyl intermediates (**3b**, **4b**, **5b** and **6b**) were characterised in a similar process. The NMR spectra of these intermediates differed in relation to the fluorophenyl group compared to the phenyl group. In particular, the proton resonances of H-2'/6' and H-3'/5' in

the ^{1}H NMR spectra appeared as a characteristic doublet of doublets and pseudo triplet, respectively. Using **5b** as an example, this occurred at δ 7.77 (J = 8.7, 4.9 Hz) and δ 7.52 (J = 8.7 Hz) respectively (Figure 2.12). In the ^{13}C NMR spectrum, C-4' appeared as a doublet at δ 163.2 with a huge coupling constant of J = 248.0 Hz due to it being directly bonded to the fluorine atom. The *ortho* coupled carbon resonances, C-3'/5', appeared as a doublet at δ 117.4 with J = 23.2 Hz and the *meta* coupled C-2'/6' was present at δ 130.6 (J = 9.3 Hz) (Figure 2.13).
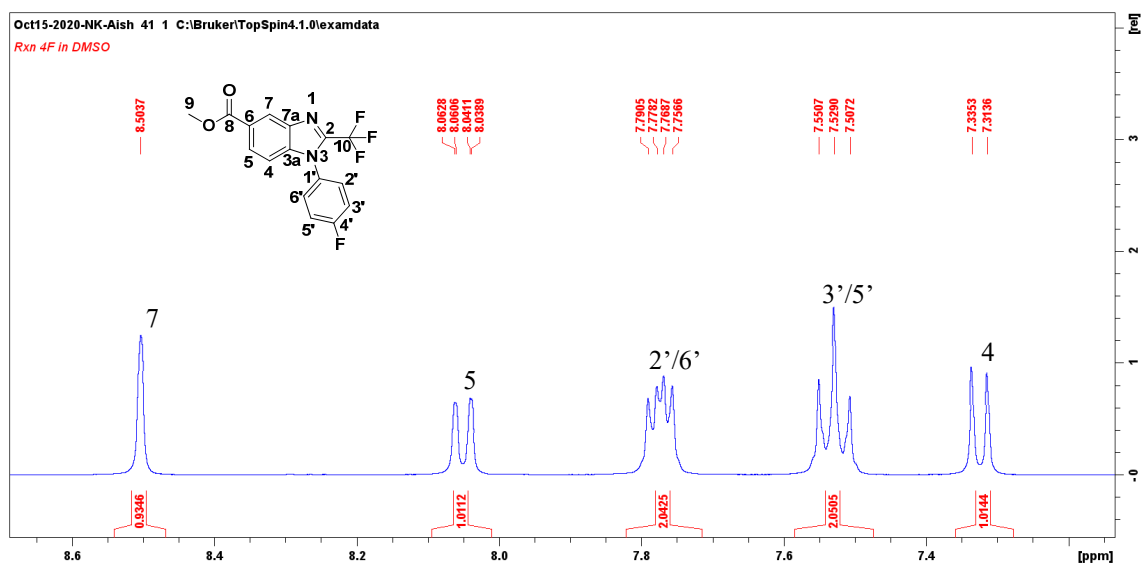
Figure 2.12 ^{1}H NMR spectrum of methyl 1-(4-fluorophenyl)-2-(trifluoromethyl)-1H-benzo[d]imidazole-5-carboxylate **5b**
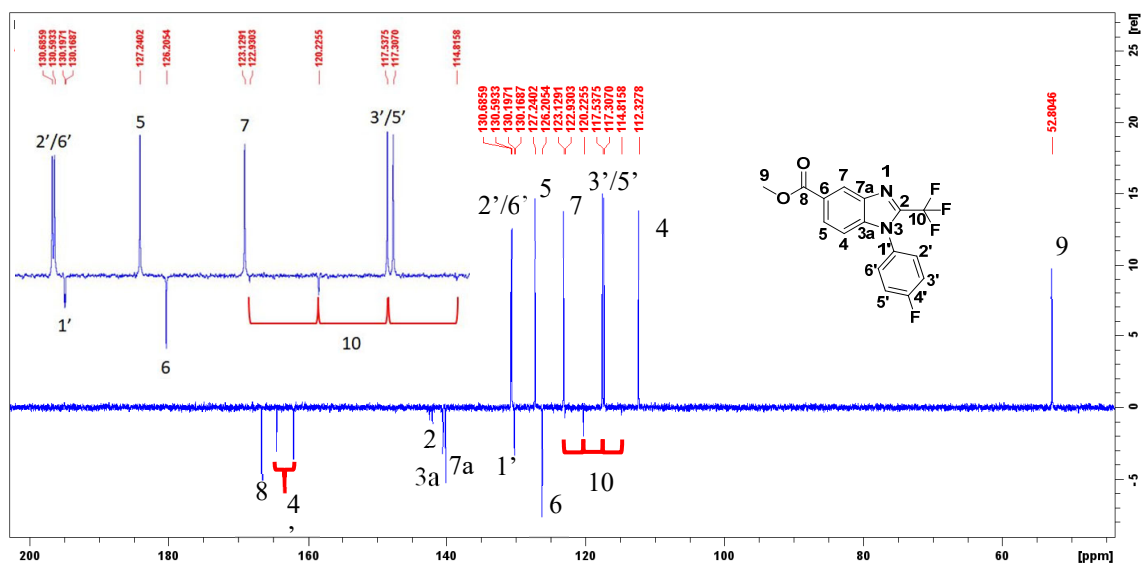
Figure 2.13 ^{13}C NMR spectrum of methyl 1-(4-fluorophenyl)-2-(trifluoromethyl)-1H-benzo[d]imidazole-5-carboxylate **5b**
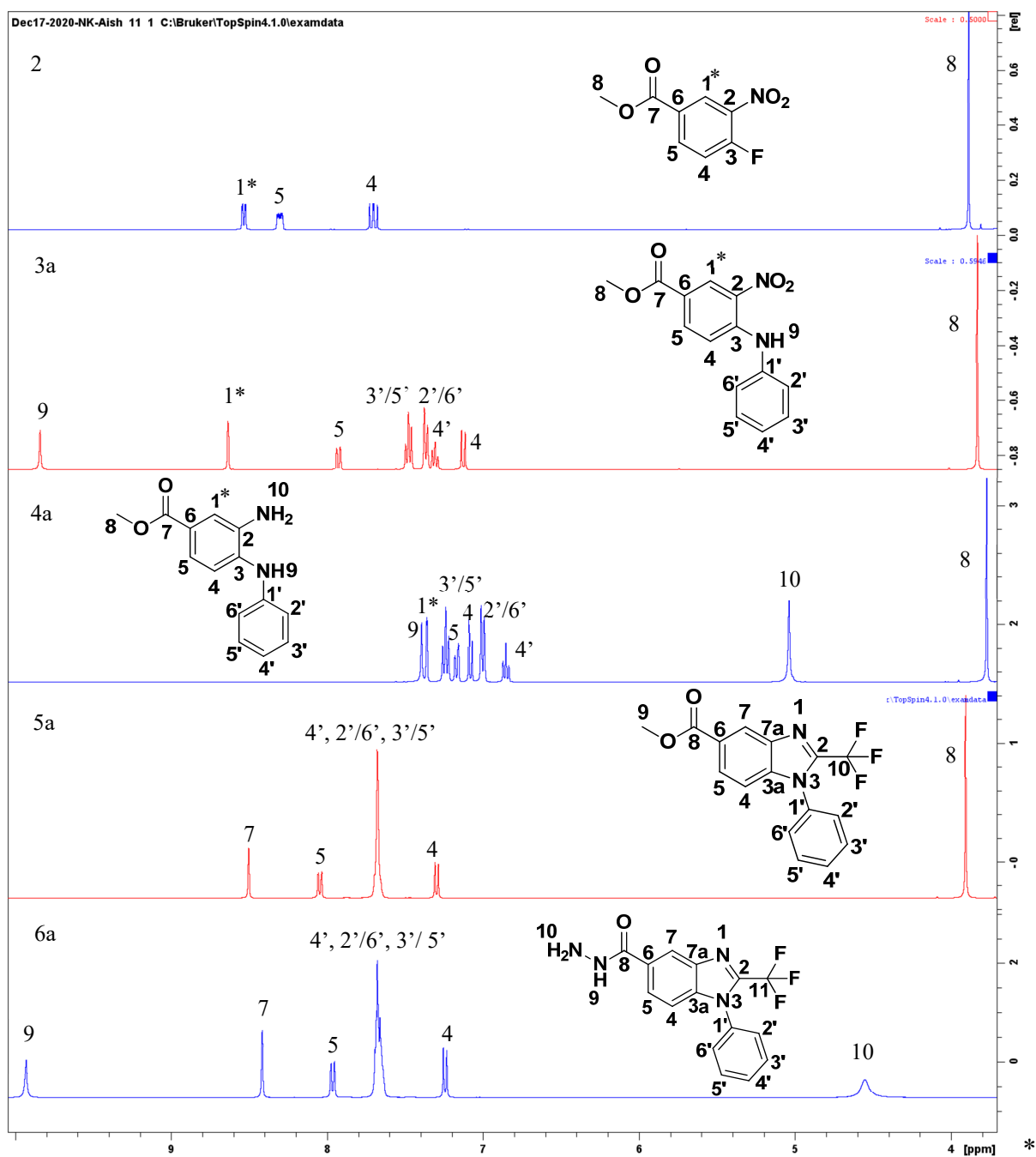
Note: H-1* and 7 are the same proton

Figure 2.14 ^{1}H NMR overlay of intermediates **2**, **3a**, **4a**, **5a** and **6a**

Figure 2.14 shows a nice overlay of the ^{1}H NMR spectra of all intermediates **2** through to **6a**. In general, the proton resonances of the aromatic ring of the benzimidazole were fairly constant in the nitro precursor **3a** and the two benzimidazoles **5a** and **6a**. These three resonances are

depicted as H-7, H-5, and H-4 in **5a** and **6a** and H-1*, H-5 and H-4 in **3a**. Only in the case of the diamino intermediate **4a** did these three resonances become more shielded and occupy the same region as the phenylamine proton resonances. Interestingly, following intermediates **2**, **3a** and **4a**, one can see a notable shielding of H-5, as the amino groups are added to the aromatic ring, indicating the electronic effects of the amino groups adding electron density to H-5 through lone pair donation to the ring.

2.3.2 Characterisation of benzimidazole-oxadiazoles hybrids (**7a-l**)

Formation of the oxadiazole moiety and the synthesis of **7a** was confirmed by the disappearance of the NH-9 and NH-10 proton resonances of the hydrazide, and the appearance of a two-proton multiplet resonance at δ 8.16 (H-2'''/6''') that overlapped with H-5, and a three-proton multiplet at δ 7.63-7.65 (H-3'''-H-5''') situated right next to the proton resonances of the phenyl ring attached to the benzimidazole (Figure 2.15). The proton resonances of the benzimidazole and phenyl moieties were similar to the precursor **6a**. Strong COSY correlations could be seen between H-7, H-5, and H-4 of the benzimidazole moiety and H-2'''/6''' and H-3'''-H-6''' of the phenyl ring attached to the oxadiazole (Figure 2.16).

The ^{13}C NMR spectrum of **7a** showed similar resonances of the benzimidazole and phenyl ring carbon resonances to the precursor **6a**. These were the protonated carbon resonances C-4', 3'/5', 2'/6', 5, 7 and 4 at δ 131.0, 130.5, 128.0, 125.0, 120.3, 113.4 respectively and the singlet resonances C-2, 7a, 3a, 1', 6 and 8 at δ 141.5 (q, J = 38.4 Hz), 140.6, 139.5, 134.0, 119.9 and 118.9 (q, J = 272.3 Hz) respectively. The oxadiazole carbon resonances C-2" and C-5" were present at δ 164.58 and 164.53. These resonances can be interchanged. The four carbon resonances of the phenyl ring attached to the oxadiazole ring could be seen at δ 132.5 (C-4'''), 129.9 (C-3'''/5'''), 127.1 (C-2'''/6''') and 123.8 (C-1''') (Figure 2.17).
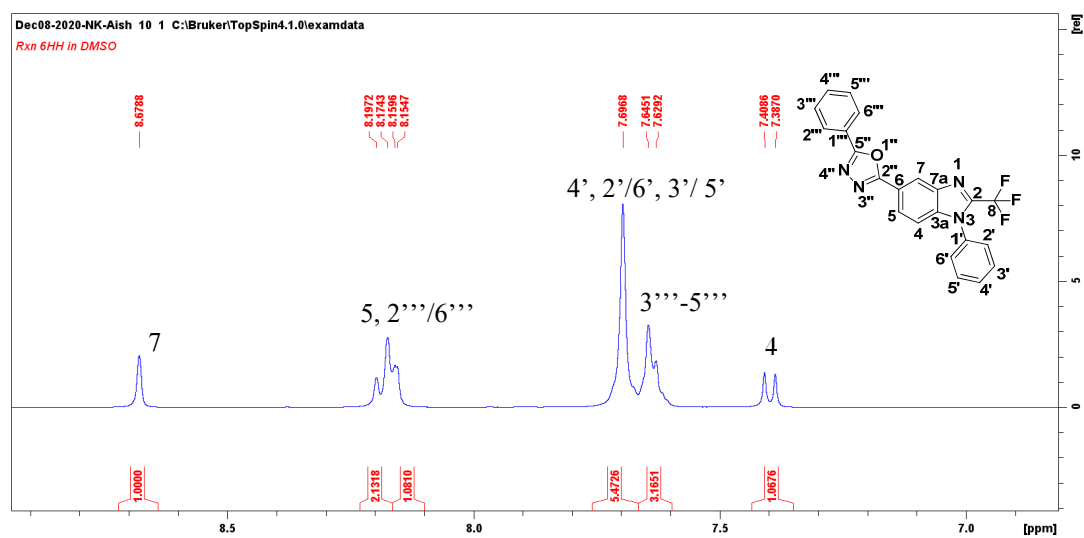
Figure 2.15 ^{1}H NMR spectrum of 2-phenyl-5-(1-phenyl-2-(trifluoromethyl)-1*H*-benzo[d]imidazole-5-yl)-1,3,4-oxadiazole **7a**
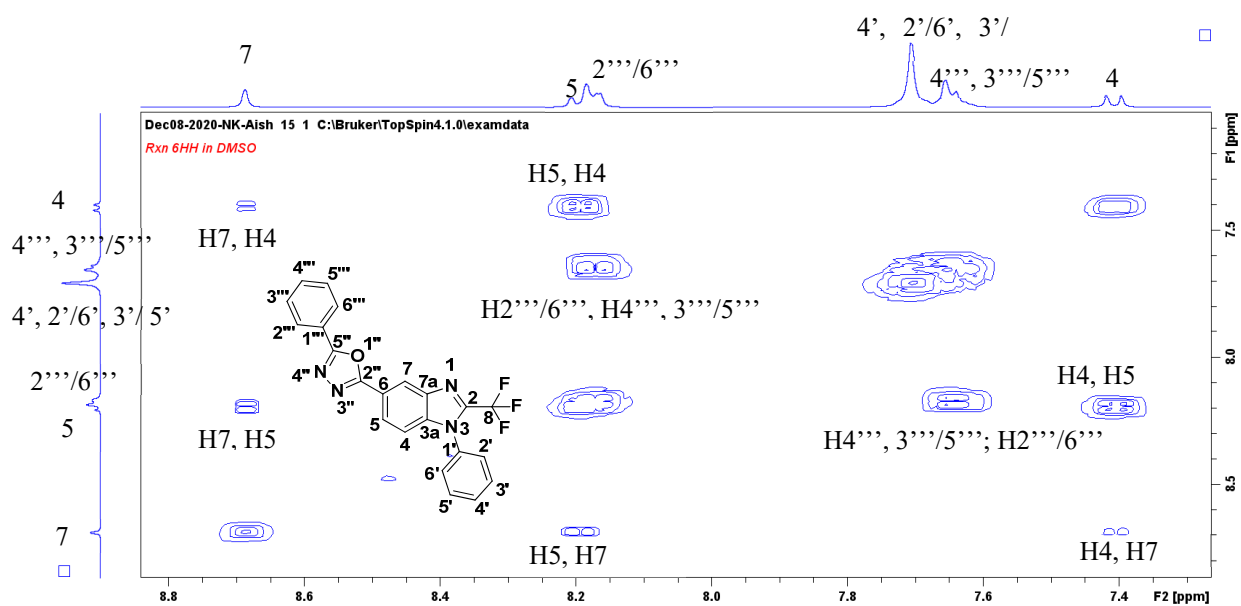
Figure 2.16 COSY spectrum of 2-phenyl-5-(1-phenyl-2-(trifluoromethyl)-1*H*-benzo[d]imidazole-5-yl)-1,3,4-oxadiazole **7a**
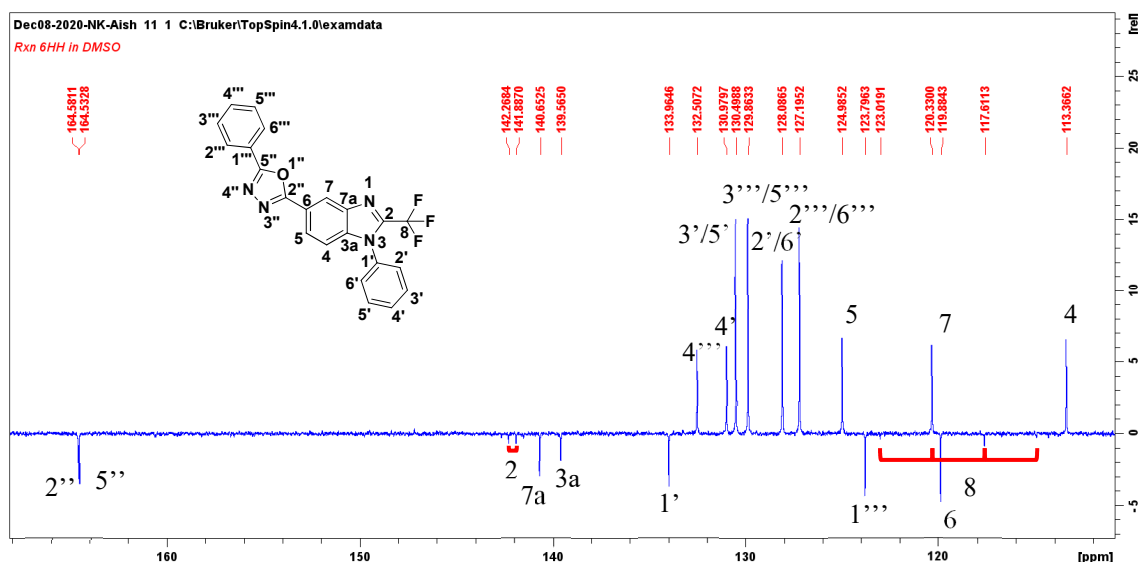
Figure 2.17 ^{13}C NMR spectrum of 2-phenyl-5-(1-phenyl-2-(trifluoromethyl)-1*H*-benzo[d]imidazole-5-yl)-1,3,4-oxadiazole **7a**

Heteronuclear multiple bond coherence (HMBC) correlations confirmed the assignments, H-7 and H-5 showing a correlation to C-3a at δ 139.5 and H-4 showing a correlation to C-7a. C-6 showed correlations to both H-5 and H-4. The oxadiazole carbon C-2" showed correlations to H-5 and H-7. At the same time, C-5" was seen correlating to H-2'''/6'''. The confirmation of assignment of H-2'''/6''' allowed C-4''' to be distinguished from C-4' as an HMBC correlation was seen between C-4''' and H-2'''/6'''. Likewise, C-1''' was identified by HMBC correlations to H-3'''/5''' and C-1' showed correlations to the proton resonance multiplet assigned to H-2'-H-6'. These correlations are depicted in Figure 2.18 and Figure 2.19.

The other eleven final compounds were elucidated using a similar method of deduction with the presence of the various substituents on the phenyl rings affecting the chemical shift and allowing for better visualisation of the splitting protons or causing extra splitting, in the case of fluorine.

All final compounds **7a-7l** were confirmed by both HRMS (Table 2.2) and elemental analysis. The required high resolution mass for **7h** for some unknown reason could not be detected, however the elemental analysis results are in good agreement with calculated values. For **7j**, the high resolution mass (*m/z* 521.1084) was in good agreement with calculated value (*m/z* 521.1071), however elemental analysis did not yield good results, and was not in agreement with calculated values.
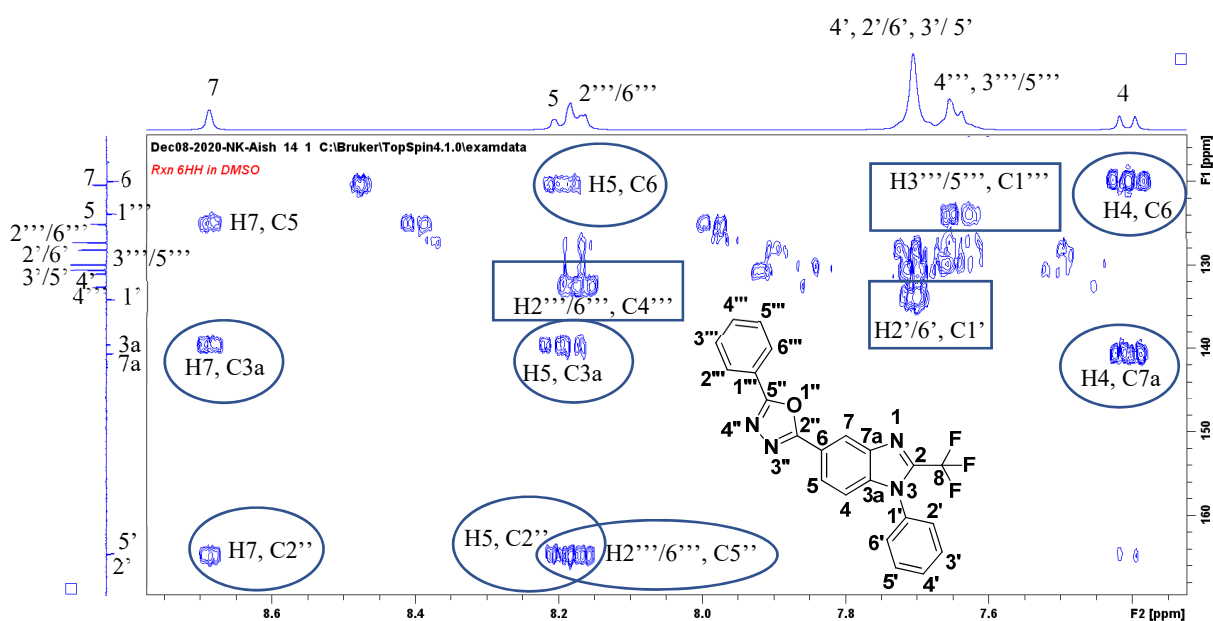
Figure 2.18 Expanded HMBC spectrum of **7a**
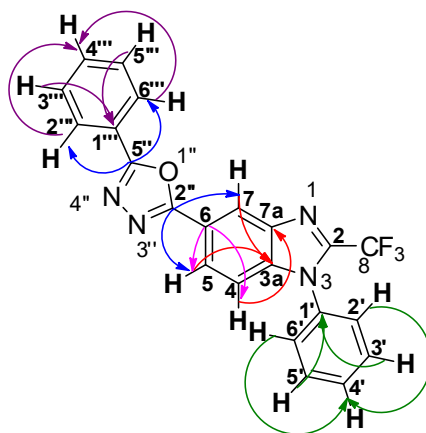
Figure 2.19 Graphical representation of HMBC correlations used to elucidate **7a**

2.4   Single Crystal X-Ray Diffraction of compound (7l)

In order to gain greater insight into the structure of the compounds synthesised, a single crystal X-Ray diffraction of compound **7l** containing a 4-fluorophenyl ring on the benzimidazole scaffold and 4-methoxyphenyl ring on the oxadiazole moiety was obtained. The crystals were grown by slow evaporation of the solvent (methanol). The crystal had a space group of P-1, and its crystal system was triclinic. The oxadiazole and benzimidazole moieties were planar with the two phenyl groups bending out of the plane, the oxadiazole phenyl ring bending out slightly at 16.47° and the fluorophenyl group attached to the benzimidazole bending out of the plane almost perpendicularly at 80.17°. The fluorine atoms of the CF_3 group were found to be disordered over three positions. PART instructions were used to model the disorder and 80% site occupancy was assigned to the major component. An ORTEP diagram of the crystal structure of **7l** is shown in Figure 2.20.
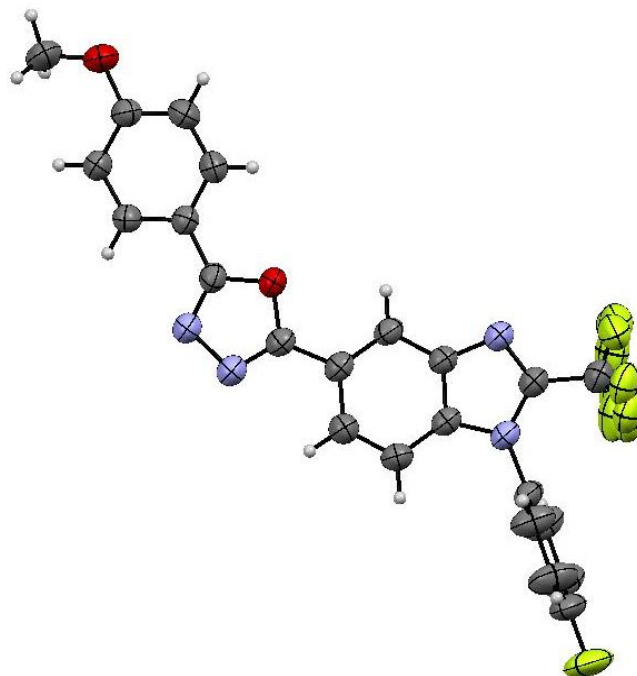
Figure 2.20 Crystal structure of 2-(1-(4-Fluorophenyl)-2-(trifluoromethyl)-1*H*-benzo[d]imidazole-5-yl)-5-(4-methoxyphenyl)-1,3,4-oxadiazole **7l**

2.5   Antibacterial assay of the benzimidazole-oxadiazole hybrids

The synthesised benzimidazole-oxadiazole hybrids (**7a-l**) were tested for their antibacterial activity against six strains of bacteria: two Gram-positive strains (*Staphylococcus aureus* and Methicillin-resistant *Staphylococcus aureus*) and four Gram-negative (*Klebsiella pneumoniae*, *Escherichia coli*, *Salmonella typhimurium* and *Pseudomonas aeruginosa*). Ciprofloxacin and metronidazole, two known antibiotics, were used as positive controls. Dimethyl sulfoxide (DMSO) was used to dissolve the samples and prepare the samples for the bioassay. It was also used as a negative control. DMSO alone did not display any antibacterial activity in the assay used.

Ciprofloxacin exhibited a broad range of antibacterial activities against all six bacterial strains tested. However, metronidazole only showed activity against *K. pneumoniae*. Metronidazole is more selective towards Gram-negative anaerobic bacteria that belong to the *Bacteroides* and Gram-positive bacteria such as peptostreptococci (Freeman et al., 1997). It was chosen as a control since it also contains an imidazole core nucleus, similar to the compounds synthesised in this work.

A preliminary antibacterial disk diffusion assay was used to screen the compounds for their ability to inhibit bacterial growth. Table 2.3 shows that almost all compounds were active against *K. pneumoniae*, with a few compounds also being active against *S. aureus* and *P. aeruginosa*. With regard to the intermediates, only **6b**, the hydrazide with a fluorinated phenyl group showed activity against *K. pneumoniae*. None of the other intermediates were active. The compounds were completely inactive against MRSA, *E. coli* and *S. typhimurium*.

Table 2.3 Disk diffusion screening results for the benzimidazole-oxadiazole hybrid molecules and intermediates leading to its synthesis

Compounds	Gram-positive		Gram-negative			
	Sa	MRSA	Ec	St	Kp	Pa
7a	-	-	-	-	A	-
7b	-	-	-	-	A	-
7c	-	-	-	-	A	-
7d	-	-	-	-	-	-
7e	A	-	-	-	A	A
7f	A	-	-	-	A	A
7g	-	-	-	-	A	-
7h	-	-	-	-	A	-
7i	-	-	-	-	A	-
7j	-	-	-	-	A	A
7k	A	-	-	-	A	A
7l	-	-	-	-	A	-
5a	-	-	-	-	-	-
5b	-	-	-	-	-	-
6a	-	-	-	-	-	-
6b	-	-	-	-	A	-
DMSO	-	-	-	-	-	-
Ciprofloxacin	A	A	A	A	A	A
Metronidazole	-	-	-	-	A	-

Sa = *S. aureus*, MRSA = Methicillin-resistant *S. aureus*, Ec = *E. coli*, St = *S. typhimurium*, Kp = *K. pneumoniae*, Pa = *P. aeruginosa*, A indicates that a zone of inhibition was observed in the assay. A "-" denotes that no zone of inhibition was observed.

The active compounds were then tested for their minimum bactericidal concentration (MBC) using a modified disk diffusion method. Five of the compounds, four of which had electron donating methyl and methoxy groups on the phenyl ring attached to the oxadiazole moiety, showed excellent activity against *K. pneumoniae*. These were **7e-f** and **7k-l**, showing a minimum bactericidal concentration (MBC) of 19, 18, 4 and 17 μM respectively (Table 2.4).

In addition, the bromo derivative **7b** showed an MBC of 16 μM. Four other compounds, **7c** and **7g-i** were also active against *K. pneumoniae*, but an order of magnitude greater, showing MBC values of between 124-147 μM. Only one compound, **7e**, the methyl derivative was active against *P. aeruginosa* with an MBC of 149 μM.

Table 2.4 Minimum bactericidal concentration (MBC in μM) of benzimidazole-oxadiazole hybrids against *K. pneumoniae* and *P. aeruginosa*

Compounds	R₁	R₂	Kp	Pa
7a	H	H	*	-
7b	H	Br	16	-
7c	H	Cl	142	-
7d	H	F	-	-
7e	H	CH₃	19	149
7f	H	CH₃O	18	*
7g	F	H	147	-
7h	F	Br	124	-
7i	F	Cl	136	-
7i	F	F	*	-
7k	F	CH₃	4	*
7l	F	CH₃O	17	-
Ciprofloxacin			12	3
Metronidazole			*	*

Kp = *Klebsiella pneumoniae*, Pa = *Pseudomonas aeruginosa*, * indicates activity >500 μM and "-" denotes no activity

In general, compounds where the phenyl moiety on the benzimidazole ring was fluorinated showed better activity than those that were not. The exception was the brominated derivatives **7b** and **7h**. Here, the compound with a benzimidazole phenyl group that was not fluorinated showed higher activity (16 μM) whereas when fluorinated, this activity decreased to 124 μM. However, the methyl derivative **7e**, which showed a MBC of 19 μM had a significant increase in activity when the phenyl group on the benzimidazole was fluorinated in **7k**, increasing

activity to 4 μM, better than that of ciprofloxacin, active in the same assay at 12 μM. It is interesting to note that **7a**, without any substitution on the phenyl rings at both the benzimidazole and oxadiazole was inactive, and that substitution on these rings was necessary for activity against *K. pneumoniae*.

These results indicated that on this particular scaffold, an electron donating group on the phenyl moiety attached to the oxadiazole was necessary for good activity, and that a fluorine at the *para* position of the phenyl group attached to the benzimidazole in general, increased activity. The best substitution pattern was observed by **7k**, which showed an MBC of 4 μM, three fold better than the standard ciprofloxacin.

The antibacterial study revealed that molecular hybridisation of the two pharmacophores produced a compound with enhanced bioactivity compared to their parent molecules. It would be interesting to investigate the effect of other substituents at the phenyl group of the benzimidazole in future work. Future work will also involve determining the cytotoxicity of the highly active compounds.

Chapter 3 Conclusion and future work

Due to the potential of both benzimidazoles and oxadiazoles to produce hit compounds for antibacterial activity, these two scaffolds were hybridised into a single molecule. The design of benzimidazole-oxadiazole hybrids was also based on previous unsuccessful attempts in hybridising benzimidazoles with other moieties.

The benzimidazole scaffold formed the basis of the final molecules and was synthesised in four efficient steps, including esterification of the acid precursor, nucleophilic aromatic substitution, reduction of the nitro group and cyclisation to the benzimidazole. All four steps were very efficient and yields of the stepwise intermediates were in the 85-95% range. As a precursor to forming the oxadizazole, the benzimidazole esters were converted to the hydrazides, in yet again a very efficient reaction with yields of over 95%. Molecular hybridisation occurred by reacting *N*-phenyl or *N*-fluorophenyl benzimidazole hydrazides **6a-b**, synthesised in this five-step synthetic route, with *para*-substituted benzoic acids in the presence of POCl$_3$ to form 2,5-phenyl-substituted oxadiazoles on the benzimidazole scaffold. Twelve hybrid molecules **7a-l** were successfully synthesised bearing halogens, electron-donating substituents, or an unsubstituted oxadiazole phenyl ring. Optimising the mole ratio of the benzoic acid to 2 moles proved to be a simple and efficient reaction with varying yields of 70 to 97%. In contrast, cyclisation with strongly electron-withdrawing groups had workup issues and in general was unsuccessful.

The antibacterial assay validated that hybridisation of two pharmacophores enhanced the bioactivity of the molecule, as the benzimidazole esters and hydrazides showed no activity against all the six bacterial strains used. However, when the benzimidazole scaffold was hybridised with the oxadiazole moiety, four compounds (**7b**, **7e-f** and **7l**) exhibited good

activity of 16-19 µM against *K. pneumoniae*. Furthermore, **7k** was identified as a hit molecule, as it had an MBC value of 4 µM, three-fold better than the standard ciprofloxacin and can be further developed into an antibacterial agent to aid in the battle against antimicrobial resistance.

Current work

The benzimidazole ester **5a-b** and hydrazide **6a-b** intermediates are being investigated for their cell viability and cytotoxicity against three cancer cell lines (HepG2, HEK 293 and Caco-2) through the colorimetric 3-(4,5-dimethylthiazol-2-yl)-2,5-diphenyl tetrazolium bromide (MTT) assay. Currently, the compounds are being screened against HepG2 cancer cells.

Future Work

Future work will involve exploring the effect of varying the substituent's position on the phenyl ring of the benzimidazole and introducing further groups to the phenyl ring of the oxadiazole. Molecular docking studies would also be carried out to determine the mode of action and bactericidal targets **7k** has against *K. pneumoniae.* Future work will also involve enhancing the drug-like qualities of the hit molecule by improving the hydrophilicity with the introduction of more polar groups, a sugar molecule or converting it into a salt.

Chapter 4 Experimental

4.1 General experimental procedures and instrumental techniques

Sigma-Aldrich supplied all chemicals *via* Capital Lab, South Africa. All organic solvents were redistilled and dried according to standard procedures. Thin-layer chromatography (TLC) was performed with silica gel 60 F_{254} plates from Merck using a 1:4 ethyl acetate: hexane mobile phase to record the retention factor. TLC was also used to monitor reactions to completion. Products were purified by column chromatography using silica gel (60-120 mesh) with ethyl acetate: hexane mobile phase as the eluent. Melting points of the intermediates and final compounds were recorded using a Stuart Scientific SMP3 apparatus and are uncorrected. The Perkin Elmer 100 FT-IR spectrophotometer was used to record IR spectra with a universal attenuated total reflectance sampling accessory. ^{1}H NMR, ^{13}C NMR and all 2D NMR spectra were analysed on a Bruker Avance instrument operating at 400 MHz. Chemical shifts were reported as δ values (ppm) relative to an internal standard of tetramethylsilane (TMS) or the solvent line of DMSO-d_6 (2.50 ppm for ^{1}H and 39.52 ppm for ^{13}C). The distance between the splitting patterns was calculated via coupling constants (J) using the Bruker TopSpin 4.1.0 software. A Bruker micro TOF-Q II ESI instrument operating at ambient temperature was used to obtain High-Resolution Mass spectra. Elemental analysis was performed with an elementar vario EL cube analyser. Single-crystal XRD analysis was obtained using the Bruker SmartAPEX2.

4.2 Synthesis

4.2.1 Preparation of methyl 4-fluoro-3-nitrobenzoate (2)

4-Fluoro-3-nitrobenzoic acid (1) (6.25 g, 33.8 mmol) was dissolved in 54.0 mL methanol, after which 6.9 mL concentrated sulfuric acid was added dropwise at room temperature. The reaction mixture was refluxed in an oil bath for 3 h at 80 °C. Upon completion, the reaction mixture was poured into an ice slurry and a white precipitate formed immediately. The precipitate was filtered, washed with (3 x 20 mL) cold water, and air-dried to afford the pure 4-fluoro-3-nitrobenzoate, in a 93% yield.
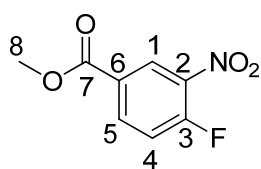
Methyl 4-fluoro-3-nitrobenzoate (2), Rf 0.58 (ethyl acetate:hexane 1:4), white powder, 93% yield, mp 65-66 °C, IR (KBr) υ_{max}: 3063 (C-H), 1713 (C=O), 1614 (C=C) cm^{-1}; ^{1}H NMR (DMSO, 400 MHz) δ 8.53 (1H, dd, J = 7.5, 2.1 Hz, H-1), 8.30 (1H, ddd, J = 8.7, 4.2, 2.1 Hz, H-5), 7.70 (1H, dd, J = 11.0, 8.7 Hz, H-4), 3.88 (3H, s, H-8); ^{13}C NMR (DMSO, 100 MHz) δ 164.3 (C-7), 157.7 (d, J_{CF} = 268.3 Hz, C-3), 137.2 (d, J = 10.5 Hz, C-5), 127.5 (d, J = 1.6 Hz, C-1), 127.1 (d, J = 3.7 Hz, C-6), 119.8 (d, J = 21.8 Hz, C-4), 53.4 (C-8). C-2 could not be detected.

4.2.2 Nucleophilic aromatic substitution reaction with anilines

4-Fluoro-3-nitrobenzoate (2) (3.50 g, 17.6 mmol) was dissolved in 35.0 mL ethanol and aniline (3.2 mL, 35.2 mol) or 4-fluoroaniline (3.3 mL, 35.2 mol). The reaction mixture was refluxed for 6 h and monitored by TLC. On completion, the ethanol was removed under reduced pressure. The residue was re-dissolved in ethyl acetate and extracted with 4 N HCl, to remove excess aniline or 4-fluoroaniline. The combined ethyl acetate layers were washed with (2 x 30 mL) water. The organic layer was dried with magnesium sulphate and concentrated under

reduced pressure. The phenyl **3a** and fluorophenyl **3b** nitrobenzoate esters were obtained in 98% and 96% yield, respectively.
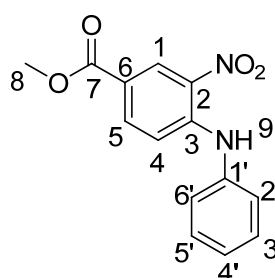
Methyl 3-nitro-4-(phenylamino)benzoate (**3a**), Rf 0.67 (ethyl acetate:hexane 1:4), dark orange crystals, 98% yield, mp 126-127 °C, IR (KBr) υ_{max}: 3326 (N-H, 2° amine), 2924 (C-H), 1717 (C=O), 1623 (C=C) cm^{-1}; ^{1}H NMR (DMSO, 400 MHz) δ 9.83 (1H, s, H-9), 8.63 (1H, d, J = 1.7 Hz, H-1), 7.92 (1H, dd, J = 8.9, 1.8 Hz, H-5), 7.47 (2H, t, J = 8.0 Hz, H-3'/5'), 7.36 (2H, d, J = 8.0 Hz, H-2'/6'), 7.30 (1H, t, J = 8.0 Hz, H-4'), 7.12 (1H, d, J = 8.8 Hz, H-4), 3.83 (3H, s, H-8); ^{13}C NMR (DMSO, 100 MHz) δ 165.1 (C-7), 145.9 (C-3), 138.5 (C-1'), 135.9 (C-5), 132.5 (C-2), 130.1 (C-3'/5'), 128.6 (C-1), 126.7 (C-4'), 125.6 (C-2'/6'), 118.4 (C-6), 116.8 (C-4), 52.6 (C-8).
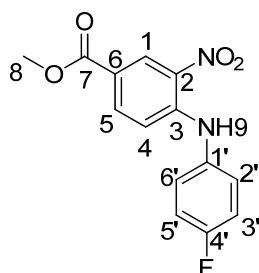
Methyl 4-((4-fluorophenyl)amino)-3-nitrobenzoate (**3b**), Rf 0.70 (ethyl acetate:hexane 1:4), light orange crystals, 90% yield, mp 157-158 °C, IR (KBr) υ_{max}: 3317 (N-H, 2° amine), 2960 (C-H), 1718 (C=O), 1623 (C=C) cm^{-1}; ^{1}H NMR (DMSO, 400 MHz) δ 9.81 (1H, s, H-9), 8.64 (1H, d, J = 1.6 Hz, H-1), 7.92 (1H, dd, J = 8.9, 1.7 Hz, H-5), 7.41 (2H, dd, J = 8.7, 5.2 Hz, H-2'/6'), 7.31 (2H, t, J = 8.7 Hz, H-3'/5'), 7.01 (1H, d, J = 8.7 Hz, H-4), 3.83 (3H, s, H-8); ^{13}C NMR (DMSO, 100 MHz) δ 165.1 (C-7), 160.7 (d, J_{CF} = 243.5 Hz, C-4'), 146.3 (C-3), 136.0 (C-5), 135.0 (C-1'), 132.4 (C-2), 128.6 (C-1), 128.4 (d, J = 8.8 Hz, C-2'/6'), 118.3 (C-6), 116.9 (d, J = 23.4 Hz, C-3'/5'), 116.8 (C-4), 52.6 (C-8).

4.2.3 Nitro group reduction

The nitrobenzoates **3a** (4.65 g, 16.0 mmol) and **3b** (4.28 g, 15.7 mmol) were reduced by 10% activated palladium on carbon (0.4 g). The intermediates **3a-b** were each dissolved in 47 mL

absolute ethanol in a two neck round bottom flask and flushed with nitrogen gas. The catalyst was added to the flask and flushed again with nitrogen to ensure an oxygen free atmosphere. Hydrogen gas was then slowly introduced to the flask via a bladder balloon and the flask was evacuated three times. The reaction was stirred under hydrogen atmosphere for twenty hours **3a** or four hours **3b** until completion (monitored by TLC). Upon completion, the reaction mixture was filtered through a celite 545 bed to remove the Pd/C and the catalyst deactivated in an acidic medium. The filtrate was evaporated under reduced pressure and the crude product purified by column chromatography (ethyl acetate: hexane, 20: 80 **4a**; 30:70 **4b**) to yield a white solid with a yield of 92% **4a** and 87% **4b**.
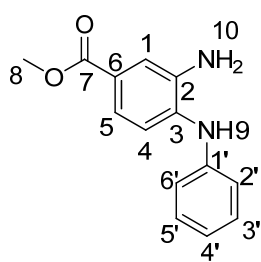
Methyl 3-amino-4-(phenylamino)benzoate (**4a**), Rf 0.28 (ethyl acetate:hexane 1:4), white solid, 92% yield, mp 88-89 °C, IR (KBr) υ_{max}: 3454 (N-H, 1° amine), 3381 (N-H, 2° amine), 2948 (C-H), 1687 (C=O), 1588 (C=C) cm^{-1}; ^{1}H NMR (DMSO, 400 MHz) δ 7.39 (1H, s, H-9), 7.35 (1H, d, *J* = 1.6 Hz, H-1), 7.23 (2H, t, *J* = 8.1 Hz, H-3'/5'), 7.17 (1H, dd, *J* = 8.3, 1.6 Hz, H-5), 7.07 (1H, d, *J* = 8.3 Hz, H-4), 7.00 (2H, d, *J* = 7.7 Hz, H-2'/6'), 6.85 (1H, t, *J* = 7.3 Hz, H-4'), 5.04 (2H, s, H-10), 3.76 (3H, s, H-8); ^{13}C NMR (DMSO, 100 MHz) δ 166.7 (C-7), 143.6 (C-3), 139.2 (C-1'), 134.5 (C-2), 129.5 (C-3'/5'), 122.6 (C-6), 120.6 (C-4'), 119.1 (C-5), 118.1 (C-2'/6'), 116.8 (C-4), 116.1 (C-1), 51.9 (C-8).
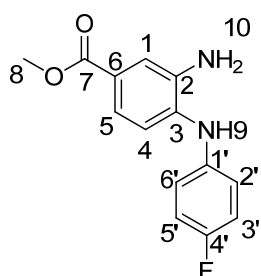
Methyl 3-amino-4-((4-fluorophenyl)amino)benzoate (**4b**), Rf 0.20 (ethyl acetate:hexane 1:4), white solid, 87% yield, mp 133-134 °C, IR (KBr) υ_{max}: 3425 (N-H, 1° amine), 3382 (N-H, 2° amine), 2952 (C-H), 1682 (C=O), 1508 (C=C), 1298 (C-O), 1158 (C-F); ^{1}H NMR (DMSO, 400 MHz) δ 7.37 (1H, s, H-9), 7.35 (1H, d, *J* = 1.8 Hz, H-1), 7.16 (1H, dd, *J* = 7.9, 1.4 Hz, H-5), 7.08 (2H, t, *J* = 8.7 Hz, H-3'/5'), 7.01 (2H, dd, *J* = 8.7, 4.8 Hz, H-2'/6'), 6.98 (1H, d, *J* = 8.0

Hz, H-4), 5.01 (2H, s, H-10), 3.76 (3H, s, H-8); ^{13}C NMR (DMSO, 100 MHz) δ 166.9 (C-7), 157.2 (d, J_{CF} = 236.5 Hz, C-4'), 139.8 (C-1'), 138.8 (C-3), 135.2 (C-2), 122.2 (C-6), 120.3 (d, J = 8.1 Hz, C-2'/6'), 119.3 (C-5), 116.1 (d, J = 22.2 Hz, C-3'/5'), 116.0 (C-1), 115.9 (C-4), 51.9 (C-8).

4.2.4 Preparation of methyl 1-phenyl-2-(trifluoromethyl)-1*H*-benzo[d]imidazole-5-carboxylate **5a** and methyl 1-(4-fluorophenyl)-2-(trifluoromethyl)-1*H*-benzo[d]imidazole-5-carboxylate **5b**

The amino intermediates **5a** (3.47 g, 14.3 mmol) and **5b** (3.16 g, 12.1 mmol) were synthesised by cyclisation of the phenylenediamine esters **4a** and **4b** with trifluoroacetic acid (2.8 mL, 36.5 mmol) and trifluoroacetic anhydride (8.5 mL, 60.9 mmol) under reflux at 70°C for 2 h. The reaction mixture was then added to 150 mL water and basified with the addition of sodium hydrogen carbonate (pH 8). The residue was dissolved in water and extracted in 100 mL ethyl acetate. The organic layer was washed with a brine solution (1 x 100 mL), dried with magnesium sulphate, and concentrated under reduced pressure. The intermediates were purified by column chromatography (ethyl acetate: hexane, 10: 90 **5a**; 15: 85 **5b**) to yield a viscous yellow liquid with a yield of 87% **5a** and 90% **5b**.
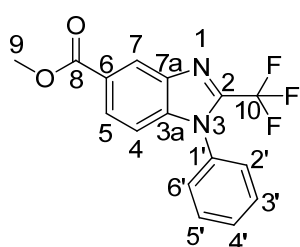
Methyl 1-phenyl-2-(trifluoromethyl)-1H-benzo[d]imidazole-5-carboxylate (**5a**), Rf 0.63 (ethyl acetate:hexane 1:4), viscous yellow liquid, 87% yield, IR (KBr) υ_{max}: 2954 (C-H), 1717 (C=O), 1621 (C=C) cm^{-1}; ^{1}H NMR (DMSO, 400 MHz) δ 8.50 (1H, s, H-7), 8.04 (1H, dd, J = 8.7, 1.3 Hz, H-5), 7.67 (5H, bs, H-2'-6'), 7.29 (1H, d, J = 8.7 Hz, H-4), 3.90 (3H, s, H-9); ^{13}C NMR (DMSO, 100 MHz) δ 166.5 (C-8), 142.1 (q, J = 38.3 Hz, C-2), 140.4 (C-3a), 140.1 (C-7a), 133.9 (C-1'), 130.9 (C-4'), 130.5 (C-3'/5'), 128.0 (C-2'/6'), 127.2 (C-5), 126.1 (C-6), 123.1 (C-7), 118.9 (q, J = 272.2 Hz, C-10), 112.3 (C-4), 52.7 (C-9).
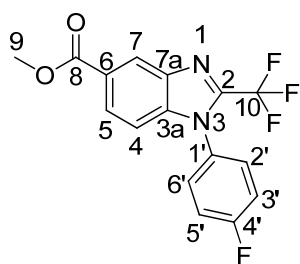
Methyl 1-(4-fluorophenyl)-2-(trifluoromethyl)-1H-benzo[d]imidazole-5-carboxylate (**5b**), Rf 0.65 (ethyl acetate/hexane 1:4), viscous yellow liquid, 90% yield, IR (KBr) υ_{max}: 2955 (C-H), 1716 (C=O), 1621 (C=C) cm⁻¹; ¹H NMR (DMSO, 400 MHz) δ 8.50 (1H, s, H-7), 8.05 (1H, dd, J = 8.7, 0.9 Hz, H-5), 7.77 (2H, dd, J = 8.7, 4.9 Hz, H-2'/6'), 7.52 (2H, t, J = 8.7 Hz, H-3'/5'), 7.32 (1H, d, J = 8.7 Hz, H-4), 3.90 (3H, s, H-9); ¹³C NMR (DMSO, 100 MHz) δ 166.6 (C-8), 163.2 (d, J = 248.0 Hz, C-4'), 142.2 (q, J = 38.2 Hz, C-2), 140.5 (C-3a), 140.1 (C-7a), 130.6 (d, J = 9.3 Hz, C-2'/6'), 130.1 (d, J = 2.9 Hz, C-1'), 127.2 (C-5), 126.2 (C-6), 123.1 (C-7), 118.8 (q, J = 272.2 Hz, C-10), 117.4 (d, J = 23.2 Hz, C-3'/5'), 112.3 (C-4), 52.8 (C-8).

4.2.5 Synthesis   of   1-phenyl-2-(trifluoromethyl)-1*H*-benzo[d]imidazole-5-carbohydrazide **6a** and 1-(4-fluorophenyl)-2-(trifluoromethyl)-1*H*-benzo[d]imidazole-5-carbohydrazide **6b**

The benzimidazole intermediates **5a** (3.60 g, 11.5 mmol) and **5b** (3.60 g, 10.8 mmol) were refluxed for eight hours in 12 mL absolute ethanol and hydrazine hydrate (2.2 mL, 46.1 mmol). The reaction was monitored by TLC. The resultant residue was added to an ice slurry, where a white precipitate formed. This was filtered and air-dried to yield 96% **6a** and 98% **6b**.
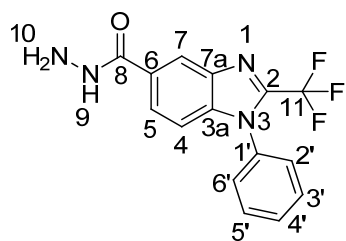
1-Phenyl-2-(trifluoromethyl)-1H-benzo[d]imidazole-5-carbohydrazide (**6a**), white powder, 96% yield, mp 145-146 °C, IR (KBr) υ_{max}: 3544 (N-H, 1° amine), 3307 (N-H, 2° amine), 1602 (C=O) cm⁻¹; ¹H NMR (DMSO, 400 MHz) δ 9.93 (1H, s, H-9), 8.41 (1H, s, H-7), 7.96 (1H, dd, J = 8.7, 1.2 Hz, H-5), 7.65 (5H, m, H-2'-6'), 7.24 (1H, d, J =

8.7 Hz, H-4), 4.54 (2H, s, H-10); ^{13}C NMR (DMSO, 100 MHz) δ 166.1 (C-8), 141.4 (d, J = 37.9 Hz, C-2), 140.1 (C-7a), 139.1 (C-3a), 134.1 (C-1'), 130.8 (C-4'), 130.5 (C-3'/5'), 129.9 (C-6), 128.1 (C-2'/6'), 125.8 (C-5), 120.3 (C-7), 119.0 (q, J = 271.9 Hz, C-11), 111.8 (C-4); HRMS (neg) (*m/z*): 319.0814 [M-H] (calculated for $C_{15}H_{10}F_3N_4O$, 319.0807).
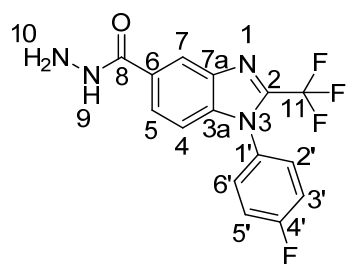
1-(4-Fluorophenyl)-2-(trifluoromethyl)-1H-benzo[d]imidazole - 5-carbohydrazide (**6b**), white powder, 98% yield, mp 148-149 °C, IR (KBr) υ_{max}: 3543 (N-H, 1° amine), 3307 (N-H, 2° amine), 3055 (C-H), 1603 (C=O) cm^{-1}; ^{1}H NMR (DMSO, 400 MHz) δ 9.92 (1H, s, H-9), 8.40 (1H, s, H-7), 7.96 (1H, d, J = 8.7 Hz, H-5), 7.75 (2H, dd, J = 8.6, 4.9 Hz, H-2'/6'), 7.52 (2H, t, J = 8.7 Hz, H-3'/5'), 7.26 (1H, d, J = 8.7 Hz, H-4), 4.56 (2H, s, H-10); ^{13}C NMR (DMSO, 100 MHz) δ 166.1 (C-8), 163.1 (d, J = 247.9 Hz, C-4'), 141.5 (q, J = 38.4 Hz, C-2), 140.0 (C-3a), 139.2 (C-7a), 130.6 (d, J = 9.3 Hz, C-2'/6'), 130.3 (d, J = 2.8 Hz, C-1'), 129.9 (C-6), 125.8 (C-5), 120.2 (C-7), 117.4 (q, J = 271.9 Hz, C-11), 117.3 (d, J = 23.3 Hz, C-3'/5'), 111.8 (C-4); HRMS (pos) (*m/z*): 417.1009 [M+H+DMSO] (calculated for $C_{17}H_{17}F_4N_4O_2S$, 417.1008).

4.2.6 General procedure of the formation of benzimidazole-oxadiazole hybrids **7a-l**

The benzimidazole carbohydrazide intermediate **6a** (0.2 g, 0.62 mmol) and benzoic acid (1.24 mmol) was mixed in a 50 mL round bottom flask with 2 mL POCl$_3$. The mixture was reacted for 16 h at 70 °C. On completion, the reaction was basified (pH 8) using sodium hydroxide, extracted with ethyl acetate (3 x 10 mL), and washed with brine solution (1 x 10 mL). The organic layer was dried over anhydrous magnesium sulphate, concentrated under reduced pressure, and purified by column chromatography (ethyl acetate: hexane, 7: 93) to obtain **7a** in a yield of 70%.

The same procedure was performed for the hybrids **7b** to **7l**, and using **6a** and **6b**, respectively.
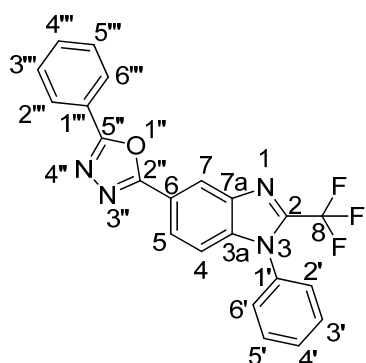
2-*Phenyl-5-(1-phenyl-2-(trifluoromethyl)-1H-benzo[d]imidazole-5-yl)-1,3,4-oxadiazole* (**7a**), Rf 0.42 (ethyl acetate:hexane 1:4), white powder, 70.2% yield, 179-180 °C, IR (KBr) υ_{max}: 3069 (C-H), 1622 (C=C) cm^{-1}; ^{1}H NMR (DMSO, 400 MHz) δ 8.76 (1H, s, H-7), 8.18 (1H, d, J = 9.2 Hz, H-5), 8.16 (2H, m, H-2'''/6'''), 7.69 (5H, s, H-4', H-2'/6', H-3'/5'), 7.63-7.65 (3H, m, H-3'''-H-5'''), 7.39 (1H, d, J = 8.7 Hz, H-4); ^{13}C NMR (DMSO, 100 MHz) δ 164.58* (C-2''), 164.53* (C-5''), 141.5 (q, J = 38.4 Hz, C-2), 140.6 (C-7a), 139.5 (C-3a), 134.0 (C-1'), 132.5 (C-4'''), 131.0 (C-4'), 130.5 (C-3'/5'), 129.9 (C-3'''/5'''), 128.0 (C-2'/6'), 127.1 (C-2'''/6'''), 125.0 (C-5), 123.8 (C-1'''), 120.3 (C-7), 119.9 (C-6), 118.9 (q, J = 272.3 Hz, C-8), 113.4 (C-4); HRMS (pos) (*m/z*): 407.1132 [M+H] (calculated for $C_{22}H_{14}F_3N_4O$, 407.1120); Anal. Calc. for CHN: C, (65.02); H, (3.22); N, (13.79). Found: C, (66.90); H, (3.41); N, (14.15). * Resonances can be interchanged.
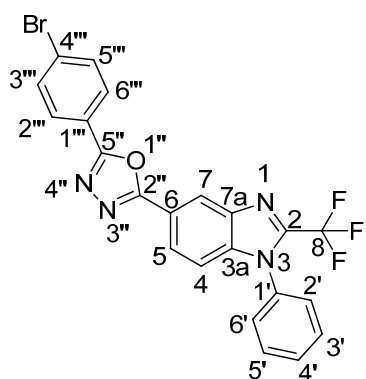
2-*(4-Bromophenyl)-5-(1-phenyl-2-(trifluoromethyl)-1H-benzo[d]imidazol-5-yl)-1,3,4-oxadiazole* (**7b**), Rf 0.50 (ethyl acetate:hexane 1:4), white powder, 70.0% yield, 186-187 °C, IR (KBr) υ_{max}: 3466 (C-H), 1601 (C=C) cm^{-1}; ^{1}H NMR (DMSO, 400 MHz) δ 8.69 (1H, s, H-7), 8.18 (1H, d, J = 8.7 Hz, H-5), 8.10 (2H, d, J = 8.3 Hz, H-2'''/6'''), 7.84 (2H, d, J = 8.3 Hz, H-3'''/5'''), 7.69 (5H, s, H-4', H-2'/6', H-3'/5'), 7.40 (1H, d, J = 8.7 Hz, H-4); ^{13}C NMR (DMSO, 100 MHz) δ 164.8 (C-2''), 163.9 (C-5''), 142.1 (d, J = 37.9 Hz, C-2), 140.6 (C-7a), 139.6 (C-3a), 133.9 (C-1'), 132.9 (C-3'''/5'''), 130.9 (C-4'), 130.5 (C-3'/5'), 129.1 (C-2'''/6'''), 128.0

(2'/6'), 126.1 (C-4'''), 125.0 (C-5), 123.0 (C-1'''), 120.4 (C-7), 119.7 (C-6), 118.9 (q, J = 272.2 Hz, C-8), 113.3 (C-4); HRMS (pos) (*m/z*): 563.0385 [M+H+DMSO] (calculated for $C_{24}H_{19}BrF_3N_4O_2S$, 563.0364); Anal. Calc. for CHN: C, (54.45); H, (2.49); N, (11.55). Found: C, (53.25); H, (2.80); N, (11.24).

2-(4-Chlorophenyl)-5-(1-phenyl-2-(trifluoromethyl)-1H-benzo[d]imidazol-5-yl)-1,3,4-oxadiazole (**7c**), Rf 0.47 (ethyl acetate:hexane 1:4), white powder, 83.8% yield, 173-174 °C, IR (KBr) υmax: 3467 (C-H), 1595 (C=C) cm⁻¹; ¹H NMR (DMSO, 400 MHz) δ 8.68 (1H, s, H-7), 8.16-8.19 (3H, m, H-5, H-2'''/6'''), 7.69-7.72 (5H, m, H-2'-H-6', H-3'''/5'''), 7.39 (1H, d, J = 8.7 Hz, H-4); ¹³C NMR (DMSO, 100 MHz) δ 164.7 (C-2''), 163.7 (C-5''), 142.0 (q, J = 38.3 Hz, C-2), 140.6 (C-7a), 139.5 (C-3a), 137.2 (C-4'''), 133.9 (C-1'), 130.9 (C-4'), 130.5 (C-3'/5'), 130.0 (C-3'''/5'''), 128.9 (C-2'''/6'''), 128.0 (2'/6'), 125.0 (C-5), 122.6 (C-1'''), 120.4 (C-7), 119.7 (C-6), 118.9 (q, J = 272.1 Hz, C-8), 113.3 (C-4); HRMS (pos) (*m/z*): 519.0892 [M+H+DMSO] (calculated for $C_{24}H_{19}ClF_3N_4O_2S$, 519.0869); Anal. Calc. for CHN: C, (59.94); H, (2.74); N, (12.71). Found: C, (58.22); H, (3.11); N, (12.03).

2-(4-Fluorophenyl)-5-(1-phenyl-2-(trifluoromethyl)-1H-benzo[d]imidazol-5-yl)-1,3,4-oxadiazole (**7d**), Rf 0.44 (ethyl acetate:hexane 1:4), white powder, 76.0% yield, 170-171 °C, IR (KBr) υmax: 3063 (C-H), 1615 (C=C) cm⁻¹; ¹H NMR (DMSO, 400 MHz) δ 8.67 (1H, s, H-7), 8.21 (2H, dd, J = 8.2, 5.6 Hz, H-2'''/6'''), 8.17 (1H, d, J = 8.7 Hz, H-5), 7.69 (5H, m, H-2'-6'), 7.46 (2H, t, J = 8.7 Hz, H-3'''/5'''), 7.39 (1H, d, J = 8.7 Hz, H-4); ¹³C NMR (DMSO, 100 MHz) δ 164.6 (d, J = 250.5 Hz, C-4'''), 164.5 (C-2''), 163.7 (C-5''), 142.0 (d, J = 38.1 Hz, C-

2), 140.6 (C-7a), 139.5 (C-3a), 133.9 (C-1'), 130.9 (C-4'), 130.4 (C-3'/5'), 129.9 (d, J = 9.5 Hz, C-2'''/6'''), 128.0 (C-2'/6'), 124.9 (C-5), 120.4 (d, J = 3.0 Hz, C-1'''), 120.3 (C-7), 119.8 (C-6), 118.9 (q, J = 272.2 Hz, C-8), 117.1 (d, J = 22.5 Hz, C-3'''/5'''), 113.3 (C-4); HRMS (pos) (m/z): 503.1179 [M+H+DMSO] (calculated for $C_{24}H_{19}F_4N_4O_2S$, 503.1165); Anal. Calc. for CHN: C, (62.27); H, (2.85); N, (13.20). Found: C, (63.55); H, (2.90); N, (13.49).
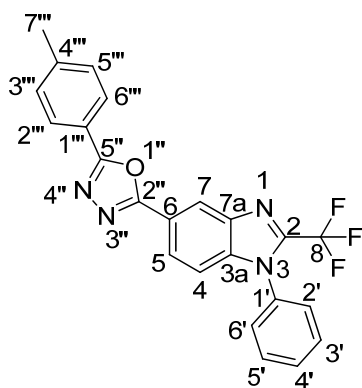
2-(1-phenyl-2-(trifluoromethyl)-1H-benzo[d]imidazol-5-yl)-5-(p-tolyl)-1,3,4-oxadiazole (**7e**), Rf 0.44 (ethyl acetate:hexane 1:4), white powder, 89.6% yield, 173-174 °C, IR (KBr) υ_{max}: 2928 (C-H), 1619 (C=C) cm^{-1}; ^{1}H NMR (DMSO, 400 MHz) δ 8.66 (1H, s, H-7), 8.17 (1H, d, J = 8.7 Hz, H-5), 8.04 (2H, d, J = 8.0 Hz, H-2'''/6'''), 7.69 (5H, m, H-2'-6'), 7.43 (2H, d, J = 8.0

Hz, H-3'''/5'''), 7.39 (1H, d, J = 8.7 Hz, H-4), 2.40 (3H, s, H-7'''); ^{13}C NMR (DMSO, 100 MHz) δ 164.6 (C-5''), 164.3 (C-2''), 142.6 (C-4'''), 142.0 (q, J = 38.3 Hz, C-2), 140.6 (C-7a), 139.5 (C-3a), 133.9 (C-1'), 130.9 (C-4'), 130.4 (C-3'/5'), 130.4 (C-3'''/5'''), 128.0 (C-2'/6'), 127.1 (C-2'''/6'''), 124.9 (C-5), 121.0 (C-1'''), 120.2 (C-7), 119.9 (C-6), 118.9 (q, J = 271.9 Hz, C-8), 113.3 (C-4), 21.6 (C-7'''); HRMS (pos) (m/z): 443.1083 [M+Na] (calculated for $C_{23}H_{15}F_3N_4NaO$, 443.1096); Anal. Calc. for CHN: C, (65.71); H, (3.60); N, (13.33). Found: C, (65.91); H, (3.58); N, (13.08).
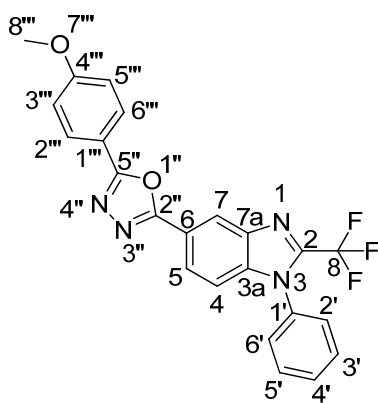
2-(4-Methoxyphenyl)-5-(1-phenyl-2-(trifluoromethyl)-1H-benzo[d]imidazol-5-yl)-1,3,4-oxadiazole (**7f**), Rf 0.22 (ethyl acetate:hexane 1:4), white powder, 97.7% yield, 169-170 °C, IR (KBr) υ_{max}: 2838 (C-H), 1614 (C=C) cm^{-1}; ^{1}H NMR (DMSO, 400 MHz) δ 8.68 (1H, s, H-7), 8.19 (1H, d, J = 8.7 Hz, H-5), 8.11 (2H, d, J = 8.7 Hz, H-2'''/6'''), 7.70 (5H, s, H-

2'-6'), 7.40 (1H, d, J = 8.7 Hz, H-4), 7.17 (2H, d, J = 8.8 Hz, H-3'''/5'''), 3.87 (3H, s, H-7''');

^{13}C NMR (DMSO, 100 MHz) δ 164.5 (C-5''), 164.1 (C-2''), 162.6 (C-4'''), 142.0 (q, J = 38.6 Hz, C-2), 140.6 (C-7a), 139.4 (C-3a), 133.9 (C-1'), 130.9 (C-4'), 130.4 (C-3'/5'), 129.0 (C-2'''/6'''), 128.1 (C-2'/6'), 124.9 (C-5), 120.1 (C-7), 120.0 (C-6), 118.9 (q, J = 271.8 Hz, C-8), 116.1 (C-1'''), 115.3 (C-3'''/5'''), 113.3 (C-4), 56.0 (C-8'''); HRMS (pos) (*m/z*): 515.1382 [M+H+DMSO] (calculated for C$_{25}$H$_{22}$F$_3$N$_4$O$_3$S, 515.1365); Anal. Calc. for CHN: C, (63.30); H, (3.46); N, (12.84). Found: C, (64.44); H, (3.85); N, (12.94).

2-(1-(4-Fluorophenyl)-2-(trifluoromethyl)-1H-benzo[d] imidazol-5-yl)-5-phenyl-1,3,4-oxadiazole (**7g**), Rf 0.44 (ethyl acetate:hexane 1:4), white powder, 85.1% yield, 183-184 °C, IR (KBr) υ$_{max}$: 1526, 1510 cm^{-1}; ^{1}H NMR (DMSO, 400 MHz) δ 8.71 (1H, s, H-7), 8.22 (1H, d, J = 8.7 Hz, H-5), 8.19 (2H, m, H-2'''/6'''), 7.80 (2H, dd, J = 8.6, 4.9 Hz, H-2'/6'), 7.62-7.66 (3H, m, H-3'''-H-5'''), 7.56 (2H, t, J = 8.6 Hz, H-3'/5'), 7.44 (1H, d, J = 8.7 Hz, H-4); ^{13}C NMR (DMSO, 100 MHz) δ 164.6 (C-2''), 164.5 (C-5''), 163.2 (d, J = 248.0 Hz, C-4'), 142.0 (d, J = 38.2 Hz, C-2), 140.6 (C-7a), 139.7 (C-3a), 132.5 (C-4'''), 130.7 (d, J = 9.4 Hz, C-2'/6'), 130.2 (d, J = 2.9 Hz, C-1'), 129.8 (C-3'''/5'''), 127.2 (C-2'''/6'''), 124.9 (C-5), 123.7 (C-1'''), 120.3 (C-7), 119.9 (C-6), 118.9 (q, J = 268.0 Hz, C-8), 117.4 (d, J = 23.1 Hz, C-3'/5'), 113.3 (C-4); HRMS (pos) (*m/z*): 503.1187 [M+H+DMSO] (calculated for C$_{24}$H$_{19}$F$_4$N$_4$O$_2$S, 503.1165); Anal. Calc. for CHN: C, (62.27); H, (2.85); N, (13.20). Found: C, (61.79); H, (2.77); N, (12.98).
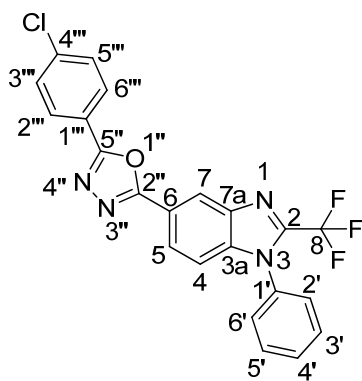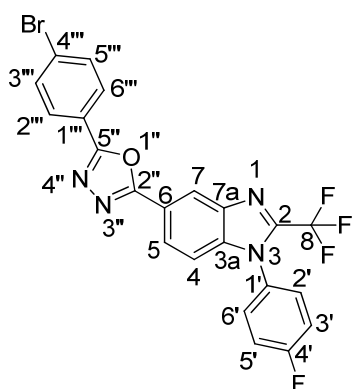

2-(4-Bromophenyl)-5-(1-(4-fluorophenyl)-2-(trifluoromethyl)-1H-benzo[d]imidazol-5-yl)-1,3,4-oxadiazole (**7h**), Rf 0.52 (ethyl acetate:hexane 1:4), white powder, 78.3% yield, 192-193 °C, IR (KBr) υ$_{max}$: 3085 (C-H), 1601 (C=C) cm^{-1}; ^{1}H NMR (DMSO, 400 MHz) δ 8.67 (1H, s, H-7), 8.17 (1H, d, J = 8.7 Hz, H-5), 8.09

(2H, d, *J* = 8.4 Hz, H-2'''/6'''), 7.82 (2H, d, *J* = 8.4 Hz, H-3'''/5'''), 7.79 (2H, dd, *J* = 9.0, 5.2 Hz, H-2'/6'), 7.54 (2H, t, *J* = 8.6 Hz, H-3'/5'), 7.42 (1H, d, *J* = 8.7 Hz, H-4); ^{13}C NMR (DMSO, 100 MHz) δ 164.7 (C-2''), 163.8 (C-5''), 163.2 (d, *J* = 247.9 Hz, C-4'), 142.1 (d, *J* = 38.2 Hz, C-2), 140.6 (C-7a), 139.7 (C-3a), 132.9 (C-3'''/5'''), 130.7 (d, *J* = 9.2 Hz, C-2'/6'), 130.2 (d, *J* = 2.8 Hz, C-1'), 129.0 (C-2'''/6'''), 126.1 (C-4'''), 124.9 (C-5), 123.0 (C-1'''), 120.4 (C-7), 119.7 (C-6), 118.9 (q, *J* =273.1 Hz, C-8), 117.4 (d, *J* = 23.2 Hz, C-3'/5'), 113.3 (C-4); Anal. Calc. for CHN: C, (52.51); H, (2.20); N, (11.13). Found: C, (52.80); H, (2.20); N, (11.01).

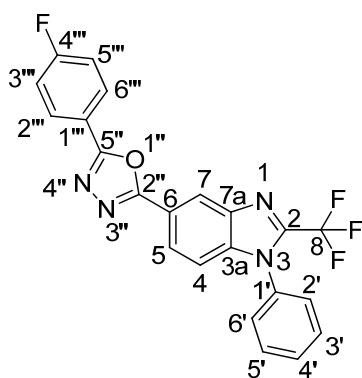*2-(4-Chlorophenyl)-5-(1-(4-fluorophenyl)-2-(trifluoromethyl)-1H-benzo[d]imidazol-5-yl)-1,3,4-oxadiazole* (**7i**), Rf 0.52 (ethyl acetate:hexane 1:4), white powder, 61.3% yield, 215-216 °C, IR (KBr) υ_{max}: 3464 (C-H), 1604 (C=C) cm^{-1}; ^{1}H NMR (DMSO, 400 MHz) δ 8.70 (1H, s, H-7), 8.20 (1H, dd, *J* = 8.5, 1.3 Hz, H-5), 8.16 (2H, d, *J* = 8.5 Hz, H-2'''/6'''), 7.79 (2H, dd, *J* = 8.7,

4.9 Hz, H-2'/6'), 7.70 (2H, d, *J* = 8.5 Hz, H-3'''/5'''), 7.55 (2H, t, *J* = 8.7 Hz, H-3'/5'), 7.43 (1H, d, *J* = 8.7 Hz, H-4); ^{13}C NMR (DMSO, 100 MHz) δ 164.7 (C-2''), 163.7 (C-5''), 163.2 (d, *J* = 247.9 Hz, C-4'), 142.1 (q, *J* = 38.1 Hz, C-2), 141.6 (C-7a), 139.7 (C-3a), 137.2 (C-4'''), 130.7 (d, *J* = 9.3 Hz, C-2'/6'), 130.2 (d, *J* = 2.8 Hz, C-1'), 130.0 (C-3'''/5'''), 128.9 (C-2'''/6'''), 124.9 (C-5), 122.6 (C-1'''), 120.3 (C-7), 119.7 (C-6), 118.9 (q, *J* = 272.1 Hz, C-8), 117.4 (d, *J* = 23.3 Hz, C-3'/5'), 113.3 (C-4); HRMS (pos) (*m/z*): 537.0786 [M+H+DMSO] (calculated for $C_{24}H_{18}ClF_4N_4O_2S$, 537.0775); Anal. Calc. for CHN: C, (57.59); H, (2.42); N, (12.21). Found: C, (55.55); H, (2.63); N, (11.67).
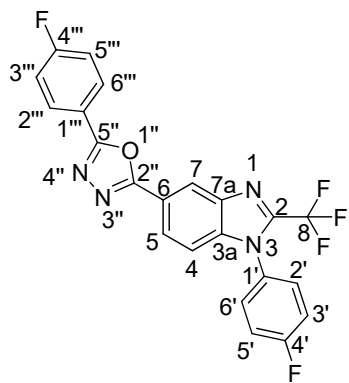
2-(4-Fluorophenyl)-5-(1-(4-fluorophenyl)-2-(trifluoromethyl)-1H-benzo[d]imidazol-5-yl)-1,3,4-oxadiazole (**7j**), Rf 0.46 (ethyl acetate:hexane 1:4), white powder, 82.6% yield, 195-196 °C, IR (KBr) υ_{max}: 3074 (C-H), 1610 (C=C) cm^{-1}; ^{1}H NMR (DMSO, 400 MHz) δ 8.67 (1H, s, H-7), 8.22 (2H, dd, J = 8.7, 5.4 Hz, H-2'''/6'''), 8.18 (1H, dd, J = 8.7, 1.1 Hz, H-5), 7.79 (2H, dd, J = 8.8, 4.9 Hz, H-2'/6'), 7.54 (2H, t, J = 8.7 Hz, H-3'/5'), 7.47 (2H, t, J = 8.8 Hz, H-3'''/5'''), 7.42 (1H, d, J = 8.7 Hz, H-4); ^{13}C NMR (DMSO, 100 MHz) δ 164.6 (d, J = 250.4 Hz, C-4'''), 164.5 (C-2''), 163.7 (C-5''), 163.2 (d, J = 248.0 Hz, C-4'), 142.1 (q, J = 38.1 Hz, C-2), 140.6 (C-7a), 139.7 (C-3a), 130.7 (d, J = 9.3 Hz, C-2'/6'), 130.2 (d, J = 2.3 Hz, C-1'), 129.9 (d, J = 9.3 Hz, C-2'''/6'''), 125.0 (C-5), 120.4 (d, J = 3.0 Hz, C-1'''), 120.3 (C-7), 119.8 (C-6), 118.9 (q, J = 272.2 Hz, C-8), 117.4 (d, J = 23.4 Hz, C-3'/5'), 117.1 (d, J = 22.4 Hz, C-3'''/5'''), 113.3 (C-4); HRMS (pos) (*m/z*): 521.1084 [M+H+DMSO] (calculated for $C_{24}H_{18}F_5N_4O_2S$, 521.1071).
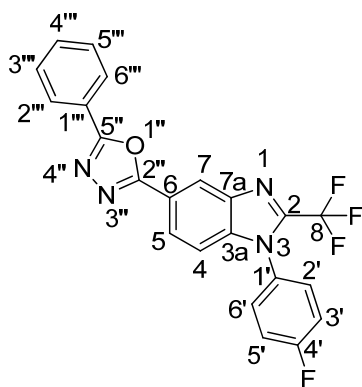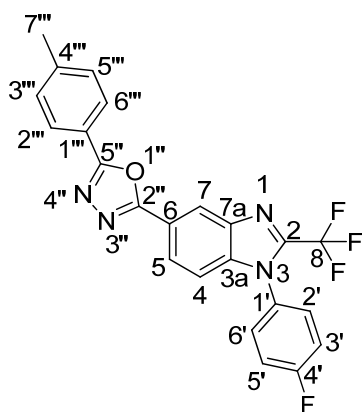

2-(1-(4-fluorophenyl)-2-(trifluoromethyl)-1H-benzo[d]imidazol-5-yl)-5-(p-tolyl)-1,3,4-oxadiazole (**7k**), Rf 0.46 (ethyl acetate:hexane 1:4), white powder, 88.1% yield, 162-163 °C, IR (KBr) υ_{max}: 3479 (C-H), 1620 (C=C) cm^{-1}; ^{1}H NMR (DMSO, 400 MHz) δ 8.69 (1H, s, H-7), 8.20 (1H, d, J = 8.7 Hz, H-5), 8.07 (2H, d, J = 8.0 Hz, H-2'''/6'''), 7.79 (2H, dd, J = 8.7, 4.9 Hz, H-2'/6'), 7.55 (2H, t, J = 8.7 Hz, H-3'/5'), 7.42 (2H, d, J = 8.0 Hz, H-3'''/5'''), 7.41 (1H, d, J = 8.4 Hz, H-4), 2.42 (3H, s, H-7'''); ^{13}C NMR (DMSO, 100 MHz) δ 164.6 (C-5''), 164.3 (C-2''), 163.2 (d, J = 247.9 Hz, C-4'), 142.7 (C-4'''), 142.1 (d, J = 38.0 Hz, C-2), 140.6 (C-7a), 139.7 (C-3a), 130.7 (d, J = 9.3 Hz, C-2'/6'), 130.3 (C-3'''/5'''), 130.2 (d, J = 2.9 Hz, C-1'), 127.1 (C-2'''/6'''), 124.9 (C-5), 121.0 (C-1'''), 120.2 (C-7), 119.9 (C-6), 118.9 (q, J =

272.1 Hz, C-8), 117.4 (d, J = 23.1 Hz, C-3'/5'), 113.3 (C-4), 21.6 (C-7'''); HRMS (pos) (*m/z*): 517.1328 [M+H+DMSO] (calculated for $C_{25}H_{21}F_4N_4O_2S$, 517.1321); Anal. Calc. for CHN: C, (63.02); H, (3.22); N, (12.78). Found: C, (61.44); H, (3.42); N, (12.09).
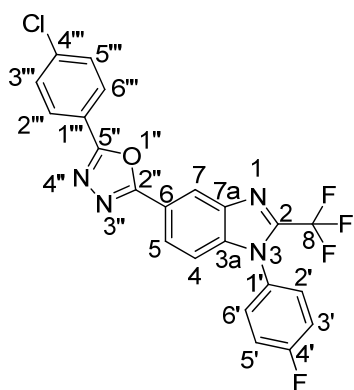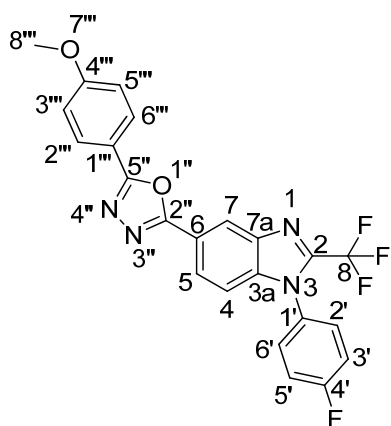
2-(1-(4-Fluorophenyl)-2-(trifluoromethyl)-1H-benzo[d]imidazole-5-yl)-5-(4-methoxyphenyl)-1,3,4-oxadiazole (**7l**), Rf 0.28 (ethyl acetate:hexane 1:4), white powder, 97.1% yield, 211-212 °C, IR (KBr) υ_{max}: 1608 (C=C) cm⁻¹; ¹H NMR (DMSO, 400 MHz) δ 8.64 (1H, s, H-7), 8.16 (1H, d, J = 8.7 Hz, H-5), 8.09 (2H, d, J = 8.7 Hz, H-2'''/6'''), 7.79 (2H, dd, J = 8.7, 4.9 Hz, H-2'/6'), 7.54 (2H, t, J = 8.7 Hz, H-3'/5'), 7.41 (1H, d, J = 8.7 Hz, H-4), 7.15 (2H, d, J = 8.8 Hz, H-3'''/5'''), 3.86 (3H, s, H-8'''); ¹³C NMR (DMSO, 100 MHz) δ 164.4 (C-5''), 164.0 (C-2''), 163.2 (d, J = 245.8 Hz, C-4'), 162.5 (C-4'''), 142.1 (d, J = 38.1 Hz, C-2), 140.6 (C-7a), 139.6 (C-3a), 130.7 (d, J = 9.4 Hz, C-2'/6'), 130.2 (d, J = 2.8 Hz, C-1'), 129.0 (C-2'''/6'''), 124.9 (C-5), 120.2 (C-7), 120.0 (C-6), 118.9 (q, J = 272.2 Hz, C-8), 117.4 (d, J = 23.3 Hz, C-3'/5'), 116.1 (C-1'''), 115.3 (C-3'''/5'''), 113.3 (C-4), 56.0 (C-8'''); HRMS (pos) (*m/z*): 533.1286 [M+H+DMSO] (calculated for $C_{25}H_{21}F_4N_4O_3S$, 533.1271); Anal. Calc. for CHN: C, (60.80); H, (3.11); N, (12.33). Found: C, (60.78); H, (3.29); N, (12.11).

4.3 Antibacterial assay

4.3.1 Preliminary screening

The twelve final benzimidazole-oxadiazole hybrid molecules and four benzimidazole intermediates (**5a-b** and **6a-b**) were tested for their antibacterial activity against two Gram-positive and four Gram-negative bacterial strains. These strains included *Staphylococcus aureus* ATCC 25923 and Methicillin-resistant *Staphylococcus aureus* ATCC 700699,

Klebsiella pneumonia ATCC 31488, *Escherichia coli* ATCC 25922, *Salmonella typhimurium* ATCC 14026 and *Pseudomonas aeruginosa* ATCC 27853, respectively. Ciprofloxacin and metronidazole were used as standards and for comparison. The bacteria were grown overnight in Nutrient Broth (Biolab, South Africa) at 37 ºC in a shaking incubator at 100 rpm. The bacterial concentration was adjusted to 0.5 McFarland's Standard with sterile distilled water using a DEN-1B McFarland densitometer (Latvia). Mueller-Hinton agar (MHA) plates (Biolab, South Africa) were lawn inoculated with the different strains of bacteria. A solution of the twelve hybrid molecules **7a-l** and the four benzimidazole intermediates were prepared by dissolving 1 mg of the compound in 1 mL of DMSO. Then 10 µL of the solution was spotted on inoculated agar plates containing the bacterial strains. The plates were then left to incubate in an oven for 24 hours at 37 °C. The compounds that displayed partial or complete inhibition zones were tested for their minimum bactericidal concentration (MBC).

4.3.2 Minimum bactericidal concentration (MBC) determination

A two-fold serial dilution of the partial and completely active compounds was prepared with DMSO to make ten standards (500 – 0.98 µg/L) in triplicate. A 5 µL aliquot of each standard solution was spotted on lawn-inoculated MHA plates, which were incubated at 37 °C for 24 hours. The lowest concentration that exhibited an inhibition zone was recorded as the MBC value (µg mL^{-1} converted to µM). The MBC assay was performed in triplicate to ensure that results were reproducible.

4.4 Single crystal X-Ray determination

Single crystals of **7l** were grown overnight in methanol by slow evaporation. A suitable crystal was selected, and its structure determined on a Bruker APEX-II CCD diffractometer. The

crystal was kept at 296.15 K during data collection. Using Olex2 (Dolomanov et al., 2009), the structure was solved with the SHELXT (Sheldrick, 2015b) structure solution program using Intrinsic Phasing and refined with the SHELXL (Sheldrick, 2015a) refinement package using Least Squares minimisation.

References

Abdel-Wahab, S.M., Abdelsamii, Z.K., Abdel-Fattah, H.A., El-Etrawy, A.S., Georghiou, P.E. Synthesis and antimicrobial evaluation of selected new benzimidazole-acetamido conjugates. International Journal of Pharmaceutical Chemistry, 2016, 6, 149-159. DOI: https://doi.org/10.7439/ijpc

Acar Çevik, U., Sağlık, B.N., Osmaniye, D., Levent, S., Kaya Çavuşoğlu, B., Karaduman, A.B., Atlı Eklioğlu, Ö., Özkay, Y., Kaplancıklı, Z.A. Synthesis, anticancer evaluation and molecular docking studies of new benzimidazole- 1,3,4-oxadiazole derivatives as human topoisomerase types I poison. Journal of Enzyme Inhibition and Medicinal Chemistry, 2020, 35, 1657-1673. DOI: https://doi.org/10.1080/14756366.2020.1806831

Adegoke, A.A., Faleye, A.C., Singh, G., Stenström, T.A. Antibiotic resistant superbugs: assessment of the interrelationship of occurrence in clinical settings and environmental niches. Molecules, 2016, 22, 29. DOI: https://doi.org/10.3390/molecules22010029

Ainsworth, C. The condensation of aryl carboxylic acid hydrazides with orthoesters. Journal of the American Chemical Society, 1955, 77, 1148-1150. DOI: https://doi.org/10.1021/ja01610a019

Ainsworth, C. 1,3,4-Oxadiazole. Journal of the American Chemical Society, 1965, 87, 5800-5801. DOI: https://doi.org/10.1021/ja00952a056

Ainsworth, C., Hackler, R.E. Alkyl-1,3,4-oxadiazoles. Journal of Organic Chemistry, 1966, 31, 3442-3444. DOI: https://doi.org/10.1021/jo01348a531

Akkoç, S. Design, synthesis, characterization, and in vitro cytotoxic activity evaluation of 1,2-disubstituted benzimidazole compounds. Journal of Physical Organic Chemistry, 2020, 34, e4125. DOI: https://doi.org/10.1002/poc.4125

Alasmary, F.A., Snelling, A.M., Zain, M.E., Alafeefy, A.M., Awaad, A.S., Karodia, N. Synthesis and evaluation of selected benzimidazole derivatives as potential antimicrobial agents. Molecules, 2015, 20, 15206-15223. DOI: https://doi.org/10.3390/molecules200815206

Alfahad, M., Jasim, M.H.M., Qazzaz, M.E., Alassaf, F.A., Abed, M.N. Proton pump inhibitors and peptic ulcer management: Antioxidant mechanisms. Journal of Drug Delivery and Therapeutics, 2021, 11, 242-246. DOI: https://doi.org/10.22270/jddt.v11i4-s.4955

Alimi Livani, Z., Safakish, M., Hajimahdi, Z., Soleymani, S., Zabihollahi, R., Aghasadeghi, M.R., Alipour, E., Zarghi, A. Design, synthesis, molecular modeling, in silico ADME studies and anti-HIV-1 assay of new diazocoumarin derivatives. Iranian Journal of Pharmaceutical Research, 2018, 17, 65-77. DOI: https://www.ncbi.nlm.nih.gov/pmc/articles/PMC6447871/

Altıntop, M.D., Sever, B., Akalın Çiftçi, G., Turan-Zitouni, G., Kaplancıklı, Z.A., Özdemir, A. Design, synthesis, in vitro and in silico evaluation of a new series of oxadiazole-based anticancer agents as potential Akt and FAK inhibitors. European Journal of Medicinal Chemistry, 2018, 155, 905-924. DOI: https://doi.org/10.1016/j.ejmech.2018.06.049

Aly, A.A., Brase, S., Hassan, A.A., Mohamed, N.K., Abd El-Haleem, L.E., Nieger, M. Synthesis of new planar-chiral linked [2.2]paracyclophanes-N-([2.2]paracyclophanylcarbamoylamino)-[2.2]paracyclophane-4-carboxamide, [2.2]paracyclophanyl-substituted triazolthiones and -

substituted oxadiazoles. Molecules, 2020, 25, 3315. DOI: https://doi.org/10.3390/molecules25153315

Ansari, J.A. Drug interaction and pharmacist. Journal of Young Pharmacists, 2010, 2, 326-331. DOI: https://doi.org/10.4103/0975-1483.66807

Asghar, S.F., Yasin, K.A., Aziz, S. Synthesis and cyclisation of 1,4-disubstituted semicarbazides. Natural Product Research, 2010, 24, 315-325. DOI: https://doi.org/10.1080/14786410802435935

Augustine, J.K., Vairaperumal, V., Narasimhan, S., Alagarsamy, P., Radhakrishnan, A. Propylphosphonic anhydride (T3P®): an efficient reagent for the one-pot synthesis of 1,2,4-oxadiazoles, 1,3,4-oxadiazoles, and 1,3,4-thiadiazoles. Tetrahedron, 2009, 65, 9989-9996. DOI: https://doi.org/10.1016/j.tet.2009.09.114

Ayoub, M.A. Small molecules targeting heterotrimeric G proteins. European Journal of Pharmacology, 2018, 826, 169-178. DOI: https://doi.org/10.1016/j.ejphar.2018.03.003

Azizian, H., Esmailnejad, A., Fathi Vavsari, V., Mahernia, S., Amanlou, M., Balalaie, S. Pantoprazole derivatives: Synthesis, urease inhibition assay and in silico molecular modeling studies. ChemistrySelect, 2020, 5, 4580-4587. DOI: https://doi.org/10.1002/slct.202000578

Bahri, F., Shadi, M., Mohammadian, R., Javanbakht, S., Shaabani, A. Cu-decorated cellulose through a three-component Betti reaction: An efficient catalytic system for the synthesis of 1,3,4-oxadiazoles via imine CH functionalization of N-acylhydrazones. Carbohydrate Polymers, 2021, 265, 118067. DOI: https://doi.org/10.1016/j.carbpol.2021.118067

Baig, M.H., Ahmad, K., Adil, M., Khan, Z.A., Khan, M.I., Lohani, M., Khan, M.S., Kamal, M.A. Drug discovery and in silico techniques: A mini-review. Enzyme Engineering, 2014, 4. DOI: https://doi.org/10.4172/2329-6674.1000123

Bandarage, U., Hare, B., Parsons, J., Pham, L., Marhefka, C., Bemis, G., Tang, Q., Moody, C.S., Rodems, S., Shah, S., Adams, C., Bravo, J., Charonnet, E., Savic, V., Come, J.H., Green, J. 4-(Benzimidazol-2-yl)-1,2,5-oxadiazol-3-ylamine derivatives: Potent and selective p70S6 kinase inhibitors. Bioorganic & Medicinal Chemistry Letters, 2009, 19, 5191-5194. DOI: https://doi.org/10.1016/j.bmcl.2009.07.022

Bandyopadhyay, P., Sathe, M., Ponmariappan, S., Sharma, A., Sharma, P., Srivastava, A.K., Kaushik, M.P. Exploration of in vitro time point quantitative evaluation of newly synthesized benzimidazole and benzothiazole derivatives as potential antibacterial agents. Bioorganic & Medicinal Chemistry Letters, 2011, 21, 7306-7309. DOI: https://doi.org/10.1016/j.bmcl.2011.10.034

Bansal, Y., Silakari, O. The therapeutic journey of benzimidazoles: A review. Bioorganic & Medicinal Chemistry, 2012, 20, 6208-6236. DOI: https://doi.org/10.1016/j.bmc.2012.09.013

Barbero, M., Cadamuro, S., Dughera, S. The efficient o-benzenedisulfonimide catalyzed synthesis of benzothiazoles, benzoxazoles and benzimidazoles. ARKIVOC, 2012, 9, 262-279. DOI: https://doi.org/10.3998/ark.5550190.0013.923

Behalo, M.S. An efficient one-pot catalyzed synthesis of 2,5-disubstituted-1,3,4-oxadiazoles and evaluation of their antimicrobial activities. RSC Advances, 2016, 6, 103132-103136. DOI: https://doi.org/10.1039/c6ra22663a

Benet, L.Z., Hosey, C.M., Ursu, O., Oprea, T.I. BDDCS, the Rule of 5 and drugability. Advanced Drug Delivery Reviews, 2016, 101, 89-98. DOI: https://doi.org/10.1016/j.addr.2016.05.007

Bhati, S., Kumar, V., Singh, S., Singh, J. Synthesis, characterization, antimicrobial, anti-tubercular, antioxidant activities and docking simulations of derivatives of 2-(pyridin-3-yl)-1H-benzo[d]imidazole and 1,3,4-oxadiazole analogy. Letters in Drug Design & Discovery, 2020, 17, 1047-1059. DOI: https://doi.org/10.2174/1570180816666191122105313

Bhatia, S., Pai, A., Rao, R., Srinivas, S., Shetty, V. Insect bite like rash induced by bendamustine – A common presentation with an uncommon cause. Our Dermatology Online, 2020, 11, e152.1-e152.5. DOI: https://doi.org/10.7241/ourd.2020e.152

Bhutani, R., Pathak, D.P., Kapoor, G., Husain, A., Iqbal, M.A. Novel hybrids of benzothiazole-1,3,4-oxadiazole-4-thiazolidinone: Synthesis, in silico ADME study, molecular docking and in vivo

anti-diabetic assessment. Bioorganic Chemistry, 2019, 83, 6-19. DOI: https://doi.org/10.1016/j.bioorg.2018.10.025

Bishop, B.C., Chelton, E.T., Jones, A.S. The antibacterial activity of some fluorine-containing benzimidazoles Biochemical Pharmacology, 1964, 13, 751-754. DOI: https://doi.org/10.1016/0006-2952(64)90011-5

Bistrović, A., Krstulović, L., Stolić, I., Drenjančević, D., Talapko, J., Taylor, M.C., Kelly, J.M., Bajić, M., Raić-Malić, S. Synthesis, anti-bacterial and anti-protozoal activities of amidinobenzimidazole derivatives and their interactions with DNA and RNA. Journal of Enzyme Inhibition and Medicinal Chemistry, 2018, 33, 1323-1334. DOI: https://doi.org/10.1080/14756366.2018.1484733

Bonnett, R. The chemistry of the vitamin B_{12} group. Chemical Reviews, 1963, 63, 573-605. DOI: https://doi.org/10.1021/cr60226a002

Borsoi, A.F., Coldeira, M.E., Pissinate, K., Macchi, F.S., Basso, L.A., Santos, D.S., Machado, P. Ultrasound-assisted synthesis of 2-amino-1,3,4-oxadiazoles through NBS-mediated oxidative cyclization of semicarbazones. Synthetic Communications, 2017, 47, 1319-1325. DOI: https://doi.org/10.1080/00397911.2017.1324626

Bosch, F., Rosich, L. The contributions of Paul Ehrlich to pharmacology: A tribute on the occasion of the centenary of his Nobel Prize. Pharmacology, 2008, 82, 171-179. DOI: https://doi.org/10.1159/000149583

Bosquesi, P.L., Melo, T.R.F., Vizioli, E.O., Santos, J.L.D., Chung, M.C. Anti-inflammatory drug design using a molecular hybridization approach. Pharmaceuticals, 2011, 4, 1450-1474. DOI: https://doi.org/10.3390/ph4111450

Boström, J., Hogner, A., Llinas, A., Wellner, E., Plowright, A. Oxadiazoles in medicinal chemistry. Journal of Medicinal Chemistry, 2011, 55, 1817-30. DOI: https://doi.org/10.1021/jm2013248

Breijyeh, Z., Jubeh, B., Karaman, R. Resistance of gram-negative bacteria to current antibacterial agents and approaches to resolve it. Molecules, 2020, 25, 1340. DOI: https://doi.org/10.3390/molecules25061340

Brink, N.G., Folkers, K. Vitamin B_{12}. VI. 5,6-dimethylbenzimidazole, a degradation product of vitamin B_{12}. Journal of the American Chemical Society, 1950, 72, 4442-4443. DOI: https://doi.org/10.1021/ja01166a027

Calligari, P., Bobone, S., Ricci, G., Bocedi, A. Molecular investigation of SARS–CoV-2 proteins and their interactions with antiviral drugs. Viruses, 2020, 12, 445. DOI: https://doi.org/10.3390/v12040445

Capoci, I.R.G., Sakita, K.M., Faria, D.R., Rodrigues-Vendramini, F.A.V., Arita, G.S., de Oliveira, A.G., Felipe, M.S., Maigret, B., Bonfim-Mendonça, P.S., Kioshima, E.S., Svidzinski, T.I.E. Two new 1,3,4-oxadiazoles with effective antifungal activity against *Candida albicans*. Frontiers in Microbiology, 2019, 10, 2130. DOI: https://doi.org/10.3389/fmicb.2019.02130

Carbone, M., Li, Y., Irace, C., Mollo, E., Castelluccio, F., Di Pascale, A., Cimino, G., Santamaria, R., Guo, Y.-W., Gavagnin, M. Structure and cytotoxicity of phidianidines A and B: First finding of 1,2,4-oxadiazole system in a marine natural product. Organic Letters, 2011, 13, 2516-2519. DOI: https://doi.org/10.1021/ol200234r

Carilli, A., Favis, G., Sundharkrishnan, L., Hajdenberg, J. Severe dermatologic reactions with bendamustine: A case series. Case Reports in Oncology, 2014, 7, 465-470. DOI: https://doi.org/10.1159/000365324

Chandrakantha, B., Shetty, P., Nambiyar, V., Isloor, N., Isloor, A.M. Synthesis, characterization and biological activity of some new 1,3,4-oxadiazole bearing 2-flouro-4-methoxy phenyl moiety. European Journal of Medicinal Chemistry, 2010, 45, 1206-1210. DOI: https://doi.org/10.1016/j.ejmech.2009.11.046

Chaturvedi, A.K., Verma, A.K., Thakur, J.P., Roy, S., Bhushan Tripathi, S., Kumar, B.S., Khwaja, S., Sachan, N.K., Sharma, A., Chanda, D., Shanker, K., Saikia, D., Negi, A.S. A novel synthesis of 2-arylbenzimidazoles in molecular sieves-MeOH system and their antitubercular activity.

Bioorganic & Medicinal Chemistry, 2018, 26, 4551-4559. DOI: https://doi.org/10.1016/j.bmc.2018.07.049

Chauhan, J., Ravva, M.K., Sen, S. Harnessing autoxidation of aldehydes: *in situ* iodoarene catalyzed synthesis of substituted 1,3,4-oxadiazole, in the presence of molecular oxygen. Organic Letters, 2019, 21, 6562-6565. DOI: https://doi.org/10.1021/acs.orglett.9b02542

Cheddie, A. 2018. *Synthesis, characterisation and antibacterial activity of benzimidazole derivatives.* PhD Dissertation, University of Kwa-Zulu Natal.

Cheddie, A., Shintre, S.A., Bantho, A., Mocktar, C., Koorbanally, N.A. Synthesis and antibacterial activity of a series of 2-trifluoromethylbenzimidazole-thiazolidinone derivatives. Journal of Heterocyclic Chemistry, 2020, 57, 299-307. DOI: https://doi.org/10.1002/jhet.3777

Cheong, J.E., Zaffagni, M., Chung, I., Xu, Y., Wang, Y., Jernigan, F.E., Zetter, B.R., Sun, L. Synthesis and anticancer activity of novel water soluble benzimidazole carbamates. European Journal of Medicinal Chemistry, 2018, 144, 372-385. DOI: https://doi.org/10.1016/j.ejmech.2017.11.037

Chigurupati, S., Maharajan, M.K., Abhinayani, G., Sravya, N. Designing and biological evaluation of new benzimidazole compounds. Chemical Science Transactions, 2013, 2, 922-926. DOI: https://doi.org/10.7598/cst2013.431

Chimirri, A., Grasso, S., Molica, C., Monforte, A.M., Monforte, P., Zappalà, M., Bruno, G., Nicolò, F., Witvrouw, M., Jonckeere, H., Balzarini, J., De Clercq, E. Structural features and anti-human immunodeficiency virus (HIV) activity of the isomers of 1-(2',6'-difluorophenyl)-1*H*,3*H*-thiazolo[3,4-*a*]benzimidazole, a potent non-nucleoside HIV-1 reverse transcriptase inhibitor. Antiviral Chemistry and Chemotherapy, 1997, 8, 363-370. DOI: https://doi.org/10.1177/095632029700800409

Chimirri, A., Grasso, S., Monforte, A.M., Monforte, P., Zappalà, M. Anti-HIV agents. I: Synthesis and in vitro anti-HIV evaluation of novel 1*H*,3*H*-thiazolo[3,4-*a*]benzimidazoles. IL Farmaco, 1991, 46, 817-823. DOI: https://europepmc.org/abstract/MED/1685321

Chimirri, A., Grasso, S., Monforte, P., Rao, A., Zappalà, M., Monforte, A.M., Pannecouque, C., Witvrouw, M., Balzarini, J., De Clercq, E. Synthesis and biological activity of novel 1*H*,3*H*-thiazolo[3,4-*a*]benzimidazoles: non-nucleoside human immunodeficiency virus type 1 reverse transcriptase inhibitors. Antiviral Chemistry & Chemotherapy, 1999, 10, 211-217. DOI: https://doi.org/10.1177/095632029901000405

Crowther-Gibson, P., Govender, N., Lewis, D.A., Bamford, C., Brink, A., von Gottberg, A., Klugman, K., du Plessis, M., Fali, A., Harris, B., Keddy, K., Botha, M. Part IV. Human infections and antibiotic resistance. South African Medical Journal, 2011, 101, 567-578. DOI: https://www.samj.org.za/index.php/samj/article/view/5102

Desai, N., Kotadiya, G. Microwave-assisted synthesis of benzimidazole bearing 1,3,4-oxadiazole derivatives: screening for their *in vitro* antimicrobial activity. Medicinal Chemistry Research, 2014, 23, 4021-4033. DOI: https://doi.org/10.1007/s00044-014-0978-0

Dhotre, B.K., Patharia, M.A., Khandebharad, A.U., Raut, S.V., Pathan, M.A. Microwave-assisted synthesis and molecular docking studies of fluorinated 1,3,4-oxadiazole derivatives as antimicrobial agent. Russian Journal of Bioorganic Chemistry, 2020, 46, 1110-1116. DOI: https://doi.org/10.1134/s1068162020060059

Dhumal, S.T., Deshmukh, A.R., Bhosle, M.R., Khedkar, V.M., Nawale, L.U., Sarkar, D., Mane, R.A. Synthesis and antitubercular activity of new 1,3,4-oxadiazoles bearing pyridyl and thiazolyl scaffolds. Bioorganic & Medicinal Chemistry Letters, 2016, 26, 3646-3651. DOI: https://doi.org/10.1016/j.bmcl.2016.05.093

Dobrotă, C., Paraschivescu, C.C., Dumitru, I., Matache, M., Baciu, I., Ruţă, L.L. Convenient preparation of unsymmetrical 2,5-disubstituted 1,3,4-oxadiazoles promoted by Dess–Martin reagent. Tetrahedron Letters, 2009, 50, 1886-1888. DOI: https://doi.org/10.1016/j.tetlet.2009.02.054

Dokla, E.M.E., Abutaleb, N.S., Milik, S.N., Li, D., El-Baz, K., Shalaby, M.-A.W., Al-Karaki, R., Nasr, M., Klein, C.D., Abouzid, K.A.M., Seleem, M.N. Development of benzimidazole-based derivatives as antimicrobial agents and their synergistic effect with colistin against gram-negative

bacteria. European Journal of Medicinal Chemistry, 2020, 186, 111850. DOI: https://doi.org/10.1016/j.ejmech.2019.111850

Dolman, S.J., Gosselin, F., O'Shea, P.D., Davies, I.W. Superior reactivity of thiosemicarbazides in the synthesis of 2-amino-1,3,4-oxadiazoles. Journal of Organic Chemistry, 2006, 71, 9548-9551. DOI: https://doi.org/10.1021/jo0618730

Dolomanov, O.V., Bourhis, L.J., Gildea, R.J., Howard, J.A.K., Puschmann, H. OLEX2: a complete structure solution, refinement and analysis program. Journal of Applied Crystallography, 2009, 42, 339-341. DOI: https://doi.org/10.1107/S0021889808042726

Du, L.-H., Luo, X.-P. Efficient one-pot synthesis of benzimidazoles under solvent-free conditions. Synthetic Communications, 2010, 40, 2880-2886. DOI: https://doi.org/10.1080/00397910903340629

Du, Y., Wan, Z., Chen, L., Wu, L. One pot solvent-free solid state synthesis, photophysical properties and crystal structure of substituted azole derivatives. Journal of Molecular Structure, 2019, 1193, 315-325. DOI: https://doi.org/10.1016/j.molstruc.2018.12.095

Dubois, N., Glynn, D., McInally, T., Rhodes, B., Woodward, S., Irvine, D.J., Dodds, C. On DABAL-Me$_3$ promoted formation of amides. Tetrahedron, 2013, 69, 9890-9897. DOI: https://doi.org/10.1016/j.tet.2013.08.062

El-Sayed, N.A., Nour, M.S., Salem, M.A., Arafa, R.K. New oxadiazoles with selective-COX-2 and EGFR dual inhibitory activity: Design, synthesis, cytotoxicity evaluation and *in silico* studies. European Journal of Medicinal Chemistry, 2019, 183, 111693. DOI: https://doi.org/10.1016/j.ejmech.2019.111693

El-Sayed, W.A., El-Essawy, F.A., Ali, O.M., Nasr, B.S., Abdalla, M.M., Abdel-Rahman, A.A.H. Anti-HIV activity of new substituted 1,3,4-oxadiazole derivatives and their acyclic nucleoside analogues. Zeitschrift für Naturforschung C, 2009, 64, 773-778. DOI: https://doi.org/10.1515/znc-2009-11-1203

El Dareer, S.M., Tillery, K.F., Rose, L.M., Posey, C.F., Struck, R.F., Stiller, S.W., Hill, D.L. Metabolism and disposition of a thiazolobenzimidazole active against human immunodeficiency virus-1. Drug Metabolism and Disposition, 1993, 21, 231-235.

Elshihawy, H., Hammad, M. Molecular modeling studies and synthesis of fused heterocyclic compounds with potential inhibitory activities of menthionine synthase catalysed reaction. Organic Chemistry: An Indian Journal, 2013, 9, 41-57.

Eswayah, A., Khaliel, S., Saad, S., Shebani, N., Fhid, O., Belaid, A., Alsharif, T., Elforjane, H., Saadalla, Y., Baga, E. Synthesis and analgesic activity evaluation of some new benzimidazole derivatives. American Journal of Chemistry and Application, 2017, 4, 30-35.

Fan, Y., He, Y., Liu, X., Hu, T., Ma, H., Yang, X., Luo, X., Huang, G. Iodine-mediated domino oxidative cyclization: One-pot synthesis of 1,3,4-oxadiazoles via oxidative cleavage of C(sp2)–H or C(sp)–H bond. Journal of Organic Chemistry, 2016, 81, 6820-6825. DOI: https://doi.org/10.1021/acs.joc.6b01135

Fischbach, M.A. Combination therapies for combating antimicrobial resistance. Current Opinion in Microbiology, 2011, 14, 519-523. DOI: https://doi.org/10.1016/j.mib.2011.08.003

Fischer, O. Über die aufspaltung des imidazol- und oxazolringes. Journal für Praktische Chemie, 1905, 73, 419-446. DOI: https://doi.org/10.1002/prac.19060730128

Freeman, C.D., Klutman, N.E., Lamp, K.C. Metronidazole. A therapeutic review and update. Drugs, 1997, 54, 679-708. DOI: https://doi.org/10.2165/00003495-199754050-00003

Fry, D.C. Protein-protein interactions as targets for small molecule drug discovery. Biopolymers, 2006, 84, 535-552. DOI: https://doi.org/10.1002/bip.20608

Fu, R., Yang, Y., Ma, Y., Yang, F., Li, J., Chai, W., Wang, Q., Yuan, R. Microwave-promoted direct amidation of unactivated esters catalyzed by heteropolyanion-based ionic liquids under solvent-free conditions. Tetrahedron Letters, 2015, 56, 4527-4531. DOI: https://doi.org/10.1016/j.tetlet.2015.05.118

Gaba, M., Gaba, P., Uppal, D., Dhingra, N., Bahia, M.S., Silakari, O., Mohan, C. Benzimidazole derivatives: search for GI-friendly anti-inflammatory analgesic agents. Acta Pharmaceutica Sinica B, 2015, 5, 337-342. DOI: https://doi.org/10.1016/j.apsb.2015.05.003

Gaba, M., Mohan, C. Development of drugs based on imidazole and benzimidazole bioactive heterocycles: recent advances and future directions. Medicinal Chemistry Research, 2016, 25, 173-210. DOI: https://doi.org/10.1007/s00044-015-1495-5

Gaba, M., Singh, D., Singh, S., Sharma, V., Gaba, P. Synthesis and pharmacological evaluation of novel 5-substituted-1-(phenylsulfonyl)-2-methylbenzimidazole derivatives as anti-inflammatory and analgesic agents. European Journal of Medicinal Chemistry, 2010, 45, 2245-2249. DOI: https://doi.org/10.1016/j.ejmech.2010.01.067

Gao, Q., Liu, S., Wu, X., Zhang, J., Wu, A. Direct annulation of hydrazides to 1,3,4-oxadiazoles via oxidative C(CO)–C(methyl) bond cleavage of methyl ketones. Organic Letters, 2015, 17, 2960-2963. DOI: https://doi.org/10.1021/acs.orglett.5b01241

Garcia-Aranda, M.I., Gonzalez-Padilla, J.E., Gomez-Castro, C.Z., Gomez-Gomez, Y.M., Rosales-Hernandez, M.C., Garcia-Baez, E.V., Franco-Hernandez, M.O., Castrejon-Flores, J.L., Padilla-Martinez, I.I. Anti-inflammatory effect and inhibition of nitric oxide production by targeting COXs and iNOS enzymes with the 1,2-diphenylbenzimidazole pharmacophore. Bioorganic & Medicinal Chemistry, 2020, 28, 115427. DOI: https://doi.org/10.1016/j.bmc.2020.115427

Garg, S., Raghav, N. 2,5-Diaryloxadiazoles and their precursors as novel inhibitors of cathepsins B, H and L. Bioorganic Chemistry, 2016, 67, 64-74. DOI: https://doi.org/10.1016/j.bioorg.2016.05.003

Ge, M., Feng, J., Huang, H., Gou, X., Hua, C., Chen, B., Zhao, J. NO_2-Fe (II)Pc-catalyzed synthesis of 2-ferrocenyl-5-aryl-1,3,4-oxadiazoles and study of antifungal activity. Journal of Heterocyclic Chemistry, 2019, 56, 3297-3302. DOI: https://doi.org/10.1002/jhet.3725

Gejalakshmi, S., Dhanalakshmi, S., Harikrishnan, N. Synthesis characterization and evaluation of novel substituted azole derivatives. Der Pharma Chemica, 2018, 10, 76-81. DOI: https://www.derpharmachemica.com/archive.html

Glomb, T., Świątek, P. Antimicrobial activity of 1,3,4-oxadiazole derivatives. International Journal of Molecular Sciences, 2021, 22, 6979. DOI: https://doi.org/10.3390/ijms22136979

Glomb, T., Szymankiewicz, K., Świątek, P. Anti-cancer activity of derivatives of 1,3,4-oxadiazole. Molecules 2018, 23, 3361. DOI: https://doi.org/10.3390/molecules23123361

Goldschmidt, H. Ueber die einwirkung von hydroxylamin auf diketone (About the effect of hydroxylamine on diketone). Berichte der Deutschen Chemischen Gesellschaft (Reports from the German Chemical Society), 1883, 16, 2176-2180.

Gomtsyan, A. Heterocycles in drugs and drug discovery. Chemistry of Heterocyclic Compounds, 2012, 48, 7-10.

Gontijo, V.S., Viegas, F.P.D., Ortiz, C.J., de Freitas Silva, M., Damasio, C.M., Rosa, M.C., Campos, T.G., Couto, D.S., Tranches Dias, K.S., Viegas, C. Molecular hybridization as a tool in the design of multi-target directed drug candidates for neurodegenerative diseases. Current Neuropharmacology, 2020, 18, 348-407. DOI: https://doi.org/10.2174/1385272823666191021124443

Gozelle, M., Suloglu, A.K., Selmanoglu, G., Ramazanoglu, N., Acik, L., Gumus, F. Studies on the synthesis, characterization, cytotoxic activities and plasmid DNA binding of platinum(II) complexes having 2-substituted benzimidazole ligands. Polyhedron, 2019, 161, 298-308. DOI: https://doi.org/10.1016/j.poly.2019.01.028

Grant, M.A. Protein structure prediction in structure-based ligand design and virtual screening. Combinational Chemistry & High Throughput Screening, 2009, 12, 940-960. DOI: https://doi.org/10.2174/138620709789824718

Green, L., Livingstone, K., Bertrand, S., Peace, S., Jamieson, C. UV-induced 1,3,4-oxadiazole formation from 5-substituted tetrazoles and carboxylic acids in flow. Chemistry – A European Journal, 2020, 26, 14866-14870. DOI: https://doi.org/10.1002/chem.202002896

Gu, Q., Li, P. 2016. Biosynthesis of vitamins by probiotic bacteria. *In:* Rao, V. & Rao, L. G. (eds.) *Probiotics and prebiotics in human nutrition and health.* London: IntechOpen.

Gündüz, M.G., Tahir, M.N., Armaković, S., Özkul Koçak, C., Armaković, S.J. Design, synthesis and computational analysis of novel acridine-(sulfadiazine/sulfathiazole) hybrids as antibacterial agents. Journal of Molecular Structure, 2019, 1186, 39-49. DOI: https://doi.org/10.1016/j.molstruc.2019.03.010

Guo, Y., Xu, T., Bao, C., Liu, Z., Fan, J., Yang, R., Qin, S. Design and synthesis of new norfloxacin-1,3,4-oxadiazole hybrids as antibacterial agents against methicillin-resistant *Staphylococcus aureus* (MRSA). European Journal of Pharmaceutical Sciences, 2019, 136, 104966. DOI: https://doi.org/10.1016/j.ejps.2019.104966

Gupta, S., Agarwal, P.K., Kundu, B. Catalyst/ligand-free synthesis of benzimidazoles and quinazolinones from amidines via intramolecular transamination reaction. Tetrahedron Letters, 2010, 51, 1887-1890. DOI: https://doi.org/10.1016/j.tetlet.2010.02.019

Hamdani, S.S., Khan, B.A., Hameed, S., Batool, F., Saleem, H.N., Mughal, E.U., Saeed, M. Synthesis and evaluation of novel *S*-benzyl- and *S*-alkylphthalimide- oxadiazole -benzenesulfonamide hybrids as inhibitors of dengue virus protease. Bioorganic Chemistry, 2020, 96, 103567. DOI: https://doi.org/10.1016/j.bioorg.2020.103567

Hashtroudi, M.S., Nia, S.S., Asadollahi, H., Balalaie, S. Microwave promoted synthesis of benzimidazole derivatives under solvent free conditions. Indian Journal of Heterocyclic Chemistry, 2000, 9, 307-308.

Haskins, W.T., Hudson, C.S. Improvements in the preparation of L-tartaric acid from racemic tartaric acid through resolution by a substituted benzimidazole base. Journal of the American Chemical Society, 1939, 61, 1266-1268. DOI: https://doi.org/10.1021/ja01874a076

Heravi, M.M., Sadjadi, S., Oskooie, H.A., Shoar, R.H., Bamoharram, F.F. Heteropolyacids as heterogeneous and recyclable catalysts for the synthesis of benzimidazoles. Catalysis Communications, 2007, 9, 504-507. DOI: https://doi.org/10.1016/j.catcom.2007.03.011

Heravi, M.M., Tajbakhsh, M., Ahmadi, A.N., Mohajerani, B. Zeolites. Efficient and eco-friendly catalysts for the synthesis of benzimidazoles. Monatshefte für Chemie 2006, 137, 175-179. DOI: https://doi.org/10.1007/s00706-005-0407-7

Heravi, M.M., Zadsirjan, V. Prescribed drugs containing nitrogen heterocycles: an overview. RSC Advances, 2020, 10, 44247-44311. DOI: https://doi.org/10.1039/d0ra09198g

Hirschberg, E., Gellhorn, A., Gump, W.S. Laboratory evaluation of a new nitrogen mustard, 2-[di-(2-chloroethyl)amino-methyl]benzimidazole, and of other 2-chloroethyl compounds. American Association for Cancer Research, 1957, 17, 904-910.

Hobrecker, F. Ueber reductionsprodukte der nitracetamidverbindungen (About reduction products of nitroacetamide compounds). Berichte der Deutschen Chemischen Gesellschaft (Reports from the German Chemical Society), 1872, 5, 920-924.

Hölljes, E.L., Wagner, E.C. Some reactions of nitriles as acid anammonides. Journal of Organic Chemistry, 1944, 09, 31-49. DOI: https://doi.org/10.1021/jo01183a005

Homan, K.T., Tesmer, J.J. Molecular basis for small molecule inhibition of G protein-coupled receptor kinases. ACS Chemical Biology, 2014, 10, 246-256. DOI: https://doi.org/10.1021/cb5003976

Hooda, T., Sharma, S., Goyal, N. Synthesis, *in silico* designing, microbiological evaluation and structure activity relationship of novel amide derivatives of 1-(2,4-dinitrophenyl)-2-(3-methylbenzo[b]thiophen-6-yl)-1*H*-benzo[d]imidazole-5-carboxylic acid. Polycyclic Aromatic Compounds, 2021, 1-13. DOI: https://doi.org/10.1080/10406638.2020.1869793

Howe, R.K. A novel benzimidazole reaction. Journal of Organic Chemistry, 1969, 34, 2983-2985. DOI: https://doi.org/10.1021/jo01262a040

Hughes, D., Karlén, A. Discovery and preclinical development of new antibiotics. Upsala Journal of Medical Sciences, 2014, 119, 162-169. DOI: https://doi.org/10.3109/03009734.2014.896437

Huisgen, R. 1,5,-Electrocyclizations—An important principle of heterocyclic chemistry. Angewandte Chemie, 1980, 19, 947-973. DOI: https://doi.org/10.1002/anie.198009473

Huisgen, R., Sauer, J., Sturm, H. Acylierung 5-substitutierter tetrazole zu 1.3.4-oxdiazolen (Acylation of 5-substituted tetrazole to 1,3,4-oxdiazoles. Angewandte Chemie, 1958, 70, 272-273.

Hutchings, M.I., Truman, A.W., Wilkinson, B. Antibiotics: past, present and future. Current Opinion in Microbiology, 2019, 51, 72-80. DOI: https://doi.org/10.1016/j.mib.2019.10.008

Ibrahim, H.A., Awadallah, F.M., Refaat, H.M., Amin, K.M. Design, synthesis and molecular modeling study for some new 2-substituted benzimidazoles as dual inhibitors for VEGFR-2 and c-Met. Future Medicinal Chemistry, 2018, 10, 493-509. DOI: https://doi.org/10.4155/fmc-2017-0174

Ibrahim, T.S., Tala, S.R., El-Feky, S.A., Abdel-Samii, Z.K., Katritzky, A.R. Benzotriazole reagents for the syntheses of Fmoc-, Boc-, and Alloc-protected amino acids. Synlett, 2011, 22, 2013-2016. DOI: https://doi.org/10.1055/s-0030-1261160

Indu, P., Rameshkumar, M.R., Arunagirinathan, N., Al-Dhabi, N.A., Valan Arasu, M., Ignacimuthu, S. Raltegravir, Indinavir, Tipranavir, Dolutegravir, and Etravirine against main protease and RNA-dependent RNA polymerase of SARS-CoV-2: A molecular docking and drug repurposing approach. J Infect Public Health, 2020, 13, 1856-1861. DOI: https://doi.org/10.1016/j.jiph.2020.10.015

Insa, D., Wakode, S., Sharma, A. Valuable insight into recent biological activities of different benzimidazoles. Current Trends in Pharmacy and Pharmaceutical Chemistry, 2019, 1, 1-22.

Iqbal, H., Verma, A., Yadav, P., Alam, S., Shafiq, M., Mishra, D., Khan, F., Hanif, K., Negi, a.s., Chanda, D. Antihypertensive effect of a novel angiotensin II receptor blocker fluorophenyl benzimidazole: contribution of cGMP, voltage-dependent calcium channels, and BK_{Ca} channels to vasorelaxant mechanisms. Frontiers in Pharmacology, 2021, 12, 611109.

Izgi, S., Sengul, I.F., Şahin, E., Koca, M.S., Cebeci, F., Kandemir, H. Synthesis of 7-azaindole based carbohydrazides and 1,3,4-oxadiazoles; antioxidant activity, α-glucosidase inhibition properties and docking study. Journal of Molecular Structure, 2022, 1247, 131343. DOI: https://doi.org/10.1016/j.molstruc.2021.131343

Jha, K.K., Samad, A., Kumar, Y., Shaharyar, M., Khosa, R.L., Jain, J., Kumar, V., Singh, P. Design, synthesis and biological evaluation of 1,3,4-oxadiazole derivatives. European Journal of Medicinal Chemistry, 2010, 45, 4963-4967. DOI: https://doi.org/10.1016/j.ejmech.2010.08.003

Jiang, Q., Qi, X., Zhang, C., Ji, X., Li, J., Liu, R. Oxidant- and hydrogen acceptor-free palladium catalyzed dehydrogenative cyclization of acylhydrazones to substituted oxadiazoles. Organic Chemistry Frontiers, 2018, 5, 386-390. DOI: https://doi.org/10.1039/C7QO00749C

Jiménez-Juárez, R., Cruz-Chávez, W., de Jesús-Ramírez, N., Castro-Ramírez, G.I., Uribe-González, I., Martínez-Mejía, G., Ruiz-Nicolás, R., Aguirre-Alvarado, C., Castrejón-Jiménez, N.S., García-Pérez, B.E. Synthesis and antimycobacterial activity of 2,5-disubstituted and 1,2,5-trisubstituted benzimidazoles. Frontiers in chemistry, 2020, 8, 433. DOI: https://doi.org/10.3389/fchem.2020.00433

John, S.E., Gulati, S., Shankaraiah, N. Recent advances in multi-component reactions and their mechanistic insights: a triennium review. Organic Chemistry Frontiers, 2021, 8, 4237-4287. DOI: https://doi.org/10.1039/D0QO01480J

Kahl, D.J., Hutchings, K.M., Lisabeth, E.M., Haak, A.J., Leipprandt, J.R., Dexheimer, T., Khanna, D., Tsou, P.-S., Campbell, P.L., Fox, D.A., Wen, B., Sun, D., Bailie, M., Neubig, R.R., Larsen, S.D. 5-Aryl-1,3,4-oxadiazol-2-ylthioalkanoic acids: A highly potent new class of inhibitors of Rho/Myocardin-Related Transcription Factor (MRTF)/Serum Response Factor (SRF)-mediated gene transcription as potential antifibrotic agents for scleroderma. Journal of Medicinal Chemistry, 2019, 62, 4350-4369. DOI: https://doi.org/10.1021/acs.jmedchem.8b01772

Kalinin, A.A., Mamedov, V.A., Rizvanov, I.K., Efremov, Y.Y., Levin, Y.A. Cyclodehydration of 3-{α-[(2-aminophenyl)amino]benzylidene}-2-oxo-1,4-dihydroquinoxaline into 2,2'-bisbenzimidazole with elimination of the benzylidene fragment. Chemistry of Heterocyclic Compounds, 2000, 36, 226-227. DOI: https://doi.org/10.1007/bf02283560

Kamanna, K. 2019. Synthesis and pharmacological profile of benzimidazoles. *In:* Marinescu, M. (ed.) *Chemistry and applications of benzimidazole and its derivatives.* London: IntechOpen.

Kangani, C.O., Kelley, D.E., Day, B.W. One pot direct synthesis of oxazolines, benzoxazoles, and oxadiazoles from carboxylic acids using the Deoxo-Fluor reagent. Tetrahedron Letters, 2006, 47, 6497-6499. DOI: https://doi.org/10.1016/j.tetlet.2006.07.032

Kanwal, A., Ahmad, M., Aslam, S., Naqvi, S.A.R., Saif, M.J. Recent advances in antiviral benzimidazole derivatives: A mini review. Pharmaceutical Chemistry Journal, 2019, 53, 179-187. DOI: https://doi.org/10.1007/s11094-019-01976-3

Karaburun, A.Ç., Kaya Çavuşoğlu, B., Acar Çevik, U., Osmaniye, D., Sağlık, B.N., Levent, S., Özkay, Y., Atlı, Ö., Koparal, A.S., Kaplancıklı, Z.A. Synthesis and antifungal potential of some novel benzimidazole-1,3,4-oxadiazole compounds. Molecules, 2019, 24, 191. DOI: https://doi.org/10.3390/molecules24010191

Kashid, B.B., Ghanwat, A.A., Khedkar, V.M., Dongare, B.B., Shaikh, M.H., Deshpande, P.P., Wakchaure, Y.B. Design, synthesis, in vitro antimicrobial, antioxidant evaluation, and molecular docking study of novel benzimidazole and benzoxazole derivatives. Journal of Heterocyclic Chemistry, 2019, 56, 895-908. DOI: https://doi.org/10.1002/jhet.3467

Kasten, F.H. Paul Ehrlich: pathfinder in cell biology. 1. Chronicle of his life and accomplishments in immunology, cancer research, and chemotherapy. Biotechnic & Histochemistry, 1996, 71, 2-37. DOI: https://doi.org/10.3109/10520299609117128

Katikireddy, R., Marri, S., Kakkerla, R., Murali Krishna, M.P.S., Gandamalla, D., Reddy, Y.N. Synthesis, anticancer activity and molecular docking studies of hybrid benzimidazole-1,3,4-oxadiazol-2-N-alkyl/aryl amines. Polycyclic Aromatic Compounds, 2021, 1-15. DOI: https://doi.org/10.1080/10406638.2021.1959352

Kattimani, P.P., Kamble, R.R., Meti, G.Y. Expedient synthesis of benzimidazoles using amides. RSC Advances, 2015, 5, 29447-29455. DOI: https://doi.org/10.1039/c5ra00021a

Kaur, J., Soto-Velasquez, M., Ding, Z., Ghanbarpour, A., Lill, M.A., Van Rijn, R.M., Watts, V.J., Flaherty, D.P. Optimization of a 1,3,4-oxadiazole series for inhibition of Ca^{2+}/calmodulin-stimulated activity of adenylyl cyclases 1 and 8 for the treatment of chronic pain. European Journal of Medicinal Chemistry, 2019, 162, 568-585. DOI: https://doi.org/10.1016/j.ejmech.2018.11.036

Keri, R.S., Rajappa, C.K., Patil, S.A., Nagaraja, B.M. Benzimidazole-core as an antimycobacterial agent. Pharmacological Reports, 2016, 68, 1254-1265. DOI: https://doi.org/10.1016/j.pharep.2016.08.002

Kerru, N., Gummidi, L., Maddila, S., Gangu, K.K., Jonnalagadda, S.B. A review on recent advances in nitrogen-containing molecules and their biological applications. Molecules, 2020, 25, 1909. DOI: https://doi.org/10.3390/molecules25081909

Khalili, S.B., Sardarian, A.R. KF/Al_2O_3: an efficient solid heterogeneous base catalyst in one-pot synthesis of benzimidazoles and bis-benzimidazoles at room temperature. Monatshefte für Chemie, 2012, 143, 841-846. DOI: https://doi.org/10.1007/s00706-011-0647-7

Khan, D., Ahmed, N., Alsharif, M.A., Alahmdi, M.I., Mukhtar, S. SeO_2 mediated synthesis of selected heterocycles by oxidative C-C bond cleavage of acetophenone derivatives. ChemistrySelect, 2019, 4, 7585-7590. DOI: https://doi.org/10.1002/slct.201901216

Khan, M.T., Nadeem, H., Khan, A.U., Abbas, M., Arif, M., Malik, N.S., Malik, Z., Javed, I. Amino acid conjugates of 2-mercaptobenzimidazole provide better anti-inflammatory pharmacology and improved toxicity profile. Drug Development Research, 2020, 81, 1057-1072. DOI: https://doi.org/10.1002/ddr.21728

Khan, S.A., Ahuja, P., Husain, A. Oxidative cyclization of Isoniazid with Fluoroquinolones: synthesis, antibacterial and antitubercular activity of new 2,5-disubstituted-1,3,4-oxadiazoles. Journal of the Chinese Chemical Society, 2017, 64, 918-924. DOI: https://doi.org/10.1002/jccs.201600199

Krishnanjaneyulu, I., Saravanan, G., Vamsi, J., Supriya, P., Bhavana, J., Kumar, M. Synthesis, characterization and antimicrobial activity of some novel benzimidazole derivatives. Journal of Advanced Pharmaceutical Technology & Research, 2014, 5, 21-27. DOI: https://doi.org/10.4103/2231-4040.126983

Kumar, A., Maurya, R.A., Saxena, D. Diversity-oriented synthesis of benzimidazole, benzoxazole, benzothiazole and quinazolin-4(3H)-one libraries via potassium persulfate-CuSO$_4$-mediated oxidative coupling reactions of aldehydes in aqueous micelles. Molecular Diversity, 2010, 14, 331-341. DOI: https://doi.org/10.1007/s11030-009-9170-8

Kuo, M.R., Morbidoni, H.R., Alland, D., Sneddon, S.F., Gourlie, B.B., Staveski, M.M., Leonard, M., Gregory, J.S., Janjigian, A.D., Yee, C., Musser, J.M., Kreiswirth, B., Iwamoto, H., Perozzo, R., Jacobs, W.R., Jr., Sacchettini, J.C., Fidock, D.A. Targeting tuberculosis and malaria through inhibition of enoyl reductase: compound activity and structural data. Journal of Biological Chemistry, 2003, 278, 20851-20859. DOI: https://doi.org/10.1074/jbc.M211968200

Ladenburg, A. Derivate von diaminen (Derivatives of diamines). Berichte der Deutschen Chemischen Gesellschaft (Reports from the German Chemical Society), 1875, 8, 677-678. DOI: https://doi.org/10.1002/cber.187500801209

Ladenburg, A., Rügheimer, L. Ueber die aldehydine (About the aldehydes). Berichte der Deutschen Chemischen Gesellschaft (Reports from the German Chemical Society), 1878, 11, 1656-1661. DOI: https://doi.org/10.1002/cber.187801102113

Lashkari, M., Roudbaraki, S.J., Ghashang, M. Preparation of 1,3,4-oxadiazole derivatives via supported and unsupported phosphinium dibromide reagents. Canadian Journal of Chemistry, 2020, 98, 670-675. DOI: https://doi.org/10.1139/cjc-2020-0185

Lazar, C., Kluczyk, A., Kiyota, T., Konishi, Y. Drug evolution concept in drug design: 1. Hybridization method. Journal of Medicinal Chemistry, 2004, 47, 6973-6982. DOI: https://doi.org/10.1021/jm049637+

Lellmann, E., Hailer, R. Ueber einige amidirte amidinbasen (On some amidated amidine bases). Berichte der Deutschen Chemischen Gesellschaft (Reports from the German Chemical Society), 1893, 26, 2759-2763. DOI: https://doi.org/10.1002/cber.18930260381

Leonard, N.J., Curtin, D.Y., Peck, K.M. Sulfonate salts of substituted benzimidazoles. Journal of the American Chemical Society, 1947, 69, 2459-2461. DOI: https://doi.org/10.1021/ja01202a062

Li, C., Dickson, H.D. A mild, one-pot preparation of 1,3,4-oxadiazoles. Tetrahedron Letters, 2009, 50, 6435-6439. DOI: https://doi.org/10.1016/j.tetlet.2009.08.084

Li, Q., Kang, C. Mechanisms of action for small molecules revealed by structural biology in drug discovery. International Journal of Molecular Sciences, 2020a, 21, 5262. DOI: https://doi.org/10.3390/ijms21155262

Li, Q., Kang, C. A practical perspective on the roles of solution NMR spectroscopy in drug discovery. Molecules, 2020b, 25, 2974. DOI: https://doi.org/10.3390/molecules25132974

Li, T., Wen, G., Li, J., Zhang, W., Wu, S. A useful synthesis of 2-acylamino-1,3,4-oxadiazoles from acylthiosemicarbazides using potassium iodate and the discovery of new antibacterial compounds. Molecules, 2019, 24, 1490. DOI: https://doi.org/10.3390/molecules24081490

Lotfi, B., Mustafa, B., Leila, L., Salima, M. Electrocyclization of semicarbazone; A novel route of green synthesis of 2,5-disubstituted-1,3,4-oxadiazoles. International Journal of Electrochemical Science, 2011, 6, 1991-2000.

Lukyanov, D.B., Vazhnova, T., Cherkasov, N., Casci, J.L., Birtill, J.J. Insights into Brønsted acid sites in the zeolite mordenite. Journal of Physical Chemistry C, 2014, 118, 23918-23929. DOI: https://doi.org/10.1021/jp5086334

Makane, V.B., Krishna, V.S., Krishna, E.V., Shukla, M., Mahizhaveni, B., Misra, S., Chopra, S., Sriram, D., Azger Dusthackeer, V.N., Rode, H.B. Novel 1,3,4-oxadiazoles as antitubercular agents with limited activity against drug-resistant tuberculosis. Future Medicinal Chemistry, 2019, 11, 499-510. DOI: https://doi.org/10.4155/fmc-2018-0378

Mamedov, V., Kalinin, A., Gubaidullin, A., Gorbunova, E., Litvinov, I. Quinoxaline—benzimidazole rearrangement in the synthesis of benzimidazole-based podands. Russian Journal of Organic Chemistry, 2006, 42, 1532-1543. DOI: https://doi.org/10.1134/S1070428006100241

Marinescu, M. 2019. Introductory chapter: Short insight in synthesis and applications of benzimidazole and its derivatives. *In:* Marinescu, M. (ed.) *Chemistry and applications of benzimidazole and its derivatives.* London: IntechOpen.

Marri, S., Kakkerla, R., Krishna, M., Rajam, M. Synthesis and antimicrobial evaluation of isoxazole-substituted 1,3,4-oxadiazoles. Heterocyclic Communications, 2018, 24, 285-292. DOI: https://doi.org/10.1515/hc-2018-0137

Matheau-Raven, D., Dixon, D.J. General α-amino 1,3,4-oxadiazole synthesis via late-stage reductive functionalization of tertiary amides and lactams. Angewandte Chemie, 2021, 60, 19725-19729. DOI: https://doi.org/10.1002/anie.202107536

Méhes, J., Decsi, L., Várszegi, M.K., Hideg, H., Hankovszky, O.H. Inhibitory effect of 1-alkylbenzimidazoles on gastric secretion in the rat. Journal of Pharmacy and Pharmacology, 1966, 18, 551-552. DOI: https://doi.org/10.1111/j.2042-7158.1966.tb07930.x

Mikhailov, I., Artyushkina, Y., Dushenko, G., Minkin, V. Synthesis and spectral-luminescent properties of 2,5-diaryl-1,3,4-oxadiazoles and their chelate complexes with cadmium(II). Russian Journal of General Chemistry, 2020, 89, 2165-2169. DOI: https://doi.org/10.1134/S107036321910030X

Mohan, C.D., Anilkumar, N.C., Rangappa, S., Shanmugam, M.K., Mishra, S., Chinnathambi, A., Alharbi, S.A., Bhattacharjee, A., Sethi, G., Kumar, A.P., Basappa, Rangappa, K.S. Novel 1,3,4-oxadiazole induces anticancer activity by targeting NF-κB in hepatocellular carcinoma cells. Frontiers in Oncology, 2018, 8. DOI: https://doi.org/10.3389/fonc.2018.00042

Monforte, A.M., De Luca, L., Buemi, M.R., Agharbaoui, F.E., Pannecouque, C., Ferro, S. Structural optimization of N_1-aryl-benzimidazoles for the discovery of new non-nucleoside reverse transcriptase inhibitors active against wild-type and mutant HIV-1 strains. Bioorganic & Medicinal Chemistry, 2018, 26, 661-674. DOI: https://doi.org/10.1016/j.bmc.2017.12.033

Moussebois, C., Lenaers, R., Eloy, F. Synthèse de l'oxadiazole-1,2,4 (Synthesis of 1,2,4-oxadiazole). Helvetica Chimica Acta, 1962, 45, 446-449. DOI: https://doi.org/10.1002/hlca.19620450204

Nadi, I., Bouanis, M., Benhiba, F., Nohair, K., Nyassi, A., Zarrouk, A., Jama, C., Bentiss, F. Insights into the inhibition mechanism of 2,5-bis (4-pyridyl)-1,3,4-oxadiazole for carbon steel corrosion in hydrochloric acid pickling via experimental and computational approaches. Journal of Molecular Liquids, 2021, 342, 116958. DOI: https://doi.org/10.1016/j.molliq.2021.116958

Naeimi, H., Babaei, Z. Microwave-assisted practical and simple method for heterocyclization of *o*-phenylenediamine and aldehydes using DDQ as oxidant agent. Green Chemistry Letters and Reviews, 2017, 10, 129-133. DOI: https://doi.org/10.1080/17518253.2017.1314555

Nagao, I., Ishizaka, T., Kawanami, H. Rapid production of benzazole derivatives by a high-pressure and high-temperature water microflow chemical process. Green Chemistry, 2016, 18, 3494-3498. DOI: https://doi.org/10.1039/c6gc01195k

Narasimhan, B., Sharma, D., Kumar, P. Benzimidazole: a medicinally important heterocyclic moiety. Medicinal Chemistry Research, 2012, 21, 269-283. DOI: https://doi.org/10.1007/s00044-010-9533-9

Nguyen, L.H.T., Nguyen, T.T.T., Dang, M.-H.D., Tran, P.H., Doan, T.L.H. Heterocyclic reaction inducted by Bronsted-Lewis dual acidic Hf-MOF under microwave irradiation. Molecular Catalysis, 2021, 499, 111291. DOI: https://doi.org/10.1016/j.mcat.2020.111291

Nieto, C., Cabildo, P., García, M., Claramunt, R., Alkorta, I., Elguero, J. An experimental and theoretical NMR study of NH-benzimidazoles in solution and in the solid state: Proton transfer and tautomerism. Beilstein Journal of Organic Chemistry, 2014, 10, 1620-1629. DOI: https://doi.org/10.3762/bjoc.10.168

Noor, A., Qazi, N.G., Nadeem, H., Khan, A.-u., Paracha, R.Z., Ali, F., Saeed, A. Synthesis, characterization, anti-ulcer action and molecular docking evaluation of novel benzimidazole-pyrazole hybrids. Chemistry Central Journal, 2017, 11, 85. DOI: https://doi.org/10.1186/s13065-017-0314-0

Olofson, R.A., Michelman, J.S. Furazan. Journal of Organic Chemistry, 1965, 30, 1854-1859. DOI: https://doi.org/10.1021/jo01017a034

Panneer Selvam, T., Radhika, P.P., Janagaraj, S., Kumar, A.S. Synthesis of novel 2-substituted benzimidazole derivatives as potential anti microbial agents. Research in Biotechnology, 2011, 2, 50-57.

Parascandola, J. The theoretical basis of Paul Ehrlich's chemotherapy. Journal of the History of Medicine and Allied Sciences, 1981, 36, 19-43. DOI: https://doi.org/10.1093/jhmas/xxxvi.1.19

Paris, J.-M. 2012. Chirality in antibacterial agents. *In:* Carreira, E. M. & Yamamoto, H. (eds.) *Comprehensive Chirality.* Amsterdam: Elsevier.

Parizadeh, N., Alipour, E., Soleymani, S., Zabihollahi, R., Aghasadeghi, M.R., Hajimahdi, Z., Zarghi, A. Synthesis of novel 3-(5-(alkyl/arylthio)-1,3,4-oxadiazol-2-yl)-8-phenylquinolin-4(1*H*)-one derivatives as anti-HIV agents. Phosphorus, Sulfur, and Silicon and the Related Elements, 2018, 193, 225-231. DOI: https://doi.org/10.1080/10426507.2017.1394302

Perin, N., Hok, L., Bec, A., Persoons, L., Vanstreels, E., Daelemans, D., Vianello, R., Hranjec, M. *N*-substituted benzimidazole acrylonitriles as *in vitro* tubulin polymerization inhibitors: Synthesis, biological activity and computational analysis. European Journal of Medicinal Chemistry, 2021, 211, 113003. DOI: https://doi.org/10.1016/j.ejmech.2020.113003

Phillips, M.A. CCCXVII.—The formation of 2-substituted benziminazoles. Journal of the Chemical Society, 1928, 2393-2399. DOI: https://doi.org/10.1039/JR9280002393

Pinder, J.L., Davis, R.E., Charrier, J.-D. A facile, one-pot procedure for the formation of benzimidazoles from esters using DABAL-Me$_3$, an air stable source of AlMe$_3$. Tetrahedron Letters, 2014, 55, 4853-4855. DOI: https://doi.org/10.1016/j.tetlet.2014.06.026

Piwowarek, K., Lipińska, E., Hać-Szymańczuk, E., Kieliszek, M., Ścibisz, I. *Propionibacterium* spp.—source of propionic acid, vitamin B12, and other metabolites important for the industry. Applied Microbiology and Biotechnology, 2018, 102, 515-538. DOI: https://doi.org/10.1007/s00253-017-8616-7

Prabhu, G., Sureshbabu, V.V. Hypervalent iodine(V) mediated mild and convenient synthesis of substituted 2-amino-1,3,4-oxadiazoles. Tetrahedron Letters, 2012, 53, 4232-4234. DOI: https://doi.org/10.1016/j.tetlet.2012.05.154

Rabie, A.M. Four three-winged nitrogenous heterocyclic derivatives of citric acid scaffold: The first synthesis and characterization of these newly discovered fan-like compounds. Russian Journal of Organic Chemistry, 2021, 57, 417-421. DOI: https://doi.org/10.1134/s1070428021030131

Radhamanalan, R., Alagumuthu, M., Nagaraju, N. Synthesis and drug efficacy validations of racemic-substituted benzimidazoles as antiulcer/antigastric secretion agents. Future Medicinal Chemistry, 2018, 10, 1805-1820. DOI: https://doi.org/10.4155/fmc-2017-0214

Rahimi, S., Soleimani, E. Synthesis of 2-substituted benzimidazole, coumarin, benzo[*b*][1,4]oxazin and dihydropyrimidinone derivatives using core-shell structured Fe$_3$O$_4$@SiO$_2$-ZnCl$_2$ nanoparticles as an effective catalyst. Results in Chemistry, 2020, 2, 100060. DOI: https://doi.org/10.1016/j.rechem.2020.100060

Ramazani, A., Rezaei, A. Novel one-pot, four-component condensation reaction: An efficient approach for the synthesis of 2,5-disubstituted 1,3,4-oxadiazole derivatives by a Ugi-4CR/aza-Wittig sequence. Organic Letters, 2010, 12, 2852-2855. DOI: https://doi.org/10.1021/ol100931q

Ramprasad, J., Kumar Sthalam, V., Linga Murthy Thampunuri, R., Bhukya, S., Ummanni, R., Balasubramanian, S., Pabbaraja, S. Synthesis and evaluation of a novel quinoline-triazole analogs for antitubercular properties via molecular hybridization approach. Bioorganic & Medicinal Chemistry Letters, 2019, 29, 126671. DOI: https://doi.org/10.1016/j.bmcl.2019.126671

Rane, R.A., Telvekar, V.N. Synthesis and evaluation of novel chloropyrrole molecules designed by molecular hybridization of common pharmacophores as potential antimicrobial agents. Bioorganic & Medicinal Chemistry Letters, 2010, 20, 5681-5685. DOI: https://doi.org/10.1016/j.bmcl.2010.08.026

Rao, A., Chimirri, A., De Clercq, E., Monforte, A.M., Monforte, P., Pannecouque, C., Zappalà, M. Synthesis and anti-HIV activity of 1-(2,6-difluorophenyl)-1*H*,3*H*-thiazolo[3,4-a]benzimidazole structurally-related 1,2-substituted benzimidazoles. IL Farmaco, 2002, 57, 819-823. DOI: https://doi.org/10.1016/s0014-827x(02)01300-9

Rathore, A., Sudhakar, R., Ahsan, M.J., Ali, A., Subbarao, N., Jadav, S.S., Umar, S., Yar, M.S. *In vivo* anti-inflammatory activity and docking study of newly synthesized benzimidazole derivatives bearing oxadiazole and morpholine rings. Bioorganic Chemistry, 2017, 70, 107-117. DOI: https://doi.org/10.1016/j.bioorg.2016.11.014

Raut, S.V., Tidke, A.D., Dhotre, B.K., Pathan, M.A. Synthesis of 3-[5-(substituted phenyl)-[1,3,4] oxadiazol-2-yl]-1*H*-indazole. Polycyclic Aromatic Compounds, 2021, 41, 1147-1158. DOI: https://doi.org/10.1080/10406638.2019.1665552

Ravi, O., Shaikh, A., Upare, A., Singarapu, K.K., Bathula, S.R. Benzimidazoles from aryl alkyl ketones and 2-amino anilines by an iodine catalyzed oxidative C(CO)-C(alkyl) bond cleavage. Journal of Organic Chemistry, 2017, 82, 4422-4428. DOI: https://doi.org/10.1021/acs.joc.7b00165

Reddy, D.M.S., Anisetti, R.N., Prasad, K., Sannigrahi, S., Reddy, P. Synthesis, characterization and biological evaluation of some novel 2-substituted mercaptobenzimidazole derivatives. Pharmaceutical Chemistry Journal, 2011, 44, 642-645. DOI: https://doi.org/10.1007/s11094-011-0537-7

Reddy, P.L., Arundhathi, R., Tripathi, M., Rawat, D.S. CuI nanoparticles mediated expeditious synthesis of 2-substituted benzimidazoles using molecular oxygen as the oxidant. RSC Advances, 2016, 6, 53596-53601. DOI: https://doi.org/10.1039/c6ra11678g

Reichart, B., Kappe, C.O. High-temperature continuous flow synthesis of 1,3,4-oxadiazoles via *N*-acylation of 5-substituted tetrazoles. Tetrahedron Letters, 2012, 53, 952-955. DOI: https://doi.org/10.1016/j.tetlet.2011.12.043

Reygaert, W.C. An overview of the antimicrobial resistance mechanisms of bacteria. AIMS Microbiol, 2018, 4, 482-501. DOI: https://doi.org/10.3934/microbiol.2018.3.482

Rickes, E.L., Brink, N.G., Koniuszy, F.R., Wood, T.R., Folkers, K. Comparative data on vitamin B_{12} from liver and from a new source, *Streptomyces griseus*. Science, 1948, 108, 634-635. DOI: https://doi.org/10.1126/science.108.2814.634-a

Roth, T., Morningstar, M.L., Boyer, P.L., Hughes, S.H., Buckheit, R.W., Jr., Michejda, C.J. Synthesis and biological activity of novel nonnucleoside inhibitors of HIV-1 reverse transcriptase. 2-Aryl-substituted benzimidazoles. Journal of Medicinal Chemistry, 1997, 40, 4199-4207. DOI: https://doi.org/10.1021/jm970096g

Saglam, M.F., Gündogdu, A., Hora, M., Kandemir, H., Sengul, I.F. Synthesis of pyrrolo[3,2-c]carbazole-2-carbohydrazides and pyrrolo[3,2-c]carbazol-2-yl-1,3,4-oxadiazoles and their *in vitro* antibacterial evaluation. Synthetic Communications, 2021, 51, 3164-3174. DOI: https://doi.org/10.1080/00397911.2021.1966040

Sasmal, P.K., Sasmal, S., Abbineni, C., Venkatesham, B., Rao, P.T., Roshaiah, M., Khanna, I., Sebastian, V.J., Suresh, J., Singh, M.P., Talwar, R., Shashikumar, D., Reddy, K.H., Frimurer, T.M., Rist, Ø., Elster, L., Högberg, T. Synthesis and SAR studies of benzimidazole derivatives as melanin concentrating hormone receptor 1 (MCHR1) antagonists: Focus to detune hERG inhibition. MedChemComm, 2011, 2, 385-389. DOI: https://doi.org/10.1039/C1MD00015B

Sayahi, M.H., Khoshneviszadeh, M., Soheilizad, M., Saghanezhad, S.J., Mahdavi, M. Efficient copper-catalyzed synthesis of 2-arylbenzimidazole derivatives by reaction of 1-fluoro-2-nitrobenzene with benzamidine hydrochlorides. Chemistry of Heterocyclic Compounds, 2018, 54, 351-354. DOI: https://doi.org/10.1007/s10593-018-2272-4

Schoepf, A.M., Salcher, S., Hohn, V., Veider, F., Obexer, P., Gust, R. Synthesis and characterization of Telmisartan-derived cell death modulators to circumvent imatinib resistance in chronic myeloid leukemia. ChemMedChem, 2020a, 15, 1067-1077. DOI: https://doi.org/10.1002/cmdc.202000092

Schoepf, A.M., Salcher, S., Obexer, P., Gust, R. Overcoming imatinib resistance in chronic myelogenous leukemia cells using non-cytotoxic cell death modulators. European Journal of Medicinal Chemistry, 2020b, 185, 111748. DOI: https://doi.org/10.1016/j.ejmech.2019.111748

Scott, J.M., Molloy, A.M. The discovery of vitamin B_{12}. Annals of Nutrition & Metabolism, 2012, 61, 239-245. DOI: https://doi.org/10.1159/000343114

Selvaraj, K., Nasarullah, Z., Kannan, K. Synthesis and biological evaluation of sulfonamide-based 1,3,4-oxadiazole derivatives. Bulletin of the Chemical Society of Ethiopia, 2019, 33, 307-319. DOI: https://doi.org/10.4314/bcse.v33i2.11

Sethi, P., Bansal, Y., Bansal, G. Synthesis and PASS-assisted evaluation of coumarin–benzimidazole derivatives as potential anti-inflammatory and anthelmintic agents. Medicinal Chemistry Research, 2018, 27, 61-71. DOI: https://doi.org/10.1007/s00044-017-2036-1

Shah, P., Westwell, A.D. The role of fluorine in medicinal chemistry. Journal of Enzyme Inhibition and Medicinal Chemistry, 2007, 22, 527-540. DOI: https://doi.org/10.1080/14756360701425014

Sheldrick, G.M. Crystal structure refinement with SHELXL. Acta Crystallographica Section C Structural Chemistry, 2015a, 71, 3-8. DOI: https://doi.org/10.1107/s2053229614024218

Sheldrick, G.M. SHELXT– Integrated space-group and crystal-structure determination. Acta Crystallographica Section A Foundations and Advances, 2015b, 71, 3-8. DOI: https://doi.org/10.1107/s2053273314026370

Shi, L., Zhang, N. Applications of solution NMR in drug discovery. Molecules, 2021, 26, 576. DOI: https://www.mdpi.com/1420-3049/26/3/576

Shingare, R., Patil, Y., Sangshetti, J., Patil, D.R., Rajani, D.D., Madje, B. Synthesis, biological evaluation and docking study of some novel isoxazole clubbed 1,3,4-oxadiazoles derivatives. Medicinal Chemistry Research, 2018, 27, 1283-1291. DOI: https://doi.org/10.1007/s00044-018-2148-2

Siwach, A., Verma, P.K. Therapeutic potential of oxadiazole or furadiazole containing compounds. BMC Chemistry, 2020, 14, 70. DOI: https://doi.org/10.1186/s13065-020-00721-2

Smitha, G., Sreekumar, K. Highly functionalized heterogeneous dendrigraft catalysts with peripheral copper moieties for the facile synthesis of 2-substituted benzimidazoles and 2,2-disubstituted benzimidazoles. RSC Advances, 2016, 6, 18141-18155. DOI: https://doi.org/10.1039/C5RA28046J

Song, D., Ma, S. Recent development of benzimidazole-containing antibacterial agents. ChemMedChem, 2016, 11, 646-659. DOI: https://doi.org/10.1002/cmdc.201600041

Song, Z.-L., Zhu, Y., Liu, J.-R., Guo, S.-K., Gu, Y.-C., Han, X., Dong, H.-Q., Sun, Q., Zhang, W.-H., Zhang, M.-Z. Diversity-oriented synthesis and antifungal activities of novel pimprinine derivative bearing a 1,3,4-oxadiazole-5-thioether moiety. Molecular Diversity, 2021, 25, 205-221. DOI: https://doi.org/10.1007/s11030-020-10048-8

Srinivas, K., Sivakumar, G., Ramesh Kumar, C., Ananth Reddy, M., Bhanuprakash, K., Rao, V.J., Chen, C.-W., Hsu, Y.-C., Lin, J.T. Novel 1,3,4-oxadiazole derivatives as efficient sensitizers for dye-sensitized solar cells: A combined experimental and computational study. Synthetic Metals, 2011, 161, 1671-1681. DOI: https://doi.org/10.1016/j.synthmet.2011.06.001

Srivastava, R., Gupta, S.K., Naaz, F., Sen Gupta, P.S., Yadav, M., Singh, V.K., Singh, A., Rana, M.K., Gupta, S.K., Schols, D., Singh, R.K. Alkylated benzimidazoles: Design, synthesis, docking, DFT analysis, ADMET property, molecular dynamics and activity against HIV and YFV. Computational Biology and Chemistry, 2020, 89, 107400. DOI: https://doi.org/10.1016/j.compbiolchem.2020.107400

Stecoza, C.E., Nitulescu, G.M., Draghici, C., Caproiu, M.T., Olaru, O.T., Bostan, M., Mihaila, M. Synthesis and anticancer evaluation of new 1,3,4-oxadiazole derivatives. Pharmaceuticals, 2021, 14, 438. DOI: https://doi.org/10.3390/ph14050438

Stollé, R. Ueber die ueberführung der secundären säurehydrazide in derivate des furodiazols, pyrrodiazols und thiodiazols (On the conversion of secondary acid hydrazides into derivatives of furodiazole, pyrrodiazole and thiodiazole). Berichte der Deutschen Chemischen Gesellschaft (Reports from the German Chemical Society), 1899, 32, 797-798. DOI: https://doi.org/10.1002/cber.189903201122

Stone, O.J., Mullins, J.F. First use of thiabendazole in creeping eruption Texas Reports on Biology and Medicine, 1963, 21, 422-424.

Sun, M., Zhao, L., Yu, Y.-L., Ding, M.-W. DEAD-mediated oxidative Ugi/Aza-Wittig reaction for the synthesis of 5-(1,2,3,4-tetrahydroisoquinolin-1-yl)-1,3,4-oxadi--azoles starting from (*N*-isocyanimine)triphenylphosphorane. Synthesis, 2021, 53, 1365-1371.

Sunil, R., Pal, S., Jayashree, A. Molecular hybridization-An emanating tool in drug design. Medicinal Chemistry, 2019, 9, 93-95.

Sunke, R., Edupuganti, S., Nallapati, S., Medishetty, R., Kulkarni, P., Kapavarapu, R., Ramudu, B., Parsa, K., Pal, M. Copper-catalyzed domino reaction involving nitro as an unexpected leaving group: Construction of dibenzo-fused azepinone ring. Advanced Synthesis & Catalysis, 2016, 358, 3201-3205. DOI: https://doi.org/10.1002/adsc.201600748

Taha, M., Imran, S., Alomari, M., Rahim, F., Wadood, A., Mosaddik, A., Uddin, N., Gollapalli, M., Alqahtani, M.A., Bamarouf, Y.A. Synthesis of oxadiazole-coupled-thiadiazole derivatives as a potent β-glucuronidase inhibitors and their molecular docking study. Bioorganic & Medicinal Chemistry, 2019, 27, 3145-3155. DOI: https://doi.org/10.1016/j.bmc.2019.05.049

Taha, M., Rahim, F., Zaman, K., Selvaraj, M., Uddin, N., Farooq, R.K., Nawaz, M., Sajid, M., Nawaz, F., Ibrahim, M., Khan, K.M. Synthesis, α-glycosidase inhibitory potential and molecular docking study of benzimidazole derivatives. Bioorganic Chemistry, 2020, 95, 103555. DOI: https://doi.org/10.1016/j.bioorg.2019.103555

Tambe, M., Choudhari, A., Sarkar, D., Sangshetti, J., Patil, D.R., Gholap, S. Design, synthesis and biological screening of novel 1,3,4-oxadiazoles as antitubercular agents. ChemistrySelect, 2018, 3, 13304-13310. DOI: https://doi.org/10.1002/slct.201802227

Tandon, V.K., Kumar, M. $BF_3 \cdot Et_2O$-promoted one-pot expeditious and convenient synthesis of 2-substituted benzimidazoles and 3,1,5-benzoxadiazepines. Tetrahedron Letters, 2004, 45, 4185-4187. DOI: https://doi.org/10.1016/j.tetlet.2004.03.117

Tantray, M.A., Khan, I., Hamid, H., Alam, M.S., Dhulap, A., Kalam, A. Synthesis of benzimidazole-based 1,3,4-oxadiazole-1,2,3-triazole conjugates as glycogen synthase kinase-3β inhibitors with antidepressant activity in *in vivo* models. RSC Advances, 2016, 6, 43345-43355. DOI: https://doi.org/10.1039/c6ra07273a

Taylor, E.C., McKillop, A. Reaction of 2,3-diphenylquinoxaline with amide ion. An unusual ring contraction. Journal of Organic Chemistry, 1965, 30, 2858-2859. DOI: https://doi.org/10.1021/jo01019a521

Theuretzbacher, U., Outterson, K., Engel, A., Karlén, A. The global preclinical antibacterial pipeline. Nature Reviews Microbiology, 2020, 18, 275-285. DOI: https://doi.org/10.1038/s41579-019-0288-0

Tiemann, F., Krüger, P. Ueber amidoxime und azoxime (About amidoxime and azoxime). Berichte der Deutschen Chemischen Gesellschaft (Reports from the German Chemical Society), 1884, 17, 1685-1698. DOI: https://doi.org/10.1002/cber.18840170230

Todorova, T.T., Ermenlieva, N., Tsankova, G. 2017. Vitamin B12: Could it be a promising immunotherapy? *In:* Metodiev, K. (ed.) *Immunotherapy - Myths, reality, ideas, future.* London: IntechOpen.

Tumosienė, I., Peleckis, A., Jonuškienė, I., Vaickelionienė, R., Kantminienė, K., Šiugždaitė, J., Beresnevičius, Z.J., Mickevičius, V. Synthesis of novel 1,2- and 2-substituted benzimidazoles with high antibacterial and antioxidant activity. Monatshefte für Chemie, 2018, 149, 577-594. DOI: https://doi.org/10.1007/s00706-017-2066-x

v. Niementowski, S. Neue methoden der darstellung der anhydroverbindungen (New methods of preparing anhydrous compounds). Berichte der Deutschen Chemischen Gesellschaft (Reports from the German Chemical Society), 1897, 30, 3062-3071. DOI: https://doi.org/10.1002/cber.189703003124

Valent, P., Groner, B., Schumacher, U., Superti-Furga, G., Busslinger, M., Kralovics, R., Zielinski, C., Penninger, J.M., Kerjaschki, D., Stingl, G., Smolen, J.S., Valenta, R., Lassmann, H., Kovar, H.,

Jäger, U., Kornek, G., Müller, M., Sörgel, F. Paul Ehrlich (1854-1915) and his contributions to the foundation and birth of translational medicine. Journal of Innate Immunity, 2016, 8, 111-120. DOI: https://doi.org/10.1159/000443526

Veerasamy, R., Roy, A., Karunakaran, R., Rajak, H. Structure–activity relationship analysis of benzimidazoles as emerging anti-inflammatory agents: An overview. Pharmaceuticals, 2021, 14, 663. DOI: https://doi.org/10.3390/ph14070663

Viegas Junior, C., Danuello, A., Bolzani, V., Barreiro, E., Fraga, C. Molecular hybridization: A useful tool in the design of new drug prototypes. Current Medicinal Chemistry, 2007, 14, 1829-1852. DOI: https://doi.org/10.2174/092986707781058805

Vosátka, R., Krátký, M., Švarcová, M., Janoušek, J., Stolaříková, J., Madacki, J., Huszár, S., Mikušová, K., Korduláková, J., Trejtnar, F., Vinšová, J. New lipophilic isoniazid derivatives and their 1,3,4-oxadiazole analogues: Synthesis, antimycobacterial activity and investigation of their mechanism of action. European Journal of Medicinal Chemistry, 2018, 151, 824-835. DOI: https://doi.org/10.1016/j.ejmech.2018.04.017

Wang, Q., Mgimpatsang, K.C., Konstantinidou, M., Shishkina, S.V., Dömling, A. 1,3,4-Oxadiazoles by Ugi-tetrazole and Huisgen reaction. Organic Letters, 2019a, 21, 7320-7323. DOI: https://doi.org/10.1021/acs.orglett.9b02614

Wang, W., Yafeng, T., Wan, Y., Gu, S.-X., Ju, X.-L., Luo, X., Liu, G. Insights into the key structural features of N_1-aryl-benzimidazoles as HIV-1 NNRTIs using molecular docking, molecular dynamics, 3D-QSAR, and pharmacophore modeling. Structural Chemistry, 2019b, 30, 385-397. DOI: https://doi.org/10.1007/s11224-018-1204-3

Wang, Z. 2010. Phillips-Ladenburg benzimidazole synthesis. *In:* Wang, Z. (ed.) *Comprehensive organic name reactions and reagents.* Hoboken, New Jersey: John Wiley.

Weidenhagen, R. Eine neue synthese von benzimidazol-derivaten (A new synthesis of benzimidazole derivatives). Berichte der Deutschen Chemischen Gesellschaft (Reports from the German Chemical Society), 1936, 69, 2263-2272. DOI: https://doi.org/10.1002/cber.19360691010

Weir, C.B., Le, J.K. *Metronidazole,* 2021, Treasure Island (FL), StatPearls Publishing Copyright © 2022, StatPearls Publishing LLC., p.

Wen, L., Jian, W., Shang, J., He, D. Synthesis and antifungal activities of novel thiophene-based stilbene derivatives bearing an 1,3,4-oxadiazole unit. Pest Management Science, 2019, 75, 1123-1130. DOI: https://doi.org/10.1002/ps.5229

WHO. 2021. *Drug resistance in bacteria. Antimicrobial resistance* [Online]. Available: https://www.who.int/news-room/fact-sheets/detail/antimicrobial-resistance [Accessed 20th October 2021].

Wishart, D.S., Feunang, Y.D., Guo, A.C., Lo, E.J., Marcu, A., Grant, J.R., Sajed, T., Johnson, D., Li, C., Sayeeda, Z., Assempour, N., Iynkkaran, I., Liu, Y., Maciejewski, A., Gale, N., Wilson, A., Chin, L., Cummings, R., Le, D., Pon, A., Knox, C., Wilson, M. DrugBank 5.0: a major update to the DrugBank database for 2018. Nucleic Acids Research, 2018, 46, D1074-D1082. DOI: https://doi.org/10.1093/nar/gkx1037

Witkop, B. Paul Ehrlich and his magic bullets-revisited. Proceedings of the American Philosophical Society, 1999, 143, 540-557.

Woolley, D. Some biological effects produced by benzimidazole and their reversal by purines. Journal of Biological Chemistry, 1944, 152, 225-232.

Wright, J.B. The chemistry of the benzimidazoles. Chemical Reviews, 1951, 48, 397-541.

Wu, Q., Braveenth, R., Zhang, H., Bae, I.-J., Kim, M., Chai, K. Oxadiazole-based highly efficient bipolar fluorescent emitters for organic light-emitting diodes. Molecules, 2018, 23, 843. DOI: https://doi.org/10.3390/molecules23040843

Wu, Z., Anh, N.T.P., Yan, Y.J., Xia, M.B., Wang, Y.H., Qiu, Y., Chen, Z.L. Design, synthesis and biological evaluation of AT_1 receptor blockers derived from 6-substituted aminocarbonyl benzimidazoles. European Journal of Medicinal Chemistry, 2019, 181, 111553. DOI: https://doi.org/10.1016/j.ejmech.2019.07.056

Wu, Z., Xia, M.B., Bertsetseg, D., Wang, Y.H., Bao, X.L., Zhu, W.B., Tao, X., Chen, P.R., Tang, H.S., Yan, Y.J., Chen, Z.L. Design, synthesis and biological evaluation of novel fluoro-substituted benzimidazole derivatives with anti-hypertension activities. Bioorganic Chemistry, 2020, 101, 104042. DOI: https://doi.org/10.1016/j.bioorg.2020.104042

Xie, C., Han, X., Gong, J., Li, D., Ma, C. One-pot strategy of copper-catalyzed synthesis of 1,2-disubstituted benzimidazoles. Organic & Biomolecular Chemistry, 2017, 15, 5811-5819. DOI: https://doi.org/10.1039/c7ob00945c

Yadavalli, V.D.N., Vaidya, J.R. 2020. Applications of ionic liquids in chemical reactions. *In:* Inamuddin & Asiri, A. M. (eds.) *Nanotechnology-based industrial applications of ionic liquids.* Cham: Springer International Publishing.

Yang, W., Gadgil, P., Krishnamurthy, V.R., Landis, M., Mallick, P., Patel, D., Patel, P.J., Reid, D.L., Sanchez-Felix, M. The evolving druggability and developability space: Chemically modified new modalities and emerging small molecules. AAPS Journal, 2020, 22, 21. DOI: https://doi.org/10.1208/s12248-019-0402-2

Yaragorla, S., Vijaya Babu, P. Oxidative C_{sp3}-H functionalization of 2-methylazaarenes: A practical synthesis of 2-azaarenyl-benzimidazoles and benzothiazoles. Tetrahedron Letters, 2017, 58, 1879-1882. DOI: https://doi.org/10.1016/j.tetlet.2017.04.007

Yarmohammadi, E., Beyzaei, H., Aryan, R., Moradi, A. Ultrasound-assisted, low-solvent and acid/base-free synthesis of 5-substituted 1,3,4-oxadiazole-2-thiols as potent antimicrobial and antioxidant agents. Molecular Diversity, 2021, 25, 2367-2378. DOI: https://doi.org/10.1007/s11030-020-10125-y

Yeong, K.Y., Ang, C.W., Ali, M.A., Osman, H., Tan, S.C. Antituberculosis agents bearing the 1,2-disubstituted benzimidazole scaffold. Medicinal Chemistry Research, 2017, 26, 770-778. DOI: https://doi.org/10.1007/s00044-017-1784-2

Yin, Z., Power, D., Wang, Z., Stewart, S., Wu, X.-F. Synthesis of 1,3,4-oxadiazoles via annulation of hydrazides and benzene-1,3,5-triyl triformate under metal-free conditions. Synthesis, 2018, 50, 3238-3242. DOI: https://doi.org/10.1055/s-0037-1609481

Yoon, Y.K., Ali, M.A., Wei, A.C., Choon, T.S., Ismail, R. Synthesis and evaluation of antimycobacterial activity of new benzimidazole aminoesters. European Journal of Medicinal Chemistry, 2015, 93, 614-624. DOI: https://doi.org/10.1016/j.ejmech.2013.06.025

Zabiulla, Nagesh Khadri, M.J., Bushra Begum, A., Sunil, M.K., Khanum, S.A. Synthesis, docking and biological evaluation of thiadiazole and oxadiazole derivatives as antimicrobial and antioxidant agents. Results in Chemistry, 2020, 2, 100045. DOI: https://doi.org/10.1016/j.rechem.2020.100045

Zafer, M.M., El-Mahallawy, H.A., Abdulhak, A., Amin, M.A., Al-Agamy, M.H., Radwan, H.H. Emergence of colistin resistance in multidrug-resistant *Klebsiella pneumoniae* and *Escherichia coli* strains isolated from cancer patients. Annals of Clinical Microbiology and Antimicrobials 2019, 18, 40. DOI: https://doi.org/10.1186/s12941-019-0339-4

Zawawi, N.K., Taha, M., Ahmat, N., Wadood, A., Ismail, N.H., Rahim, F., Ali, M., Abdullah, N., Khan, K.M. Novel 2,5-disubtituted-1,3,4-oxadiazoles with benzimidazole backbone: a new class of β-glucuronidase inhibitors and *in silico* studies. Bioorganic & Medicinal Chemistry, 2015, 23, 3119-3125. DOI: https://doi.org/10.1016/j.bmc.2015.04.081

Zhao, J., Deng, Y., Jiang, Z., Qing, H. G Protein-coupled receptors (GPCRs) in Alzheimer's disease: A focus on $BACE_1$ related GPCRs. Frontiers in Aging Neuroscience, 2016, 8. DOI: https://doi.org/10.3389/fnagi.2016.00058

Zheng, Z., Liu, Q., Kim, W., Tharmalingam, N., Fuchs, B.B., Mylonakis, E. Antimicrobial activity of 1,3,4-oxadiazole derivatives against planktonic cells and biofilm of *Staphylococcus aureus*. Future Medicinal Chemistry, 2018, 10, 283-296. DOI: https://doi.org/10.4155/fmc-2017-0159

Zhong, C.-S., Cui, J.-L., Yu, S.-Y., Wang, X., Wang, N. A green and practical reduction of *N*-(4-chlorophenyl)-2-nitroaniline and its derivatives to corresponding *N*-substituted-benzene-1,2-

diamines using thiourea dioxide. Tetrahedron Letters, 2020, 61, 151599. DOI: https://doi.org/10.1016/j.tetlet.2020.151599

Zhu, J., Wang, Q., Wang, M.X. 2015. Multicomponent reactions in green pharmaceutical production. *In:* Zhu, J., Wang, Q. & Wang, M. X. (eds.) *Multicomponent reactions in organic synthesis.* Weinheim, Germany: Wiley-VCH.

Zuo, W.-Q., Wang, N.-Y., Zhu, Y.-x., Liu, L., Xiao, K.-J., Zhang, L.-D., Gao, C., Liu, Z.-H., You, X.-Y., Shi, Y.-J., Peng, C.-T., Ran, K., Tang, H., Yu, L.-T. A new series of HCV inhibitors based on a 2-(thieno[2,3*b*]pyridin-2-yl)-1,3,4-oxadiazole scaffold. RSC Advances, 2016, 6, 40277-40286. DOI: https://doi.org/10.1039/C6RA01179A